Expression, molecular interactions and functions of Ruk, a novel adaptor protein

Courtney Luke

PhD
University of Edinburgh
2005

Declaration

I declare that I am the author of this thesis. All experiments described were carried out by myself under the supervision of Dr. Vladimir L. Buchman and any contributions by third persons are clearly acknowledged. This thesis has not been submitted for any other degree or qualification.

Courtney Luke

June 2005

Acknowledgements

I am deeply grateful for Dr. Vladimir Buchman's supervision, support and patience throughout the years. Without Dr. Emma Borthwick and her support, wisdom, guidance and proofreading I doubt I would have made it through the years it has taken me to complete this thesis. The other lab members that were always good for a laugh and a drink that helped keep me sane were Dr. Natalia Ninkina, Darren Robertson, Dr. Mandy Jackson, David Longhurst and Katarina Papachroni.

Dr. Natalia Ninkina was also always willing to share her tricks of the trade with me that were extremely helpful. Julia Wanless provided great technical and a good gossip, while Dr. Ilya Merstolov and Dr. Veronika Boychenko acted as my ES cell culture gurus and taught me all about the wonders of ES cells. Dr. Ludmila Drobot was an enormous help with the GST work and Dr. Igor Korobko helped with the deletion mutation experiments.

Finally, I would like to thank the gang at Drouthy's for all the drinks and stories that made the rest of the week bearable. I would also like to thank my flatmates and friends for putting up with my occasional freakouts about my thesis and general future. Last but not least, I need to thank my parents and Andy for all their financial support and allowing me to do what I wanted to.

Abstract

The Ruk (Regulator of Ubiquitous Kinase) group of proteins is comprised of N-terminally truncated isoforms of the longest isoform, Ruk_l, (also known as CIN85, SETA and CD2BP3) which is comprised of 3 SH3 domains, a proline rich region, a serine rich region and a C-terminal coiled-coil domain. This domain organisation is very similar to the organization of CD2AP/CMS molecule and therefore these proteins are thought to form a novel multi-domain adaptor family. This protein family acts as scaffolding proteins that bridge different intracellular pathways and processes by forming multi-protein complexes. The Ruk isoforms are thought to dimerise through their common coiled-coil domain and are known to function in receptor tyrosine kinase endocytosis, actin polymerization, Rho and Arf GTPase pathways, PI3K downregulation and B and T cell development/activation. In this work I resolved the structure of the mouse *Ruk* gene, which encompasses 320 kb and contains 24 exons. There are 5 potential promoters in *Ruk* and differential usage of these promoters together with alternative splicing generate 12 types of *Ruk* mRNA, which are for the majority developmentally down-regulated; the exceptions are Ruk_t and Ruk_{h2} which are upregulated in adult testis. The 12 transcripts encode 7 different proteins and the only domain that is common for all of them is the N-terminal coiled-coil. Therefore, the coiled-coil domain was targeted for conditional inactivation using the Cre loxP system. The possibility of tissue specific inactivation will help to elucidate the function of the individual isoforms depending on which tissues are targeted. GST pulldown and co-immunoprecipitation studies have shown that isoforms are able to interact with one another through various domains. Similar

techniques have been used to elucidate the fine mechanism of the interaction between Ruk proteins and the p85α regulatory subunit of PI3-kinase.

Aims and objectives of thesis

The principal aim of the work was to characterise the *Ruk* gene, its expression and the intermolecular interactions mediated by the different domains of the encoded proteins. The specific objectives were as follows:

1. To determine the exon/intron structure of the *Ruk* gene.
2. To elucidate the expression patterns for the various splice variants of the *Ruk* transcripts.
3. Using information about the gene structure and expression to create mouse ES cells with a floxed *Ruk* gene that would eventually be used to study the conditional inactivation of the *Ruk* gene in mice.
4. To clarify the mechanism of intermolecular interactions between Ruk and the p85α regulatory subunit of PI3K.
5. To reveal the intermolecular interactions of the Ruk domains to further understand the role they play in interaction with other signalling molecules.

Table of Contents

List of Illustrations

Abbreviations

ABP	Actin binding protein
AIP1	ALG-2 interacting protein 1
ALG-2	Apoptosis-linked gene 2
Alix	ALG-2 interacting protein X
AP-2	Adaptor protein 2
ARAP3	ARF and Rho GTPase protein 3
ARF	ADP-ribosomal factor
ASAP1	ARF GTPase-activating protein 1
ASK1	Apoptosis signal-regulating kinase 1
BCR	B cell receptor
BH	BCR homology
BLNK	B-cell linker protein
bp	Base pairs
BRDG1	BCR downstream signalling 1
CAMGAP1	CIN85 associated muti-domain containing RhoGAP 1
Cbl	Casitas B-lineage lymphoma
CCP	Clathrin coated pits
CCD	Coiled-coil domain
CCV	Clathrin coated vesicle
CD2AP	CD2 adaptor protein
CD2BP3	CD2 binding protein 3
CHMP4	Chromatin-modifying protein 4
CIN85	Cbl interacting protein of 85 kb

CMS	Cas ligand with multiple SH3 domains
Dab2	Disabled-2
DH	Dbl homology
DMEM	Dulbecco's modified eagle's medium
DNA	Deoxyribonucleic acid
DOC-2	Differentially expressed in ovarian carcinoma protein 2
ECM	Extra-cellular matrix
EEA1	Early-endosomal autoantigen 1
ES	Embryonic stem cells
EGFR	Epidermal growth factor receptor
ESCRT	Endosomal sorting complex required for transport
FA	Focal adhesion
FAK	Focal adhesion kinase
FBS	Feotal bovine serum
GAP	GTPase activating protein
GEF	Guanine nucleotide exchange factor
GST	Glutathione S-transferase
HBS	HEPES buffered saline
HEPES	N-(2-Hydroxyethyl)piperazine-N'-(2-ethanesulfonic acid), 4-(2-Hydroxyethyl)piperazine-1-ethanesulfonic acid
HIP1R	Huntingtin interacting protein 1 related
HIV	Human immunodeficiency virus
HRP	Horse radish peroxidase
IP	Immunoprecipation

IRS-1	Insulin receptor substrate-1
Kb	Kilobase
LAAT	Lysophosphatydic acid acyl transferase activity
LAT	Linker for activated T cells
LBPA	Lysobiphophatidic acid
LPA	Lysophosphatidic acid
MCS	Multiple cloning site
ml	Milliliter
μg	Microgram
μl	microliter
MVB	Multi-vesicular body
nm	Nanometer
PA	Phosphatidic acid
PBS	Phosphate buffered Saline
PCR	Polymerase chain reaction
PDGF	Platelet derived growth factor
Pfu	Phage forming units
PH	Pleckstrin homology
PI3K	Phosphoinositide 3-phosphate kinase
PLC-γ2	Phosphoinositide phospholipase C-gamma-2
PRD	Proline-rich domain
PtdIns	Phosphatidylinositol
PtdIns(3)P	Phosphatidylinositol-3-phosphate
PtdIns(3,4)P_2	Phosphatidylinositol-3,4-diphosphate

$PtdIns(3,4,5)P_3$	Phosphatidylinositol-3,4,5-triphosphate
PtdIns(4)P	Phosphatidylinositol-4-monophosphate
$PtdIns(4,5)P_2$	Phosphatidylinositol-4,5-diphosphate
PTEN	Phosphatase located on chromosome ten
RING	Really interesting new gene
RNA	Ribonucleic acid
RTK	Receptor tyrosine kinase
RT-PCR	Reverse transcriptase polymerase chain reaction
Ruk	Regulator of ubiquitous kinase
SB1	SETA binding protein 1
SETA	SH3 domain expressed in tumorigenic astrocytes
SH2	Src homology 2 domain
SH3	Src homology domain 3
SH3KBP1	SH3-domain kinase binding protein 1
SHIP1	SH2-containing inositol phosphatase 1
Sos1	Son of Sevenless
STAP-1	Stem cell adaptor protein 1
TBS	Tris-buffered saline
TCR	T cell receptor
UIM	Ubiqitin interacting motif
UV	Ultraviolet

Chapter 1:
Introduction

1.1 Ruk gene and protein structure

Ruk, regulator of ubiquitous kinase, is a recently identified group of multidomain adaptor proteins that are involved in various cellular signalling cascades. Different orthologues of this group were isolated by five research teams and subsequently each team has independently named the proteins. For the extent of this work, the Ruk based naming system created by the Buchman group will be used, as the other naming systems fail to comprehensively distinguish between the different isoforms that have since emerged.

The Ruk family appears to be evolutionarily conserved in higher eukaryotes, and orthologues have been found in a variety of vertebrate species ranging from fish to human. However, there are no obvious orthologues found in lower eukaryotes such as *Drosophila melanogaster, Caenorhabditis elegans* or yeast, indicating a specific role in higher eukaryotes (Dikic, 2002). When initially cloned, many groups only isolated a single isoform; the exception was the Buchman lab that isolated three different isoforms (Gout *et al.*, 2000). Thus until recently there were only four known isoforms of Ruk: Ruk_l, Ruk_m, Ruk_s and $Ruk_{\Delta A}$. Furthermore, prior to the research presented here, the size of the gene was unknown; sequence comparison to the known genome and flourescent in situ hybridisation studies had placed it on the X chromosome (Hyatt *et al.*, 2000; Narita *et al.*, 2001; Kost and Buchman, unpublished results). When the research presented in this thesis was begun, the Genome Projects had yet to complete either the human or mouse genome sequencing and it was not possible to acheive the entire *Ruk* gene structure through computer analysis alone.

The basic structure of the Ruk proteins is illustrated below in Figure 1.1. The

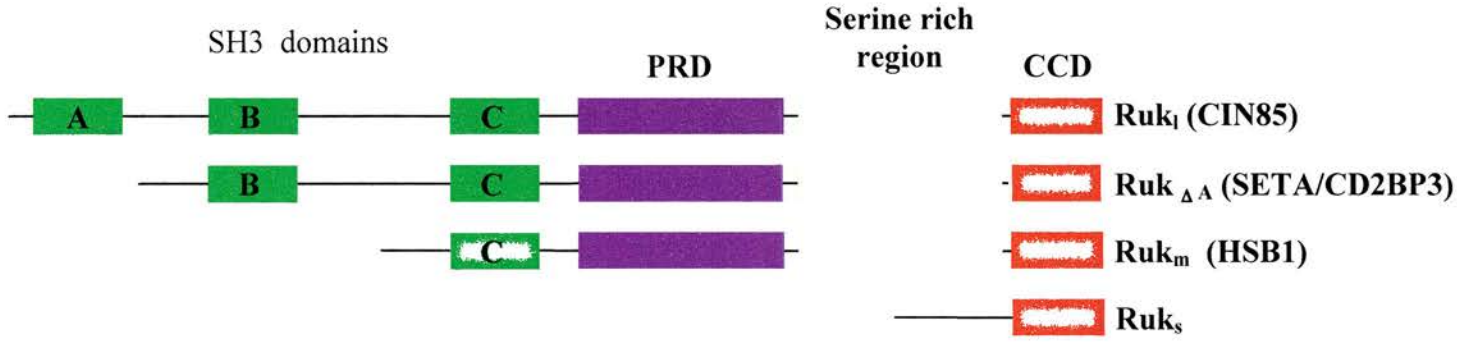

Figure 1.1: The various protein isoforms of Ruk that were initially isolated in 2000 by various groups, including the Buchman lab. Ruk$_l$ is the longest with three SH3 domains (A, B and C), followed by a proline rich domain, a serine rich domain and a coiled-coil domain. The Ruk$_l$ protein was also named CIN85. The Ruk$_{\Delta A}$ isoform is comprised of two SH3 domains (B and C), the proline rich, serine rich and coiled-coil domains. This isoform was also named SETA and CD2BP3. Ruk$_m$ contains a single SH3 domain (C), a proline rich domain, serine rich domain and coiled-coil domain. This Ruk$_m$ isoform has also been named HSB1. The smallest isoform is Ruk$_s$ which is comprised of only a CCD and has no other names. Adapted from Buchman *et al.*, 2002.

longest isoform, Ruk_l, is comprised of three SH3 (Src homology 3) domains of the N-terminus followed by a PRD (proline rich domain), and a serine rich region followed by a CCD (coiled-coil domain) at the C-terminus. The smaller isoforms derive from N-truncations of this longest isoform until all that is left is a CCD in the smallest isoform, Ruk_s (see Figure 1.1). Comparison between Ruk_l and all known proteins showed that it had an uncanny similarity to the adaptor protein CD2AP/CMS in that they shared a common overall domain structure. Ruk_l and CD2AP/CMS also share 39% identity and 54% similarity in their amino acid sequences (Dikic, 2002). The similarities between the two proteins were further shown by the fact that the SH3 domains of Ruk_l and CD2AP/CMS share a higher sequence similarity to each other than any other SH3 domain (Dikic, 2002). The similarities between CD2AP/CMS and Ruk_l point to a novel family of adaptor proteins comprised of the Ruk isoforms and CD2AP/CMS.

1.2 Ruk isoforms mediate interactions

1.2.1 Intermolecular interactions of Ruk isoforms

The multi-domain structure of the Ruk isoforms indicates that they are capable of several simultaneous interactions. While the Ruk SH3 domains bind PRD containing proteins, the Ruk PRD can also bind proteins containing SH3 domains. Furthermore, the CCD may dimerise the Ruk isoforms leading to an even greater number of combinatorial possibilities (Dikic, 2002). However, it should be noted that most of the proteins identified so far as Ruk interactors are PRD containing proteins that bind to one or more of the Ruk SH3 domains. In order to find more Ruk binding partners, recent work has identified a novel Ruk SH3 binding consensus

sequence (PXXXPR) that is found in the PRD of Ruk interactors (Kowanetz *et al.*, 2003a; Kurakin *et al.*, 2003). The importance of this specific binding motif is highlighted by the fact that the mutation of the arginine is capable of abrogating Ruk binding (Kowanetz *et al.*, 2003a; Kowanetz *et al.*, 2003b). While database investigations have yielded many proteins with the Ruk SH3 binding sequence, only a subset actually interacts with Ruk isoforms; therefore, it is thought that residues outside of the motif may determine the specificity and affinity of binding to the Ruk molecules (Kowanetz *et al.*, 2003a; Kowanetz *et al.*, 2004). This hypothesis is supported by a recent database search by Kowanetz *et al.* (2004) that identified several putative Ruk_1 binding proteins that contained the PXXXPR motif, however co-immunoprecipitations proved that many of these proteins were unable to bind Ruk_1. It is possible that the residues surrounding the binding sequence are able to participate in the binding or they may alter the structure of the protein around the motif in some way to affect the SH3 domain binding.

The implication from the available data is that Ruk isoforms, specifically Ruk_1, serve as scaffolding proteins by clustering different proteins that direct intracellular processes and dynamically exchanging binding partners depending on intra- and intercellular conditions (Figure 1.2). The transient nature of complexes based around Ruk isoforms may help to coordinate and distinguish the various steps of the pathways in which they are involved.

For instance, Ruk_1 based protein clustering may be key to some of the processes that Ruk_1 is involved. This hypothesis is supported by the fact that some proteins, such as ASAP1 and ARAP3, can only be found in a single complex when Ruk_1 is present (Kowanetz *et al.*, 2004). In such cases these proteins may function

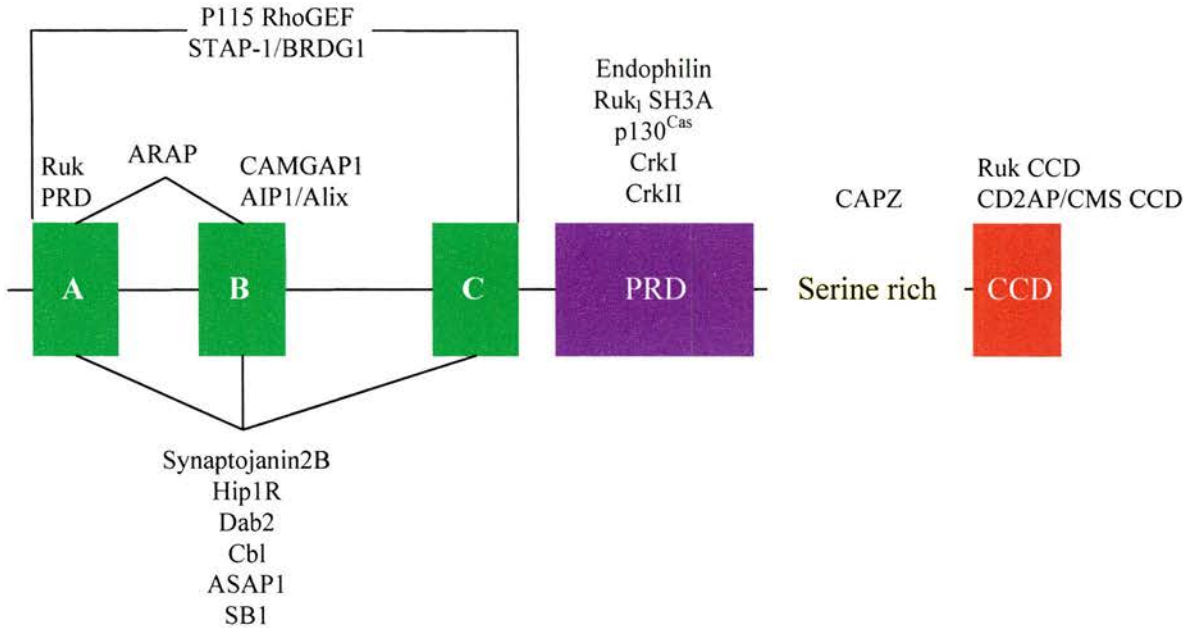

Figure 1.2: The many interactions of the Ruk isoforms. The multi-domain structure allows several different interactions to occur simultaneously and for Ruk based multi-protein complexes to bridge different cell processes. Most of the known interactions occur through the Ruk SH3 domains, and several different interactors depend on two or more SH3 domains for maximum binding efficiency. Some SH3-domain containing proteins interact with the prolein rich domain of the Ruk isoforms, and only CAPZ is known to interact with the serine rich domain. The coiled-coil domain is thought to dimerise the isoforms and interact with CD2AP/CMS.

coordiantely only due to Ruk_I mediated clustering. Due to the low affinity binding between the PXXXPR motifs of PRD containing proteins and the SH3 domains of Ruk_I, the rapid exchange of binding partners depending on their concentrations, compartmentalisation or post-translational modifications can occur (Kowanetz *et al.*, 2004).

1.2.2 Ruk intramolecular interactions and dimerisation

It has recently been discovered that the PRD of the Ruk proteins also contains the consensus sequence for Ruk SH3 domains, indicating either an autoinibitory or dimerisation mechanism (see Section 6.5). The PRD of the Ruk isoforms contains a PPKKPR motif that binds with high specificity but low affinity to the SH3A domain, which may prevent SH3B and C from interacting with other proteins (Kowanetz *et al.*, 2003a). It is thought that higher affinity interactions are able to "break" open the Ruk_I protein by interfering with the intramolecular binding and allowing all three SH3 domains to interact with various other proteins (Kowanetz *et al.*, 2003a; Borthwick *et al.*, 2004). According to Borthwick *et al.* (2004) the SH3A-PRD bond occurs between the different Ruk isoforms resulting in a Ruk dimer that is closed to lower affinity interactions (see Figure 6.2).

The PRD-SH3A interaction is not the only mechanism for dimerisation evident in the Ruk proteins. It is well known that CCDs are able to mediate dimerisation in other proteins and it is predicted that they may do so in the Ruk isoforms to create hetero or homodimers (Watanabe *et al.*, 2000). Recent work using a yeast two-hybrid system and GST-fusion proteins has confirmed that the CCD allows different Ruk isoforms to interact with one another, thereby supporting their

dimerisation (Borthwick *et al.*, 2004). All Ruk isoforms contain a CCD (see Figure 1.1), unlike the PRD that is only present in some isoforms, and there is some evidence that heterodimerisation does play a role in endocytosis (see Section 1.3.1). This dimerisation ability increases the number of simultaneous interactions and combinatorial possibilities of protein interactions based around Ruk dimers.

1.3 Ruk_I

The most studied of the isoforms is Ruk_I that was independently cloned three times in 2000 from human and rat cells (Borinstein *et al.*, 2000; Take *et al.*, 2000; Gout *et al.*, 2000). Take *et al.* (2000) named the human orthologue of Ruk_I that they cloned CIN85 (c-Cbl interacting protein of 85kDa) as it was an approximately 85 kDa protein that interacted with c-Cbl. This isolation of human Ruk_I cDNA was from a library derived from T cells (Take *et al.*, 2000) and this cDNA was shown to also be expressed in adult human heart, brain, placenta, lung, liver, skeletal muscle, kidney, pancreas and all human derived cancer cell lines tested (Take *et al.*, 2000). Gout *et al.* (2000) reported cloning the same isoform along with two smaller isoforms from newborn rat tissues and named them regulator of ubiquitious kinase (Ruk) after the inhibition of PI3K (phosphoinositide 3-phosphate kinase) that they observed. Borinstein *et al.* (2000) cloned Ruk_I from an adult rat brain library as a longer isoform of rat $Ruk_{\Delta A}$ they had earlier cloned and designated SETA (SH3 domain expressed in tumorigenic astrocytes) (Bogler *et al.*, 2000).

Most recently, another functional homologue of the Ruk_I protein was isolated from yeast termed Sla1 (Stamenova *et al.*, 2004). Ruk_I is smaller than Sla1 but the two have a 34% overall similarity which is relatively high in such circumstances

(Stamenova *et al.*, 2004). Both proteins share structural similarities as they both have three SH3 domains in the N-terminus with similar spacing between the domains and a CCD; both function as scaffolding proteins in endocytosis by interacting with functional homologues of Cbl (Stamenova *et al.*, 2004). The mere existence of a functional homologue of Ruk_I in lower eukaryotes is evidence that the Ruk_I role in endocytosis is highly important and integral to cellular homeostasis.

As previously stated, Ruk_I is the longest isoform of the Ruk family and thus theoretically provides the most opportunity for binding. Currently, this theory is proven only because Ruk_I is the most extensively studied isoform. Detailed below are the different pathways that Ruk_I plays a role in and the specific proteins that it is known to interact with.

1.3.1 Ruk_I has a role in endocytosis

1.3.1.1 Overview of CCP (clathrin coated pit)/CCV (clathrin coated vesicle) formation

CCPs are formed at specific locations on the cell membrane, "coated pit zones", possibly due to the presence of the phosphoiniositides PtdIns(4,5)P_2 and PtdIns(3,4,5)P_3 and key adaptor proteins (Mousavi *et al.*, 2004). Quite possibly these "coated pit zones" are lipid rafts, as evidenced by the necessity of high cholesterol levels in the invagination process (Rodal *et al.*, 1999; Subtil *et al.*, 1999). It is interesting to note that lipid rafts attenuate EGFR (epidermal growth factor receptor) signalling, possibly through cholesterol dependent changes in the physical properties of the plasma membrane that affects the conformation of EGFR (Chen and Resh, 2002; Pike and Casey, 2002; Westover *et al.*, 2003). The most plausible view

of CCP formation is that it is a two-step process: endocytic adaptors specify the location of the CCP, and clathrin is drawn to the location by adaptors that bind and polymerise clathrin, thereby stabilizing the CCP (Mousavi *et al.*, 2004).

Epsin and Eps15 play a key role in both targeting the location and drawing clathrin to the pit, as it has been shown that Epsin and Eps15 bind membrane bound PtdIns(4,5)P_2 and initiate membrane curvature (Mousavi *et al.*, 2004). Following membrane localization, Epsin complexes with and clusters AP-2 (adaptor protein complex 2; possibly through Eps15 acting as an adaptor) that results in clathrin translocation and polymerization (Mousavi *et al.*, 2004). Epsin is displaced from the complex, leaving a CCP lined with AP-2 and other adaptor proteins. In this scheme, the integral ability of clathrin to form curvatures does not initiate CCP formation but does serve to support the curvature of the coated pit once it is formed (Mousavi *et al.*, 2004).

When the shallow coated pits have formed, they become deeply invaginated pits through the actions of dynamin and endophilin (Hill *et al.*, 2001; Huttner and Schmidt, 2002). The GTPase ability of dynamin provides the necessary energy for the transition while endophilin can cause the curvature through its LAAT activity (lysophosphatydic acid acyl transferase; Hill *et al.*, 2001). When the "neck" of the CCP is sufficiently formed, dynamin, synaptojanin1 and endophilin act in concert to close it and perform the scission of the CCV from the membrane (Hill *et al.*, 2001). It is thought that the GTP bound to dynamin provides the necessary energy, while endophilin converts the inverted cone shaped lipids of the neck to cone shaped, causing curvature of the membrane and eventual budding off.

A specific type of endocytosis is RTK (receptor tyrosine kinase) internalization, and Cbl, a Ruk$_1$ interactor, is one of the key proteins involved in several of the steps of this internalisation. During endocytosis, Cbl not only functions as a multi-domain adaptor protein, it also acts as a ubiquitin ligase (Joazeiro *et al.*, 1999). The monoubiquitination of activated RTKs by Cbl may facilitate the targeting of the RTK to the CCP; many of the endocytic proteins, such as Eps15 and epsin, also have an ability to recognize and bind ubiquitin through their UIM (ubiquitin interacting motif) (Haglund *et al.*, 2003a; Haglund *et al.*, 2003b). The scheme that ubiquitin helps to draw the RTK to the CCP is controversial however, as there is evidence that ubiquitin is unnecessary to targeting the RTK for internalization (Duan *et al.*, 2003). It is almost universally accepted that multiple monoubiquitination is needed to target the RTK to lysosomal degradation, however.

Once the RTK is targeted to the CCP, Cbl continues to monoubiqutinate the protein throughout the endocytic process at several sites thereby allowing different ubiquitin binding proteins (Hrs and TSG101) to recognize the RTKs by specific and unique ubiquitnated sites (Haglund *et al.*, 2003b). In this manner, multiple monoubiquitination throughout endocytosis targets the vesicle for transport along the ESCRT (endsomal sorting complex required for transport) pathway that leads to the sorting of receptors for lysosomal degradation and the termination of their signals (Haglund *et al.*, 2003b, Jiang and Sorkin, 2003). This multiple monoubiquitination may specify a higher rate of endocytosis and a more efficient degradation than a single monoubiquitination event does (Haglund *et al.*, 2003b).

1.3.1.2 The role of Ruk$_I$ in RTK internalisation

In RTK signalling it has been found that Ruk$_I$ plays an essential role in receptor endocytosis and degradation of signals by bringing together several different components that are necessary for the internalization of activated RTKs (Figures 1.3 and 1.4). So far, Ruk$_I$ has been implicated in the down-regulation of four different RTKs from three different subfamilies: EGFR, c-Met, c-Kit and PDGFR (Petrelli *et al.*, 2002; Soubeyran *et al.*, 2002; Szymkiewicz *et al.*, 2002). Several of the Ruk$_I$ binding proteins have been implicated in the various stages of CCV formation. At the shallow CCP stage, Ruk$_I$ interacts with Hip1R, Dab-2, endophilin and possibility even AP-2 (Dikic, 2003; Kowanetz *et al.*, 2004). Ruk$_I$ may also help to target RTKs to developing CCPs through its interactions with Cbl and later may help the CCV to move into the cell through the Ruk$_I$ binding of Rho and Arf GTPase interacting proteins (see Section 1.3.2; Figure 1.3; Figure 1.4).

However, this simplistic view of Ruk$_I$ working in conjunction with other proteins to promote endocytosis is not entirely accurate. Recent work has shown that in different cellular conditions, Ruk$_I$ can inhibit RTK endocytosis (Schmidt *et al.*, 2003b). This shows that Ruk$_I$ may act as a cellular "switch" between different cellular processes with the result dependent on intracellular concentrations of the various Ruk$_I$ interactors.

Ruk$_I$ based multi-protein complexes serve to bridge and coordiante the action of proteins that are directly involved in endocytosis (endophilin and synaptojanin) and proteins that are indirectly needed for endocytosis (Rho GTPases). Another such link that may be key to the endocytic process is the influence of Ruk$_I$ on PtdIns levels and the endocytic process. Ruk$_I$ was initially identified as a negative regulator of

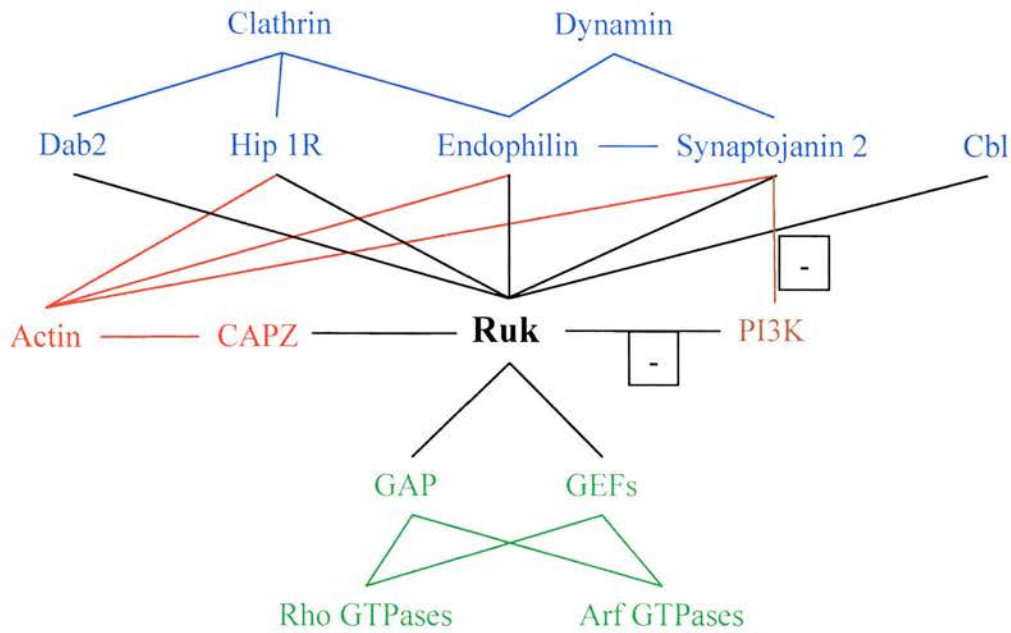

Figure 1.3: An interaction map showing the role of Ruk_l in endocytosis and its binding partners. Ruk_l and possibly other isoforms are involved in many of the pathways leading to RTK endocytosis and Ruk based multi-protein complexes link together these pathways. The Rho and Arf GTPase pathways are in green, actin associations are in red, the proteins associated with endocytosis are in blue, the PI3K pathway is in brown and Ruk interactions are in black.

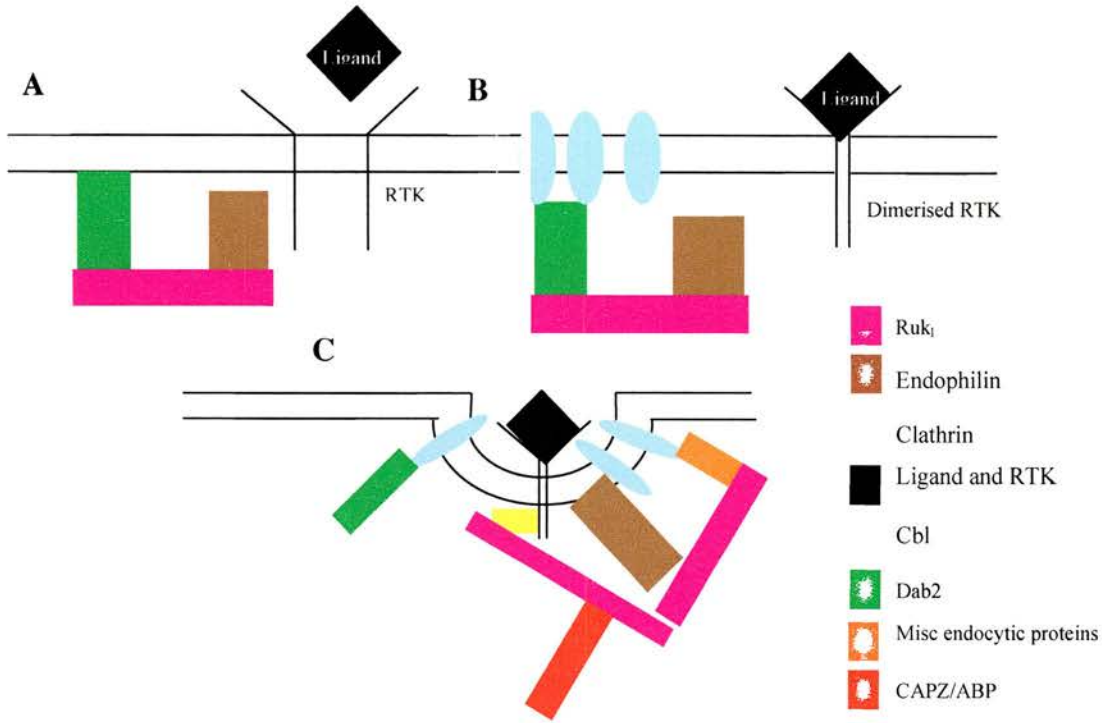

Figure 1.4: A schematic diagram of the formation of CCVs and the role of Ruk in early endocytosis. Ruk isoforms are located on the cell membrane due to its association with Dab2 (A). Ligand association causes the dimerisation of the RTK and subsequent polymerisation of clathrin. Cbl becomes associated with the RTK (B). Ruk dissociates from Dab2 and interacts with Cbl. While the CCP is forming Ruk interacts with ABPs such as CAPZ and other endocytic proteins such as Hip1R.

PI3K and later found to interact with SHIP1 (Src homology 2 domain-containing inositol-5-phosphotase; Gout *et al.*, 2000; Kowanetz *et al.*, 2004). As discussed below in Section 1.3.4, SHIP1 and synaptojanin are 5' phosphatases that produce PtdIns(3,4)P_2 from the PI3K product PtdIns(3,4,5)P_3 and PI3K produces PtdIns(3,4,5)P_3 from PtdIns(4,5)P_2 (Giuriato *et al.*, 2003). Therefore, it is theoretically possible that Ruk_I acts to suppress PI3K activity leading to higher levels of PtdIns(4,5)P_2 while simultaneously, in certain cells, increasing SHIP1 and synaptojanin activity. The combination of these actions would lead to an accumulation of PtdInsP_2 at the site of Ruk_I expression, which is essential for the localisation of endocytic machinery.

In an interesting note, it seems that dimerisation with the other Ruk isoforms is crucial to Ruk_I promoting receptor trafficking, as Ruk_I lacking the CCD does not localise to the punctate structures that Ruk_I does (Watanabe *et al.*, 2000) and endocytosis is impaired in cells expressing this mutant form (Soubeyran *et al.*, 2002; Kowanetz *et al.*, unpublished data). With this evidence, it seems that the hetero or homodimerisation of Ruk isoforms and the combinations of proteins induced by dimerisation is needed to form essential endocytic protein complexes.

1.3.1.3 Ruk_I may bridge actin and endocytosis

As mentioned above, it is possible that Ruk_I based multi-protein complexes could link specific endocytic processes to the actin cytoskeleton (Figures 1.3 and 1.4), which is thought to play a role in endocytosis. While the role of actin in yeast endocytosis is fairly well known, its full involvement in endocytocis in higher eukaryotes remains relatively unknown. Much like in yeast, recent evidence in

higher eukaryotes points to the involvement of actin in specifying the site of formation for clathrin lattices and the eventual formation of CCPs by localizing the endocytic protein complexes to specific sites in the plasma membrane (Engqvist-Goldstein and Drubin, 2003).

The specific localization of endocytic machinery by actin is important to organize the cell cortex and maintain or establish cell polarity (Engqvist-Goldstein and Drubin, 2003). Actin polymerization, which is partially controlled by CAPZ (capping protein (actin filament) muscle Z-line), another Ruk_I binding protein, may also play a role in providing the force necessary for the scission of CCVs from the plasma membrane when working in conjunction with dynamin and synaptojanin, another Ruk_I interactor (Hutchings *et al.*, 2003; Engqvist-Goldstein and Drubin, 2003). The third role of actin in endocytosis is in the propulsion of newly formed CCVs away from the cell membrane (Engqvist-Goldstein and Drubin, 2003). With its many interactors, Ruk_I may play a role in some or all of these processes.

The current evidence points to a transient relationship between actin and endocytic machinery at specific points in the formation of CCVs, and Ruk_I could possibly play a role in targeting ABPs (actin binding protein) to specific protein complexes in the endocytic process due to its multiple binding motifs and dimerisation ability. Furthermore, it has been hypothesized that Ruk_I specializes in low affinity binding that would facilitate the creation of many different protein complexes such as those necessary to transiently target actin to specific points in the formation of CCVs.

1.3.1.4 The role of interaction between Hip1R and Ruk$_I$ in endocytosis

Ruk$_I$ has recently been identified as a binding partner of Hip1R (Huntingtin interacting protein 1 related), a protein that binds directly to F-actin and is implicated in the early stages of CCP formation (Engqvist-Goldstein *et al.*, 2001; Kowanetz *et al.*, 2004). Hip1R is an evolutionarily conserved protein that binds and polymerises clathrin via its CCD (Engqvist-Goldstein *et al.*, 2001). This protein is one of the many adaptor proteins that help to target clathrin to specific "coated pit zones" and it dimerises to physically link F-actin to the clathrin lattices and CCPs (Engqvist-Goldstein *et al.*, 2001). It is possible that Hip1R interactions with other proteins such as Ruk$_I$ that play a role in the transient nature of the actin-CCP binding and that Hip1R and its binding partners serve to localize actin to the necessary steps in CCP formation (eg: early shallow pits, constricted necks etc). Recent evidence of Hip1R silencing by RNAi, shows that in the absence of Hip1R, actin and the endocytic machinery are constitutively bound producing an overabundance of CCPs while lacking CCVs (Engqvist-Goldstein *et al.*, 2004). This evidence points to the necessity of Hip1R or its binding partners in the maintenance of the limited association between actin and endocytosis to specific points in the formation of CCVs.

Kowantez *et al.* (2004) showed that Ruk$_I$ interacts with Hip1R and suggests that this interaction plays a role in clustering Hip1R at the membrane, possibly facilitating its ability to polymerise clathrin and helping to form CCPs (Figures 1.3 and 1.4). Furthermore, their research showed that, in a manner similar to many other Ruk$_I$ binding partners, more than one SH3 domain increased the ability of Ruk$_I$ to bind to Hip1R with the highest amount of Hip1R being bound when all three SH3

domains are present. The SH3 domains of Ruk_I bind to the PSPAPR (amino acid 1025) and PSIAPR (amino acid 1044) motifs found in the PRD of Hip1R (Kowanetz *et al.*, 2004).

1.3.1.5 The role of interaction between Dab2/DOC-2 and Ruk_I in endocytosis

Dab2/DOC-2 (disabled-2/differentially-expressed in ovarian carcinoma 2) is a multidomain protein that acts as an adaptor in the endocytic pathway through its interactions with PtdIns(4,5)P_2, clathrin and associated proteins such as AP-2 (Mishra *et al.*, 2002). The functional sites of the protein bind and polymerise multiple clathrin molecules, which helps to form the CCP, while simultaneously binding other proteins involved in the endocytic process such as Ruk_I and myosin IV (Mishra *et al.*, 2002). Myosin IV is a motor protein that associates with actin filaments and generates the force for membrane protrusions, retractions and the propulsion of vesicles away from the plasma membrane (Engqvist-Goldstein and Drubin, 2003).

It has been shown that in unstimulated cells, Dab2/DOC-2 binds to clathrin and Ruk_I on the cell surface independently of the RTK, and when cells are stimulated, Dab2/DOC-2 translocates Ruk_I with its constitutively bound endophilin to the forming clathrin lattice (Figure 1.4, Kowanetz *et al.*, 2003b). Similar to the manner in which CD2AP/CMS is thought to cluster CD2 to the T-cell surface, Ruk_I helps to cluster Dab2/DOC-2 to the cell surface, possibly helping to bring the multiple clathrin complexes close together and facilitating the lattice formation (Kowanetz *et al.*, 2003b). Once in the location of the forming CCP, Ruk_I dissociates from Dab2/DOC-2 in order to bind to Cbl; Cbl and Dab2/DOC-2 compete with one

another for binding to Ruk_I and Cbl has the higher binding affinity (Kowanetz *et al.*, 2003b).

The Ruk_I binding site (PKPAPR) is found within the Dab2/DOC-2 carboxyl terminus (amino acid 713 to 718 on the mouse Dab2 p96 splice variant) and is able to bind all three SH3 domains of Ruk_I (Kowanetz *et al.*, 2003b). Multiple SH3 domains may be necessary for efficient binding since SH3-AB, SH3-BC and SH3-ABC all associated to a higher degree than individual SH3 domains (Kowanetz *et al.*, 2003b).

1.3.1.6 The role of interaction between Cbl and Ruk_I in endocytosis

Two of the Cbl proteins, c-Cbl and Cbl-b (collectively known as Cbl), contain a tyrosine kinase binding domain, a RING finger domain, a PRD and an ubiquitin associating domain and both have similar functions *in vivo* (Thien and Langdon, 2001). This multi-domain structure indicates several different binding partners including RTKs, non-receptor tyrosine kinases and SH3 containing proteins such as Grb2 and Ruk_I (Thien and Langdon, 2001). The Cbl proteins work in a variety of pathways as adaptors that bring together several different interactors through their multiple binding domains. These other roles for Cbl are mentioned in their own contexts below. Cbl was initially identified as an adaptor protein and only relatively recently has its role in receptor endocytosis become clear. As has been mentioned above, Cbl is now known as a negative regulator of receptor tyrosine kinases that act by ubiquinating activated RTKs and targeting them for internalisation and signal degradation.

Cbl's role in receptor endocytosis is negatively regulated by the Rho GTPase Cdc42 (cell division cycle 42; see Section 1.3.2 for Rho GTPases). The Cdc42 effector p85Cool-1/β-Pix (cloned out of library-1/Pax interaction factor) is a Cbl binding partner that also binds to active Cdc42, and the p85Cool-1/β-Pix-Cdc42-Cbl complex that is formed prevents Cbl ubiquitination of activated RTK (Wu *et al.*, 2003). Since p85Cool-1/β-Pix is only able to interact with GTP-bound Cdc42, the inhibition of RTK ubiquitination by C-Cbl is transient, allowing for the eventual targeting of the RTK for degradation and the temporal regulation of the RTK signals (Wu *et al.*, 2003).

In addition to ubiquitinating RTKs, Cbl acts in receptor endocytosis as an actin polymerisation inhibitor (Scaife *et al.*, 2003). Cbl is spatially relocated by PDGFR stimulation to PDGFR induced actin dorsal ruffles where it inhibits the Rho GTPase Rac. Rac is able to nucleate actin assembly and the appearance of dorsal ruffles in response to PDGFR stimulation requires Src, PI3K and Rac (Scaife *et al.*, 2003). Cbl only inhibits Rac activity but this is sufficient for the full abrogation of dorsal ruffles (Scaife *et al.*, 2003).

Human c-Cbl has a single Ruk_I binding site in the PRD at amino acids 824 to 829 (PKPFPR); human Cbl-b also has a single binding site at amino acids 906 to 911 (PKPRPR) (Kurakin *et al.*, 2003). All three SH3 domains can individually bind Cbl, but the efficiency of binding is increased when two or more SH3 domains are present with the most efficient binding occurring with SH3A or SH3C in conjunction with SH3B (Take *et al.*, 2000; Kowanetz *et al.*, 2003a). The amount of Cbl bound to Ruk_I increases with increasing binding efficiency, leading to the conclusion that Ruk_I

serves as an adaptor protein that can cluster together two or three Cbl molecules which results in the stabilisation of the Cbl-RTK complex (Kowanetz *et al.*, 2003a).

The binding of Ruk_I to Cbl can cause an inhibition of RTK endocytsis depending on the cellular conditions. In confluent cells, Ruk_I actually inhibits Cbl binding to EGFR and subsequent endocytosis (Schmidt *et al.*, 2003b). The inhibition of Cbl activity is possibly due to cytoskeletal changes in confluent cells that may influence Ruk_I interactions with c-Cbl and activated EGFR (Schmidt *et al.*, 2003b).

Cbl is tyrosine phosphorylated when it is bound to an activated RTK, a function that is independent of its ubiquitin ligase ability. Ruk_I-Cbl binding is initially independent of the RTK tyrosine phosphorylation of Cbl, but the amount of interaction between the two molecules is increased when Cbl is phosphorylated (Take *et al.*, 2000; Soubeyran *et al.*, 2002). To explain this phenomenon, it has been hypothesised that growth factor induced tyrosine phosphorylation of Cbl causes a conformational shift that opens or stabilises the PXXXPR motif leading to Ruk_I binding (Kowanetz *et al.*, 2003a). One of the consequences of Ruk_I and Cbl interaction is Ruk_I monoubiquitination by Cbl, but Ruk_I is not targeted for degradation, possibly because multi-monoubiquitination is necessary for targeting for lysosomal degradation (Verdier *et al.*, 2002). Verdier *et al.* (2002) also reported that both Ruk_m and Ruk_s are ubiquitinated by Cbl indicating that other isoforms are capable of indirectly interacting with c-Cbl via heterodimerisation with Ruk_I.

1.3.1.7 The role of interaction between AIP1/Alix and Ruk_I in endocytosis

Along with its roles in apoptosis and focal adhesions, Chatellard-Causse *et al.* (2002) showed that AIP1/Alix, a Ruk_I and $Ruk_{\Delta A}$ interactor, is able to interact with

endophilins and induce cytoplasmic vacuolisation. AIP1/Alix has been implicated in promoting membrane curvature through its interaction with EIAV (equine infectious anemia virus), a protein with a Gag domain, and controlling the formation of endosomes containing LBPA (lysobiphophatidic acid) *in vivo* (Strack *et al.*, 2003; Matsuo *et al.*, 2004).

Furthermore, recent work has shown that AIP1/Alix indirectly associates with EGFR regardless of its activation state; this binding appears to be independent of either Cbl or Ruk_I involvement indicating the presence of another unknown protein in the EGFR-AIP1/Alix complex (Schmidt *et al.*, 2004). Interestingly, the co-expression of AIP1/Alix and Ruk_I is able to increase their respective indirect interactions with EGFR while simultaneously weakening the interaction between Ruk_I and Cbl (Schmidt *et al.*, 2004). When the expression of AIP1/Alix was increased it reduced the tyrosine phosphorylation of Cbl and the ubiquitination EGFR (Schmidt *et al.*, 2004), and thus AIP1/Alix acts to attenuate the Cbl-EGFR interaction and subsequent phosphorylation or ubiquitination events and in this manner acts to inhibit EGFR endocytosis. Therefore, the interaction of Ruk_I may act as a method of bridging the pro-endocytic effects of Cbl and the anti-endocytic effects of AIP1/Alix to create a well-balanced effect on cellular signalling.

In addition to early endocytosis, the fact that AIP1/Alix is involved in the later stages of endosomal sorting is becoming increasingly apparent. AIP1/Alix has been found to interact with the intracellular transport and sorting machinery such as CHMP4 (chromatin-modifying protein 4) and ESCRT (endosomal sorting complex required for transport) proteins.

It has been shown that AIP1/Alix binds to the some of the CHMP4 class of

proteins, especially CHMP4b, via the C-terminal half of the AIP1/Alix protein, this interaction is independent of the tyrosine phosphorylation state of AIP1/Alix (Katoh *et al.*, 2003; Katoh *et al.*, 2004; Katoh *et al.,* 2003). Through this interaction with CHMP4 proteins, AIP1/Alix may link the ESCRTIII and ESCRTI complexes and may also indirectly linkall three ESCRT complexes together (Martin-Serrano *et al.*, 2003; Strack *et al.*, 2003; von Schwedler *et al.*, 2003).

These interactions point to functional differences between the two halves of the AIP1/Alix protein; the N-terminal half that binds endophilin (Trioulier *et al.*, 2004) is involved in early events governing the sorting of ubquitinated endosomal cargo and the C-terminal half plays an unknown role in the ESCRT pathway. It has been hypothesised that N-terminal binding to either Ruk_I/$Ruk_{\Delta A}$ (the binding motif begins at amino acid 740; Kurakin *et al.*, 2003) may play a role in changing the conformation of AIP1/Alix and allows the C-terminal half to interact with CHMP4 and later endosomal trafficking proteins (Katoh *et al.*, 2003; Strack *et al.*, 2003). This ability of AIP1/Alix to bind to both early and late endosomal trafficking proteins indicates a possible link between the internalisation machinery and the MVB sorting complexes (Katoh *et al.*, 2003).

As can be expected from a protein that is known to bind both Ruk_I and $Ruk_{\Delta A}$, the main Ruk SH3 domain that binds to AIP1/Alix is the SH3B domain while neither SH3A nor SH3C seem to mediate the interaction (Chen *et al.*, 2000; Schmidt *et al.*, 2003a).

1.3.1.8 The role of interaction between endophilin and Ruk_I in endocytosis

Since endophilin is constitutively bound to the PRD of Ruk_I, it is possible that

Ruk isoforms bring additional endophilin to the forming pit through the Ruk$_I$-Dab2 interaction (Figure 1.4; Petrelli *et al.*, 2002; Soubeyran *et al.*, 2002). Once at the shallow pit, endophilin is able to interact with the membrane to help produce or maintain the initial membrane curvature necessary for the formation of the CCP (Petrelli *et al.*, 2002; Soubeyran *et al.*, 2002; Kowanetz *et al.*, 2003b).

Endophilin is involved in several steps of endocytosis, from invagination through to uncoating the vesicle when it is internalised (Mousavi *et al.*, 2004). Endophilins are drawn to the developing CCP and help to form CCVs through three mechanisms. Firstly, endophilin has an intrinsic lysophosphatydic acid acyl transferase activity by binding to lysophosphatidic acid (LPA) and transferring arachidonate to it, thereby producing phosphatidic acid (PA) and changing the membrane curvature (Schmidt *et al.*, 1999; Mousavi *et al.*, 2004). Secondly, endophilin directly binds to the cellular membrane and cause the invagination of shallow coated pits independently of its LAAT activity that helps to form the deeply invaginated CCPs (Farsad *et al.*, 2001). Lastly, endophilin interacts with dynamin, a protein that binds to GTP and hydrolyses it to GDP thereby providing the necessary energy to produce membrane curvature and scission (Hill *et al.*, 2001; Mousavi *et al.*, 2004). This interaction between endophilin and dynamin is crucial to the formation of the late CCP that is linked to the cellular membrane by a narrow neck and the eventual release of the CCP from the membrane to form a CCV.

1.3.1.9 The role of interaction between the synaptojanins and Ruk$_I$ in endocytosis

A PXXXPR motif exists in both isoforms of synaptojanin, but an interesting

example of the selectivity of Ruk_I binding is seen in the fact that Ruk_I interacts with synaptojanin2 but not synaptojanin1 (Kowanetz *et al.*, 2004). One of the splice variants of synapotjanin2, synaptojanin2B1, binds to all three SH3 domains of Ruk_I through the PVPKPR motif that starts at amino acid 1244 (Kowanetz *et al.*, 2004). This indicates that while they are very similar, each synaptojanin isoform has a different physiological function due to their unique binding partners (Rusk *et al.*, 2003).

Both synaptojanin1 and synaptojanin2 are known to hydrolyse some of the phopshoinositides including PtdIns(4,5)P_2 and PtdIns(3,4,5)P_3 and plays a role in the formation of CCPs and later stages of CCV movement (Rusk *et al.*, 2003). Unlike synaptojanin1, synaptojanin2 is thought to play a role in targeting the activated RTK to the forming CCP and in lipid hydrolysis in the earlier stages of endocytosis (Rusk *et al.*, 2003). The theory is that a delicate balance of PtdIns(3,4,5)P_3 and PtdIns(4,5)P_2 is necessary for the formation of CCPs in the appropriate places on the plasma membrane and this balance is maintained by kinases and phosphatases such as PI3K and synaptojanin2 (Rusk *et al.*, 2003). Synaptojanin2 is capable of interacting with endophilin and Ruk_I and it currently seems that at least endophilin is required for the localisation and activation of synaptojanin2 to the developing CCP (Figure 1.3; Schuske *et al.*, 2003). The result of the Ruk_I/synaptojanin2 interaction is unknown other than that synaptojanin2B1 is able to form an inducible link between Ruk_I and RTKs; when synaptojanin2B1 was overexpressed, the amount of Ruk_I found complexed with activated EGFR increased (Kowanetz *et al.*, 2004). When cells expressing both Ruk_I and synaptojanin2B1 were stimulated, the amount of Ruk_I interacting with synaptojanin2B1 also increased (Kowanetz *et al.*, 2004).

Synaptojanin2 interaction with Ruk_I may link the down-regulation of EGFR-stimulated PI3K production of PtdIns(3,4,5)P_3 to the phospholipid's hydrolysis and thus attenuates signal transduction to a greater degree than either protein alone could.

Synaptojanin1 also interacts with dynamin, endophilin and amphiphysin except these interactions are found during the later stages of CCP formation when the narrow "neck" has formed and is crucial to the scission reaction (Schuske *et al.*, 2003). It is thought that the multi-protein complex of synaptojanin1-amphiphysin-dynamin-endophilin provides the necessary lipid modifications and energy required to produce scission of the CCP from the membrane (Hill *et al.*, 2001; Lafer, 2002). Later in the endocytic process, synaptojanin1 plays a crucial role in reducing PtdInsP_2 levels on the CCV that in turn cause a loss of clathrin binding proteins that are localised to the membrane by the presence of PtdInsP_2 (eg: AP2 and Dab2) (Schuske *et al.*, 2003; Verstreken *et al.*, 2003). When the clathrin binding proteins are lost, clathrin becomes dissociated from the membrane and the uncoated vesicle is able to become an early endosome.

1.3.1.10 Intersectin acts similarly to Ruk_I in endocytosis

A protein with analogous function to Ruk_I, intersectin, was isolated in 1998 (Yamabhai *et al.*, 1998). Intersectin has, similar to Ruk_I, been implicated in the regulation of clathrin-mediated endocytosis through its five different SH3 domains that are known to interact with proteins necessary for endocytosis (Yamabhai *et al.*, 1998). Of the five SH3 domains, the two carboxyl terminal SH3 domains of intersectin share over 50% homology with the SH3 domains of Ruk_I placing the two proteins among the most closely related SH3 domain sequences found in public

databases (Kowanetz *et al.*, 2004). This high homology and functional similarity implies cooperation between the Ruk_I and intersectin in the assembly of endocytic proteins around activated RTKs.

1.3.1.11 Overview of Ruk_I action in endocytosis

Ruk_I is known to interact with several different proteins that play key roles in endocytosis such as Cbl and endophilin. It is thought that Dab-2/DOC2 draws the Ruk_I-endophilin complex to the developing CCP where Ruk_I dissociates from Dab-2/DOC2 in order to interact with Cbl (see Figure 1.4). The activated RTK tyrosine phosphorylates Cbl that in turn ubiquintinates the activated RTKs, thus starting the internalisation process. At the developing CCP, Ruk_I also binds to other endocytic proteins such as synaptojanin2, AIP1/Alix, Hip1R and CAPZ. Through these interactions, Ruk_I acts as a scaffolding protein that spatio-temporally coordinates RTK internalisation with the actin rearrangements necessary for the process.

1.3.2 Certain GTPase accessory proteins interact with Ruk_I

GTPases act in a variety of pathways, including endocytosis and FA formation. For a review of GTPase function in FA formation, please see Section 1.3.3. GTPase function is dependent on a wide variety of GTPase accessory proteins, some of which are known to interact with Ruk_I. Therefore, in addition to directly acting in endocytosis as a scaffolding/adaptor protein, Ruk_I is able to influence the endocytic process through interactions with Arf and Rho GTPase accessory proteins (Figure 1.5). Several of these GTPase accessory proteins are also dependent on PI3K activity, thereby providing another mechanism through which

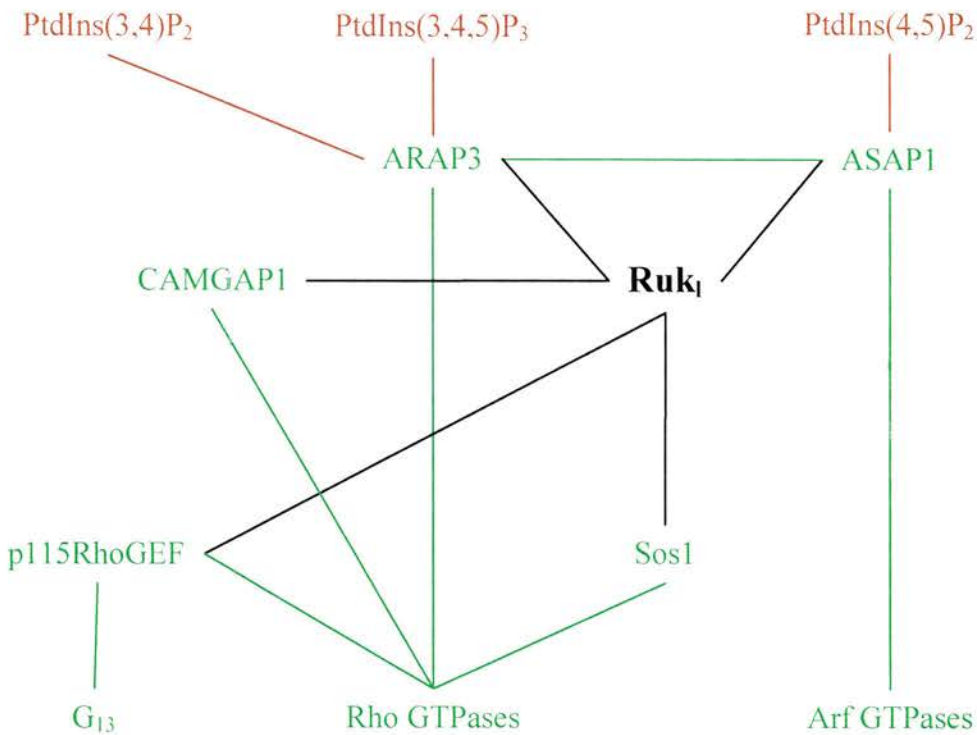

Figure 1.5: The Ruk_I interactors in Arf and Rho GTPases. Ruk_I is known to interact with several Arf and Rho GTPase accessory proteins, and through these interactions Ruk_I may affect endosomal transport and other functions of Arf and Rho GTPases. Ruk_I links together the Arf and Rho GTPases through their respective accessory proteins ARAP3 and ASAP1. The Rho and Arf GTPase pathways are in green, the PtdInsP dependent pathways are in brown and Ruk interactions are in black.

Ruk_I may influence GTPase activity. While it not known what exact effect Ruk_I has on GTPase activity, it can be theorised that Ruk_I bridges the gap between those proteins providing the energy (GTPases), membrane targeting proteins, PtdInsPs (PI3K) and the proteins directly involved in endocytosis (ie: RTKs, Cbl, etc.).

1.3.2.1 Overview of Arf and Rho GTPase accessory proteins

GTPase proteins are in their active form when bound to GTP, and are inactive after hydrolysis occurs and the GTPase is bound to GDP. This change in activity states may be due to conformational changes as some domains of GTPase proteins posses an ability to change their conformation based on the presence of GTP or GDP (Erickson and Cerione, 2004). Two of the GTPase subclasses, Rho and Arf GTPases, utilise several different types of accessory proteins to facilitate their GTPase activity. One type of these GTPase accessory proteins is the guanine nucleotide exchange factors (GEFs) that are postive regulators of GTPase proteins. As the name implies, GEFs recognise the inactive form of GTPase that is bound to GDP and exchange GDP for GTP to activate the GTPase (Erickson and Cerione, 2004). Another type of GTPase accessory protein is the negative regulator that activates GTPase function [GTPase activating proteins (GAPs)] and thus catalyses the formation of GTPase-GDP (Nie *et al.*, 2003).

1.3.2.2 Rho GTPases act in endocytosis

Numerous evidences exist that suggest that GTPases act to spatially coordinate membrane trafficking in response to the extracellular signals and regulate the efficiency of clathrin-dependent endocytosis (Qualmann and Mellor, 2003). RhoA

plays a role in endocytosis as evidenced by a constitutively activated form that is able to block RTK internalization (Lamaze *et al.*, 1996). However, it is unknown how exactly RhoA acts in endocytosis. It may be that RhoA-GDP is necessary to target certain proteins to the forming CCP, much like the Arf1-GDP form is necessary to target specific proteins to invaginating areas of the Golgi apparatus.

The Rho GTPase, Rac, binds directly to synaptojanin2 (see Section 1.3.1.9) and lipid kinases and through these proteins may play a role in maintaining PtdIns levels (Malecz *et al.*, 2000). Whereas synaptojanin2 hydrolyses PtdIns(3,4,5)P_3 to form PtdIns(3,4)P_2, another protein activated by Rac, the type 1 PtdIns(4)P 5-kinases, synthesises PtdIns(4,5)P_2 through phosphorylating PtdIns(4)P (Tolias *et al.*, 1995). As synaptojanin2 is also able to hydrolyse PtdIns(4,5)P_2 to PtdIns(4)P, it is thought that Rac encourages the endocytic cycle by facilitating the turnover of PtdIns(4,5)P_2 throughout the cycle.

One of the Rho GTPases that is essential to many steps of the endocytic process is Cdc42. Early in the endocytic process activated Cdc42 is able to block the internalization of RTKs through its interactions with Cbl (see Section 1.3.1.6; Wu *et al.*, 2003). Another endocytic protein that interacts indirectly with Cdc42 is intersectin, which stimulates the activation of Cdc42 through a Cdc42 specifc GEF (Hussain *et al.*, 2001). Cdc42 activates (N)-WASP (normal Wiskott-Aldrich syndrome protein) and actin assembly through the Arp2/3 complex (actin related protein) providing another link between actin and the endocytic process (Hussain *et al.*, 2001). Possibly, these interactions are key to the transient appearance of actin at the "neck" that provides some of the mechanical force needed for scission and the movement of the CCV away from the cell membrane (Engqvist-Goldstein and

Drubin, 2003). Later in the endocytic process, Cdc42 also affects the sorting of internalized RTKs through its downstream effector the tyrosine kinase ACK (activated Cdc42 kinase), which helps to accelerate the traffic of internalized EGFR to lysosome (Manser *et al.*, 1993; Teo *et al.*, 2001).

Other Rho GTPases involved in endocytosis include RhoD that is co-localised with early endosomes and possibly helps to align the endosomes with actin, thus providing the force necessary for endosomal movement (Murphy *et al.*, 1996). RhoD acts through the sequential activation of Diaphanous and Src; Diaphanous is able to nucleate actin ploymerisation and reorganize microtubles to form a parallel array of actin filaments (Gasman *et al.*, 2003).

Late endosomes/MVBs (multi-vesicular bodies) also co-localise with Cdc42 that theoretically may regulate WASP/Arp2/3-dependent actin remodeling on the surface of the vesicles prior to fusion to the lysosome (Eitzen *et al.*, 2002). As the internalized EGFR enters the late endosomal vesicle, it triggers the activation of another Rho GTPase, RhoB (Gampel and Mellor, 2002). The exact nature of RhoB activity is unknown, but overexpression of activated RhoB impedes the transfer of EGFR from the MVB to the lysosome (Gampel *et al.*, 1999). Since it is hard to see any physiological purpose for blocking receptor transfer in this manner, it is possible that overexpression of RhoB is distorting the normal function of RhoB that is seen at endogenouse RhoB levels (Qualmann and Mellor, 2003).

1.3.2.3 Arf GTPases are involved in vesicular transport

Unlike the Rho GTPases that are known to play a role directly in endocytosis, the Arf GTPases are thought to act in vesicular transport to and from the ER to the

Golgi apparatus (Hinners and Tooze, 2003). These proteins seem to play a role in the recycling of proteins from the Golgi apparatus to the cellular membrane and in actin rearrangements; they may link retro and anterograde vesicular trafficking with the actin cytoskeleton (Hinners and Tooze, 2003). Currently, six Arf GTPases have been identified in mammals and are divided into three classes based on their shared structures: Arf1, -2, and –3 are grouped into Class I, Arf4 and –5 are Class II, and Arf6 is Class III (Nie *et al.*, 2003). Out of these six Arfs, the most extensive work has been done on the functions of Arf1 and Arf6. The molecular importance of the Arf GTPases is highlighted by the fact that they are highly conserved in all eukaryotic genomes so far examined (Nie *et al.*, 2003).

Both Arf1 and 6 are able to interact with the clathrin adaptor proteins AP1 and AP3, and together they produce the coated pits necessary for vesicle formation (Hinners and Tooze, 2003). Arf6 stimulates the activity of PIP 5-kinase which produces PtdIns(4,5)P_2, the lipid that is crucial to protein targeting to the membrane and PI3K function (Brown *et al.*, 2001). Thus, the emerging theme of the Arf family is the regulation of lipid composition; they help to recruit coat proteins and trap cargo or cargo receptors (Nie *et al.*, 2003).

Arf1 has been localized to the Golgi apparatus and helps to form COPI (coat protein I) coats on developing vesicles by drawing and localizing the COPI protein complex to specific sites on the Golgi apparatus (Franco *et al.*, 1998). Through this interaction, Arf1 has been implicated in ER-Golgi and intra-Golgi transport, endosome-endosome fusion and synaptic vesicle formation (Kirchhausen, 2000). In addition to directly interacting with the COPI protein complex to form vesicles, Arf1 has been shown to recruit type I PtdInsP 5-kinase to Golgi membranes which would

lead to an increase in PtdIns(4,5)P_2 levels (Jones *et al.*, 2000). Arf1 can also affect the recruitment of paxillin to focal adhesions that provides a link between vesicular trafficking and the actin cytoskeleton (Norman *et al.*, 1998).

Arf6 is localized to the plasma membrane and is thought to play a key role in endocytosis (D'Souza-Schorey *et al.*, 1995). This protein regulates membrane and protein cycling to and from plasma membranes primarily through its ability to stimulate PtdInsP 5-kinase which produces PtdIns(4,5)P_2 (Brown *et al.*, 2001). The recycling of membranes also influences the actin cytoskeleton that is located along the plasma membrane, as well as regulating the polymerization of cortical actin and cell spreading through its effectors (Randazzo *et al.*, 2000b; Schafer *et al.*, 2000; Brown *et al.*, 2001).

1.3.2.4 Rab GTPases spatial-temporally coordiante endocytosis

In addition to Arf and Rho GTPases, Rab GTPases also play a role in endocytosis. So far, approximately 40 different Rab proteins have been discovered and each is thought to be associated with a specific organelle or pathway (Somsel Rodman and Wandinger-Ness, 2000). Out of the Rabs already functionally characterised, twelve of them are localised to the endocytic pathway; these Rabs are thought to be involved in the spatial-temporal coordination of endocytosis through their function as scaffolding proteins (Somsel Rodman and Wandinger-Ness, 2000). The Rabs involved in endocytosis are known to bind several effectors including cytokeletal components (Somsel Rodman and Wandinger-Ness, 2000).

Among the twelve Rabs involved in endocytosis, Rabs 4, 5, 7 and 11 have been extensively studied. Rabs 4 and 11 are known to be involved in receptor

recycling from endosomes back to the plasma membrane. Rab 4 regulates the relatively fast recycling of early endosomes back to the plasma membrane (van der Sluijs *et al.*, 1991; van der Sluijs *et al.*, 1992), while Rab 11 is involved in a slower membrane recycling process (Sheff *et al.*, 1999). Rab 5 acts later in the endosomal process than Rab 4; Rab 5 is mainly involved in the internalisation of molecules via CCVs and the fusion of early endosomes (Bucci *et al.*, 1992; Gorvel *et al.*, 1991). Rab 7 acts downstream of Rab 5; it regulates the maturation of early to late endosomes (Feng *et al.*, 1995).

While there are no known direct interactions between Ruk_I and the Rabs, it should be noted that the Ruk_I interactors c-Cbl, CD2AP/CMS and PI3K bind to Rab 4 and Rab 5 (Cormont *et al.*, 2003; Chamberlain *et al.*, 2004). CD2AP/CMS acts as a multiprotein adaptor by binding both Cbl and Rab 4 while simultaneously co-localising with Rab 7 (Cormont *et al.*, 2003). The evidence suggests that CD2AP/CMS, through its interactions with Rab 4 and c-Cbl, regulates endosomal morphology and may play a role in trafficking between early and late eondsomes (Cormont *et al.*, 2003). It should be noted that when Ruk_I is overexpressed in Cos7 cells, small vesicular structures develop which co-localise with Rab 7 making it possible that Ruk_I interacts with c-Cbl and Rab 7 in a manner similar to CD2AP/CMS (Dr. E. Borthwick, unpublished observations).

The p85α subunit of PI3K, another Ruk_I interactor, binds to Rab 5 and has recently been discovered to act as a GAP to Rab 5 and 4 and the Rho GTPases Cdc42 and Rac 1 (Chamberlain *et al.*, 2004). PI3K is known to co-localise with Rab 5 and 4 and this lipid kinase is thought to help regulate endocytosis through determining how long the Rabs remain in an active, GTP-bound, state (Chamberlain *et al.*, 2004).

Thus, because of its interaction with p85α, Ruk_I may affect endocytosis through both Rab and Rho GTPases.

1.3.2.5 The role of interaction between ASAP1 and Ruk_I in endocytosis

ASAP1 is a Ruk_I interactor that is a mainly cytosolic protein that is a GAP for Arf1, Arf5 and in a much less detectable manner Arf6 (Brown *et al.*, 1998). The GAP activity of ASAP1 is dependent on the presence of PtdIns(4,5)P_2 (Brown *et al.*, 1998). Src and the focal adhesion kinase Pyk2 both phosphorylate ASAP1 and it is able to interact with FAK (focal adhesion kinases; Kruljac-Letunic *et al.*, 2003). *In vivo*, it is thought that Pyk2 and Src act in concert to phosphorylate ASAP1 which inhibits its Arf GAP ability, but this regulation of ASAP1 activity could also be achieved through fluctuations in the levels of PtdIns(4,5)P_2 (Kruljac-Letunic *et al.*, 2003). By binding Ruk_I through its proline-rich domain and interacting primarily with the first proline-rich region of Pyk2, ASAP1 could be a part of one or several multi-protein complexes that link membrane trafficking and cytoskeletal changes during cell movement (Randazzo *et al.*, 2000a; Kruljac-Letunic *et al.*, 2003). The theory that there are multi-protein complexes based around or containing ASAP1 is supported by the observations that ASAP1 is able to homodimerise, allowing a greater number of protein interactions than a single protein (Brown *et al.*, 1998).

ASAP1 is another protein that binds with a higher affinity to all three Ruk_I SH3 domains than to any single or pairing of the domains, and the binding motif (PVPLPR) begins at amino acid 1036 (Kowanetz *et al.*, 2004). Overexpressed ASAP1 increases the rate of EGFR recycling in a manner dependent on both an intact Ruk_I binding site and an Arf GTPase ability, thus indicating that interactions

with both proteins are necessary for the role of ASAP1 in RTK recycling (Kowanetz *et al.*, 2004). The overexpression of ASAP1 with Ruk_I showed that ASAP1 had a lessened localisation to focal adhesions with both ASAP1 and Ruk_I co-localised to vesicular structures (Kowanetz *et al.*, 2004). This phenomenon may possibly be due to the competition of Ruk_I with Pyk2 and FAK for binding to ASAP1. The binding between overexpressed Ruk_I and ASAP1 may prevent Pyk2 from phosphorylating ASAP1 and thereby constitutively links the endocytic machinery with the Arf GTPase family (Figure 1.5).

1.3.2.6 The role of interaction between ARAP3 and Ruk_I in endocytosis

ARAP3 is a PI3K effector and a Ruk_I interactor that is known to act as a GAP of both Arf and Rho GTPases. ARAP3 may link the endocytic functions of Arf6 and Rac (Santy and Casanova, 2002). Krugmann *et al.* (2002) showed that ARAP3 is highly dependent on an interaction with PtdIns(3,4,5)P_3 to act as a specific GAP for Arf6, but also functions to a lesser extent when interacting with PtdIns(3,4)P_2. ARAP3 translocates to the plasma membrane by binding PtdIns(3,4,5)P_3 and through this interaction, connects the PI3K pathway with various functions of Arf6 including cell ruffling and movement (Krugmann *et al.*, 2002). Unlike ARAP3's Arf GAP function, its Rho GAP function is independent of PtdIns in any form and is thus a constitutive function of the protein (Santy and Casanova, 2002). Taken together, the evidence points to ARAP3 transiently linking Rac and Arf6 activity depending on the availability of PtdIns(3,4,5)P_3.

The SH3A and SH3B domains of Ruk_I bind to ARAP3 at three sites: PVPKPR (amino acid 94), PEPSPR (amino acid 129) and PPQPPR (amino acid 389)

(Kowanetz *et al.*, 2004). ARAP3 and ASAP1 are only found in a complex when they are both bound to Ruk_I, and this complex allows Ruk_I to influence and coordinate the functions of Rho GTPases, Arf GTPases and endosomal machinery (Kowanetz *et al.*, 2004). However, the exact result of Ruk_I interacting with ARAP3 is unknown. Possibly, the Ruk_I interaction with ARAP3 serves to link the endocytic machinery, actin polymerisation and PI3K inhibition with Rac and Arf6 actions.

1.3.2.7 CAMGAP1 interacts with Ruk_I

Recently, it was discovered that Ruk_I interacts with and stimulates a novel RhoGAP called CAMGAP1 (CIN85 associated multi-domain containing RhoGAP 1) (Sakakibara *et al.*, 2004). This new RhoGAP acts specifically towards Rac1 and Cdc42 (Figure 1.5), both of which are thought to play roles in endosomal protein sorting. The CAMGAP1 interactors point to a role for CAMGAP1 in endocytosis and vesicular transport possibly in concert with Ruk_I actions (Sakakibara *et al.*, 2004). However, since this protein was only recently discovered, it is not known what exact role CAMGAP1 plays or even what pathways CAMGAP1 plays a role in.

The CAMGAP1 PRD between amino acids 452 to 475 has been shown to interact with the Ruk_I SH3B domain only (Sakakibara *et al.*, 2004). It is conceivable that $Ruk_{\Delta A}$ is also able to interact with this protein because $Ruk_{\Delta A}$ has the SH3B domain in common with Ruk_I. Due to the unknown nature of Ruk_I influence on CAMGAP1, it cannot be said if the proposed $Ruk_{\Delta A}$ interaction is dominant negative or results in a completely unique downstream reaction.

1.3.2.8 p115 RhoGEF interacts with Ruk_I

p115 RhoGEF binds to Ruk_I and has been identified as a GAP for the G_{12}

family of G proteins while also acting as a GEF for a Rho GTPase (Hart *et al.*, 1998; Figure 1.5). However, while it catalyses the GTPase activity of both G_{12} and G_{13}, only the association with the activated α subunit of G_{13} stimulated p115 RhoGEF's Rho GEF activity (Hart *et al.*, 1998). The theory behind the selective nature of the GEF activity of p115 RhoGEF is that the $G\alpha_{13}$ not only binds to its primary G protein binding domain, it also interacts with a second domain that somehow creates an active configuration for p115's Rho GEF ability (Wells *et al.*, 2002). According to this theory, the binding of $G\alpha_{12}$ to the primary binding site of p115 RhoGEF does not induce the same binding to the secondary site and thus does not increase its GEF activity (Wells *et al.*, 2002). The GEF ability of p115 RhoGEF is specific to the RhoA GTPase, therefore p115 RhoGEF provides an inducible link between the G_{13} functions (eg: cellular motility and secretory pathways) and RhoA functions (eg: early endocytosis) (Hart *et al.*, 1998; Neves *et al.*, 2002).

Most of the Rho GEFs with similar structure (the RGL-containing RhoGEFs) to p115 RhoGEF have been found to heterodimerise with each other, but uniquely, p115 RhoGEF is only able to form homodimers (Chikumi *et al.*, 2004). Theoretically, this dimerisation may form an inhibitory mechanism on p115 RhoGEF action as the interaction can close the protein off from further interactions (Chikumi *et al.*, 2004). Together with the ability of p115 RhoGEF to bind to Ruk_I, this points to the possibility of several multi-protein complexes that are able to bridge the many different pathways that both proteins are involved. SH3A and SH3C of Ruk_I bind to p115 RhoGEF at amino acid 771, at the Ruk_I binding motif PKPRPR (Kowanetz *et al.*, 2004). The exact physiological result of Ruk_I binding to p115 RhoGEF is unknown. In one scenario, Ruk_I may competitively inhibit the p115 RhoGEF Rho

GEF ability, thereby keeping RhoA inactive and bound to GDP. In this manner, RhoA-GDP may target specific proteins to the forming CCP. Alternatively, Ruk_I may constitutively activate the Rho GEF ability and prevent RhoA-GDP from targeting specific proteins to the CCP.

1.3.2.9 Sos1 interacts with Ruk_I

Sos1 (Son of Sevenless) is a GEF of Ras or Rac, depending on what protein is binding its C terminal PRD; the Sos1 PRD contains several SH3 binding motifs including a binding motif for Ruk_I (Figure 1.5; Nimnual and Bar-Sagi, 2002). The binding partners that determine the GEF activity of Sos1 competitively bind to the same motifs, thereby controlling the downstream effects of RTK signalling (Innocenti *et al.*, 2002). For instance, the Sos1-Grb2 complex that determines a Ras specific GEF activity is disrupted by RTK activation that phosphorylates Sos1, preventing it from interacting with Grb2. This forms a transient activation of Ras pathways through the GEF activity of Sos1 (Innocenti *et al.*, 2002). On the other hand, the Sos1-E3b1-Eps8 complex is longer lived and its Rac GEF ability and downstream signals are sustained throughout growth factor stimulation (Innocenti *et al.*, 2002). This complex has recently been shown to include the p85 subunit of PI3K (Innocenti *et al.*, 2003). Sos1 also preferentially binds the PI3K product PtdIns(3,4,5)P_3, thus allowing PI3K two mechanisms to induce Sos1's Rac GEF activity (Innocenti *et al.*, 2003). The tyrosine phosphorylation of Sos1 by Abl has been shown as necessary to stimulate its Rac GEF activity and may favour generation of the multi-protein complex that is also necessary for the Rac GEF activity of Sos1 (Sini *et al.*, 2004). Through Sos1, the activities of Ras and Rac-GEF

complexes are spatio-temporally coordinated to the necessary areas for maximum benefit to the cell (Scita *et al.*, 2001; Innocenti *et al.*, 2003). This is seen in the ability of Eps8 to bind Rac GEF activating multi-protein complexes and Sos-1 while also binding F-actin, which directs the Rac GEF to the sites where Rac mediated actin remodelling is necessary (Scita *et al.*, 2001; Innocenti *et al.*, 2003).

Sos1 activation may also be regulated by an intramolecular interaction. Research on hSos1 has shown that a small region upstream of the DH (Dbl homology) domain interacts with the PH (Pleckstrin homology) domain of hSos1 and 'closes' the protein to lower affinity interactions when in unstimulated circumstances (Jorge *et al.*, 2002). Growth factor stimulation causes a disruption of this intramolecular interaction, possibly through tyrosine phosphorylation or binding to PtdIns(3,4,5)P_3, and allows other proteins to interact with hSos1 to induce Ras or Rac GEF activity (Jorge *et al.*, 2002).

While it is known that Sos1 binds to Ruk$_I$, it is currently unknown how or what the results of this interaction are (Watanabe *et al.*, 2000). Due to a PRD being found in Sos1, it can be assumed that the interaction is governed by one or more of the Ruk$_I$ SH3 domains but no in depth research has been done on the binding to confirm this. Possibly, the Ruk$_I$ interaction serves to link the Rac or Ras GEF activity to the other pathways in which Ruk$_I$ plays a role.

1.3.2.10 Overview of GTPase accessory protein interaction with Ruk$_I$

While playing a direct role in RTK internalization, Ruk$_I$ also influences the process through its interaction with GTPase accessory proteins. Several Rho GTPases play a direct role in endocytosis by binding to endocytic proteins, and Arf

GTPases provide the energy necessary for CCV movement. Finally, Rab GTPases are known to spatio-temporally coordinate endocytosis. While Ruk_I directly interacts with Rho and Arf GTPase accessory proteins, there is no evidence of Ruk_I interacting with Rab GTPases. However, Ruk_I is known to co-localise with Rab7 in vesicular-like structures. The exact action of Ruk_I in the context of GTPase accessory proteins is unknown, but it may serve as a scaffolding protein that links together pathways as diverse as PI3K activity, endocytosis and GTPase activity.

1.3.3 Ruk_I has role in focal adhesions

In addition to acting in receptor endocytosis, certain GTPases such as Rho GTPases act in FA (focal adhesion) formation (Sastry and Burridge, 2000). Through several interactors, Ruk_I plays a role in FA pathways and may provide a similar scaffolding function to that it plays in RTK endocytosis (Figure 1.6). ASAP1, the known Ruk_I interactor, also co-localises to FAs, and may provide a link between the Arf GTPases and FAs. Arf GTPases have been implicated in targeting FA proteins to and from the FAs via the vesicle trafficking pathway (reviewed in Sastry and Burridge, 2000). Furthermore, Ruk_I interacts with the key FA components $p130^{Cas}$, Crk I and Crk II (Watanabe *et al.*, 2000).

1.3.3.1 Focal adhesions

FAs are large multi-protein complexes where integrin receptors link the actin cytoskeleton within the cell to the ECM (extra-cellular matrix). They serve at least two known functions: to transmit force/tension at adhesion sites to maintain strong attachments to the ECM and to act as signalling centers that integrate many intracellular pathways; this allows FAs to function in cell migration, proliferation

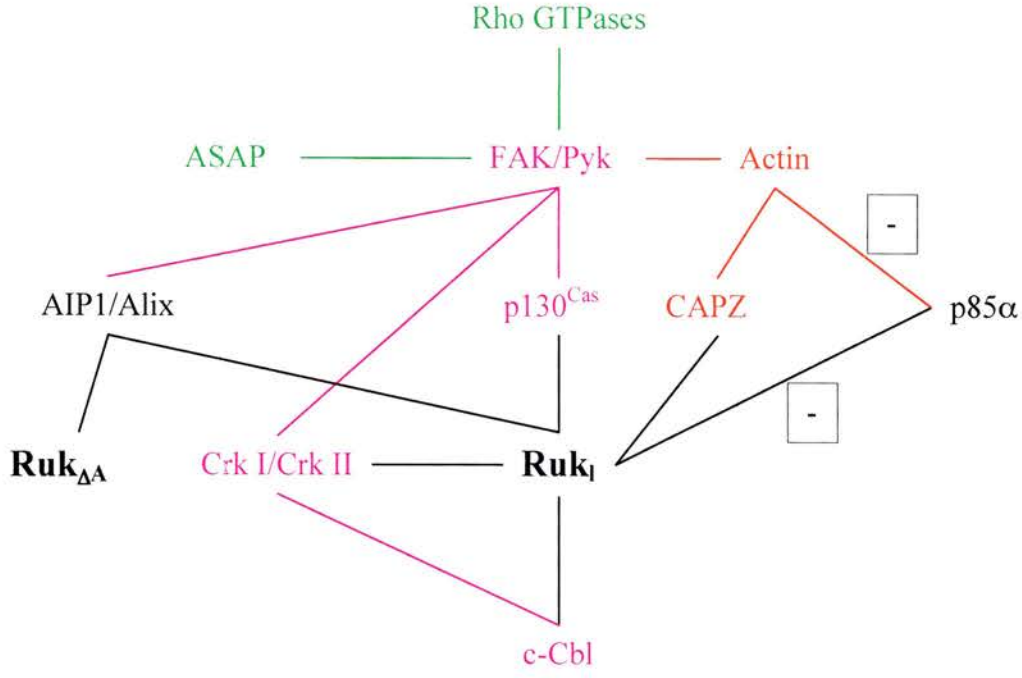

Figure 1.6: The interactions of Ruk_I in focal adhesions. Ruk_I and $Ruk_{\Delta A}$ both play a role in FA formation and possibly link their formation to other processes such as cellular growth and division. The FA related proteins are shown in magenta, and the actin related proteins are in red. The Ruk isoforms and p85α proteins are in black.

and embryogenesis (Petit and Thiery, 2000; Sastry and Burridge, 2000). FAK and Src kinase both localize to FAs and play key roles in almost all its functions (Parsons, 2003). Src kinase has an ability to regulate FAK tyrosine phosphorylation and function, while FAK acts as a point of convergance for multiple signalling pathways (Parsons, 2003).

The activation of RhoA is a key step in the initialization of FA formation through its ability to stimulate actin-myosin contractility via a kinase cascade (Sastry and Burridge, 2000). It should be noted that the Ruk_I interactor p115RhoGEF is a RhoA specific GEF that possibly links Ruk_I with the formation of FAs and other interactors may also link Ruk_I to the composition of FAs. The FA is a dynamic structure as it assembles and disperses as necessary when cells migrate or enter mitosis (Sastry and Burridge, 2000). The transience of FAs requires a close coordination of Rho GTPases, G-protein-coupled receptors, receptor tyrosine kinases, microtubules and actin.

1.3.3.2 The role of interaction between $p130^{Cas}$ and Ruk_I in FAs

One of the FA proteins that Ruk_I binds to is $p130^{Cas}$. $p130^{Cas}$ is a scaffolding/adaptor protein that was originally identified as an interactor with Crk and Src proteins (Bouton *et al.*, 2001). $p130^{Cas}$ helps to maintain the signalling equilibrium between actin cytoskeleton organization, cell migration and Src transformation by using its domains in differential and cooperative ways (Bouton *et al.*, 2001; Huang *et al.*, 2002). However, the regulation and function of many of the $p130^{Cas}$ protein complexes remain unknown (Bouton *et al.*, 2001). It has been recently hypothesized that $p130^{Cas}$ activity opposes that of another key FA

scaffolding/adaptor protein, paxillin, and together they regulate cell morphology and motlity (Feller, 2001).

What is known is that $p130^{Cas}$ is phosphorylated by FAK, which causes it to translocate to FAs (Polte and Hanks, 1995; Harte *et al.*, 1996). In fact, the role played by $p130^{Cas}$ is essential to the function of FAK, as mutants that lack the binding motif for $p130^{Cas}$ show compromised signalling to the downstream FAK effectors that influence the assembly or breakdown of FAs at the leading edges of migrating cells (Parsons, 2003). $p130^{Cas}$ is also thought to play an essential role in cytoskeletal regulation because $p130^{Cas}$ null cells contain short, disorganized actin filaments (Bouton *et al.*, 2001). However, while it is a key component in FA function, it is not essential for FA formation as non-functional FAs are able to form without $p130^{Cas}$ (Bouton *et al.*, 2001).

Both the SH2 and SH3 domains of Src associate with the C-terminal region of $p130^{Cas}$ in a complex manner (Nakamoto *et al.*, 1996). Upon the initial binding between the SH3 of Src and the $p130^{Cas}$ C terminus, the kinase phosphorylates a tyrosine within the $p130^{Cas}$ C-terminus which opens both proteins to further binding between Src's SH2 domain and the $p130^{Cas}$ C terminus (Nakamoto *et al.*, 1996). Recent work shows that $p130^{Cas}$ can activate Src because $p130^{Cas}$ binding interfers with autoinhibitory intramolecular interactions and stabilizes Src into an active conformation (Burnham *et al.*, 2000). This gives $p130^{Cas}$ the dual functions of being a substrate and activator of Src. The other effect of tyrosine phosphorylation of $p130^{Cas}$ by Src is that it allows $p130^{Cas}$ to interact with the Crk proteins, which is an essential signal for the formation of pseudopodia and cell migration through the relocation and activation of Rac GTPase (Cho and Klemke, 2002).

Proteins associated with the FA are able to transmit growth and survival signals from the ECM and therefore are able to play a role in cell cycle progression and proliferation. Through its interactions with FAK, Src and the Crks, $p130^{Cas}$ probably plays a key role in this signal transmission. Several studies point to the necessity of the $p130^{Cas}$-FAK and $p130^{Cas}$-Src interactions in cell proliferation (Bouton *et al.*, 2001).

CD2AP/CMS and $p130^{Cas}$ interact via the CD2AP/CMS PRD and $p130^{Cas}$ SH3 domain. Therefore the structural similarities between CD2AP/CMS and Ruk_I indicate that Ruk_I and $p130^{Cas}$ may interact in the same way (Figure 1.6; Bouton *et al.*, 2001). However, an alternative mechanism for Ruk_I interaction would be between the Ruk_I SH3 domains and the PRD of $p130^{Cas}$. It is currently unknown which of these is the precise method of interaction and what the physiological result of such an interaction is. However, it should be noted that recent work has shown that the interaction between CMS and $p130^{Cas}$ is stronger than that between Ruk_I and CMS indicating that Ruk_I competes for binding with CMS. In this manner, Ruk_I may subtly attenuate CMS binding and its effects on $p130^{Cas}$ based signalling (Tibaldi and Reinherz, 2003).

1.3.3.3 The role of interaction between Crk I and Crk II and Ruk_I in FAs

Crk I and Crk II, collectively called Crk, bind to Ruk_I and are known as adaptor proteins with functions in cell migration and actin remodeling. They are also thought to exert specific functions in the assembly, disassembly and regeneration of the FAs that generate the mechanochemical force required for changing cell shapes (Klemke *et al.*, 1998; Cho and Klemke, 2000). Crk proteins also play essential roles

in T and B cell activation pathways (see Sections 1.3.5 and 1.3.6). Also found in this family is the CRKL (Crk like) protein that has a significant similarity to the Crks and thus is able to interact with some of the same proteins as Crk I and II (Feller, 2001). CRKL is not known to directly bind Ruk_I but does bind with some Ruk_I interactors such as SHIP1 and PI3K (Sattler *et al.*, 2001).

Crk II is more abundant than Crk I in almost all cell types analysed but their basic domain structure is very similar, both proteins contain SH3 and SH2 domains (Matsuda *et al.*, 1992). Crk I has a single SH3 domain (SH3(1)) while Crk II has two (SH3(1) and SH3(2)) with a 50 aa spacer region between them (Matsuda *et al.*, 1992). As of yet, no specific SH3(2) binding has been found and all of the binding observed has been via the SH3(1) or the Crk SH2 domains (Feller, 2001).

The functions of Crk II are most likely negatively regulated by tyrosine phosphorylation by Abl at amino acid 221, a tyrosine residue is lacking in CrkI, which is therefore not regulated in this manner (Feller *et al.*, 1994; Escalante *et al.*, 2000). It is thought that tyrosine phosphorylation at amino acid 221 might cause an intramolecular interaction between the SH2 domain and the motif surrounding amino acid 221 that impedes the SH3(1) domain from interacting with its binding partners (Feller *et al.*, 1994). This hypothesis was supported by the finding that PTP1B is able to dephosphorylate amino acid 221 leading to the activation of Crk II (Takino *et al.*, 2003). With the discovery of both the kinase (Abl) and phosphatase (PTP1B) that regulate CrkII activity, it becomes theoretically possible that the changing tyrosine phosphorylation state of Crk II can partially account for rapid and dynamic cytoskeletal reorganization following growth factor stimulation (Escalante *et al.*, 2000).

Further down the C-terminus of Crk II, in the linker region between the SH3 domains that is not contained in Crk I, are several regulatory elements that govern Crk II's ability to bind Abl and FAK. Deletion mutants for the C-terminal region have shown increased phosphorylation of $p130^{Cas}$ and FAK that leads to their hyper-activation and increased numbers of FAs (Zvara *et al.*, 2001). Since both Crk proteins interact with the almost the same proteins, it may be that this region unique to Crk II acts to regulate both Crk I and Crk II based protein interactions (Zvara *et al.*, 2001). This mechanism of regulation may be used to attenuate the strength of the signals that converge on the FAs.

From the lack of a PRD in the Crk proteins and the observation that both Crk proteins bind to Ruk_I, it can be assumed that the SH3(1) domain binds to the PRD of Ruk_I. The nature of this interaction also makes it possible that more than just the Ruk_I isoform binds to the Crks. However, similar to other Ruk_I interactors, it is currently unknown how exactly the proteins interact or what the result of such an interaction is. Phosphorylated Cbl is also known to interact with Crk proteins following certain stimulations in certain cell types (eg: T and B cell activation, Epo stimulation); Ruk_I may play a role in these protein complexes, but the exact function of Cbl-Crk complexes is currently unknown (Feller, 2001). Recent work points to a possible role of the Crk and its binding partners in growth factor responses because Cbl and Crk are recruited to lipid rafts in neurites and growth factor stimulation leads to the formation of lamellipodia in a Crk dependent manner (Haglund *et al.*, 2004). The indications are that the Crk is an effector of c-Cbl that leads to actin reorganization.

Yet another way in which Ruk_I influences Crk activity, is through their common binding partner PI3K. The PRD of the p85α and β subunits of PI3K contain binding motifs for Crk SH3(1) but there are only a few reports of a stable interaction between the two proteins (Fukui *et al.*, 1998; Feller, 2001). Recent findings show that active Crk is able to stimulate PI3K function along the PKB/Akt pathway (Akagai *et al.*, 2000). It is unknown whether Ruk_I binding to any of the proteins involved in this complex inhibits or encourages these interactions (Figure 1.6).

1.3.3.4 AIP1/Alix draws Ruk_I to FAs

It is thought that another way for Ruk_I to co-localise with FAs is through interaction with AIP1/Alix, a protein involved in both endocytic and apoptotic pathways. Recent work shows that AIP1/Alix staining coincides with cytoskeletal proteins and that small amounts of Ruk_I and large amounts of AIP1/Alix can be found in FAK or PYK-2 immunoprecipitates (Figure 1.6; Schmidt *et al.*, 2003a). The amount of AIP/Alix co-immunoprecipitated by PYK-2 is increased with increased expression of Ruk_I, possibly through the association of Ruk_I with other binding partners in the FAs such as $p130^{Cas}$ or Crk (Schmidt *et al.*, 2003a). While Ruk_I is able to bind to FA proteins when present, it cannot intrinsically localise to FAs and AIP1/Alix is needed to translocate it to FAs in order for Ruk_I to interact with FA associated proteins (Schmidt *et al.*, 2003a).

Recent work has shown that Ruk_I enhances cellular adhesion, while AIP1/Alix is able to reduce the level of focal adhesion kinase phosphorylation levels to antagonise cellular adhesion (Schmidt *et al.*, 2003a). Interestingly, the pro-

adhesive effects of Ruk_I are abolished when it is no longer able to bind AIP1/Alix, indicating that the pro-adhesive effects may be a result of the Ruk_I-AIP1/Alix binding (Schmidt *et al.*, 2003a). Thus, Ruk_I may be a negative regulator of AIP1/Alix actions, although the pro-adhesive effects may also be due to other interactions.

Another interesting phenomenon is that AIP1/Alix binds to PYK-2 in a Ca^{2+} dependent manner, evidenced by increased Ca^{2+} levels leading to a greater amount of AIP1/Alix being associated with PYK-2 (Schmidt *et al.*, 2003a). Possibly, this is a negative feedback mechanism for FAs to detach from the ECM when Ca^{2+} levels reach high enough to begin the Ca^{2+} dependent apoptotic pathways. Ruk_I may be involved in this negative regulatory mechanism by linking different pathways such as PLC-γ Ca^{2+} influx to AIP1/Alix dependent apoptosis.

1.3.3.5 p85α acts in FAs

Ruk_I was identified as a PI3K negative regulator through its interaction with p85α. However, recent work has shown that p85α acts independently of PI3K to downregulate the formation of stress fibers and FAs (Section 1.4.3.4; Jimenez *et al.*, 2000). It has been found that PDGFR stimulation activates the Cdc42 pathways and subsequently p85α, which in turn causes a decrease in the amounts of stress fibers and FAs (Jimenez *et al.*, 2000). While the exact mechanism of p85α action is unknown, it is thought that the interaction between p85α and Cdc42 protects the RhoGTPase and conserves it in its GTP bound form that prevents it from causing actin rearrangements.

p85α and Ruk_I interact with one another with Ruk_I inhibiting PI3K activity

(Section 1.3.4), and therefore it is not inconceivable that Ruk_I also plays a role in the down-regulation of FA formation via its interaction with p85α (Gout *et al.*, 2000). The pro-adhesive effect of the over-expression of Ruk_I, as discussed above, may be partially due to its inhibition of the interaction between p85α and Cdc42.

1.3.3.6 Overview of Ruk_I action in FAs

While Ruk_I is not intrinsically drawn to FAs, it does interact with several key components of FA formation and function such as $p130^{Cas}$, Crk, AIP1/Alix and p85α. Additionally, Ruk_I influences FAs through its interaction with GTPase accessory proteins as discussed in Section 1.3.2. The ability of Ruk_I to form multi-protein complexes may provide a link between FA formation/function to other pathways such as PI3K activation and RTK endocytosis to coordinate the pathways according to the cellular needs.

1.3.4 Ruk_I negatively regulates PI3K activity

1.3.4.1 PI3K overview

While the PI3K family of lipid kinases is composed of several different classes based on their substrate specificity and activators, Ruk_I has been shown to interact specifically with Class I_A PI3Ks through their p85α regulatory subunit (Gout *et al.*, 2000). Each PI3K of this class is composed of a heterodimer of a p110 catalytic subunit (α, β or δ) and an adaptor subunit (p85α, p85β, p55α or p50α; collectively called p85) that binds to and regulates the activity of the p110 subunit (Fruman *et al.*, 1998; Wymann and Pirola, 1998). Class I_A PI3Ks phosphorylate PtdIns at the 3' position producing PtdIns(3)P, PtdIns(3,4)P_2 and PtdIns(3,4,5)P_3,

with a marked *in vivo* preference for the PtdIns(4,5)P_2 substrate used to produce PtdIns(3,4,5)P_3 (Fruman *et al.*, 1998; Wymann and Pirola, 1998).

The PI3K hetereodimer is translocated to the plasma membrane and activated through the p85 mediated interactions: the SH2 domain binds directly to RTKs, PRD containing proteins are bound through its SH3 domain (ie: Cbl, Ruk_1) and the PRD binds to proteins with SH3 domains (ie: Grb2, Src, Abl) (Fruman *et al.*, 1998; Wymann and Pirola, 1998). p85 is also capable of interacting with PtdIns(3,4,5)P_3 and PtdIns(4,5)P_2 in competition with IRS-1 and other PtdIns interactors (Rameh *et al.*, 1995). This PtdIns binding serves as an inherent negative feedback mechanism to PI3K activity; the p85 subunit binds to the increasing numbers of PtdIns(3,4,5)P_3 thereby preventing PI3K from binding to and phosphorylating PtdIns(4,5)P_2.

Of course, the p85 subunit is a key regulator of PI3K ability, although not in the traditionally accepted manner of conformational changes. Instead of inducing the p110 subunit to change into an active conformation, p85 subunit binding may serve to stabilise the existing conformation of p110 (Yu *et al.*, 1998). In concurrence with this hypothesis, it has been shown that the p110α subunit is thermally unstable at 37° but when bound to the p85 subunit the PI3K holoenzyme maintains its kinase activity (Yu *et al.*, 1998). It has also been discovered that each isoform of p85 has a specific response to different growth factor stimulation, some isoforms bind certain RTKs better than others (Inukai *et al.*, 2001). This and other research has indicated that appropriate PI3K signalling is maintained by a precise balance of regulatory subunits (Inukai *et al.*, 2001; Ueki *et al.*, 2002).

1.3.4.2 PtdIns(3,4,5)P_3 dependent pathways

The PtdIns phospholipids play important roles in many signalling pathways. As they are bound to the plasma membrane, they mainly serve to localise proteins to the plasma membrane in order to bring them into closer proximity to their upstream effectors and downstream substrates.

One of the main effects of PtdIns(3,4,5)P_3 production is the activation of Akt/PKB and its downstream effects (Kandel and Hay, 1999). Akt/PKB (protein kinase B) is translocated to the plasma membrane through its binding to PtdIns(3,4,5)P_3 but it is not activated by this binding (Frech *et al.*, 1997). Instead, another PtdIns(3,4,5)P_3 binding protein, PDK1 (phosphoinositide dependent kinase), is necessary for the phosphorylation and activation of Akt/PKB (Currie *et al.*, 1999). PtdIns(3,4,5)P_3 binding is unnecessary for PDK1 activation, showing that the function of the lipid is to bring together the kinase and its substrate in order for the enzymatic reaction to occur. There are multiple downstream effects of Akt/PKB including insulin signal transduction, cell survival through BAD (Bcl2-antagonist of cell death) and transcription through the Forkheads (Vanhaesebroeck and Waterfield, 1999; Cantley, 2002). Activation of this pathway has also been shown to move the cell into the cell cycle and increase protein synthesis, both of which control cell size (Cantley, 2002).

PtdIns(3,4,5)P_3 binding also stimulates Rho and Arf GEFs (see Section 1.3.2). All Rho specific GEFs contain PH domains specific for PtdIns(3,4,5)P_3, while only a subset of Arf GEFs that are insensitive to the drug brefeldin A bind to PtdIns(3,4,5)P_3 (Vanhaesebroeck and Waterfield, 1999). Another mechanism linking Rho and Arf GTPases with PtdIns(3,4,5)P_3 is through the PH domain of certain

GAPs, such as the centaurins, $GAP1^{m}$ and $GAP1^{IP4BP}$ that bind to PtdIns(3,4,5)P_3 with high specificity (Leevers *et al.*, 1999; Vanhaesebroeck and Waterfield, 1999). These interactions implicate PtdIns(3,4,5)P_3 and PI3K in cytoskeletal reorganisations and vesicular trafficking (see 1.3.1). PtdIns(3,4,5)P_3, via RhoGTPases, has recently been implicated in the induction of localised actin polmerisation in response to growth factor stimulation (Insall and Weiner, 2001; Hilpela *et al.*, 2004).

Another major effector of PI3K is the Tec family of tyrosine kinases that plays a role in both B and T cell activation and signal transduction. For a more comprehensive overview of PI3K in B and T cells (see Sections 1.3.5 and 1.3.6).

PI3K is also known as an effector in cellular response to insulin stimulation. The insulin bound form of the insulin receptor tyrosine kinase phosphorylates the IRS-1 protein, which enables it to interact with and activate PI3K (Inukai *et al.*, 1997). In turn, the proteins (such as PKB) that are activated via PI3K production of PtdIns(3,4,5)P_3 generate the cellular signals for the metabolism of glucose including glucose transport, the suppression of gluconeogenesis the inhibition of lipolysis and the stimulation of glycogen synthesis (Alessi and Downes, 1998; Khan and Pessin, 2002). All of the PI3K regulatory subunits are bind to IRS-1 but it seems that the p50α subunit has the highest affinity for the protein (Inukai *et al.*, 1997). However, mice deficient in the p85α subunit but expressing p50α have a higher sensitivity to insulin and are hypoglycaemic, indicating that p85α also plays key a role in the response to insulin (Teruchi *et al.*, 1999).

1.3.4.3 p85α acts independently of p110

A recent study showed that the amount of p85α found in cells is much higher

than that of p110, meaning there is a naturally occurring imbalance of the two subunits (Ueki *et al.*, 2002). This pool of unbound p85α is thought to exist mainly as a dimer, a form that inhibits p85α SH3 domain interactions; the phosphorylation of p85α releases the inherent intermolecular inhibition of the dimer (Harpur *et al.*, 1999). Therefore, it is possible for the p85α subunits to act independently of the PI3K heterodimer. Research now shows that p85α fucntions in actin cytoskeletal rearrangements, especially in the down regulation of stress fiber formation (Jimenez *et al.*, 2000). PDGFR stimulation is now known to activate the Cdc42 pathway via the p85α subunit and cause a decrease in stress fibers and FAs (Jimenez *et al.*, 2000). The hypothesis is that the interaction between p85α and Cdc42 protects the RhoGTPase from GAP activity and maintains it in its GTP bound active state that inhibits actin cytoskeletal rearrangements, as detailed above in 1.3.3.5 (Okkenhaug and Vanhaesebroeck, 2001).

Another independent role for p85α is as a putative oncogene (Jimenez *et al.*, 2000). Confirming this possibility, p85α has been shown to act in p53-mediated apoptosis as a signal transducer in cellular responses to oxidative stress (Yin *et al.*, 1998). It is thought that p85α acts downstream of p53, without any noticeable effect on the lipid kinase activity of PI3K (Yin *et al.*, 1998). While these PI3K independent pathways are important, it is clear that the greatest physiological effect of the p85α protein is as the regulatory subunit of PI3K.

1.3.4.4 Ruk$_I$ inhibits PI3K function through an interaction with p85α

Previously the only known manner of negatively regulating PI3K activity was

through proteins that remove phosphates from the PtdIns produced by PI3K. Among these lipid phosphatases are PTEN that removes the 3' phosphate and SHIP1 that removes the 5' phosphate (see Section 1.3.5.6). Thus until the discovery of Ruk_I, there were no known specific p85α inhibitors, but it is now known that Ruk_I directly binds to p85α and inhibits the lipid kinase ability of the p110 subunit (Gout *et al.*, 2000). This interaction is thought to cause a conformational shift in the p85α protein that disables its binding ability to the p110 protein, and thereby compromises PI3K lipid kinase activity (Gout *et al.*, 2000).

Previous research has shown that post-natal sympathetic and sensory neurons over-expressing Ruk_I have an increased rate of apoptosis that can be blocked through the PI3K inhibitors and the co-injection of some of the smaller Ruk isoforms (Gout *et al.*, 2000). For instance, Ruk_m has no effect by itself but when co-injected with Ruk_I lead to a decrease of Ruk_I-induced apoptosis; the same result was seen when Ruk_I was co-injected with Akt or constitutively activated PI3K (Gout *et al.*, 2000). A possible interpretation of these results is that the dimerisation of different isoforms of Ruk somehow prevents Ruk_I from interacting with p85α, possibly through the folding of the heterodimer into a non-active configuration.

Recently, Ueki *et al.* (2002) proposed that PtdIns(3,4,5)P_3 levels are regulated by a p85α binding partner that also increases the activity of SHIP1 or PTEN. Could this unknown binding partner be Ruk_I? After all, Ruk_I has been shown to bind to both p85α and SHIP1, and Ruk_I does inhibit PI3K lipid kinase activity (Figure 1.7). If the binding of Ruk_I to p85α was necessary for Ruk_I's ability to bind and activate SHIP1, it would explain why PtdIns(3,4,5)P_3 levels are actually increased in mice

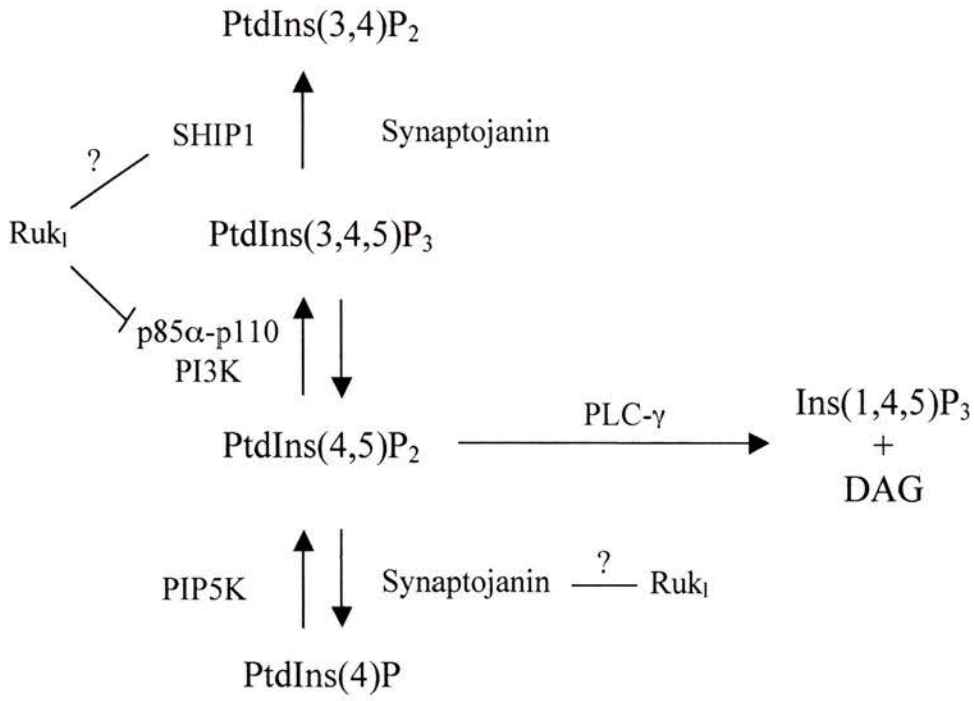

Figure 1.7: The cycling between different forms of PtdIns and the kinases and phosphatases involved in the cycling. Ruk isoforms may be essential to this cycling through their inhibition of PI3K and may link PI3K to PlC-γ2 and SHIP1 functions to produce a subtler attenuation of PI3K functions.

heterozygous for the p85α gene null mutation (Ueki *et al.*, 2002). In mice heterozygous for the null mutation, the amount of p85α available for association with Ruk_I would naturally be decreased leading to the removal of Ruk_I inhibition of PI3K and Ruk_I promotion of SHIP1 phosphatase ability. The combined effects of the decrease of p85α binding to Ruk_I leads to an inevitable increase in the amount of PtdIns(3,4,5)P_3. This connection between Ruk_I, p85α and SHIP1 would also correlate with the hypothesis that several Ruk_I interactions culminate in an increase of PtdInsP_2 levels at CCP hotspots (see 1.3.1.2).

There is also a possibility that Ruk_I influences glucose metabolism as is seen in the recent evidence pointing to the existence of a PI3K independent insulin response pathway (Khan and Pessin, 2002). A component of this pathway is a Cbl-CrkII complex that localises to lipid rafts in order to stimulate glucose uptake and metabolism (Khan and Pessin, 2002). As stated above, Ruk_I is known to associate with both Cbl and CrkII and may participate in the complexes they form. Thus, Ruk_I may play a role in linking the PI3K-dependent and independent glucose metabolism pathways together and creating the proper homeostasis between the two pathways necessary for cellular metabolism.

Overall, the inhibition of p85α activity by Ruk_I leads to the balancing of key cellular activities that are mediated by PI3K and p85α as mentioned above. Without Ruk_I, the cellular pathways would not be properly attenuated and would be detrimental, leading to among other possibilities, cancer, diabetes or a compromised immune system as can be seen by the roles of Ruk_I and PI3K in B and T cells.

1.3.5 Ruk$_I$ acts in B cell activation

Ruk$_I$ is known to interact with several proteins that are involved in B cell maturation and activation including BLNK (B cell linker protein) and Cbl (Figure 1.8). Similar to its role in endocytosis, Ruk$_I$ acts as a scaffold that links together the different pathways involved in B cell activation.

1.3.5.1 Overview of B cell receptor activation and pathways

BCR (B cell receptor) activation and aggregation is initiated by the binding of the BCR ligand and results in Src kinase family clustering and subsequent phosphorylation of certain tyrosines. This phosphorylation causes the tyrosine kinase Syk to be recruited to the BCR complex and phosphorylated, both of which enables the phosphorylation and activation of BLNK (B-cell linker protein; Benschop *et al.*, 2001). Concomitantly, the BCR also activates the NF-κB pathway that compliments the BLNK-PLCγ2 pathway (Wang and Clarke, 2003). The importance of the BCR to both mature and immature B-cells is highlighted by the fact that in its absence, pre-B cells do not mature and mature B cells die; this indicates that a basal level of signalling is necessary for the maturation and maintenance of B cells (Wang and Clarke, 2003).

It has been shown that the BCR and PLCγ2 are recruited into lipid rafts with the activation of the BCR and that the downstream effectors of these proteins, Syk, BLNK, PI3K, Btk and Vav are translocated into these compartments (Aman and Ravichandran, 2000). Later in BCR activation, the SHIP1-FcγRIIB complex is also translocated to these lipid rafts in order to inhibit the BCR signal (Aman and Ravichandran, 2000). Lipid rafts are heterogeneous membrane microdomains that

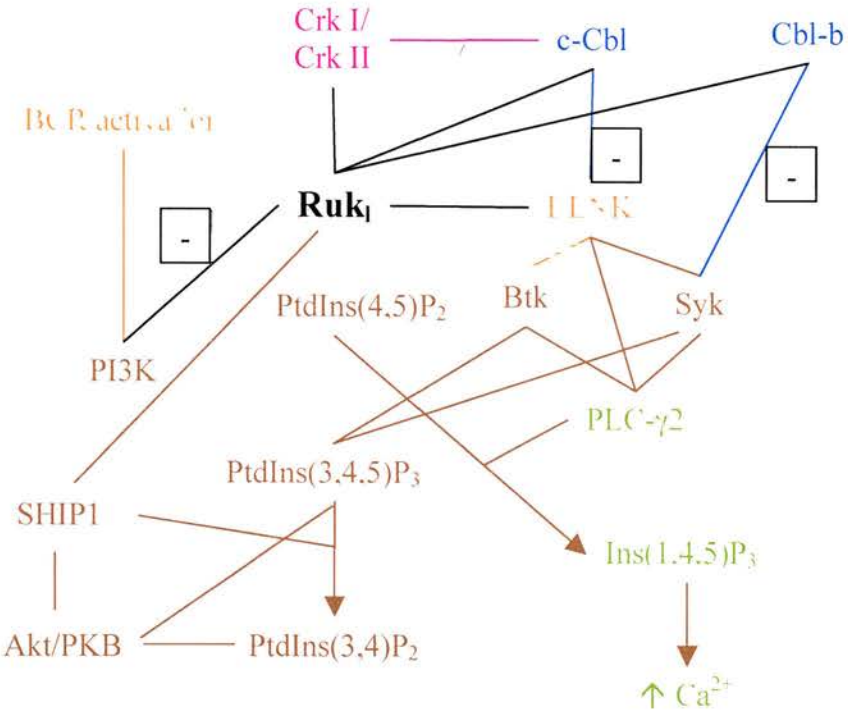

Figure 1.8: A map of Ruk$_I$ interactions in B cells. Ruk$_I$ may play a role in B cell development and maturation through its many interactors such as BLNK, SHIP1, Cbl and PI3K. In brown is the PI3K pathway, green is PLC-g2 pathway, pathways related to B cell activation are in orange, the Cbl pathways are in blue and Ruk$_I$ interactions are in black.

are enriched with cholesterol and glycosphingolipids (Pike, 2004). These areas may concentrate signalling proteins and their effectors, thereby allowing cross talk to occur between receptors and signalling pathways (Lai, 2003). Why BCR and related proteins are translocated to lipid rafts is unknown, although perhaps it serves as a mechanism for prolonging the BCR signal, as only a small amount of SHIP1 is endogenous to lipid rafts (Aman *et al.*, 2001). Recent speculations that lipid rafts form microenvironments that protect signalling pathways from negative regulators add weight to this hypothesis (Lai, 2003).

1.3.5.2 The role of interaction between BLNK and Ruk$_I$ in B cells

BLNK, which was recently found to be a Ruk$_I$ interactor (Watanabe *et al.*, 2000), was identified in 1998 as a protein that is necessary for B cell maturation (Fu *et al.*, 1998). Research into BLNK showed that inhibition of expression prevented mature B cells from forming and that there is a progressive decrease in expression from progenitor B cells to mature B cells (Minegishi *et al.*, 1999; Pappu *et al.*, 1999). BLNK is known to be tyrosine phosphorylated by Syk when the BCR pathway is activated, rendering it capable of binding to several different proteins including PLC-γ1, PLC-γ2, RhoGTPase Vav, Nck and Btk (Fu *et al.*, 1998; Pappu *et al.*, 1999; Wang and Clarke, 2003). BLNK binding brings these proteins closer to the membrane bound kinases that activate them (Wang and Clarke, 2003). BLNK is also capable of acting as an adaptor protein linking the BCR to cytoskeleton remodelling via its interactions with Vav, Nck and the Ras pathway via Grb2 (Wang and Clarke, 2003).

However, the most important interaction mediated by BLNK is that with

PLC-γ2 (Figure 1.8). It is thought that phosphorylated BLNK binds to PLC-γ2 while simultaneously binding Btk, a Tec kinase, thus bringing the two proteins into close proximity and allowing Btk to phosphorylate PLC-γ2 (Kurosaki *et al.*, 2000). In addition to the Ca^{2+} influx that is the major result of PLC-γ2 activation, the interaction between BLNK, Btk and PLC-γ2 is capable of controlling the proliferation of B cells in response to BCR stimulation. This effect is seen in BLNK deficient B cells that are unable to enter the cell cycle due to the inability of Btk to phosphorylate PLC-γ2 (Tan *et al.*, 2001).

Recent work has shown that Btk may also play an important role in PLC-γ2 activation by translocating PIP5K to the membrane where it can phosphorylate PtdIns(4)P to produce PtdIns(4,5)P_2 (Saito *et al.*, 2003). PLC-γ2 hydrolyses PtdIns(4,5)P_2 to produce Ins(1,4,5)P_3, a second messenger that binds to receptors controlling the release of Ca^{2+} from intra and extra cellular stores (Kurosaki *et al.*, 2000). In addition to producing Ins(1,4,5)P_3, PLC-γ2 hydrolysis of PtdIns(4,5)P_2 also produces diacylglycerol (DAG). Both Ca^{2+} and DAG are necessary for the activation and translocation to the nucleus of NF-κB and NFAT, signals critical to B cell survival and proliferation; hence the lack of proliferation in BLNK deficient cells (Petro and Khan, 2001; Antony *et al.*, 2004).

While the phosphorylation state of BLNK does determine its ability to interact with Btk and PLC-γ2, it does not determine its interaction with Ruk_I. However, tyrosine phosphorylation of BLNK by Syk does increase the affinity of the A and B SH3 domains of Ruk_I to its PRD, while the inability of SH3C to bind is not affected either way (Watanabe *et al.*, 2000). In human BLNK, there are Ruk_I binding

motifs at amino acids 242 to 247 (PSPLPR) and at amino acids 307 to 312 (PIPLPR; Kurakin *et al.*, 2003).

1.3.5.3 The role of interaction between Cbl and Ruk$_1$ in B cells

There is recent evidence that Cbl-b plays distinct roles in both mature and immature B cells. In mature B cells it causes the down-regulation of BCR signals in through ubiquitination of Syk, which is independent of PI3K or its downstream effectors (Sohn *et al.*, 2003). The ubiquitination of Syk causes it to be degraded and shifts the BCR toward an inactive state, thereby preventing signal transduction from the BCR (Sohn *et al.*, 2003). The role of Cbl-b is slightly different in immature B cells, as it antagonises c-Cbl function and promotes PLC-γ2 activity (Yasuda *et al.*, 2002). Syk and Lyn both phosphorylate Cbl-b allowing it to function as a scoffolding protein to complex BLNK, Btk and PLC-γ2 in lipid rafts containing the BCR and Syk. This leads to the activation of PLC-γ2 and is necessary for sustaining this activation and Ca^{2+} influx (Yasuda *et al.*, 2002). Interestingly, this interaction between Cbl-b and BLNK does not interfere with the inhibitory BLNK and c-Cbl interaction that also occurs in developing B cells, thus indicating that a balance of the two proteins may be necessary for proper homeostatis (Yasuda *et al.*, 2002).

In immature B cells the phosphorylation of BLNK allows it to directly bind c-Cbl in a manner that competes with PLC-γ2 binding to BLNK (Yasuda *et al.*, 2000). This competition allows c-Cbl to attenuate the phosphorylation of PLC-γ2 and the production of its secondary messengers (Yasuda *et al.*, 2000). Recent evidence shows that c-Cbl, much like Cbl-b, localises to the BCR and associated signalling components found in lipid rafts (Haglund *et al.*, 2004). However, it is

currently unknown if this inhibitory mechanism is retained in mature B cells. Phosphorylated c-Cbl also forms a complex with Crk after BCR activation, and this complex may play a role in BCR signal transduction (Feller, 2001).

As stated above, Ruk_I interacts with c-Cbl, Cbl-b, BLNK and Crks (Figure 1.8), and while the interaction between Ruk_I and the Cbls is well characterised in the context of receptor endocytosis, it is unknown what the role of this interaction in B cells is. There is a possibility that Ruk_I acts as a mere adaptor protein in the BLNK-Cbl complexes and helps them to form. It is also possible that Ruk_I joins these BLNK-Cbl and Crk-Cbl complexes to other pathways in B cells such as the PI3K pathway. Alternatively, Ruk_I binding may favour one complex or the other to regulate Ca^{2+} influx in a minute manner and thus fine-tune Ca^{2+} concentrations to the physiological needs of the cell.

1.3.5.4 The role of interaction between PI3K and Ruk_I in B cells

In addition to PLC-γ2 and NF-κB pathways, the PI3K pathway is also activated by BCR-antigen binding. BCR activation induces the tyrosine phosphorylation of CD19, a co-receptor, which, in turn, binds SH2 containing proteins such as p85 and intiates PI3K activation and targeting to the membrane (Marshall *et al.*, 2000). Another mechanism that may recruit PI3K to BCR complexes is the newly discovered protein BCAP, which is an adaptor protein that is tyrosine phosphorylated by Syk and Btk and promotes PI3K binding (Okada *et al.*, 2000). Another kinase found in B cells, Lyn, acts to negatively regulate the recruitment of PI3K to BCR complexes via an inhibition of this BCAP-PI3K interaction (Okada *et al.*, 2000). It is also possible that Btk has a kinase independent

function as an adaptor protein that recruits PIP5K to the membrane and consequently encourages the production of PtdIns(4,5)P_2, the substrate for both PLC-γ2 and PI3K (Saito *et al.*, 2003). In this manner, Btk may act as both a PI3K effector and an activator of PI3K (Marshall *et al.*, 2000).

The PI3K pathway is activated early in BCR signalling and the PtdIns(3,4,5)P_3 product plays a role in activating several downstream pathways that are important to the proper functioning of B cells and are key to B cell maturation (Figure 1.8; Fruman *et al.*, 1999; Okkenhaug and Vanhaesebroeck, 2003). One of the key B cell proteins that is activated by a combination of Src family phosphorylation and PtdIns(3,4,5)P_3 is Btk. As discussed above, Btk is a key integration point between the PLC-γ2 pathway and PI3K as its activation is PI3K dependent yet it regulates PLC-γ2 activation (Qiu and Kung, 2000). Another way in which PI3K may influence PLC-γ2 activity is through competitive binding of PtdIns(4,5)P_2, the lipid that both use as a substrate (Marshall *et al.*, 2000). It should be noted that while PLC-γ2 also has a PH domain that is capable of binding PtdIns(3,4,5)P_3, no direct binding has been discovered to be necessary *in vivo*, and therefore, PI3K may not directly influence PLC-γ2 activation (Fruman, 2004). Instead of directly activating PLC-γ2, the PI3K pathway and PtdIns(3,4,5)P_3 may positively regulate Ca^{2+} influx, causing it to be increased and sustained for longer, possibly though the various actions of Btk (Kurosaki *et al.*, 2000).

As discussed in Section 1.3.4.4, Ruk_I negatively regulates PI3K function in other cell types through its binding of the p85α subunit. If it also acts to negatively regulate PI3K in B cells, it may be that Ruk_I subtly attenuates PI3K signalling to maintain a delicate balance of PtdIns(3,4,5)P_3 and PtdIns(4,5)P_2 necessary for proper

BCR activation. This negative regulation may also be linked to the activities of another negative regulator of PI3K, SHIP1, which also binds to Ruk_I.

1.3.5.5 The role of interaction between SHIP1 and Ruk_I in B cells

SHIP1 is a recently discovered Ruk_I interactor (Kowanetz *et al.*, 2004) that functions as a key negative regulator of intracellular signals in hematopoietic cells: it regulates calcium flux, activates the Erk signalling cascade and influences the activation of the PKB/Akt kinase in lymphocytes (March and Ravichandran, 2002). SHIP1 seems to play an important role in the maturation of B cells as well as the regulation of mature B-cell responses through its action as a negative regulator of PI3K actions (March and Ravichandran, 2002).

FcγRIIB1 is a low affinity receptor that co-aggregates with and inhibits the BCR complex. When phosphorylated, FcγRIIB1 is able to bind SHIP1 and translocate it to the plasma membrane and the BCR (Brauweiler and Cambier, 2003). Among the results of SHIP1 binding to FcγRIIB1 is the prevention of the FcγRIIB1 pro-apoptotic signals and promotion of B cell survival (Pearse *et al.*, 1999). The pro-apoptotic signal is dependent on Btk activation of FcγRIIB1, independent of other FcγRIIB1 functions, and serves to remove those B cells that are not engaging the BCR (Pearse *et al.*, 1999). The binding of PcRIIB1 and SHIP1 may also prevent cell proliferation through the inhibition of FcγRIIB1's ability (following c-Kit activation) to induce the transcription of cyclin genes and the subsequent progression of cells through the cell cycle (Malbec *et al.*, 2001). However, the precise role of SHIP1 in the selection and proliferation of B cells is complicated by the fact that SHIP deficient mice develop autoimmune diseases, an indication that the B cells are not

properly selected against recognition of self (Okkenhaug and Vanhaesebroeck, 2003).

The function of the PtdIns(3,4)P_2 product of SHIP1 is largely unknown other than as a by-product of PI3K downregulation (March and Ravichandran, 2002; Sly *et al.*, 2003). As a functional antagonist to PI3K, SHIP1 can regulate the levels of PtdIns(3,4,5)P_3 and the subsequent activation of PI3K effectors (March and Ravichandran, 2002). In B cells, the most important PI3K effector that is inhibited by SHIP1 is Btk. Btk is removed from the membrane following the hydrolysis of PtdIns(3,4,5)P_3 which has downstream consequences for PLC-γ2 activation and Ca^{2+} influx (Bolland *et al.*, 1998).

The production of PtdIns(3,4)P_2 may play a role by attracting certain PH-domain containing proteins such as PKB/Akt and members of the PKC family (Sly *et al.*, 2003). In this manner, SHIP1 is functionally distinct from PTEN, as it may regulate the spatio-temporal nature of signalling after receptor activation by moving signal tranduction pathways away from PtdIns(3,4,5)P_3-dependent effectors to PtdIns(3,4)P_2 dependent effectors (Freeburn *et al.*, 2002).

A secondary function of SHIP1's ability to hydrolyse 5'phosphates is the hydrolysis of Ins(1,3,4,5)P_4 to Ins(1,3,4)P_3 (March and Ravichandran, 2002). This product may affect the amount of higher order InsPs such as $InsP_6$ that are thought to play an essential role in transporting mRNA out of the nucleus to the ribosomes for translation (March and Ravichandran, 2002; Sly *et al.*, 2003).

SHIP1 has also been shown to form a multiprotein complex with PI3K and CRKL, a member of the Crk family and a relative of the Ruk_I binding protein CrkII (Sattler *et al.*, 2001). Ruk_I binds both SHIP1 and PI3K but has an unknown role in

the SHIP1-CRKL-PI3K complexes; through these various multi-protein complexes, Ruk_I may link different B cell functions to maintain B cell homeostatsis.

Although, similar to many Ruk_I binding proteins, the actual effect of such binding is unknown, it is known that SHIP1 binds constitutively to all three SH3 domains of Ruk_I at amino acid 1028 (motif: PKPAPR) and amino acid 1135 (motif: PTPTPR) (Kowanetz *et al.*, 2004). Theoretically, Ruk_I could act as a link between PI3K and SHIP1 to inhibit the PI3K signal to a greater degree (Figure 1.8). Alternatively, Ruk_I interaction with SHIP1 could provide a mechanism to bridge the PI3K signal transduction pathways to other proteins that Ruk_I interacts with in the B and T lymphocytes.

1.3.5.6 The role of interaction between STAP-1/BRDG1 and Ruk_I in B cells

Another recently identified Ruk_I interactor is STAP-1 (stem cell adaptor protein 1), the mouse homologue of the human docking protein BRDG1 (BCR downstream signaling 1; Kowanetz *et al.*, 2004). STAP-1/BRDG1 is a protein found in hematopoetic stem cells that may help to maintain their undifferentiated state and plays a role in BCR signal transduction (Ohya *et al.*, 1999; Masuhara *et al.*, 2000). This protein has been identified as an effector of Tec, a member of the same kinase family as Btk (Ohya *et al.*, 1999). Tec is re-localized to the plasma membrane through its interaction with PtdIns(3,4,5)P_3 where it is phosphorylated and activated by another kinase, possibly from the Src kinase family, similar to how Btk is activated (Lucas *et al.*, 2003). Predominantly found in lymphocytes, Tec is activated by the BCR in B lymphocytes and CD28 in T lymphocytes and affects many key processes such as lymphocyte development, activation and homeostatis (Lucas *et al.*,

2003; Fruman, 2004). Due to its dependence on PtdIns(3,4,5)P_3, Tec and BRDG1 are downstream of the Ruk$_I$ interactor PI3K.

BRDG1 interacts with and is tyrosine phosphorylated by Tec, thereby activating Tec, possibly through the disruption of an autoinhibitory intramolecular interaction within Tec (Ohya *et al.*, 1999). When BRDG1 is phosphorylated after BCR stimulation, it is known to interact with several different phosphorylated proteins in a large, multi-protein complex that has multiple downstream effects on protein translation and cell proliferation (Ohya *et al.*, 1999).

A single Ruk$_I$ binding motif (PKPAPR) has been located starting at amino acid 7 in STAP-1 and it binds the SH3A and C domains of Ruk$_I$ (Kowanetz *et al.*, 2004). The physiological result of this binding is unknown, but theoretically, Ruk$_I$ serves as a TCR/BCR scaffolding protein in a manner similar to its role in receptor endocytosis. Through binding of STAP-1 and other B cell proteins, Ruk$_I$ may link B cell maturation and activation to protein translation, cellular proliferation, actin remodeling and other pathways such as PtdIns(3,4,5)P_3 production (Figure 1.8).

1.3.6 Ruk$_I$ is involved in T cell activation

Similar to the situation in B cells, Ruk$_I$ is known to bind several different proteins that are involved in T cell maturation and activation (Figure 1.9). In T cells, as in B cells, Ruk$_I$ acts as a scaffolding protein that coordiantes several different pathways leading to T cell activation.

1.3.6.1 Overview of CD2 in T cell activation

CD2 is an accessory protein expressed on the cell surface of T and NK cells, which mediates low affinity cell-cell interactions by binding to CD58 in humans and

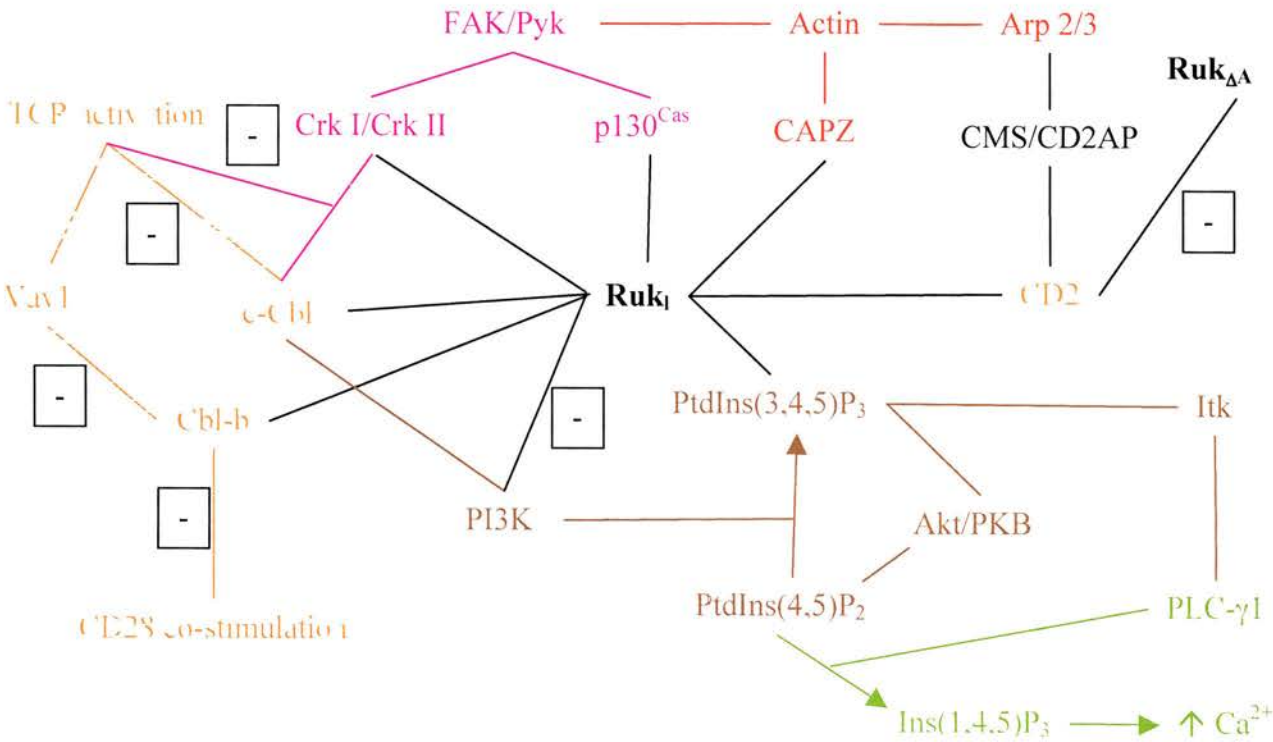

Figure 1.9: The interactions of Ruk isoforms in T cells. Much like in B cells, Ruk$_I$ possibly plays a role in T cell development and maturation through its many interactors. Ruk$_I$ and Ruk$_{\Delta A}$ both bind to CD2, leading to the inhibtion of CMS/CD2AP dependent pathways; Ruk$_I$ also serves to link CD2 with actin rearrangements through CAPZ. The pathways leading to T cell activation are in orange, the PI3K pathway is in brown, the PLC-g pathway is in green, the FA/Crk pathway is in magenta and the actin associations are in red. Ruk interactions are in black.

CD48 in rodents (Davis *et al.*, 1998; Davis *et al.*, 2003). The interaction between CD2 and CD58/CD48 is of very low affinity but high specificity, indicating that the purpose of it is to bring the membranes of the T cell and APC (antigen presenting cell) into close proximity for the TCR (T cell receptor) and antigen to interact (Dustin *et al.*, 1997). In this manner, the CD2-CD48 binding plays an important role in enhancing the co-receptor and TCR binding as well as lowering the threshold for TCR activation (Hahn *et al.*, 1992).

With ligand binding, the CD2 receptor is clustered by CD2AP to increase the affinity of the binding (Dustin *et al.*, 1998). Much like activated BCR, CD2 is co-localised to lipid rafts containing LAT (linker for T cell activation), and the cross-linking of clustered CD2 molecules and TCR activates the LAT protein through tyrosine phosphorylation (Inoue *et al.*, 2002). In turn, activated LAT results in an increased association with and activation of PI3K and PLC-γ1, leading to an increase in intracellular Ca^{2+} and other downstream effects (Inoue *et al.*, 2002; Reynolds *et al.*, 2004).

1.3.6.2 The role of interaction between CD2 and Ruk$_I$ in T cells

Ruk$_I$, with its structural similarities with CD2AP, has been identified as a binding partner with CD2. Both CD2AP and Ruk$_I$ bind to CD2 via the interaction of the cytoplasmic tail of CD2 (amino acids 322 to 339) with the SH3A domain of CD2AP and Ruk$_I$ (Hutchings *et al.*, 2003; Tibaldi and Reinherz, 2003). However, in both of these studies, it was not resolved whether a combination of two or more SH3 domains would interact with a higher affinity than SH3A alone. There are indications that other domains of Ruk$_I$ and CD2AP mediate the interactions with

CD2 since $Ruk_{\Delta A}$ is also able to interact very weakly with CD2 (Tibaldi and Reinherz, 2003).

Jurkat T cells overexpressing truncation mutants of CD2AP decreased TCR downmodulation (Hutchings *et al.*, 2003). This points to a key role for CD2AP in the proper functioning of T cells and modulating the TCR responses. However, the exact pathways stimulated by Ruk_I in T cells are unknown, possibly because its main role in T cells may be to modulate CD2AP function (Tibaldi and Reinherz, 2003). For instance, while Ruk_I is capable of binding to both CD2 and CAPZ (Figure 1.8), Tibaldi and Reinherz (2003) showed that Ruk_I blocks cytoskeleton polarisation initiated by CD2 crosslinking. It is also possible that Ruk_I binding to CD2 acts to attenuate CD2AP functions by inefficiently activating $p130^{Cas}$; a more efficient binding is known to occur between CD2AP and $p130^{Cas}$ (Tibaldi and Reinherz, 2003). This is in contrast to $Ruk_{\Delta A}$ that is unable to bind $p130^{Cas}$ at all, showing that it competes with Ruk_I and CD2AP for binding to CD2 without recruiting downstream effectors; while Ruk_I is able to activate downstream effectors to a degree (Tibaldi and Reinherz, 2003). Therefore, it can be hypothesised that $Ruk_{\Delta A}$ acts as a complete inhibitor of CD2AP dependent pathways while Ruk_I merely down-modulates them and acts as fine tuning mechanism (Figure 1.9).

It is also possible that the ability of Ruk_I to bind to CD2 is a mechanism to stabilise CD2 proteins on the cell surface in resting T-cells without fully activating downstream pathways. Tibaldi and Reinherz (2003) showed that the basal level of CD2 in Ruk_I transfected cells was higher than in $Ruk_{\Delta A}$ transfected cells, possibly due to the intramolecular interactions between the PRD and SH3A regions of Ruk_I

decreasing the amount of c-Cbl recruited to the sites of CD2 clustering (see Section 1.3.6.5).

1.3.6.3 Ruk_I links CD2 to CAPZ

Further research into Ruk_I function in T cells pointed to a role for Ruk_I to act as an adaptor between CD2 and CAPZ that directly links the cell surface receptor to the cytoskeleton (Hutchings *et al.*, 2003). CAPZ has been shown to bind to the C-terminal region of both Ruk_I and CD2AP; the binding site is outside of the CCD and endophilin binding sites (Figure 1.9; Hutchings *et al.*, 2003).

CAPZ is a barbed-end actin capping protein that serves several functions, including nucleating and regulating actin assembly. *In vivo*, CAPZ is a heterodimer with α and β subunits that are found in two different isoforms for each (α_1, α_2, β_1 and β_2); CD2AP and Ruk_I are capable of co-immunoprecipitating all four subunits but it is unclear which subunit they interact with (dos Remedios *et al.*, 2003; Hutchings *et al.*, 2003). While direct binding to CAPZ is the most obvious way in which Ruk_I affects the actin cytoskeleton, CAPZ binding to actin is also mediated by the presence of PtdInsP and $PtdInsP_2$ (dos Remedios *et al.*, 2003). When signal transduction occurs, PtdInsP and $PtdInsP_2$ cause CAPZ to become removed from actin filaments and the actin filaments are then able to polymerise (dos Remedios *et al.*, 2003). Given that Ruk_I clearly affects $PtdInsP_2$ and $PtdIns(3,4,5)P_3$ levels through a variety of interactors, this mediation of CAPZ binding provides another way for Ruk_I to affect the actin cytoskeleton.

1.3.6.4 The role of interaction between PI3K and Ruk_I in T cells

Much like its role in B cells, PI3K is critical to T cell activation and signal

transduction, mainly through its activation of Tec kinases, particularly Itk, and Akt/PKB (Salim *et al.*, 1996; Lucas *et al.*, 2003). PI3K is activated and recruited to the membrane by CD28 ligation and PI3K inhibitors cause the decreased activation of T cells (Kane and Weiss, 2003).

PLC-γ1 and subsequent Ca^{2+} influx may act downstream of PI3K through two mechanisms. The Tec kinases bind to and phosphorylate PLC-γ1 in T cells, PLC-γ1 also has an ability to directly bind PtdIns(3,4,5)P_3 (Lucas *et al.*, 2003). The PLC-γ1 downstream pathway leads to similar results as the PLC-γ2 pathway in B cells and are as important for T cell development, differentiation, function and homeostatis as PLC-γ2 is to B cells (Lucas *et al.*, 2003). However, unlike in B cells, PI3K inhibitors have little effect on sustained Ca^{2+} influx implying that the roles of the Tec kinases in T cells can be uncoupled from PtdIns(3,4,5)P_3 (Harriague and Bismuth, 2002). Other, lesser known functions of the Tec family are in regulating actin cytoskeleton rearrangements in response to TCR signalling, cell adhesion and migration (Takesono *et al.*, 2002).

In addition to activating the mTOR (target of rapamycin), Forkhead and BAD pathways, Akt/PKB has been linked to activation-induced increases in glucose metabolism (Rathmell *et al.*, 2003). This stimulation occurs in the context of T cell co-stimulation via the TCR and CD28 pathways but it is not entirely clear how this metabolic increase occurs (Frauwirth *et al.*, 2002).

Ruk_I is a known inhibitor of PI3K function in other cell types and it is feasible that it inhibits PI3K in T cells. If this is the case, Ruk_I would play a role in attenuating multiple pathways leading to T cell activation and proliferation in a manner similar to how it acts in B cells (Figure 1.9).

1.3.6.5 The role of interaction between Cbl and Ruk$_1$ in T cells

It has been shown that T cell activation requires CD28 co-stimulation in order to maintain antigen specificity, and recent evidence shows that Cbl-b regulates this necessity for CD28 through its inhibition of Vav1 (Figure 1.9; Chiang *et al.*, 2000). Vav1 inhibition allows Cbl-b to act as a negative regulator of receptor clustering and lipid raft aggregation that are key to T cell activation (Krawczyk *et al.*, 2000). CD28 co-stimulation removes Cbl-b inhibition of Vav1, creating specific T cell activation and preventing autoimmunity from developing (Krawczyk *et al.*, 2000). As would be expected, Cbl-b deficiency results in T cells that are over-stimulated through the TCR alone and lack attenuation by Cbl-b and CD28 co-stimulation, this eventually leads to T cell proliferation and autoimmunity (Bachmaier *et al.*, 2000; Chiang *et al.*, 2000).

Cbl-b has also recently been shown to negatively regulate the PI3K pathway in T cells by binding and ubiquitinating p85α (Fang *et al.*, 2001). This ubiquitination does not target p85α for degradation, instead it merely serves to functionally regulate p85α by inhibiting its recruitment to CD28 and the TCR (Fang and Liu, 2001; Fang *et al.*, 2001). Therefore, Cbl-b is able to attenuate signal transduction in T cells, via both the TCR and PI3K pathways.

However, Cbl-b is not the only Cbl family member found in T cells that plays a role in T cell activation. Recent work shows that c-Cbl negatively regulates TCR signalling through the ubiquitination of the TCRζ subunit (Wang *et al.*, 2001). Similar to the Cbl-b ubiquitination of Syk in B cells, the ubiquitination of the TCRζ subunit targets it for proteolytic degradation thereby impairing TCR signalling (Wang *et al.*, 2001).

It should be noted that c-Cbl deficient mice do not show any T cell impairment, which leads to the hypothesis that T cell activation is mediated mainly though Cbl-b (Murphy *et al.*, 1998; Naramura *et al.*, 1998). Thus the role of c-Cbl may be more in "fine-tuning" the signalling threshold of developing T cells instead of their gross development or TCR activation in mature T cells (Murphy *et al.*, 1998; Naramura *et al.*, 1998).

Following T cell activation, the tyrosine phosphorylation of c-Cbl produces binding sites for both PI3K and CrkII and induces a low affinity binding between PI3K and CrkII (Gelkop *et al.*, 2001). This low affinity binding is then able to produce a higher affinity binding between PI3K and CrkII, possibly through conformational changes of one or both of the proteins (Gelkop *et al.*, 2001). This multiprotein complex brings together their two downstream pathways and mediates their physiological effects. The interaction between c-Cbl and CrkII is thought to play a role in maintaining an anergic state, whereby T-cells are rendered non-responsive due to the TCR being stimulated without co-stimulation of co-receptors (Feller, 2001). This means that much like Cbl-b, c-Cbl also plays a role in both T cell activation and PI3K activity, albeit the effects are slightly less physiologically important as seen in c-Cbl deficient mice (Murphy *et al.*, 1998; Naramura *et al.*, 1998).

Once again, the exact role of Ruk_I in these Cbl based interactions is unknown. Ruk_I is able to bind both c-Cbl and Cbl-b leading to the possibility that it has a role in T cell activation, but what that role is remains unknown. In the case of the c-Cbl, PI3K and CrkII interaction, Ruk_I is able to bind all three proteins involved but the effect of Ruk_I on the overall multi-protein complex is unknown. In receptor

endocytosis, Ruk_I has a coordianted action tied to c-Cbl that brings about endocytosis, but it is unknown if Ruk_I has a similar function in TCRζ degradation.

It may be that Ruk_I serves to bridge the PI3K, CD2, CAPZ and Cbl pathways for the proper maintenance of T cell homeostatsis and antigen specificity. Therefore, Ruk_I may play a role in preventing auto-immunity from developing and the maintenance of T cell specificity.

1.3.7 Ruk_I interacts with SB1, an unknown protein

Borinstein *et al.* (2000) reported that the Ruk_I protein, which they called SETA, interacts with a novel protein that they named SB1 (SETA binding protein 1). The novel binding protein shares a 55% amino acid similarity with a renal tumour antigen NY-REN-45, though most of the consensus is restricted to the N-terminal half of NY-REN-45 (Borinstein *et al.*, 2000). Recent work into the recognition sequence of the Ruk_I SH3 domains shows that the mouse SB1 homologue has two putative Ruk_I recognition sites: PSPSPR at amino acids 618 to 623 and PTPAPR at amino acids 678 to 683 (Kurakin *et al.*, 2003). These sites bind with the highest affinity to SH3A when the SH3 domains were individually present, but the maximum binding efficiency was only achieved when two or more of the SH3 domains were present (Borinstein *et al.*, 2000).

Since SB1 is newly discovered, it is unknown what its exact function is. At the N terminus there is a region that contains a high similarity to the cytoplasmic region of potassium channels, however SB1 lacks other similarities to potassium channels making it unlikely that it functions as an ion transporter (Borinstein *et al.*, 2000). The PRD is thought to bind to the SH3 domains of Grb2 and to a lesser

extent Abl and Yes thus raising the possibility that SB1, Ruk_I, and their associated proteins form a complex *in vivo* (Borinstein *et al.*, 2000).

1.4 $Ruk_{\Delta A}$/SETA

The $Ruk_{\Delta A}$ isoform lacks SH3A and was independently cloned twice and named SETA (SH3 domain containing expressed in tumorigenic astrocytes) (Bogler *et al.*, 2000) or CD2BP3 (CD2 binding protein 3) (Tibaldi and Reinherz, 2003). Unlike Ruk_I which was found in many developing and adult organs, $Ruk_{\Delta A}$ was found primarily in the developing brain with no transcripts found in either adult rat or human brains (Bogler *et al.*, 2000). However, Tibaldi and Reinherz (2003) reported isolating what they named CD2BP3 from human T lymphocytes, thus indicating that there is expression of $Ruk_{\Delta A}$ in some adult human tissues.

Out of all the $Ruk_{\Delta A}$-based protein interactions so far discovered, the main interactor of $Ruk_{\Delta A}$ is AIP1/Alix that is involved in apoptotic pathways. $Ruk_{\Delta A}$ may function as a negative regulator of Ruk_I in that is able to bind to some of the same proteins but not provoke the same response as Ruk_I. An example of this competitive inhibition is seen in the interaction between Ruk_I, $Ruk_{\Delta A}$ and CD2, as detailed above in Section 1.3.6.2. However, another possible alternative is that $Ruk_{\Delta A}$ binds to some of the same proteins as Ruk_I and produces the same downstream results to reinforce Ruk_I based signals.

1.4.1 AIP1/Alix interacts with $Ruk_{\Delta A}$ and ALG-2

AIP1/Alix was initially identified as an ALG-2 (apoptosis-linked gene 2) interacting partner that participates in apoptotic pathways through its interactions with ALG-2 (Missotten *et al.*, 1999; Vito *et al.*, 1999). It was also discovered that

ALG-2 and AIP1/Alix are able to bind together only when ALG-2 is loaded with Ca^{2+}, implying that the interaction is linked to intracellular Ca^{2+} levels and the signalling mechanisms that control it (Missotten *et al.*, 1999; Vito *et al.*, 1999). This initial work also showed that overexpression of AIP1/Alix was capable of protecting some cell types from apoptosis induced by serum starvation (Vito *et al.*, 1999). Later work showed that AIP1/Alix, through its binding with ALG-2, is capable of controlling numerous apoptotic pathways that are both caspase dependent and independent (Trioulier *et al.*, 2004).

ALG-2 plays a key role in the ER-associated apoptotic complex that is independent of traditionally described microsomal and mitochondria-dependent pathways of apoptosis (Rao *et al.*, 2004). However, ALG-2 also binds to ASK1 (apopotis signal-regulating kinase 1) in a Ca^{2+} independent manner and inhibits ASK1's ability to activate the JNK apoptotic pathways (Hwang *et al.*, 2002). Another apoptotic protein that is known to interact with ALG-2 is Fas, which is activated upon dissociation from ALG-2 (Jung *et al.*, 2001). All three interacting partners point to a variety of mechanisms through which ALG-2 and its binding partner AIP1/Alix can influence apoptotic pathways.

The same PRD of AIP1/Alix interacts with both ALG-2 and $Ruk_{\Delta A}$, but the two proteins do not recognise the same binding motif. ALG-2 binds further downstream than both the Ruk SH3 binding motif or the endophilin-binding motif (see Section 1.3.1.7).

1.4.2 $Ruk_{\Delta A}$ acts in apoptosis

Initial studies into $Ruk_{\Delta A}$ showed that the isoform was associated with

malignancy due to its upregulation in half of the human gliomas tested with expression being restricted to tumorigenic cells (Bogler *et al.*, 2000). Later work done by the same lab found that $Ruk_{\Delta A}$ bound to AIP1/Alix and through this binding its associated with ALG-2, which could explain the coincidence with malignancy (Chen *et al.*, 2000). However, when $Ruk_{\Delta A}$ was overexpressed in cultured cell, the cells were more susceptible to apoptosis when exposed to UV irradiation, a contradictory result to the overexpression of $Ruk_{\Delta A}$ *in vivo* (Chen *et al.*, 2000). It may be that the different *in vitro* and *in vivo* results are attributable to an interaction with other isoforms found in the *in vivo* studies but not the *in vitro* studies. The other isoforms found *in vivo* may interact with $Ruk_{\Delta A}$ to negatively affect AIP1/Alix, possibly in conjunction with endosomal proteins (see Section 1.3.1.7), to increase cell division and growth to increase cancerous malignancy. Ruk_I is already known to negatively regulate AIP1/Alix in FAs and is a known endocytic protein. Therefore, without other isoforms to interact with $Ruk_{\Delta A}$, it interacts with AIP1/Alix to increase cellular susceptibility to apoptotic stimuli.

However, it should be noted that the involvement of $Ruk_{\Delta A}$ in the PI3K pathway was unexplored. It is possible that some of the effects on apoptosis seen by the over expression of $Ruk_{\Delta A}$ can be attributed to the dominant negative effect of $Ruk_{\Delta A}$ on the different pathways that Ruk_I is known to be involved in, including PI3K dependent survival pathways. Especially interesting would be the effect of the interaction of $Ruk_{\Delta A}$ with the proteins that trigger PLC-γ activation such as PI3K and BLNK; these proteins lead to an increase in Ca^{2+} upon which AIP1/Alix-ALG-2 binding is dependent.

1.4.3 AIP1/Alix participates in retroviral budding

AIP1/Alix is known to interact with EIAV (see Section 1.3.17), a protein involved in membrane curvature (Strack *et al.*, 2003). Recently it has been shown that AIP1/Alix binds to HIV-1 p6 (human immunodeficiency virus-1, protein 6) that is functionally equivalent to EIAV and is necessary for retroviral budding (Strack *et al.*, 2003). AIP1/Alix links this HIV protein to the ESCRT complexes that it takes over in order to bud (Strack *et al.*, 2003). Recent work has shown the necessity of AIP1/Alix and its binding partners Tsg101 and CHMP4 to the viral machinery of HIV, as they are actually enclosed along with the virus in viral packages (von Schwedler *et al.*, 2003). The interaction between $Ruk_{\Delta A}$ and AIP1/Alix may provide a mechanism for Ruk isoforms to influence HIV infection, a phenomenon seen when Ruk_m is overexpressed (Narita *et al.*, 2001).

1.5 Ruk_m

Ruk_m, an isoform lacking SH3A and B domains (see Figure 1.1), was independently cloned from human lymphocytes (Narita *et al.*, 2001) and newborn rat tissues (Gout *et al.*, 2000). The gene found in human lymphocytes by Narita *et al.* (2001) was named SH3KBP1 (SH3-domain kinase binding protein 1) while the encoded protein was named HSB1 (human Src-family kinase binding protein 1). Gout *et al.* (2000) also isolated the protein around the same time and named it Ruk_m. An interesting result obtained by over-expressing Ruk_m in human macrophage-like cells was that the isoform provided a certain amount of resistance to HIV-1 infection (Narita *et al.*, 2001). Unfortunately, this line of work was never followed through, although recent work done on the $Ruk_{\Delta A}$ interactor AIP1/Alix shows that this protein

may have a role in HIV infection. Possibly the increased resistance to HIV infection seen in Ruk_m transfected cells is a result of an inter-isoform interaction between $Ruk_{\Delta A}$ and Ruk_m that alters or inhibits AIP1/Alix function.

Unlike the extensive work done on Ruk_l and $Ruk_{\Delta A}$, Ruk_m is a relatively unknown protein and no other proteins are known to bind to it. Ruk_m may act as an antagonist to Ruk_l function because the two isoforms are able to heterodimerise and research has shown that Ruk_m can rescue cells overexpressing Ruk_l from apoptosis (Gout *et al.*, 2000).

1.6 Other isoforms

Much like Ruk_m, there is not much known about the smaller isoforms of the Ruk family: Ruk_s, Ruk_h and Ruk_t (see Figure 1.1). Due to the possibility that they may all be able to homo and heterodimerise with each other there is the prospect that they act as antagonists or negative regulators of the larger isoforms. However, there is also a likelihood that inter-isoform heterodimerisation may be able to provide an increased combination of proteins and lead to the connecting of several different pathways by the Ruk isoforms.

1.7 CD2AP/CMS is a protein similar in structure and function to Ruk_l

Unlike the Ruk proteins, CD2AP/CMS (CD2 adaptor protein/Cas ligand with multiple SH3 domains) does not have different isoforms, and this is a key difference between the two proteins. However, the structural similarity between Ruk_l and CD2AP/CMS has lead many to hypothesis that they form a new subfamily of adaptor proteins that have the ability to form multi-protein complexes that help to link different pathways together. The very nature of these multidomain proteins allows

several different proteins to come in close proximity to one another and thus interact. However, the similarities between the two proteins allow a certain amount of functional redundancy to occur. Another possibility is that the similar proteins compete with one another to bind to specific key proteins to produce a myriad of down stream effects to occur. This competition between CD2AP and Ruk isoforms for binding partners creates multi-protein complexes that occur for a transient period time thus "fine tuning" signalling cascades in response to external cellular signalling. The competition does not allow any one protein (CD2AP or Ruk_1) to overwhelmingly interact with other proteins and constitutively affect signalling cascades that would produce invariable and often detrimental downstream effects (eg: apoptosis, proliferation, motility).

1.7.1 CD2AP/CMS interacts with CD2

CD2AP was first cloned in 1998 as a key component in receptor patterning at T cell junctions that interacts with the cytoplasmic tail of CD2 (Dustin *et al.*, 1998). It was discovered that the first SH3 domain of CD2AP binds to a PRD in the last 30 residues of CD2, creating an interaction with high affinity and specificity (Dustin *et al.*, 1998). The interaction between CD2 and CD2AP is dependent on T cell activation and CD2-CD48/CD58 binding results in CD2AP mediating CD2 relocation and clustering at the T cell junction (see 1.3.5.1).

Following CD2 activation, a succession of pathways are activated including actin polymerisation by Arp2/3 and CAPZ (Hutchings *et al.*, 2003; Lynch *et al.*, 2003). This and the putative actin binding sites in CD2AP/CMS, show that CD2AP/CMS may function as an adaptor protein linking the CD2 signalling

pathway to the actin cytoskeleton. This would allow key cytoskeletal responses to external stimuli.

1.7.2 CD2AP/CMS interacts with p130^{Cas}

Shortly after the discovery of murine CD2AP the human orthologue of CD2AP, CMS (p130^{Cas} ligand with multiple SH3 domains), was discovered from the screening of a human kidney library (Kirsch *et al.*, 1999). The PRD of CMS not only bound to the SH3 domain of p130^{Cas} but also to the SH3 domains of Fyn, Src, p85α and Grb2 (Kirsch *et al.*, 1999). Kirsch *et al.* (1999) discovered that CMS and p130^{Cas} both co-localised with actin to the membrane ruffles and leading edges of cells indicating a role for CMS in multi-protein complexes leading to the invagination of cell membranes. Interestingly, punctate structures similar to those reported for Ruk$_I$ (see Section 1.3.2.4; Watanabe *et al.*, 2000; Kowanetz *et al.*, 2004; Dr. E. Borthwick, unpublished observations) were found in the cytoplasm of cells overexpressing CMS and the CMS proteins were localised to the surface of these vesicular like structures (Kirsch *et al.*, 1999).

1.7.3 CD2AP/CMS functions in kidneys

Despite the role of CD2AP in T-cell tight junctions, mice lacking CD2AP actually die 6 –7 weeks after birth of severe kidney failure (Shih *et al.*, 1999). CD2AP is developmentally upregulated during the differentiation of mesenchymal cells to epithelial cells in mouse kidneys and eventually form a crucial component in the slit diaphragm (Shih *et al.*, 1999; Lehtonen *et al.*, 2000). Due to the pathology of the kidney malfunction in knockout animals, it was hypothesised that CD2AP serves as an adaptor that anchors nephrin to the cytoskeleton thereby helping to form the slit

diaphragm of kidneys (Shih *et al.*, 1999). While CD2AP and nephrin are co-expressed and interact with one another, CD2AP is not necessary for normal expression and localisation of nephrin in developing podocytes (Li *et al.*, 2000).

Tyrosine phosphorylated nephrin and CD2AP simultaneously bind the p85α subunit of PI3K and recruit it to the slit diaphragm protein complex located at the plasma membrane (Huber *et al.*, 2003). Nephrin and CD2AP both trigger the phosphorylation of AKT on serine 473 via activation of PI3K thus stimulating the AKT dependent signalling pathways and the phosphorylation of Bad on both of its regulatory sites leading to the production of survival signals (Huber *et al.*, 2003). The suggestion that antiapopotic pathways are stimulated by the combined efforts of nephrin and CD2AP is confirmed by the observation that overexpression of nephrin significantly inhibited apopotosis while the lack of CD2AP significantly increased apoptosis (Huber *et al.*, 2003). The observation that nephrin signalling can be enhanced by podocin provides a novel way for PI3K downstream effectors to be upregulated in podocytes (Huber *et al.*, 2001). Podocin also binds to CD2AP and all three proteins, CD2AP, podocin and nephrin, are necessary for the stabilisation and normal filtration function of the slit diaphragm (Huber *et al.*, 2001).

CD2AP also plays a potentially crucial role in kidneys by interacting with polycystin-2. CD2AP partially co-localises with polycystin-2 in kidney tubules and possibly modulates the polycystin signalling pathway by forming multiprotein complexes much in the same way it acts in RTK endocytosis (Lehtonen *et al.*, 2000). The exact function of polycystin-2 is largely unknown, except that it has the potential to form multiprotein complexes with other proteins such as polycystin-1 and associated focal adhesion proteins (Wilson, 2001). Through its many domains and

binding partners, CD2AP could play a role in linking the FAs containing polycystin-1 to other signalling pathways such as P13K.

1.7.4 CD2AP/CMS functions in receptor endocytosis

Much like the structurally similar Ruk_I, CD2AP/CMS can also bind to c-Cbl via the second SH3 domain of CD2AP/CMS interacting with the PRD of c-Cbl (Kirsch *et al.*, 2001). Unlike the single motif found in c-Cbl that Ruk_I binds to, it is likely that CD2AP/CMS binds to more than one of the PXXP motifs found in the C terminus of c-Cbl (Kirsch *et al.*, 2001).

Furthering the similarities between CD2AP/CMS and Ruk_I, is the ability of CD2AP/CMS to constitutively bind endophilins via the endophilin SH3 and CD2AP/CMS PRD 1 (Lynch *et al.*, 2003). The two other PRDs may also play an insignificant role in the binding of endophilins but P1 plays the predominant role.

While binding to c-Cbl, CD2AP/CMS is able to recruit cortactin to the multiprotein complex necessary for RTK endocytosis (Lynch *et al.*, 2003). The PRD of CD2AP/CMS (specifically P2) binds to the SH3 domain of cortactin and, in turn, cortactin interacts with actin via the Arp 2/3 complex (Lynch *et al.*, 2003). The Arp2/3 complex is comprised of Arp2, Arp3, and five smaller (Arc) proteins; this complex binds to actin filaments and creates branch points at a 70° angle near ruffling membranes creating an "out-pushing" of the cell membrane (dos Remedios *et al.*, 2003). Possibly CD2AP interacts with both c-Cbl and Arp 2/3 to create this "out-pushing" and facilitate the formation of CCPs, actin provides the mechanical force necessary for the furthering of the endocytic process. This interaction is unique to CD2AP/CMS and indicates that it is capable of playing a role in endocytosis

distinct from Ruk_I.

Much like Ruk_I, CD2AP/CMS is able to bind CAPZ via the CD2AP/CMS C-terminal half (Hutchings *et al.*, 2003). This interaction may also play a role in receptor endocytosis by acting in concert with cortactin to link the actin cytoskeleton to endocytic machinery. CAPZ is an actin capping protein that nucleates and regulates actin assembly (see Section 1.3.1.3).

It is interesting to note that CD2AP/CMS might also bind directly to actin, as there are four putative actin-binding sites in the C-terminus of the protein (Kirsch *et al.*, 2001). Despite the lack of evidence pointing to a direct CD2AP/CMS-actin interaction, the presence of putative actin binding sites in CD2AP/CMS distinguishes it from Ruk_I. It is possible that CD2AP/CMS does bind directly to actin leading to unique methods of CD2AP/CMS regulation of actin cytoskeleton.

Thus, the pattern of events as hypothesised by some researchers is as follows: The RTK binds its ligand and causes the phosphorylation of c-Cbl. Phosphorylated c-Cbl is then able to recruit CD2AP/CMS, with the constitutively bound endophilin, to the activated RTK. c-Cbl is free to ubiquitinate the RTK to target it for degredation; endophilin promotes the cell membrane invagination process; and CD2AP/CMS binds to cortactin. Cortactin binds to and activates the Arp 2/3 complex and CAPZ to produce an "out-pushing" of the cell membrane, further promoting the endocytotic process.

1.8 Dimerisation is possible between CD2AP/CMS and Ruk proteins

Due to the similarity between CD2AP/CMS and Ruk_I, it is likely that a heterodimerisation can occur between it and Ruk_I, similar to the homodimerisation

between the different Ruk isoforms. This dimerisation is thought to occur through the CCD and could play a role in attenuating the function of both CD2AP/CMS and Ruk_I. Currently, only Tibaldi and Reinherz (2003) have shown a dimerisation between CD2AP/CMS and the Ruk proteins. This interaction is achieved through the SH3A domain of CD2AP/CMS binding to the PRD of Ruk_I. However, this interaction was shown to be weak and of unknown significance. Despite the unknown significance of the CD2AP/CMS and Ruk_I dimerisation, it is known that Ruk_I has a significant role in many different physiological functions. Recent work has lead to the theory that Ruk_I acts as a scaffolding protein that spatio-temporally coordiantes functions such as RTK endocytosis, FA formation, PI3K activity and B/T cell development and function.

Chapter 2:
Materials and Methods

2.1 Sterilisation techniques

All solutions and glassware for molecular biology techniques were autoclaved at 15psi for 20 minutes to ensure sterilisation. All plasticware were purchased pre-sterilised except in the case of pipette tips and microcentrifuge tubes which were autoclaved as for solutions and glassware.

2.2 Initial growth and storage of bacteria

The bacterial strains used in this molecular biology work were grown on LB agar with the appropriate antibiotic as indicated.

Stocks of bacteria strains were kept at –70°C as described below and were streaked out onto LB agar Petri dishes using a pre-sterilised plastic loop. The dishes were incubated inverted at 37°C overnight or until colonies appeared. A single colony was "picked" using a sterile pipette tip and used to inoculate ~10 ml of LB containing the appropriate antibiotic. The culture was incubated with shaking at 37°C for 16 hours.

Bacteria on Petri dishes and in liquid cultures were stored at 4°C for up to two weeks. For long-term storage of bacteria, 3 volumes of liquid culture were mixed with 1 volume sterile glycerol in sterile microcentrifuge tubes and frozen at –70°C.

2.3 Plasmid preparation

For small-scale plasmid preparation, 10ml liquid cultures were prepared as indicated above. The DNA was extracted using the Nucleospin™ (Machery-Nagel) plasmid mini-preparation kit. 1.5 ml of the overnight culture was put into a sterile 1.5 ml microcentrifuge tube and centrifuged at 13,000 rpm for 5 minutes (all given speeds are for a standard tabletop microcentrifuge). The supernatant was discarded

and another 1.5 ml of the culture was pelleted in the same tube to obtain a larger amount of starting material for DNA extraction. Thereafter, the protocol provided with the kit was followed.

For large-scale plasmid preparations, 1 ml of bacterial suspension from the 10 ml overnight cultures described above was used to inoculate 150 ml of LB broth containing the appropriate antibiotic. The culture was incubated overnight (16 hours) at 37°C with shaking. Bacteria from the entire culture were collected by centrifugation at 5,000 x g for 5 minutes and the supernatant was discarded. The protocol provided with the Maxiprep kit (Sigma-Aldrich) was then followed.

2.4 Quantification of DNA

DNA was quantified by measuring absorbance at 260 nm using a spectrophotometer as described in Sambrook and Russell, 2001.

The spectrophotometer was equilibriated with dH_2O, after which the absorbance (optical density) of a diluted DNA sample (1:100) in dH_2O was measured. The reading at 260 nm was taken and the DNA concentration was calculated from the reading using the following equation:

Concentration of DNA in sample ($^{\mu g}/_{ml}$) =Absorbance at 260nm x 50 x 100

1 OD_{260}= 50 $^{\mu g}/_{ml}$ double stranded DNA

To further confirm the quantity of DNA and its purity, a small sample of the DNA was run on an agarose gel electrophoresis as described below and compared to the known amounts of DNA found in the 1 kb and 100 bp ladders (Helena Biosciences).

2.5 Restriction endonuclease digest of plasmids

Restriction endonuclease digests served multiple purposes including verifying the identity of plasmids and constructs, subcloning fragments of DNA into the multiple cloning sites of vectors, and identifying the orientation of the ligated fragments within the vectors. These digests were performed in a similar manner as described by Sambrook and Russell, 2001.

Small-scale digests were prepared by mixing the following:

0.5-2 μg DNA

2 μl 10X Buffer (specific buffer supplied with each enzyme)

5 units of enzyme(s) (Promega unless otherwise indicated)

sterile dH_2O to 20 μl

The reaction was carried out at 37°C for 30 minutes to an hour.

Double digests were also performed, using a buffer compatible to both enzymes.

Large-scale digests were performed in order to prepare DNA fragments and plasmids for subcloning. 10-20 μg of DNA was digested with 50 units of enzyme, 5 μl of 10X buffer and sterile dH_2O to 50 μl. This mixture was incubated at 37°C for 2 to 3 hours.

2.5.1 Partial restriction digestion of DNA

20 μg of DNA was diluted with sterile dH_2O to a total volume of 270 μl and 30 μl of the appropriate 10X enzyme buffer was added. This 300 μl was split into three aliquots, 150 μl, 100 μl and 50 μl. 7 U of enzyme were added to the 150 μl aliquot and well mixed. 50 μl was removed from the first aliquot, added to the 100μl

aliquot and well mixed. 50 µl was removed from this second aliquot and added to the third, 50 µl, aliquot. All of the aliquots measured 100 µl with 6.7 µg of DNA and decreasing amount of an enzyme.

Aliquot	Initial vol.	Final vol.	Final ezyme amount	Final DNA
1	150 µl	100 µl	5.25 U	6.7 µg
2	100 µl	100 µl	1.17 U	6.7 µg
3	50 µl	100 µl	0.58 U	6.7 µg

Each of the three digests was incubated at 37°C for 45 minutes, after which the digestion was stopped and run out on a 1% gel. The necessary band was excised and purified as detailed below.

2.6 Agarose gels

1X TAE (DNA electrophoresis buffer)

40 mM Tris-acetate pH 7.6

1 mM EDTA

6X Loading buffer, DNA:

0.1% ($^{w}/_{v}$) Bromophenol blue

50% glycerol

A variety of different percentage agarose gels was used for diverse applications and the protocol used is similar to that described in Sambrook and Russell, 2001. Standard 1% agarose gels were the most commonly used, therefore that protocol will be described here. A stock of 1 % agarose solution was made to 400 ml (4 g of agarose, 400 ml of TAE) and heated in a microwave until the agarose

melted. The agarose was allowed to cool to ~55°C and EtBr was added to a concentration of 1 $^{\mu g}/_{ml}$. The gel was poured into a casting tray to a desired depth and an appropriate comb was placed in the tray.

Once the gel was set, the seal at either end was removed and the gel was placed in an electrophoresis tank. The gel was covered in a thin (0.5 to 1 cm thick) layer of TAE + EtBr solution and the combs were gently removed. DNA samples were prepared for electrophoresis by a quick centrifugation and the addition of 2 µl of 6X DNA loading buffer for every 10 µl of sample. The DNA samples were placed into the wells of gel with a DNA standard marker, either the 1 kb or the 100 bp ladder, on one side. The gel was electrophoresed at 150 volts until the dye front was at the bottom of the gel (0.75 to 1 hour), after which the DNA was visualised under UV (240 nm) and a picture taken using the gel imaging system.

2.7 Extracting specific DNA fragments from gels

For subcloning fragments, the digested DNA (Refer to section 2.5) was separated out by electrophoresis as described above using a wide tooth comb to create a larger well in the gel. After electrophoresis, the gel was examined under a long wavelength (320 nm) UV light source to lessen the chance of the DNA backbone becoming nicked by UV irradiation. The desired DNA fragment was removed from the rest of the gel by excising it with a clean scalpel blade and placed in a sterile microcentrifuge tube. The DNA was extracted from the agarose gel using either the GeneClean II kit (Anachem) or the QIAquick® Gel Extraction Kit (Qiagen) and their accompanying protocols. After elution, the DNA was quantified by agarose gel electrophoresis and stored at –20°C.

2.8 Ligations

2.8.1 Fragment preparation

Fragments were excised from 10 – 20 μg of λ DNA or plasmid DNA using enzymatic digest as described in Section 2.5; followed by extraction from a 1% agarose gel as described above.

2.8.2 Plasmid preparation

The plasmid was prepared as described in Section 2.5. Unless otherwise noted, the pBluescript SK^+ plasmid was used for the vector.

10 - 20 μg of plasmid DNA was prepared by digesting with the appropriate restriction enzymes followed by a dephosphorylating step if the overhangs were the same and there was a chance of the plasmid religating to itself. The process of dephosphorylation proceeded according to the protocol provided with the Alkaline Phosphatase (New England Biolabs). This secondary reaction was incubated at 37°C for an additional 30 to 60 minutes. Unless a blunting step (described below) was necessary, both the linearised plasmid and prospective insert digests were run out on a 1% gel and the desired DNA extracted as described above.

If necessary, an additional blunting step was performed on both the plasmid and insert so that even if the insert could not be cut with enzymes that were compatible to the plasmid, the desired ligation could still be done. The blunting step was done according to the protocol provided with the DNA polymerase I large (Klenow) fragment (Promega). The enzyme was added to the digests prior to the addition of loading dye as well as its enzyme specific 10X Buffer, dNTPs (Helena Biosciences) up to 40 mM each and up to 20 $^{\mu g}/_{ml}$ acetylated BSA (Promega). The

reaction was incubated at room temperature for 10 minutes and the blunt-ended fragment or vector was purified on agarose gel as described above and used in the ligation reaction.

2.8.3 Ligation

All ligations were done according to the protocol provided with the T4 Ligase (Promega). In a sterile 1.5 ml microcentrifuge tube, 0.5 μg of the vector was mixed together with either 0.5 μg or 1 μg of the DNA fragment, 10X T4 ligase buffer, 2 μg of acetylated BSA and 1 U of T4 ligase in the final volume of sterile dH_2O to 20 μl. The reaction was incubated at 16°C overnight.

2.8.4 Subcloning PCR fragments

Specific PCR fragments (see Section 2.11) were subcloned immediately into a plasmid using the TOPO TA cloning kit (Invitrogen) and the accompanying protocol. The resulting transformed cells were plated onto Kanamycin (50 $^{\mu g}/_{ml}$, Melford), X-gal (80 $^{\mu g}/_{ml}$, Melford) and IPTG (200 mM, Melford) plates, which were incubated inverted overnight at 37°C. The colour of the colonies was further developed by incubating the plates at 4°C for 1 hour or more. White colonies were picked to inoculate 10 ml overnight cultures in LB + Ampicillin (Sigma-Aldrich) as previously described.

2.9 Preparation of competent cells

Buffer 1:

30 mM KAc

100 mM RuCl

10 mM $CaCl_2 \cdot 2H_2O$

50 mM $MnCl_2 \cdot 4H_2O$

15% glycerol

pH 5.8 with 0.2 M Acetic Acid

Buffer 2:

10 mM MOPS

75 mM $CaCl_2 \cdot 2H_2O$

10 mM RuCl

15% glycerol

pH 6.5 with 1 M KOH

200 ml of LB was inoculated with a 10 ml overnight culture of either DH5α or BL-21 cells as described in Section 2.3. The culture was grown until the OD_{600} reached 0.2-0.4 (approximately 1 to 2 hours) and chilled on ice for 5 minutes. The cells were pelleted at 5,000 x g for 10 minutes at 4ºC and resuspended in 80 ml of ice cold Buffer 1. The suspension was incubated on ice for 5 minutes and centrifuged again at 5,000 x g for 10 minutes at 4ºC. The cells were resuspended in 8 ml of ice cold Buffer 2 and incubated on ice for 5 minutes. After the incubation, the cells were aliquoted into 50 µl, 100 µl and 200 µl amounts into pre-chilled tubes and flash

frozen (either in a dry ice ethanol bath or liquid nitrogen). The aliquots were stored at –80°C until used.

2.10 Transformation

All transformations were carried out using DH5α chemically competent cells unless otherwise stated and to the protocol described by Sambrook and Russell, 2001. The DH5a chemically competent cells were removed from the –80°C, gently thawed on ice and aliquoted into 50 ml portions. 5 µl of the ligation reaction was mixed with the cells and incubated on ice for 1 hour. The cells were heat shocked in a 42°C water bath for 45 seconds and then cooled on ice for 1-2 minutes. 500 µl of LB was added to each mixture and incubated at 37°C with shaking for 1 hour. After the incubation period, the bacteria were pelleted by centrifugation at 13,000 rpm for 30 seconds and 250 µl of LB was removed. The cells were resuspended in the remaining 250 µl; 50 µl and 100 µl portions were plated on LB agar plates with an appropriate selecting agent specific to the vector used in the ligation. These plates were incubated inverted overnight (approximately16 hours) at 37°C until colonies formed.

2.11 Conditions for RNA work

All RNA related work occurred on a dedicated bench with dedicated apparatuses that were thoroughly cleaned and RNAse free. Sterile dH_2O that was RNAse free was used for all experiments and solutions.

2.12 RNA extraction

Guanadine buffer:

4 M Guanadine Isothiocyanate

25 mM Sodium Citrate

0.5% (w/v) N-Lauroylsarcosine

0.1 M 2-Mercaptoethanol

4X Loading Buffer, RNA:

0.1% BPB

25% glycerol

300 $^{\mu g}/_{ml}$ ethidium bromide

1X MOPS

RNA extractions from mouse tissues were performed similar to Sambrook and Russell, 2001. Various tissue samples were isolated from 8 day old and adult mice. Approximately 100 mg of tissue was homogenised in 500 µl Guanidine buffer by syringing up and down with needles of gradually smaller gauge. 50 µl of 2 M Sodium Acetate (pH 4.0) was added to the homogenised samples, followed by 500 µl of Acidic Phenol (pH 4.5). The samples were thoroughly mixed and kept on ice until all the samples were finished being processed to this stage.

Further deproteinisation was performed by the addition of 100 µl Chloroform and intensive shaking for 10 seconds. Phases were separated by centrifugation at 13,000 rpm for 10 minutes, after which the aqueous phase containing the RNA was removed to a new microcentrifuge tube. The RNA was precipitated by the addition of 500 µl of isopropanol; to help precipitate the RNA the precipitation mixture was

incubated overnight at -20°C.

The next day the RNA was pelleted by centrifugation at 13,000 rpm for 20 minutes. The pellets were washed with 1 ml 70% ethanol, making sure to resuspend the RNA thoroughly; dried to evaporate all the ethanol and resuspended in 400 µl of Guanidine buffer. The process of RNA extraction was repeated with the addition of 50 µl of 2M Sodium Acetate (pH 4.0), followed by 500 µl Acidic phenol and 100 µl choloroform. The aqueous phase was again separated out by centrifugation at 13,000 rpm for 10 minutes, after which it was removed to a clean microcentrifuge tube for RNA precipitaiton. 1 ml of 100% ethanol was added to precipitate the RNA and the samples were incubated overnight at -20°C. The RNA was pelleted by centrifugation at 13,000 rpm for 20 minutes and the pellet was washed in 1 ml 70% ethanol once again making sure to break up the pellet thoroughly. The RNA was then repelleted with centrifugation at 13,000 rpm for 10 minutes.

An estimation of the relative amount of extracted RNA was made based on the size of the pellets seen with the smallest pellet designated as 1 unit and all other samples designated relative to this standard. The pellets were dried in a speed-vac microcentrifuge for approximately 25 minutes at 45°C and then re-hydrated with ice-cold sterile water according to the pellet designation. Those pellets designated as 1 unit were re-hydrated in 50 µl of H_2O, 2 units of RNA were re-hydrated in 100 µl of H_2O and 3 units were re-hydrated in 150 µl of H_2O. 15 µl of each sample was prepared for loading onto an agarose gel and the remainder was frozen at –80°C for use in RT-PCR. 10 µl 1xMOPS and 20 µl Formamide/formaldehyde solution (330 µl formaldehyde per 1 ml of Formamide) and 5 µl of RNA loading dye were added

to the 15 µl aliquots of each sample and these samples were incubated at 60°C for 10 to 15 minutes before being placed on ice.

2.13 Formaldehyde gel electrophoresis

10X RNA electrophoresis buffer:

0.2 M MOPS

50 mM NaAc

10 mM EDTA

To determine the amount of RNA in each sample a 1.25% agarose gel was prepared. 2 g of agarose was melted in 88 ml of dH_2O by boiling in a microwave and cooled to approximately 55°C. 32 ml 5X MOPS and 40 ml 17% formaldehyde were heated to 55°C and added to the melted agarose. The agarose and formaldehye mixture was allowed to set as described in Section 2.6. The gel tank was filled to almost level with the gel, but not covering the top, with 1X MOPS and the wells were filled with a 1:3 solution of formaldehyde and 1X MOPS. 7 µl of the ready to load RNA was loaded onto the gel and run at 100v for approximately 20 minutes before being examined under UV light. If the quantities of RNA were reasonably even, the gel was run further until the BPB reached the end of the gel to accurately predict the amount of RNA in each lane.

2.14 RT-PCR

The empirical gel determined the amount of RNA in each sample and was used to equalise the amount needed for the RT-PCR. 1µl of P8 spleen, brain and kidney; 2 µl of P8 heart; 2.5µl of P8 skin and testes; 5 µl adult skin and 10 µl of P8

thymus, P8 lung, adult thymus and adult testes were used for each cDNA synthesis reaction. 1 µl of 500 $^{\mu g}/_{ml}$ Oligo $(dT)_{15}$ primer (Invitrogen), 1 µl of 10mM dNTPs (Helena Biosciences) and sterile dH_2O to 12 µl per reaction were mixed together with the RNA aliquots. This mixture was heated at 65°C for 5 minutes after which, 4 µl of 5X Superscript II buffer and 2 µl of 0.1M DTT (Invitrogen) were added. The mixture was then incubated at 42°C for 2 minutes prior to the addtion of 1 µl per reaction of Superscript II (Invitrogen). This reaction was then allowed to proceed for 50 minutes at 42°C and stopped by incubation for 15 minutes at 70°C.

When the cDNA was sythesised, aliquots were taken and used in subsequent PCRs with specific primers. The remainder of the cDNA was stored at –20°C.

2.15 Polymerase Chain Reaction (PCR)

The general PCR recipe used was as stated in Sambrook and Russell, 2001.

	Reaction composition	Supplier
DNA:	1 pg to 1 µg	
Primers:	0.5 mM	Thermo-Hybaid
$MgCl_2$:	1.0-3.5 mM	Promega
dNTPs:	200 µM	Helena Biosciences
Taq:	1-5 U	Promega
10X buffer:	1X	Promega

The general PCR programme used was as follows:

Temperature	Time	
95°C	0.5 minute	\
T_M of primers -5°C	1 minute	20 to 25 cycles
72°C	0.5 minute for every 500 bp of final product	/
72°C	10 to 30 minutes	
4°C	Hold	

The T_M of the primers was calculated by the manufacturers and the Mg^{2+} concentration was determined empirically though trial PCR reactions. Final products were visualised on a 2% agarose gel as previously described in Section 2.6. For work requiring high fidelity and extensions greater than 1.5 kb, either the Roche Expand High Fidelity PCR system was used following the manufacturer's instructions or the Pfu polymerase (Promega) with the above programme and recipe.

2.15.1 Transcript amplification from cDNA

After creating the first strand cDNA using the RT-PCR protocol as described above (Section 2.14), individual transcripts were amplified using the given PCR recipe and the primers described in Section 3.2.2 and Figure 3.1. The programme used for amplification is described below. The amount of cDNA used as template in each reaction was normalized using standard L27 primers.

	Reaction composition	
DNA:	empirically determined	
Primers:	0.5 mM	
$MgCl_2$:	1.5 mM	
dNTPs:	200 μM	
Taq:	1-5 U	
10X buffer:	1X	
Temperature	Time	
94°C	0.25 minute	\
62°C	0.5 minute	45 cycles
72°C	0.5 minute	/
4°C	hold	

2.15.2 ES clone screening using PCR

ES clones were initially screened using PCR in order to determine clones that did not contain the recombined DNA (see Section 2.46). The above recipe was used with the primers and programme described in Section 4.2.2 and Figure 4.18:

	Reaction composition
DNA (from Section 2.46):	1 μg
Primers:	0.5 mM
$MgCl_2$:	2.0 mM
dNTPs:	200 μM
Taq:	1-5 U
10X buffer:	1X

Temperature	Time	
94°C	0.5 minute	\
50°C	0.5 minute	30 cycles
72°C	1 minute	/
72°C	10 minutes	
4°C	hold	

2.15.3 GST-SH3 constructs

The above general recipe and programme (Section 2.15) was used with the following primers to create a construct containing the SH3 domains tagged with GST. Full-length cDNA *Ruk*$_I$ was used as the template. The GST tagged proteins were then expressed in BL21 cells as described in Section 2.55.

SH3C primers

SH3Cfor: GCCCGAATTCCTGCAAAGTAATATTTCCATATGAG

SH3Crev: GCCTCGAGCTATGACGGAAGTAACTTCAC

2.15.4 ΔSH3 constructs

The above general recipe and programme was used with the following primers to create a *Ruk* construct lacking either SH3B or SH3C. Full-length *Ruk*$_I$ cDNA was used as the template and the products was transformed into TOPO plasmids (see Section 2.8.4).

ΔSH3B primers

dB1: GCGGCCGCCTGGCATCGGCGTCTCCGTC

dB2: GCGGCCGCGTCAGGGGAGTCGGATGAGC

ΔSH3C primers
dC1: GCGGCCGCTTTGCAGTAATCCTTGGTC

dC2: GCGGCCGCGTCAGACTTCGACAAGGAAG

2.16 Conditions for phage work

All work with phages and MRA cells took place in a sterile hood with a level floor. Between uses, the hood was sterilised with 70% EtOH and a 20 minute exposure to UV light. Separate incubators were used for the phage infected cells and regular bacteria work. A 129Ola mouse genomic library in λ FIX II vector (Stratagene) was used during this screening process.

2.17 Growing MRA cells

MRA cells from a glycerol stock were streaked out onto a 1.5% LB agar plate without any antibiotic and were incubated inverted overnight at 37°C. A single colony was picked from the plate and used to inoculate 5 ml of NZY media (Invitrogen) without antibiotic. This starter culture was incubated over the day or overnight with shaking at 37°C. $MgCl_2$ (final concentration 10 mM) and Maltose (final concentration 0.2%) was added to a larger volume, 100 to 250 ml, of NZY media and prewarmed to 37°C. The 5 ml culture was then used to inoculate the larger volume of NZY with Mg-Maltose and allowed to grow for 1-2 hours until the absorbance at 600 nm was between 0.3 and 0.6. The amount of cells in the culture were calculated using the following formula:

$$1\ OD_{600} = 7\text{-}8 \times 10^8\ \text{cells/ml}$$

The cells were collected by centrifugation at 5,000 x g for 15 minutes, after which the NZY media was carefully drained off. The MRA cells were resuspended in 40 ml of ice-cold 10mM $MgCl_2$ and kept at 4°C for up to a month.

2.18 Primary library screening

10^{10} MRA cells per 5 x 10^4 phage forming units (pfu) were mixed together in a 7 ml bijou, and incubated at room temperature for 5 to 10 minutes. 0.7% agarose in NZY was melted, cooled to 50°C and 5 ml mixed with the infected cells. The agarose and cell mixture was poured onto square (10 x 10 cm) LB agar plates and allowed to set in the hood for approximately 15 minutes. The plates were incubated inverted at 37°C overnight, after which they were chilled to 4°C for at least 30 minutes.

Three pieces of Hybond N+ (Amersham-Pharmacia) per plate were cut to 9 cm^2 and were labelled on the bottom right hand corner with the plate number, lift number and screening number. The pieces of membrane were carefully pressed onto the plates with the writing facing up so that no air bubbles occurred, and orientated with random needle punctures. After puncturing, each lift was carefully removed using forceps and placed DNA side up, writing side down, onto a clean sheet of 3MM filter paper to dry. Another lift was taken by placing another membrane onto the plate and puncturing the membrane in the same places as the first before being placed next to the first lift. This was repeated once more for the third lift. The needle holes were then carefully marked on the base of the plate.

As shown in Figure 2.1, clean trays were dotted with 2 ml aliquots per filter of Denaturing solution (0.5M NaOH), Wash solution (0.5M Tris-HCl pH 7.2) and Colony Lift Neutralising solution (0.5 M Tris, pH 7.4; 1.5 M NaCl).

The filters were each placed on the aliquot of Denaturing solution, DNA side up, for 10 minutes, followed by 2 minutes in the Wash solution aliquots and 10 minutes on an aliquot of Neutralising solution. After this process, the filters were removed to a clean sheet of 3MM filter paper to drain off excess solution. To fix the DNA to the membrane, the lifts were placed DNA side down onto a UV transilluminator for irradiation at 320 nm for 5 minutes.

2.19 Radiation work preparation

All work with radiation was performed behind certified radiation screens following prescribed protocols for containment. The bench, water bath, microcentrifuge and hybridisation chamber were both monitored before and after each use for contamination and appropriate safety precautions were taken.

2.20 Oligonucleotide probe production

STES:

50 mM NaCl

10 mM Tris-HCl, pH 7.6

1 mM EDTA

1% (w/v) SDS

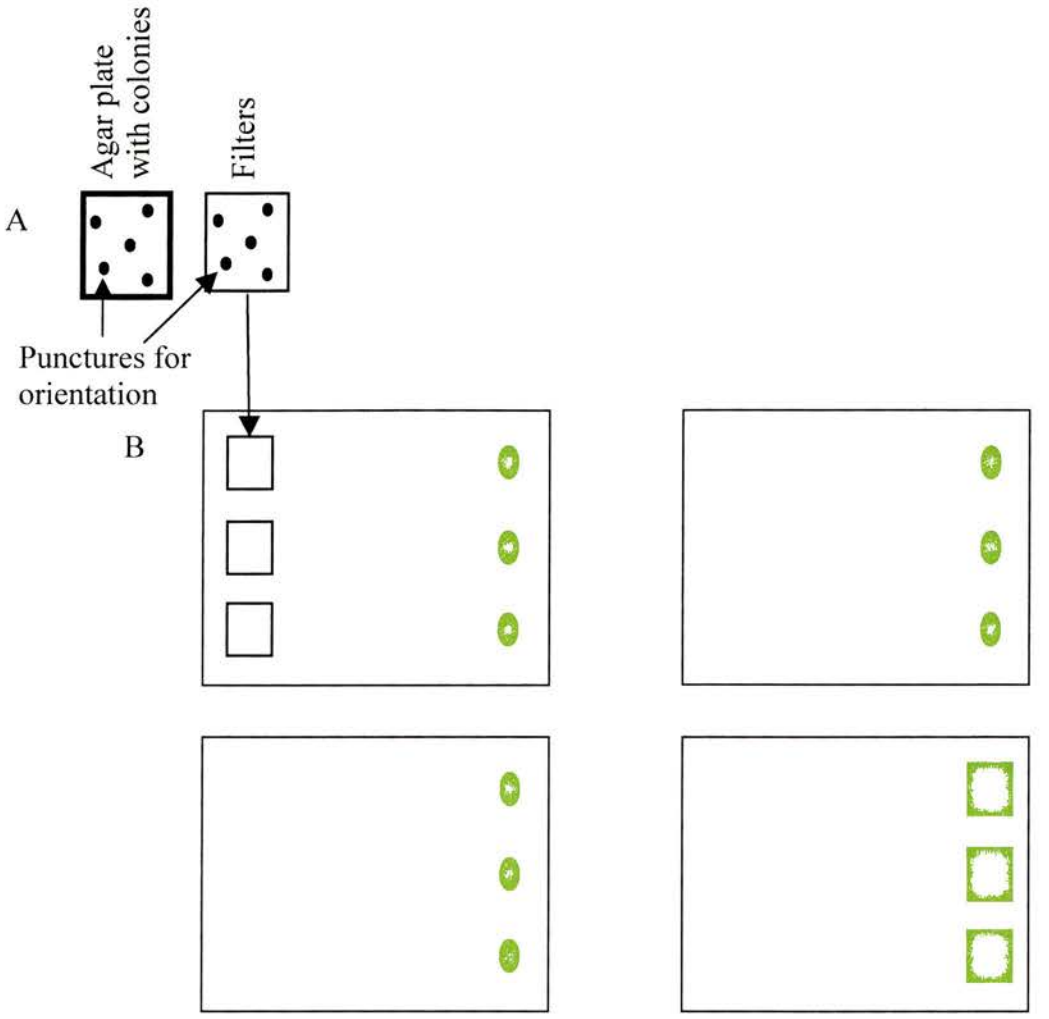

Figure 2.1: The filter is placed on the agar phage Petri dishes and both are simultaneously punctured. The filter is then placed DNA side down on Denaturing buffer (light blue), then Wash solution (yellow) and finally Neutralising solution (green).

1M NaPhos:

Empirically determined by mixing

1 M Na_2HPO_4

1 M NaH_2PO_4

until pH 7.0

All of the oligonucleotides used for hybridisation probe production were synthesised by Thermo-Hybaid Interactiva. 100 pmoles of the oligonucleotide were mixed together with 2 ml 10X T4 polynucleotide kinase buffer (Hybaid) and 60 μCi of the radionucleotide [γ-^{32}P] ATP (Amersham-Pharmacia) in a total volume of 19 μl. 1 μl of T4 polynucleotide kinase (PNK, Hybaid) was added to bring the volume to 20 μl and the reaction was incubated at 37°C for 1 hour.

[γ-^{32}P] ATP incorporation was tested by spotting 0.25 μl of the reaction onto a piece of DE81 filter paper and the initial radioactivity level was measured using a Geiger counter. A suction pump with filtering funnel was setup with a fresh filter paper No. 1 that was wetted with ice-cold 0.5 M NaPhos and the piece of DE81 paper with the reaction spotted on it was placed on the filter. The non-incorporated radionucleotide was washed away with ice-cold 0.5 M NaPhos, after which the radioactivity was measured again. The level of incorporation was taken as the percentage of radioactivity left after the washes; if the level of incorporation was less than 60%, 1 μl of T4 PNK was added and the reaction was incubated for a further hour. After the second incubation, the incorporation test was repeated. When the level of incorporation was satisfactory, the reaction was heated at 68°C for 20 minutes to inactivate the kinase and 100 ml of STES was added.

2.21 Probe purification

The oligonucleotide probe was purified on Sephadex Nick columns (Amersham-Pharmacia) according to the enclosed protocols. The preservative storage solution in the column was disposed of and the column was washed with STES buffer until all the preservative had been removed, 3 to 4 column volumes. The reaction was loaded into the column and allowed to drip into a clean eppendorf. Fraction 1 was collected by adding 300 ml of STES to the column, and fractions 2 to 7 were collected in 400 µl STES aliquots. The radioactivity of each fraction was assessed and the earliest fraction that had the highest level of radioactivity was used immediately in the hybridisation reaction.

2.22 Hybridisation with oligonucleotide probes

Oligonucleotide pre-hybridisation/hybridisation buffer:

6X SSC

1X Denhardt's reagent

10 mM NaPhos

10 $^{ug}/_{ml}$ tRNA

Denhardt's reagent

1% ($^{w}/_{v}$) Ficoll 400

1% ($^{w}/_{v}$) Polyvinylpyrrolidone

1% ($^{w}/_{v}$) Bovine Serum Albumin, Fraction V

1X SSC

3 M NaCl

0.3 M Sodium Citrate

Hybridisation of the colony lifts or Southern blots (described in Section 2.14) with oligonucleotide probes was done in a shaking water bath overnight. The lifts were heat sealed into a plastic bag with the pre-hybridisation solution (0.125 $^{ml}/_{cm^2}$) and incubated at 45°C with gentle agitation for 2-3 hours. The bag was cut open to introduce the hybridization solution (same as pre-hybridisation with purified probe added to it) and then re-heat sealed to make it watertight. The bag containing the hybridising lifts was sealed into another bag to ensure no leakage occurred and the bags covered with the heated water of the shaking water bath. Each corner was weighed down and the hybridisation proceeded at 45°C for 1-2 hours with gentle agitation after which the heating mechanism was turned off but the agitation was continued. The water and hybridisation reaction were allowed to cool overnight. Excess probe was washed from the membrane with 2x SSC/0.2 SDS at room temperature, with 3 changes for a total of 30 minutes. The membrane was exposed to X-ray film for no more than 2 hours at –80°C and developed as described below (Section 2.30). If non-specific binding occurred, the membrane was washed with 2X SSC/0.2 SDS at 37°C-50°C for 30 minutes depending on the severity of the non-specific binding.

If reprobing of the filters were necessary, they were stripped of the probe by boiling them twice in 0.1X SSC/0.1% SDS. The membrane was soaked in 2X SSC and allowed to dry at room temperature.

2.23 Identification and isolation of positive phage clones

SM buffer:

100 mM NaCl

10 mM $MgSO_4$

50 mM Tris-HCl pH 7.5

After developing the autoradiograph of the lifts, the puncture marks of the membranes were matched with their corresponding plates and the plaques that hybridized with the probe were identified. A plug of the agar from region that hybridized to the probe was taken for the 2° screening. Plugs were taken by carefully gouging out the area of interest from the rest of the dish using a glass pipette. These plugs were then placed in 0.5 ml of SM buffer, allowed to diffuse for at least 1 hour with shaking at room temperature and stored at 4°C until needed.

2.24 2° and 3° screenings

The pfu of each plug was determined by titrating the plugs taken from the initial screening. Serial dilutions were made from each diffused plug at 10^{-2}, 10^{-4}, 10^{-8}, 10^{-16} diluted in SM. 100 µl of MRA cells were mixed with 10 µl of each dilution and plated onto 10 cm circular plates as described above. The amount of phage plaques on each plate were counted and the original concentration of pfu were determined.

2° and 3° screenings occurred in the same manner as primary screenings using smaller 10 cm diameter circular plates. Screenings continued until all plaques on the plate hybridised with the probe.

2.25 Growing phage and isolating phage DNA

Phage DNA isolation Buffer 1:

300 mM NaCl

100 mM Tris-HCl pH 7.5

10 mM EDTA pH 8.0

0.2 $^{mg}/_{ml}$ BSA

store at 4°

Phage DNA isolation Buffer 2:

30% PEG 6000

3 M NaCl

Phage DNA isolation Buffer 3:

100 mM NaCl

10 mM Tris-HCl pH 7.5

1 mM EDTA pH 8.0

In a sterile microcentrifuge tube, the Mg-MRA cells and phage stock were mixed together, allowing for 5 x 10^7 pfu and 10^{10} cells. The cells and phage were left for adsorption for 5 to 10 minute at room temperature as before. $MgCl_2$ and Maltose were added to 100 to 250 ml of NZY to a final concentration of 10 mM $MgCl_2$ and 0.2% Maltose and the media was prewarmed to 37°C prior to inoculation with the phage infected MRA cells. These cells were incubated at 37°C with vigorous shaking until cell lysis and cellular debris was visible (approximately 5 to 8 hrs) after which 1µl of chloroform was added per ml of lysate.

If no cellular debris was visible after 12 hours of incubation, a 1 ml aliquot was taken and 100 µl of chloroform was added. The aliquot was incubated at 37°C with shaking for 5 to 10 minutes. If cellular debris became visible then 1 ml of choloroform was added per 50 ml of culture and the culture allowed to incubate at 37°C with shaking for 10 minutes until lysis appeared. If no lysis occurred, the phage adsportion was redone.

After lysis, the cellular debris was removed by centrifugation at 5,000 x g for 15 minutes at 4°C and the lysate was carefully removed so that no cellular debris was dislodged. A 0.5 ml aliquot of cleared lysate was taken as a stock prior to the extraction of phage DNA. To the remainder of the lysate, 0.3ml of Buffer 1 was added per 100 ml of lysate along with DNaseI (Invitrogen) to a final concentration of 10 to 15 $^{\mu g}/_{ml}$ and RNase A (Roche) to a final concentration of 30-50 $^{\mu g}/_{ml}$. This mixture was thoroughly mixed and incubated at 37°C for 30 minutes. 20 ml of ice-cold Buffer 2 was added per 100 ml of lysate and the mixture was incubated for 1 hour on ice.

PEG-precipitated phage particles were pelleted by centrifugation at 5,000 x g for 30 to 45 minutes at 4°C. The supernatant was carefully drained and the pellet resuspended in a total volume of 5 ml of Buffer 3. SDS was added to this suspension to a final concentration of 1% and Proteinase K (Invitrogen) to a final concentration of 100 $^{\mu g}/_{ml}$. The mixture was incubated at 55°C for 30 minutes to release the phage DNA. The DNA was separated from the phage proteins by two basic phenol (pH 8.0) extractions. An equal amount of phenol was added to the solution and carefully mixed by inversion, and the organic and inorganic phases were separated by centrifugation at 5,000 x g for 10 minutes. The upper, organic phase, was carefully

removed to a fresh microcentrifuge tube without disturbing the interface between the two. After the second phenol extraction the phage DNA was further purified by a 1:1 phenol:chloroform extraction. A volume of phenol that was equal to half of the volume of supernatant from the last wash was added along with the same amount of chloroform (24:1 chloroform:Isoamyl alcohol). The mixture was carefully mixed and the phases again separated by centrifugation as before, with the organic phase being taken away carefully without disturbing the interface between the two.

In order to precipitate the DNA from the aqueous phase, 1/20 of the volume of 3M NaAc pH 5.5 was added followed by 2.5 volumes of 100% EtOH. If it was immediately visible, the DNA was fished out using a plastic pipet tip and placed in 1 ml of 70% EtOH. However, if no precipitation was immediately visible, the solution was stored at –20°C overnight. DNA was pelleted by centrifugation at 5,000 x g for 5 minutes in a bench centrifuge. The pellet was washed three times in 1 ml of 70% EtOH; the DNA was repelleted by centrifugation between washes as described above. After the last wash, the pellet was allowed to dry and the DNA was dissolved in 100 µl to 200 µl of sterile dH_2O overnight at 4°C. A small aliquot of DNA was run on an agarose EtBr gel along with a known amount of marker DNA to determine the total amount and concentration of DNA isolated.

2.26 Southern blotting to nylon membranes

Blotting was carried out as described by Sambrook and Russell, 2001. The DNA of interest (1 µg of phage DNA, 20 µg of genomic DNA) digested with appropriate endonuclease(s), was run on a 1% agarose gel until the DNA was sufficiently separated. The gel was then photographed and the excess portions of the

gel were excised. In order to orientate the gel, the bottom right hand corner was also removed. The DNA was depurinated by being soaked in 0.25M HCl for 15 minutes with gentle rocking and then rinsed quickly in dH_2O to remove any traces of HCl.

2.26.1 Preparing the gel for neutral blotting

Denaturing buffer (neutral transfer to neutral membranes):

0.5 M NaOH

1.5 M NaCl

Neutralising buffer I (neutral transfer to neutral membranes):

1 M Tris (pH 7.4)

1.5 M NaCl

Alkali transfer buffer (alkali transfer to charged membranes):

0.5 N NaOH

1.5 M NaCl

To prepare the gel for neutral blotting, it was soaked in Denaturing buffer for 30 minutes with rocking, changing the solution once. The gel was rinsed again in dH_2O and soaked for 30 minutes with rocking in Neutralising buffer I, changing the solution once. To prepare the gel for alkali blotting, it was soaked in Alkali transfer buffer for 15 minutes with rocking.

2.26.2 Preparing the membrane

Neutral transfer buffer

10X SSC

While the gel was soaking, the Hybond N (neutral transfer, Amersham-

Pharmacia) or Hybond N^+ (alkali transfer, Amersham-Pharmacia) membrane was cut to a size slightly larger than the gel (~ 0.5 cm on each side) and 3MM Whatman paper was cut a size approximately ~1 cm on each side larger than the gel. Paper towels were also folded and cut to the same size as the 3MM paper. Enough 3MM paper to create a stack 2.5 cm thick and enough paper towels to form a stack 5 to 7.5 cm thick were cut to size. The membrane was rinsed in boiling dH_2O until completely wet and soaked in transfer buffer for 5 minutes along with 2 pieces of the 3MM paper cut to size.

2.26.3 Transferring the DNA to a membrane

The blotting apparatus (Figure 2.2) consisted of a tray with a raised platform in the middle and a thin sponge on the platform. Covering the sponge was a piece of 3MM paper that draped down into the wells on either side that were filled with transfer buffer. The gel was carefully laid face down and any bubbles between it and the wick were rolled out. For future orientation, the bottom right hand corner of the membrane was cut prior to the membrane being placed on top of the gel. Once again, any air bubbles were rolled out from between the gel and the membrane. The soaked 3MM papers were placed on top of the membrane with any air bubbles being rolled out, followed by the dry 3MM papers and the paper towels. A 500 g weight was placed on top of the paper towels to maintain the capillary action. The transfer was left to proceed overnight.

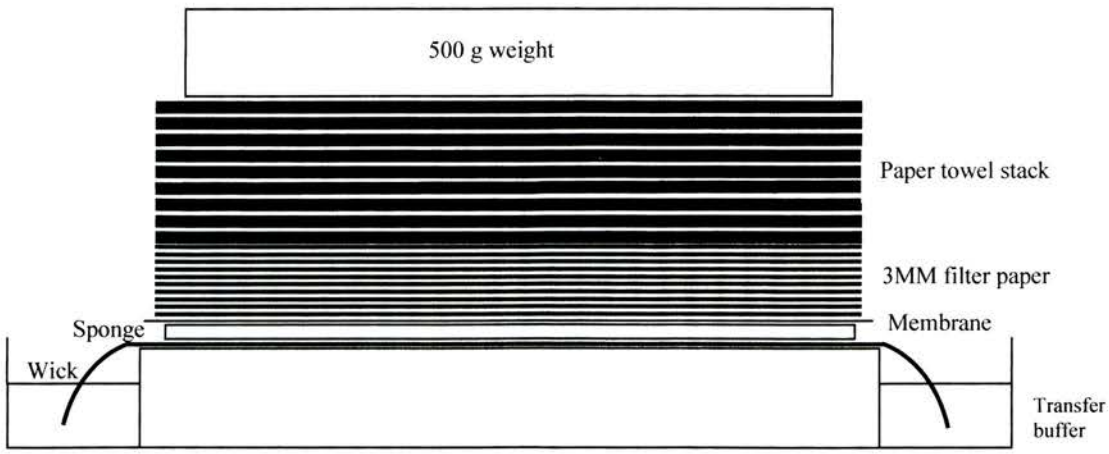

Figure 2.2: The Southern blotting apparatus.

2.26.4 Treating the membrane after transfer

Neutralising buffer II (alkali method):

0.5 M NaCl

1 M Tris-HCl

After neutral transfer, the membrane was removed from the blotting apparatus and soaked in 2X SSC for 5 minutes. The membrane was then allowed to air dry between two pieces of 3MM paper and later the DNA was cross-linked to the membrane by either baking it at 80°C for 30 minutes to 2 hours or irradiating it at 320 nm for 5 minutes.

After alkali transfer, the membrane was removed from the blotting apparatus and soaked in Neutralising buffer II for 5 minutes. Following the soak, the membrane was either dried on 3MM paper or used immediately for hybridisation.

2.27 Radioactive labeling of DNA for probe

2.27.1 Nick-translation

20-50 ng of the template DNA was mixed together with 4 µl of a mixture that includes 5X DNA polymerase buffer (Gibco); 100nM of each, dATP, dGTP and dTTP; 30 µCi of α^{32}P dCTP (Amersham-Pharmacia); and dH_2O to 16 µl. 5 pg DNase I and 5 U of DNA polymerase (Promega) were also added and the solution was thoroughly mixed. The reaction was allowed to proceed for 30 minutes at room temperature, after which the level of incorporation was tested by the TCA method as described below.

A vacuum filter was assembled, the filter covered by a piece of No 1 filter paper and the filter was wetted with 10% TCA solution. A snip of GF/A or GF/B filter paper was spotted with 0.25 µl of the reaction and the activity level of the sample was measured. The sample was moved to the filter and washed several times with 10% TCA solution. After the washes, the activity was measured again and if it was less than 30% of the original level, the reaction was allowed to continue for another 20 minutes, after which the level of incorporation was tested again. 30% incorporation was considered good and the probe was purified, while more than 65% indicated that too much template DNA was used and the labeling reaction was redone with less DNA.

The labeled probe was purified using a Nick column as previously described for oligonucleotide probe production (Section 2.18). The fraction with the highest radioactivity and the fraction prior to it were taken to precipitate the labeled DNA probe out of them. The following were added to the fraction in order to precipitate the DNA:

5 to 10 μg tRNA

$^{1}/_{20}$ volume NaAc (ph 5.5)

2.5 volumes absolute EtOH

This precipitating mixture was either snap frozen or incubated in the –20°C freezer for 2 or more hours. After the DNA precipitated out of the solution, it was pelleted by microcentrifugation at 13,000 rpm for 5 minutes. The supernatant was drained off and the pellet was allowed to dry for no more than 1 hour before being resuspended in 100 μl of dH_2O. The probe was denatured by adding 5 μl of 10N NaOH and incubated at 58°C. The NaOH was neutralised with 50 μl 2M Tris-HCl prior to the probe being introduced directly to the hybridization solution.

2.27.1 Random primer labelling

The Megaprime kit (Amersham-Pharmacia) was used to create radioactive probes to use in the Rapid-Hyb buffer (Amersham-Pharmacia). The instructions included with the kit were followed and 25 ng of template DNA was labelled with 50 μCi α^{32}P dCTP. The resulting probe was used unpurified in Rapid-Hyb buffer as described below.

2.28 Pre-hybridisation/Hybridisation of nylon membranes

2.28.1 4X SSC buffer

Southern pre-hybridisation/hybridisation buffer (neutral membranes):

4X SSC

5X Denhardt's reagent

0.2% SDS

5 mM EDTA (pH 8.0)

15 mM NaPhos (pH 7.0)

100 $^{\mu g}/_{ml}$ sonicated salmon sperm DNA

Sterile distilled water to volume

Pre-hybridisation and hybridisation of DNA probes to Southern blots occurred as described by Sambrook and Russell, 2001. For pre-hybridisation, the buffer was pre-warmed along with the roller bottle and the hybridisation chamber to 65°C. The membrane was then introduced into the roller bottle and 5 to 10 ml of pre-hybridisation buffer was added. Any air bubbles that formed between the membrane and the bottle were rolled out. Pre-hybridisation occurred for 2-3 hours, after which the radioactive probe was added. Hybridisation occurred overnight for 16-18 hours.

2.28.2 Rapid-Hyb

The hybridisation chamber, hybridisation tubes and Rapid-Hyb were all pre-heated to 65°C. The membranes were pre-hybridised in Rapid-Hyb for 15 to 60 minutes after which the probe was added to the Rapid-Hyb at a concentration of 2.5 $^{ng}/_{ml}$; hybridisation proceeded for 2 to 5 hours.

2.29 Post-hybridisation washes

2.29.1 After hybridisation in 4X SSC buffer

Post hybridisation washes occurred as described by Sambrook and Russell, 2001. After the hybridisation buffer was drained off, the filter was rinsed in the roller bottle at room temperature in 20 ml of 2X SSC. The 2X SSC was replaced by 20 ml of 2X SSC, 0.2% SDS (warmed to 65°C) and the filter was washed for 20 minutes at 65°C; the wash was repeated once. A higher stringency wash, 0.2X SSC/0.2% SDS, was sometimes used at the same conditions of the lower stringency wash.

2.29.2 After hybridisation in Rapid-Hyb

Following hybridisation, the membranes were washed with 2X SSC, 0.1% SDS at room temperature for 20 minutes. The membranes were then washed in low stringency wash (1X SSC, 0.1% SDS) at 65°C for 15 minutes. This wash was repeated once and, if necessary, was followed by two washes in high stringency wash (0.1X SSC, 0.1% SDS) at 65°C for 15 minutes.

2.30 Exposure to flim

Excess wash solution was drained off the filter and the filter was carefully wrapped in plastic wrap. The filter was sealed into the plastic wrap with tape and secured to the back of a cassette. A piece of X-Omat Kodak film (Sigma-Aldrich) was placed in the cassette between 2 Hi-Speed X intensifying screens. The cassette was incubated at –70°C for 2 to 48 hours depending on the strength of the signal on the membrane. Northern blots were typically exposed for 48 to 72 hours.

2.31 Developing flim

X-ray films were developed using normal developing techniques. The frozen cassettes were allowed to thaw to room temperature and the film inside was placed into Kodak GBX developer and replenisher (Sigma-Aldrich) for 2 minutes. The film was rinsed in H_2O and then placed in Kodak GBX fixer and replenisher (Sigma-Aldrich) with gentle agitation for 2 to 5 minutes. Excess fixer was rinsed off with H_2O and the film was allowed to air dry.

2.32 Conditions for tissue culture work

Between each use, all hoods were sprayed with 70% EtOH and UV irradiated. All bottles, gloves and hands that entered the hood were also sprayed with 70% EtOH. All solutions were stored at 4°C and pre-warmed to 37°C unless otherwise stated and all incubations were done at 37°C with 7% CO_2 unless otherwise stated. After trypsinisation of cells, the media was changed at 24 hours and thereafter 48 hours unless otherwise stated. All media was from Invitrogen unless otherwise stated and all plasticware was from Nunc.

2.33 Handling non-ES cell lines

Cos7 and Hek293 cell lines were grown in DMEM+10% FBS on 10 cm diameter dishes. For defrosting, an aliquot of the line was removed from the cryo-facility and immediately thawed in a 37° water bath. Once entirely defrosted, the cells and freezing solution were diluted into 10 ml of DMEM+FBS and centrifuged at 300 x g for 5 minutes; the media was carefully aspirated off of the cell pellet. The cells were re-suspended in 10 ml of DMEM+FBS, and plated onto 10 cm diameter

Petri dishes and incubated overnight at 37°, 5% CO_2. The media was changed after 24 hours and every 48 hours thereafter until the cells reached 90% confluency.

To prepare the cells for trypsinisation, the dish was washed in sterile PBS and 1 ml of trypsin solution was placed on the cells. The dish was incubated in the trypsin at room temperature for 5 minutes or less, until the cells became dissociated from the dish. The trypsinisation process was stopped by the addition of 10 ml DMEM+10% FBS and the cellular clumps were broken up by repeated pipetting. The suspended cells were then split into either a 1:5 or 1:4 dilution onto new 10 cm diameter Petri dishes and the volume was adjusted to 15 ml. The cells were allowed to expand in the same conditions described above until they reached 90% confluency, and they were expanded again. The night before tranformation, the cells were trypsinised and split according to how many dishes would be necessary for the experiment.

2.34 Preparation of plates for ES cell culture

An 0.1% gelatine solution was made in order to prepare plates for ES cell work. A 2% gelatine solution (Sigma-Aldrich) was warmed to 37°C and 25 ml was added to 475 ml of Tissue Culture grade water. The final 0.1% gelatine solution was filter sterilised and aliquoted out into 50 ml Corning tubes. To gelatinise the plates, enough of the 0.1% gelatine solution was added to cover the bottom surface of the plate and then aspirated off, leaving a thin layer of gelatine on the surface. The plates were then allowed to dry in the hood until the solution had completely evaporated. When dry, the plates were used immediately or covered by foil to prevent UV light from damaging the gelatine layer.

2.35 LIF preparation and titration

Cos7 cells were transfected with a LIF expression plasmid DNA (gift of A.G Smith) using Lipofectamine 2000 (Invitrogen) and following the provided protocols. The media was changed 5 hours after the addition of Lipofectamine to DMEM+10% FBS and the cells incubated at 37°C with 5% CO_2. The media was collected 48 hours after the media change into 50ml centrifuge tubes and spun at 300 x g for 5 minutes to pellet any cellular debris. The supernatant was taken off, separated into 1 ml aliquots and stored at –80°C until needed. Prior to use with electroporated ES cells, the working concentration of the LIF was empirically determined using a titration.

An aliquot of ES cells were defrosted and allowed to grow onto a 10 cm diameter dish until sub-confluent (See Section 2.36). The cells were then trypsinised as for passaging and seeded onto ten 3.5 cm diameter dishes at relatively low densities ($<10^5$ cells per cm^2). The LIF was diluted into complete media with ES FBS but without LIF (recipe below) as follows:

1:100, 1:500, 1:1000, 1:5000, 1:10,000, 1:50,000, 1:100,000, 1:500,000

As a positive control, one dish contained a known differentiation inhibiting concentration of LIF, and as a negative control, one dish contained no LIF. The cells were allowed to grow for 7 days before staining with Geimsa stain (VWR). The degree of differentiation was assessed based on cell morphology and the concentration of LIF that definitely inhibited differentiation was decided.

2.36 Defrosting ES cells

Complete media:

DMEM

10X ES FBS (HyClone)

1X MEM

1X L-glutamine

0.11 mM 2-mercaptoethanol

0.1% Penicillin-Streptomycin

LIF empirically determined (see above for titration)

The vial of ES cells were recovered from the cyro-facility and placed in the 37°C H_2O bath. To facilitate thawing, the cells were gently mixed twice during the thawing period. Using a P1000, the cells were carefully pipetted into 30 ml of complete media and spun at 300 x g for 5 minutes. The meda was aspirated off and the cells were resuspended in 15 ml of complete media. This suspension was then transferred to a 10 cm diameter gelatinised Petri dish and incubated overnight. The media was changed at 24 hours and then every 48 hours until the cells were 70% to 80% confluent when they were passaged as described below (Section 2.37).

2.37 Passaging cells

The media in the plate was aspirated off and replaced with DMEM in order to wash away the FBS. The wash was aspirated off and trypsin solution was added (the minumum amount needed to cover the bottom of the plate or well). The trypsinisation was allowed to proceed at room temperature for 5 minutes and then checked for detaching from the surface. If necessary, the side of the dish was gently

tapped to help dissociate the cells from the plate or well. Complete media was added to stop the trypsinisation process. The usual amount of complete media added was 10X the amount of trypsin solution, or the maximum that the plate or well could hold. The cells were gently pipetted up and down using a P1000 or a 10 ml pipette in order to form a single cell suspension and to remove all the cells from the gelatine layer. This suspension was then aliquoted into the necessary number of new plates or wells and incubated overnight. After 24 hours the media was changed to remove any dead cells and all traces of trypsin. The cells were then treated as normal with 48 hour changes to the media.

2.38 Preparing ES cells for electroporation

Three 10 cm diameter dishes of ES cells at 70-80% confluence were used for electroporation. To prepare the cells for elecroporation, the cells were trypsinised as for passaging except a bit longer to ensure all of the cells were dissociated and to help form a single cell suspension. The cells were gently pipetted to form a single cell suspension. The suspension was placed in a sterile 50 ml centrifuge tube and the cells pelleted by centrifugation at 300 x g for 5 minutes. The cells were washed with 50 ml of PBS, making sure to resuspend the cells thoroughly in the PBS. (The PBS was made using Tissue Culture grade water and filter sterilised. Each aliquot was re-filter sterilised immediately prior to use.) The cells were pelleted again at 300 x g for 5 minutes and the PBS gently aspirated off. The cells were finally suspended in 700 µl of PBS and gently pipetted into the elecroporation cuvette.

2.39 Preparing DNA for electroporation

50 μg of the targeting plasmid DNAwas isolated and cut with Not I for 3-4 hours. After 2 to 3 hours a 5 μl aliquot was run out on a 1% gel alongside uncut plasmid to check for complete digestion. When adequate digestion had occurred, the linearised plasmid was deproteinised by mixing with an equal amount of basic phenol and chloroform (1:1). The aqueous and organic layers were separated by centrifugation for 10 minutes at 13,000 rpm. The aqueous layer was removed to a new microcentrifuge tube and the extraction was repeated using an equal amount of chloroform. The linearised plasmid was precipitated overnight at –20°C by adding 1/20 of the volume in 3 M NaAc and 2.5 volume of 100% EtOH. The next day, the DNA was pelleted by centrifugation at 13,000 rpm for 5 minutes. The ethanol was removed and the DNA was washed with 75% EtOH three times. The DNA was left under the last 75% EtOH wash at –20°C until the ES cells were ready for electroporation. When the cells had sufficiently expanded, the EtOH was removed and the DNA was dried in the tissue culture hood. The DNA was re-dissolved in 100 μl of PBS and a small (1-2 μl) aliquot was run out on a gel to determine the concentration. If necessary, the concentration of the DNA was adjusted with the addition of more PBS to a concentration of $0.2^{\mu g}/_{\mu l}$. A 100 μl aliquot of DNA was kept on ice for electroporation and any unused DNA was stored at –20°C until needed for further electroporations.

2.40 Electroporating ES cells

The cells and DNA were gently mixed in the electroporation cuvette and the cuvette was placed in the Gene Pulsar electroporator (Bio-Rad); the capacitance and

voltage were set at 500 μF and 240 V correspondingly. The cells were electroporated and the time constant was marked down. The cuvette was removed from the electroporator and the cells were allowed to rest for 20 minutes at room temperature. 50 ml of complete media with LIF and FBS was placed in a centrifuge tube and the electroporated cells were gently transferred from the cuvette to the media. The remainder of the cells was gently rinsed from the cuvette using a P200 and P20 to get all of the cells out. The cell suspension was aliquoted out into ten 10 cm diameter dishes at varying densities by adding between 1 ml and 10 ml of the cell suspension per dish and the final volume of each plate were adjusted to 15 ml per dish with complete media. The cells were incubated overnight and the media changed at 16 hours. After the initial change, the media was changed twice a day to remove dead cells and cellular debris.

2.41 Antibiotic selection of clones

To select for cells that had successfully incorporated the plasmid into their genomic DNA, antibiotics specific to the plasmid were added to the media. 48 hours after electroporation, Geneticin (Invitrogen) was added to a final concentration of 0.15 $^{mg}/_{ml}$ to all the plates. 96 hours after electroporation, Puromycin (Sigma-Aldrich) was added to a final concentration of 1.56 $^{\mu g}/_{ml}$ to half of the plates; thus, half of the plates were under single antibiotic selection while the other half was under double antibiotic selection. The media was changed twice a day to remove dead cells and cellular debris.

2.42 Isolating colonies of ES cells

Colonies began to form within 4 to 5 days of electroporation and were ready to be expanded onto 96 well plates by 7 days.

Prior to isolating individual colonies (picking), 96 well plates were prepared by gelatinising the even numbered rows. The colonies suitable for isolation were circled on the bottom of the dish with a different coloured pen for each day of picking. The complete media in the dish was aspirated off and replaced with 10 ml of DMEM. The DMEM wash was aspirated off to remove all traces of FBS and replaced with 5 ml of DMEM to cover the cells during "picking". 10 μl of trypsin was added to each odd numbered row of a 96 well plate.

Each colony was removed from the plate by being suctioned off the bottom into a yellow tip. The colony was then transferred into the 10 μl of trypsin and allowed to rest there until the entire row had been filled. Using a multi-channel pipette, 150 μl of complete media with antibiotic(s) was added to each well and the colony was carefully pipetted up and down to separate the cells. The cell suspension was then transferred to the even, gelatanised, row next to it. When all the even numbered rows were full, the plate was incubated overnight.

Approximately 1/3 to 1/2 of the colonies did not survive picking, but those wells with cell growth were carefully marked and watched for colour change. When the media turned yellow, 5 days after picking or less, colonies were expanded onto 4 well dishes.

2.43 Expanding clones to 4 well dishes

The clones selected for expansion were washed in the 96 well plates with

200 µl of DMEM that was carefully aspirated off. 100 µl of trypsin was added to the well and allowed to incubate at room temperature for 5 minutes. 300 µl of complete media with antibiotics(s) was added to the well and pipetted up and down. The resulting cell suspension was transferred to a well of a 4 well plate that contained 750 µl of complete media with antibiotic(s) and pipetted up and down again. When the 4 well plate was full, the dish was incubated in the CO_2 incubator as described above until the cells reached 70-80% confluence.

2.44 Triplicating clones

When the clones in the 4 well plates were suitably confluent they were triplicated to prepare the cells for analysis and freezing. In order to have clones in a 4 well plate growing at approximately the same rate, each clone was matched with three other clones at approximately the same confluence and passaged. Three separate gelatinised 4 well plates were prepared with 500 µl of complete media with antibiotic(s) in each well and each was marked with the same designation (ie Dish 1). Being careful to keep corresponding wells aligned, 200 µl of the trypsinised cell mixture was added to the same well in each plate so that each plate had the same clone in their corresponding wells. The cells were incubated until the majority of clones on the plate reached 50-80% confluence and were ready to freeze.

2.45 Freezing clones

Freezing solution (store at +4°C):

DMEM

10% DMSO

20% FBS

Prior to freezing the plates, two large cardboard boxes were placed in the –80°C freezer and marked as 1° and 2°. Small polystyrene boxes were also prepared by lining them with white towel roll and strips of cling film the size of the 4 well plates were prepared. Of the triplicate plates (See Section 2.43), one of the plates was marked as 1°, one as 2° and the last as DNA.

The media on the 1° and 2° plates was aspirated off and replaced with 400 µl of the freezing solution. The plates were individually wrapped in a strip of cling film and placed in the polystyrene boxes; a maximum of 6 plates per polystyrene box and the plates designated 1° and 2° in different polystyrene boxes. The plates were kept level so that the cells were completely covered with the freezing mixture and put into the –80°C exactly level. The next day, the plates were removed from the polystyrene boxes and placed into the pre-cooled cardboard boxes. These plates can be kept at –80° for a maximum of 2 months without a substantial decrease of cell viability.

The plates marked as DNA were left to grow until 100% confluent. The media was then aspirated off the cells and the plates were frozen at –20°C overnight or until ready to extract DNA.

2.46 Isolation of DNA from ES cell clones

A master mix of STES and proteinase K (0.1 $^{mg}/_{ml}$) was heated to 55°C. 400 µl of master mix was added to each well and left at room temperature for 5 minutes, until the cells defrost and lyse. Using blunt cut pipette tips, the bottom of the well was washed with the STES mixture to remove all the cells. The viscous mixture was transferred to an appropriately marked sterile 1.5 ml microcentrifuge tube and incubated at 55°C overnight.

The next day, 400 µl of basic phenol was added and the content of the tube was mixed well for several minutes. The phases were separated by centrifugation at 13,000 rpm for 10 minutes and the upper, aqueous phase was transferred to a new sterile microcentrifuge tube. The phenol extraction was repeated once and repeated using a 1:1 phenol:chloroform mixture. After the phenol:chloroform extraction, the DNA was precipitated out of the aqueous phase by adding 1/20 (20 µl) 3M NaAc and 2X (800 µl) of 100% EtOH. When the precipitate formed, the DNA was carefully removed to a microcentrifuge tube containing 70% EtOH and centrifuged for 5 minutes at 13,000 rpm. The pellet was washed three times with 70% EtOH after which the pellet was air-dried. 100µl of sterile dH_2O was added and the DNA was left to dissolve at 4°C overnight. An aliquot of the DNA was run out on an agarose gel to determine how much DNA was extracted from the cells.

2.47 Recovery of positive clones

Any clones that appeared to be positive from the Southern hybridisation analysis were defrosted and expanded. The 1° plate containing the desired clone was removed from –80°C and placed onto dry ice for transport to the tissue culture room. Once there, the plate was removed from the dry ice and allowed to thaw slightly at room temperature. After a slight thawing, 1 ml of warmed complete media with antibiotic(s) was added to each well on the plate. When the cells were fully thawed, the media containing DMSO was carefully removed and placed into a 3.5 cm diameter dish. The volume of this dish was adjusted by adding 2 ml of complete media and it was incubated overnight as described above. The wells of the 4 well dish were filled with 500 µl of fresh complete media with antibiotic(s) and the cells

were allowed to recover with an overnight incubation. The media of both were changed at 24 hours and then 48 hours after that.

If the cells in the 3.5 cm diameter dish recovered, they were treated as normal and were grown to 80% confluence. When the cells in the 4 well dish showed signs of recovering from the freeze/thaw process, they were passaged (as in Section 2.36) and seeded onto a separate 3.5 cm diameter plate. After the plate reached 80% confluence, the cells were once again passaged and seeded onto 6 cm diameter and 3 cm diameter plates.

2.48 Freezing positive clones

When the 6 cm diameter dish was 80% confluent, the cells were prepared for long-term storage in the cryo-facility. The cells were trypsinised as for passaging and the resulting single cell suspension was removed to a 15 ml centrifuge tube. The cells were pelleted by centrifugation at 300 x g for 5 minutes and the media was carefully aspirated off. The cells were resuspended in 1 ml of freezing media and aliquoted into two cyro-tubes at 0.5 ml per tube. These cryo-tubes were placed in the middle of an Eprak box containing paper towels as insulation and incubated at –80°C overnight. After 24 hours, the cryo-tubes were removed to the liquid nitrogen storage tank for long-term storage.

2.49 Karyotyping positive clones

The postive clones were defrosted as previously described in Section 2.35 and expanded onto 10 cm diameter plates. When the 10 cm diameter plate was 80% confluent, Demecolcine (Sigma-Aldrich) was added to the media at 0.1 $^{\mu g}/_{ml}$ and the cells incubated at 37°C, 7% CO_2 for 3 hours. The cells were trypsinised as for

passaging (Section 2.36) and the single cell suspension was removed to a 15 ml centrifugation tube. The cells were pelleted by centrifugation at 300 x g for 5 minutes and resuspended in 10 ml of DMEM. After centrifugation (as above), the DMEM was aspirated off, and the cells were resuspended in the hypotonic solution (0.056 M KCl) and incubated at room temperature for 15 minutes. The cells were re-pelleted by centrifugation at 300 x g for 5 minutes.

The hypotonic solution was aspirated off and 5 ml of fixative (1:3 Acetic Acid: Methanol) was slowly dropped onto the cells. After each drop the centrifuge tube was gently flicked so that the cells were resuspended in the fixative. The suspension was incubated on ice for 20 minutes and repelleted by centrifugation at 300 x g for 5 minutes. The cells were resuspended by inversion in 5 ml of fixative and incubated for 10 minutes, repeated twice. The cells were repelleted by centrifugation at 300 x g for 5 minutes. All the fixative was removed and the cells were resuspended in 500 μl of fresh fixative.

The cell suspension was carefully dropped onto clean slides using a long form glass pipette and allowed to dry. In order to visualize the nuclei, the slides were stained with Geimsa stain and the chromosomes were counted under high-resolution bright field microscopy.

2.50 Preparation of blastocyts for microinjection

Female donor mice (wild-type, C57Bl/6) were mated to proven stud males (wild-type, C57Bl/6). The next day, the donor mice were checked for vaginal plugs and if they are present, the donors were killed by cervical dislocation 3.5 days after the mating. The ovaries, oviduct and uterus were dissected out from the donors and

placed into a sterile tissue organ dish for the removal of the blastocytes. A small incision was made in the oviduct and the blastocyts were flushed out through the uterus with ~2 ml of M2 media (Sigma-Aldrich) using a 23G needle. The media was changed three or four times to remove any follicle cells. The blastocysts were stored until used for microinjections (maximum of 8 hours) in M16 media (Sigma-Aldrich) at 37°, 5% CO_2.

2.51 Preparation of clonal ES cells for injection into blastocyts

The clones selected for microinjection were defrosted onto 3 cm diameter dishes as previously described for ES cells (Section 2.35). The cells were expanded until 50% confluent and trypsinised as for passaging; after stopping the trypsinisation process, the single cell mixture was placed in a centrifuge tube and pelleted at 300 x g for 5 minutes. The cells were resuspended in full media without LIF and repelleted at 300 x g for 5 minutes. This wash was repeated twice. The cells were finally resuspended in 250 μl M2 media (Sigma-Aldrich).

2.52 Injecting ES cells into blastocytes

The blastocytes were placed into M2 media and using micromanipulators, 12-20 clonal ES cells were injected into the blastoceol cavity. Injected blastocyts were incubated in M16 media until they were ready to be transferred to host mice.

2.53 Transferring blastocyts to psuedopregnant host mothers

Female CD1 mice were mated to vasectomized male mice 2.5 days (3 nights) before transfer. 9-10 injected blastocysts were placed into each side of the uterus of each host mouse and the pregnancy was allowed to proceed as normal.

2.54 Chimeric animals and 1° generation

Chimeric animals resulting from the injection of clonal ES cells were readily apparent because of their coat color; the browner the chimeric mice were, the higher the incorporation of clonal ES cells. When the chimeric mice were sexually mature, they were mated to female wildtype C57Bl6 mice to check if any of the clonal ES cells had differentiated into germ line progenitor cells. Once again, coat colour determined if the ES cell had contributed to the germ line.

2.55 Transient expression of proteins in Hek293 cells

2XHBS:

0.27M NaCl

1.5mM $Na_2PO_4 \bullet 7H_2O$

0.05M HEPES

pH 7.0, store at –20°C

Buffer A:

50mM Tris pH 7.5

1% Triton,

150mM NaCl

1mM EDTA

1X Complete Protease Inhibitor Cocktail (Roche)

0.01% 2-Mercaptoethanol

For expression in Hek293 cells, various cDNA encoding Ruk isoforms and deletion muntants with C terminal-FLAG tags were subcloned into pCMV vectors. Triple myc tagged p85α and ΔSH3 p85α in pcDNA3.1 vector were obtained from

Dr. Peter Shepherd (UCL, UK). Hek293 cells were cultured as described in Section 2.33 and 10 μg of each plasmid was transfected by a modified calcium method as described in Webster and Perkins (1999). After normalizing the transfection efficiencies to ensure similar expreesion levels, co-transfections of various combinations of Ruk isoform/deletion mutant plasmids and p85α expression plasmids were carried out.

Cells were split and plated at 10-20% confluency 1 hour before transfections occurred. The $CaCl_2$/HBS/DNA (61 μl 2M $CaCl_2$, 0.5 ml 2X HBS, 10 μg DNA in final volume 1 ml; amounts are for 10 cm diameter dish) precipitate was formed by gentle mixing of the components together using freshly defrosted HBS. The precipitate was carefully dropped onto the cells and incubated for 16 hours at 5% CO_2, 37°C. This media was aspirated off and the cells were washed in sterile warm PBS. Complete media was added to the dish and the cells were incubated for 24 hours in the same conditions as above.

To prepare them for lysis, the cells were washed twice with non-sterile PBS. Cold Buffer A was added and the cells were scraped from the dish. The lysis was helped with 10 passes through a 23G syringe needle. The cellular debris was pelleted with centrifugation at 300 x g for 20 minutes at 4°C; the supernatent was removed, stored on ice and protein concentrations were determined. A portion of the cell lysate was assessed using SDS-PAGE and Western blotting, while the remainder was immediately used for IPs or snap-frozen in liquid N_2 and stored at –80°C until needed. For analytical gels and Western blotting, 10 μg of protein concentrate was used per sample. After defrosting, the cell lysates were re-centrifuged as above before proceeding with IPs.

2.56 Measuring protein concentration

The cell lysates were diluted 1:10 in sterile dH_2O and this dilution was further diluted to 1:200 in Coomassie Protein Assay Reagent (Perbio). The dilution was thoroughly mixed and a 1 ml sample of this dilution was measured at 595 nm using the spectrophotometer. The constant determined with each batch of Coomassie stain used was applied to calculate the amount of protein in the sample (constant was generally 0.6 to 0.7 $OD_{595} = 1\ ^{mg}/_{ml}$).

2.57 SDS-PAGE gel analysis

4X Loading buffer:

Laemmli Sample Buffer (Bio-Rad)

10% 2-Mercaptoethanol

SDS Electrophoresis buffer for polyacrylamide gels:

25 mM Tris

250 mM Glycine

0.1% SDS

10 μg of protein was diluted to 30 μl and 10 μl of 4X loading buffer was added to prepare the samples for running on the polyacrylamide gel. The plates used for the acrylamide gel were washed with dH_2O and then 70% EtOH. The plates were assembled in the gel pouring apparatus according Bio-Rad's instructions and tested for leaks by adding dH_2O, which was then drained off.

Firstly, the running gel was mixed together in the following quantities:

Initial concentration	Final concentration
Acrylamide : bis (29:1) 30% solution	5% or 7.5%
1.25 M Tris pH 8.8	0.38 M
10% SDS	0.1%
dH_2O	to volume

In order to catalyse ploymerisation, 10% Ammonium persulfate (APS) was added to a final concentration of 0.1% and TEMED to a final concentration of 0.1%. This mixture was poured between the glass plates until it reached 2 cm from the top, and was topped off by dH_2O. The gel was allowed to polymerise for 20 minutes after which the dH_2O was poured off.

The stacking gel was then mixed together in the following quantities:

Initial concentration	Final concentration
Acrylamide : bis (29:1) 30% solution	5%
1.25 M Tris pH 6.8	0.125 M
10% SDS	2.5%
dH_2O	to volume

The catalysts were added at final concentrations of 0.25% for the APS and 0.17% for TEMED. This stacking gel was then added on top of the polymerised running gel and combs were carefully introduced into the stacking gel without creating any bubbles in the mixture. The stacking gel was then allowed to polymerise for 20 minutes.

After the gel had set, the combs were carefully removed and the wells were washed with dH_2O to remove any loose bits of gel. The plates were then removed

from the gel pouring apparatus and transferred to the gel running apparatus. The apparatus was assembled according to the manufacturer's instructions and filled with SDS running buffer.

The protein samples from Section 2.57 and 2.66 were denatured by boiling for 5 minutes and immediately cooled on ice, after which they were loaded onto the gel. 5 µl of the Kaleidoscope prestained protein standards (Bio-Rad) was run in one lane of the gel and the gel was run at 200V for 45-60 minutes until the dye front had run off and the standard proteins were sufficiently separated.

Following the gel being run, the gel running apparatus was dismantled and the gels removed from the glass plates. The stacking gel was carefully cut off the running gel and discarded. The running gel was then either stained to examine all of the proteins present in the sample or Western blotted to examine specific proteins present.

2.58 Staining acrylamide protein gels

Acrylamide gels were stained using Gelcode Blue Stain reagent (Perbio). The gel was incubated at room temperature with rocking in 100 to 200 ml dH_2O twice for 20 minutes each to remove excess SDS. The gel was then submerged in 20 ml of Gelcode reagent for an hour at room temperature with rocking until it was completely stained. Excess staining reagent was removed and the gel was incubated in dH_2O for 1 to 2 hours, changing the water as much as necessary. Fully developed gels were stored in dH_2O until a picture could be taken.

2.59 Western Blotting

For Western blotting, 4 pieces of Whatman 3MM paper and 1 piece of

Hybond P (Amersham-Pharmacia) filter membrane were cut to the size of the gel. The membrane and the blotting apparatus pads were soaked in 100% Methanol and the 3MM papers were soaked in Transfer buffer for 10 to 15 minutes. Meanwhile, the gel was soaked in running buffer for 5 minutes.

The transfer apparatus was then assembled; two 3MM papers were stacked together and placed on one of the pads and the membrane was placed on the 3MM paper. The gel was carefully placed onto the membrane and any air bubbles between the two were rolled out. The remaining two 3MM papers were stacked and placed on top of the membrane and again any air bubbles were removed. Finally, the second pad was placed on top of the 3MM paper forming a sandwich effect. The "sandwich" was placed in the blotting cassette with the membrane on the anode, positive, side of the cassette. The cassette was closed and placed in the transfer apparatus. After the apparatus was assembled, it was filled with chilled transfer buffer and run at 100V for 1 hour.

The apparatus was dismantled and the gel and membrane were carefully removed; the gel was then stained with Gelcode staining reagent to ensure that sufficient protein transfer had occurred (see Section 2.59)

2.60 Staining Western blots

The Western blot was also stained to ensure that proper transfer had occurred. The membrane was soaked in Ponceau Solution (Sigma-Aldrich) for 5 to 15 minutes or until the membrane was completely dyed. Excess dye was removed by rinsing in dH_2O for 5 minutes or until distinct protein bands were visible. If the transfer was successful, the membrane was then blocked and prepared for antibody probing.

2.61 Probing Western blots with antibodies

PBST:

1X Phosphate buffered saline

0.1% Tween 20

The Western blot was blocked by incubating it in 10% blocking agent (Marvel Instant Milk diluted in PBST) for 1 hour with shaking at room temperature. The membrane was rinsed in PBST to remove excess milk and probed with the 1° antibody diluted in 3% blocking agent. The dilution of the 1° antibody was empirically determined for every antibody and the membrane was probed for 2-3 hours at room temperature or overnight at 4°C, both with shaking. The following antibodies were used to visualize the proteins on the membrane.

Antibody	Source	Conjugate	Concentration
anti-FLAG	Sigma-Aldrich	Mouse	1:1000
anti-Myc	Santa Cruz Biotechnology	Mouse	1:1000
anti-Ruk*	Purified by Dr. E Borthwick	Rabbit	1:5000

The membrane was washed in PBST for 1 hour at room temperature, changing the solution at least six times. The process was repeated with a 2° antibody that was specific to the animal that the primary antibody was derived from, which is conjugated to horse radish peroxidase (HRP, Amersham-Pharmacia). The 2° antibody was diluted to 1:2000 in 3% blocking agent. After 1 hour of incubation, the

* The anti-Ruk antibody was raised against KLH-conjugated C-terminal peptide of Ruk and was common for mouse, rat and human proteins.

membrane was washed as before.

2.62 Exposing the membranes

In order to visualize the proteins on the membrane, a chemiluminiscent detection method (Amersham-Pharmacia) was used. The ECL solutions were mixed according to the manufacturer's instructions and incubated with the membrane for 1 minute. The membrane was removed from the solution, wrapped in transparent plastic and sealed with tape to make it watertight. A piece of Kodak X-Omat film was exposed to the membrane for 1 to 20 minutes depending on the strength of the fluorescence. Following the exposure, the film was developed in the same manner as described before in Section 2.28.

2.63 Immunoprecipitation

FLAG-tagged Ruk proteins were immunoprecipitated from cell lysates using Sepharose immobilised anti-FLAG antibody (Sigma). The coupled Sepharose beads were washed twice with PBS and resuspended in double the original volume. 15 ml of Sepharose beads were added to each lysate and incubated for 90 minutes at 4°C with shaking. The beads were then pelleted by centrifugation at 13,000 rpm for 1 minute at 4°C, with the supernatant being preserved. The beads were washed three times with Buffer A (Section 2.56) under the same conditions and twice with 0.5M NaCl. After the last wash, the beads were resuspended in 40 μl of 2X Loading buffer, boiled for 1 minute and loaded onto a SDS-PAGE gel for analysis and Western blotting.

2.64 Transformation of *E. coli* BL21 cells

BL21 cells were made chemically competent (Section 2.9) and transformed with plasmids for protein expression (Section 2.10). The selection agents used were chloramphenicol (Sigma-Aldrich, to select for the cells) and ampicillin (Sigma-Aldrich, to select for the plasmid).

2.65 Titration of GST expression

An overnight culture (10 ml) of BL21 cells transformed with a GST-fusion protein plasmid was diluted to 1:100 in prewarmed LB media containing chloramphenicol and ampicillin. This large culture was grown at 37°C with shaking (200 rpm) until the absorbance at 600 nm reached 0.4 to 0.5, approximately 2 to 3 hours. The expression of the GST fusion protein was induced by the addition of IPTG to a final concentration of 0.5 mM and 10 ml of the media was removed as the zero hour sample. The culture was then divided into two samples; one was incubated with shaking at 37°C and the other at 30°C to determine which was optimal for the protein expression. 10 ml samples were taken at 2 hours, 4 hours, 6 hours and overnight.

Each 10 ml sample was pelleted by centrifugation at 3,000 rpm for 10 minutes; the supernatant was removed and the pellets were snap frozen by incubation in liquid nitrogen for 5 minutes. The pellets were stored at –20°C until needed for protein extraction.

2.66 Small scale extraction of total bacteria proteins

The bacterial pellets were weighed and defrosted by the addition of 5 ml of Bugbuster (Novagen) per 1 g of pellet. The bacteria were resuspended in the

Bugbuster and the mixture was incubated for 5 minutes at room temperature to allow the bacteria to lyse. Cellular debris was pelleted by centrifugation at 6,000 rpm for 20 minutes at 4°C and the cell lysate was removed for protein analysis.

2.67 Large scale GST fusion protein purification

PBS+Triton:

1X PBS

1X Protease Inhibitor Cocktail

0.1% 2-Mercaptoethanol

1% Triton X-100

PBS-Triton:

1X PBS

1X Protease Inhibitor Cocktail

0.1% 2-Mercaptoethanol

Elution buffer:

5 mM Glutathione

50 mM Tris pH8.0

A 10 ml overnight culture of BL21 cells transformed with appropriate plasmid was used to inoculate 500 ml of LB with the necessary selection agents (choloramphenicol and ampicillin usually). The culture was incubated at 37°C with shaking until the absorbance of the density of the culture at 600 nm reached between 0.4 and 0.6. A 10 ml aliquot was taken as T_0, IPTG was added to a final concentration of 0.5 mM and the culture was incubated at the empirically determined

optimal temperature and for the optimal time for maximum GST fusion protein expression.

The cultures were spun at 5,000 x g for 20 minutes at 4°C in order to pellet the cells. 15 ml of Bugbuster was added to the pellet and it was incubated at room temperature with shaking for 5 minutes. The lysates were placed on ice and sonicated in 10 bursts of 20 seconds with 1 minute rests between each burst. The cellular debris was pelleted by centrifugation at 5,000 x g for 20 minutes at 4°C and the supernatant was removed. An aliquot of the sonicated lysate supernatant was taken to run on the gel.

An aliquot of Glutathione-Sepharose 4B beads (Amersham-Pharmacia) were washed three times in 1 ml PBS+Triton and pelleted by centrifugation at 13,000 rpm for 1 minute. The final supernatant was discarded and replaced with the sonicated lysate, and the mixture was incubated for 30 minutes at 4°C with gentle rotation.

The beads were pelleted by centrifugation at 13,000 rpm for 5 minutes at 4°C and then washed twice with 15 ml of PBS+Triton with centrifugation at 13,000 rpm for 5 minutes at 4°C. The beads were further washed three times with PBS-Triton. The proteins were eluted from the beads by the addition of 0.5 ml of Elution Buffer; beads were pelleted by centrifugation as before with the eluate removed as fraction 1 and the beads being washed again with 0.5 ml of Elution buffer. The protein concentration of fraction 1 was determined by measuring the absorbance at 280 nm. The elution process was continued until 0 absorbance at 280 nm was reached, with all the fractions being combined for dialysis (36 hours, 4°C, against 50 mM Tris pH 8.0).

2.68 GST pulldowns

TBS (pH 7.4):

50mM Tris

150 mM NaCl

Pulldown buffer:

TBS

0.1% NP-40

0.01% 2 Mercaptoethanol

A mastermix of 50 µl of Glutathione Sepharose beads per pulldown was placed into a microcentrifuge tube. The beads were washed in Pulldown buffer with centrifugation at 13,000 rpm for 1 minute, repeated two times and aliquoted out into microcentrifuge tubes. 0.6 to 1 µg of GST fusion protein was added and the total volume was increased to 1 ml with Pulldown buffer. This mixture was rotated at 4°C for 1 to 1.5 hours to associate the GST protein with the sepharose beads. Unbounded (if any) GST fusion proteins were washed off with Pulldown buffer; the beads were pelleted by centrifugation at 13,000 rpm for 1 minute and the wash was repeated two times. Lysates of transfected HEK293 cells normalised to have equal amounts of the various Ruk proteins were added to the GST fusion protein bounded to the beads. The total volume was increased to 1 ml and the mixture was incubated, with rotation, at 4°C for 2 hours. Unbound proteins were washed off with a solution of TBS + 0.1% NP-40, pelleting at 13,000 rpm for 1 minute, repeated four times. 30 µl of protein loading buffer was added to the washed beads and the associated proteins

were eluted off by boiling at 95°C to 100°C for 1 minute. The samples were loaded directly onto a SDS-PAGE gel as described above in Section 2.59.

Chapter 3:
The *Ruk* gene structure and expression pattern

3.1 The *Ruk* gene structure was mostly unknown

While it was previously known that there were several different isoforms of Ruk and splice variants of Ruk mRNA, information about the gene structure was very limited. One study using FISH (fluorescent in situ hybridisation) did localize the gene to the X chromosome but did not show its size or structure (Narita *et al.*, 2000). Therefore, it was decided that in order to understand the various isoforms, the gene structure needed to be elucidated through analysis of genomic clones isolated by library screenings. It was also hoped that an exact understanding of the gene structure would help to discover other *Ruk* transcripts and the origin of the Ruk isoforms would be shown. Moreover, this information was vital for designing a strategy for targeted inactivation of the *Ruk* gene and producing a knockout mouse model.

Previous studies produced very restricted information about the expression pattern of the gene. Bogler *et al.* (2000) did show that $Ruk_{\Delta A}$ was expressed in the developing brain with no expression found in the adult brain. This study also showed that $Ruk_{\Delta A}$ expression coincided with malignancy in half of the human gliomas tested. However, no extensive study had been done on the expression patterns of the various *Ruk* transcripts. The full expression pattern of the different *Ruk* transcripts may clarify the role of Ruk isoforms *in vivo*.

The results presented here show that the mouse *Ruk* gene is relatively large with 24 exons and with some introns exceeding 100 kb. There are 12 identified transcripts that are translated into 7 different protein isoforms. Furthermore, the expression pattern does indeed shed some light on the role of Ruk isoforms *in vivo*. Most of the *Ruk* transcripts are developmentally down-regulated indicating a need

for them in developing tissues. *Ruk* transcripts were largely absent from adult tissues or when present were expressed at much lower level than in developing tissues.

3.2 The *Ruk* gene structure and expression pattern was finalised

3.2.1 The Ruk gene structure was determined through genomic library screening

A 129Ola mouse genomic library was screened (as described in Sections 2.18 to 2.24) using seven different DNA probes derived from rat Ruk_l, Ruk_m and Ruk_s cDNA clones. These screenings isolated 13 λ clones containing genomic sequence (Figure 3.1). The majority of the clones did not overlap with one another as evidenced by their inability to hybridise with more than one probe and subsequent sequencing of subclones. Specific fragments carrying Ruk exonal sequences were isolated by hybridisation with oligonucleotide probes that were also derived from rat *Ruk* cDNA sequences. These fragments were subcloned and sequenced; these sequences were compared to the Mouse Genomic and EST libraries to determine *Ruk* exon/intron boundries.

The 13 genomic clones encompassed 21 exons that contained the majority of the cDNA sequence for Ruk_{xl}, Ruk_l, $Ruk_{\Delta CP}$, Ruk_m Ruk_s and Ruk_h (Figure 3.1). Almost all of the cDNA of $Ruk_{\Delta A}$ and Ruk_t was also found within these clones, with the exception of a single exon from each. A comparasion of the known sequence and the *Ruk* sequence found of the mouse EST database revealed these last three exons, bringing the total number of exons in the *Ruk* gene to 24. These additional exons were determined to be the most 5' exon of the $Ruk_{\Delta A}$, Exon 3, Exon 12 which encodes a non-binding domain sequence and the most 5' exon of Ruk_t, Exon 18 (Figure 3.2). This allowed the sequences of both $Ruk_{\Delta A}$ and Ruk_t to also be

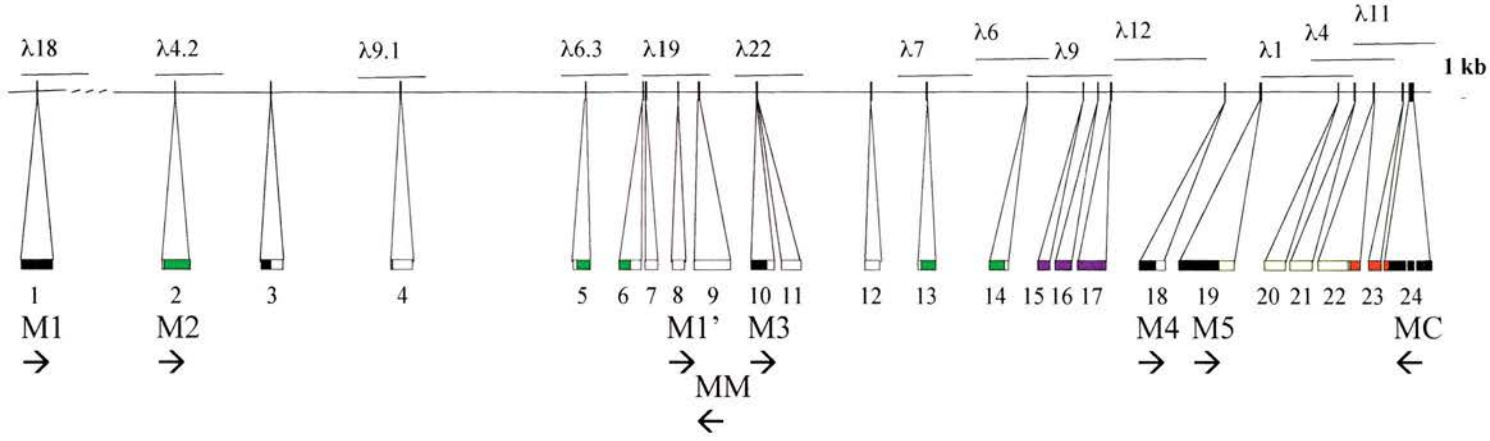

Forward primers

M1: TTCCGCCAACTTTCACTCTG

M1': GTGGAAAATGACTTCCTGCC

M2: CACAGAATGGAGCTTTCTGC

M3: GGATTTCAGGGTAGTTCTGG

M4: TGAATCTGTTTCGGCAGACC

M5: TACAGAACAGAGGGACATCC

Reverse primers

MC: TTCACTTCCATCTGCAACCG

MM: GGCAGGAAGTCATTTTCCAC

Figure 3.1: The *Ruk* exons showing the λ phage clones isolated by the cDNA library screenings. 21 of the 24 exons were discovered through the screenings while two of the exons were determined by analysis of the available mouse EST database. Also shown in this figure are the locations of the primers and their sequences used in the RT-PCR study. Adapted from Buchman *et al.*, 2000.

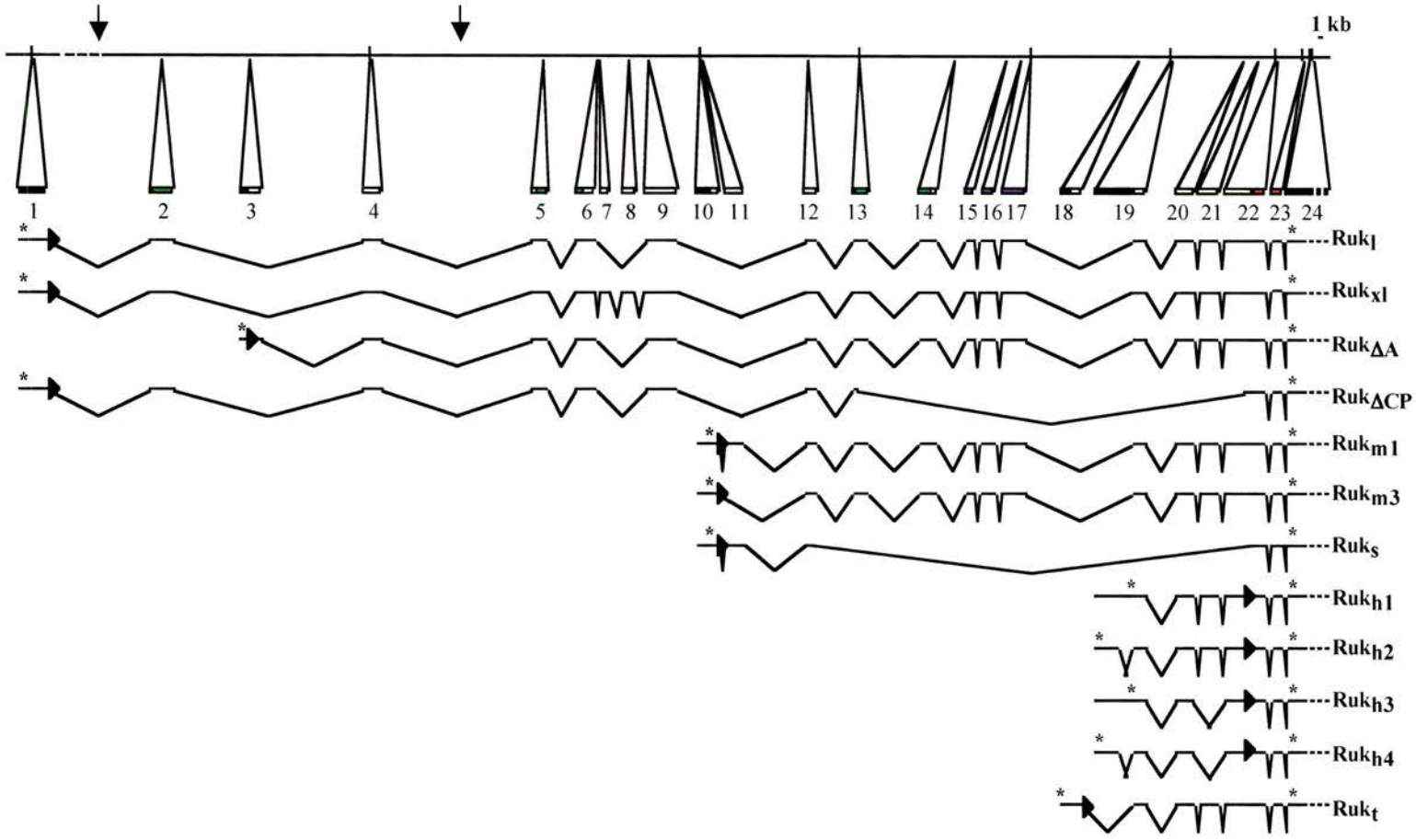

Figure 3.2: The 12 different transcripts expected from analyzing the EST clones and cDNA library. It was determined that the *Ruk* gene is over 320 kb long with some introns exceeding 100 kb (indicated by the arrows). There are 24 exons with 6 different promoters and the transcripts only share Exons 22, 23 and 24 in common with one another. Adapted from Buchman *et al.,* 2002.

completed and no other possible *Ruk* transcripts were detected through this analysis. Other combinations of exons may be possible to produce differently splice mRNA but only five potential promoters were detected during this sequence analysis.

When combined with the data from the draft sequence of the X chromosomal region that *Ruk* encompases, the data showed that the *Ruk* gene covers over 320 kb with introns measuring over 100 kb in some cases (Figure 3.2). The alignment of cDNA clone sequences (including the clones isolated and mouse and human ESTs) and the sequence of mouse genomice locus demonstrated the origin of each transcript. This work showed that there are five potential promoters located in Exons 1, 3, 10, 18 and 19, and these possible promoters together with alternative splicing produce 12 different splice variants. While there is no experimental data for the existence of these promoters, it was suggested by the fact that the transcripts began at 5' specific exons. The sequence preceeding Exon 1 is thought to contain the promoter for the longer splice variants of Ruk_l and Ruk_{xl} as well as $Ruk_{\Delta CP}$, while the 5' half of Exon 3 is the where the splice variant $Ruk_{\Delta A}$ begins. The potential promoter for the small Ruk_{m1}, Ruk_{m3} and Ruk_s splice variants is 5' to Exon 10. Ruk_t is promoted by the sequence found 5' to Exon 18 while the sequence in the 5' portion of Exon 19 serves as the start point for Ruk_{h1}, Ruk_{h2}, Ruk_{h3} and Ruk_{h4}.

In addition to their distinctive starts and 5' UTRs (Untranslated Region), some of the *Ruk* transcripts contain exons that distinguish the different transcripts. Ruk_{xl} contains all exons that Ruk_l does, as well as Exons 7 and 8 that are not found in any other transcript. These additional exons that encode a linker region between SH3B and SH3C domains of the protein, make Ruk_{xl} the longest transcript derived from *Ruk* gene. Both Ruk_{m1} and Ruk_s contain an additional exon, Exon 11, which

serves to elongate a non-domain N terminal region of the proteins. *Ruk*$_s$ is unique as it has only the 5' portion of Exon 12, while most other transcripts contain Exon 12 in its entirety.

Exon 19 is an interesting case in that the 3' portion is common to almost every transcript because it encodes the start of the serine rich domain, but the 5' UTR and promoter region in front of this exon is unique to *Ruk*$_h$ splice variants. While *Ruk*$_{h1}$ and *Ruk*$_{h3}$ utilise the entire exon, *Ruk*$_{h2}$ and *Ruk*$_{h4}$ are missing a middle portion of Exon 19. This 3' end of the exon may cause the differential expression of the *Ruk*$_h$ transcripts in developing tissues (see below).

3.2.1.1 Origin of the various *Ruk* transcripts

Ruk$_l$ is transcribed from Exons 1, 2, 4, 5, 6, 9, 12 to 17, the 3' portion of Exon 19 and Exons 20 to 24. As previously stated, *Ruk*$_{xl}$ is composed of the same exons as for *Ruk*$_l$ with the addition of Exons 7 and 8; *Ruk*$_{\Delta A}$ excludes Exons 1 and 2 in favour of Exon 3. The structure of *Ruk*$_{\Delta CP}$ is also the same as *Ruk*$_l$ except that it only contains the 5' portion of Exon 13 and excludes Exons 14, 15, 16, 17, the 3' portion of Exon 19, 20, 21 and the 5' portion of 22.

Ruk$_{m1}$ and *Ruk*$_{m3}$ are very similar, as they are comprised of Exon 10, 12 to 17, the 3' half of Exon 19, and Exons 20 to 24. *Ruk*$_{m1}$ varies from *Ruk*$_{m3}$ in that it contains Exon 11 as well as the exons it has in common with *Ruk*$_{m3}$. *Ruk*$_s$ contains Exons 10 and 11 as well as the 5' end of Exon 12, but following those exons, it is composed of the 3' end of Exon 22, Exon 23 and Exon 24.

The *Ruk*$_{h1}$ and *Ruk*$_{h2}$ transcripts are very similar to one another, as they contain Exons 19 through to 24; these two transcripts vary only in the presence of the middle portion of Exon 19 that is present in *Ruk*$_{h1}$ and lacking in *Ruk*$_{h2}$. *Ruk*$_{h3}$ is

similar to *Ruk*$_{h1}$, except Exon 21 is missing, as it is in *Ruk*$_{h4}$, which is otherwise similar to *Ruk*$_{h2}$. *Ruk*$_{l}$ is closely aligned to the *Ruk*$_{h}$ transcripts, except instead of the 5' portion of Exon 19 it is primed by Exon 18.

Analysis of the coding regions of the Ruk cDNA shows that from the 12 different splice variants of *Ruk*, 7 different isoforms of Ruk protein are formed (Figure 3.3). It is predicted from the genomic data that the longest isoforms are Ruk$_{l}$ and Ruk$_{xl}$, which are translated from *Ruk*$_{l}$ and *Ruk*$_{xl}$, respectively. These isoforms are indistinguishable from one another and are both called Ruk$_{l}$, and as previously stated, these isoforms contain three SH3 domains in the N terminus, followed by a proline-rich region, a serine rich region and a CCD (coiled-coil domain). While it looks considerably shorter than *Ruk*$_{l}$ and *Ruk*$_{xl}$, *Ruk*$_{\Delta CP}$ has the most in common with them than the other transcripts because they share the same starting sequence and promoter. Thus, the Ruk$_{l}$ and Ruk$_{\Delta CP}$ isoforms share a N-terminus sequence and SH3A domain that is found in no other isoform. In addition to the SH3A domain, Ruk$_{\Delta CP}$ is composed of SH3B and the CCD (coiled-coil domain) by themselves without the SH3C, proline rich and serine rich domains.

The other isoforms derived from the *Ruk* transcripts each represent an N terminal truncation of the long isoform which leads to the absence of certain binding domains. As was previously known (Bogler *et al*, 2000; Tibaldi and Reinherz, 2003) Ruk$_{\Delta A}$ differs from Ruk$_{l}$ only in its lack of SH3A but does contain an exclusive start codon and N-terminus sequence that is encoded by the Exon 3. The Ruk$_{m}$ isoform that is derived from the *Ruk*$_{m1}$ and *Ruk*$_{m3}$ transcripts lacks the SH3A and SH3B domains but otherwise contains the same binding domains as Ruk$_{l}$. Much like for Ruk$_{l}$ and Ruk$_{\Delta CP}$, Exon 10 is shared by the *Ruk*$_{m}$ and *Ruk*$_{s}$ transcripts and encodes a

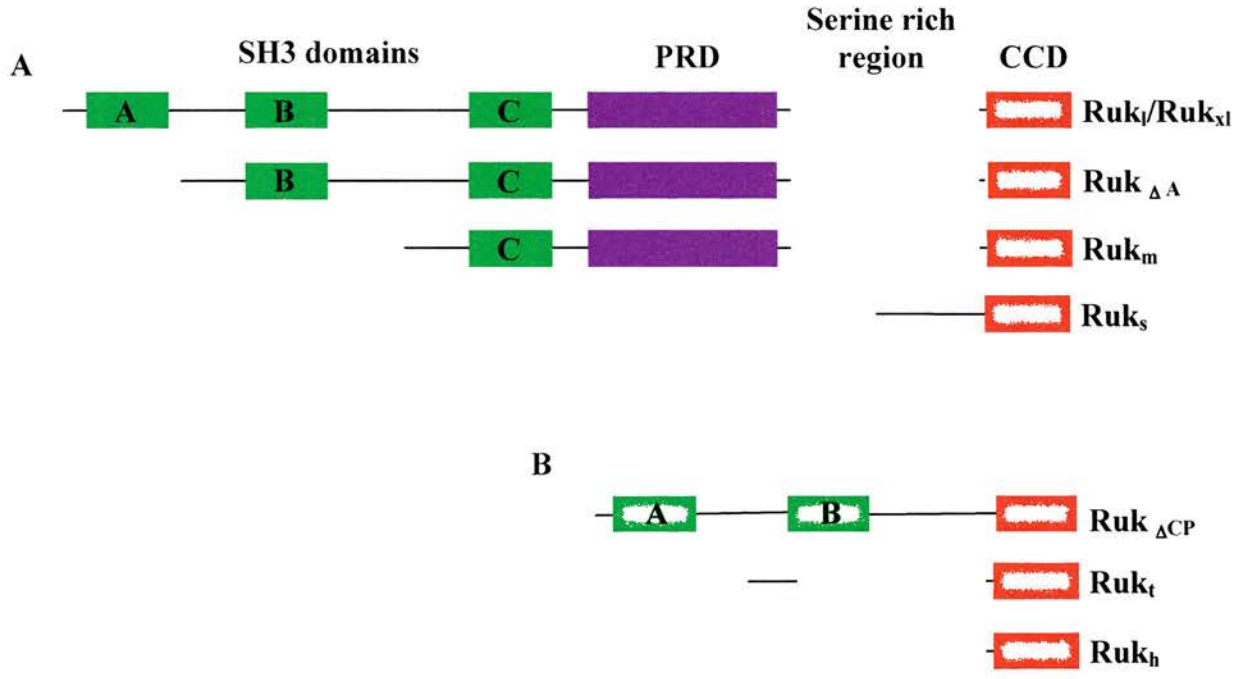

Figure 3.3: The 7 different Ruk isoforms currently known. The previously described isoforms include Ruk$_l$, Ruk$_{\Delta A}$, Ruk$_m$ and Ruk$_s$ (A). The analysis of additional cDNA and EST clones pointed to the possibility of three other isoforms, Ruk$_{\Delta CP}$, Ruk$_t$ and Ruk$_h$ As its name implies, Ruk$_{\Delta CP}$ contains two SH3 domains, A and B, and the CCD, and it lacks the SH3C domain, the PRD and serine rich regions. Ruk$_t$ is a smaller isoform that 13 contains only the serine rich region and the CCD, while Ruk$_h$ is slightly smaller than Ruk$_t$ and contains the C terminal portion of the serine rich region and the CCD. As can be seen, the only common domain between all of the isoforms is the CCD that is thought to allow the isoforms to dimerise with one another. Adapted from Buchman *et al.,* 2002.

common start-codon and N-terminus sequence for Ruk_m and Ruk_s. The Ruk_s isoform is the smallest isoform as it consists of the unique N-terminus sequence that does not encode any known domains and the CCD. The four *Ruk*$_h$ transcripts are translated into a single isoform, Ruk_h, which lacks a middle portion of the serine rich region while maintaining the CCD in its entirety. Finally, the Ruk_t isoform begins with a unique N terminus and continues with the C terminal half of Ruk_l, the serine rich region and CCD. As can be seen in Figure 3.3, the Ruk isoforms differ greatly from one another and the only common domain that is conserved in every isoform is the CCD.

3.2.2 The expression pattern of Ruk transcripts was determined

Tissue was collected from a male 8 day old (P8) mouse and an adult male mouse for RNA isolation as described in Section 2.12. The tissues taken from the P8 mouse were: skin, brain, lung, kidneys, testis, spleen, heart and thymus. Only the testis, thymus and skin were taken from the adult mouse. The mRNA was isolated from these tissue samples and the first-strand cDNA was synthesised from this RNA using Superscript II (Invitrogen) reverse transcriptase and oligo(dT) primers (see Section 2.14). Using the cDNA as a template and the oligonucleotide primers shown in Figure 3.1, several different *Ruk* splice variants were amplified.

Oligonucleotide M1 (5' TTCCGCCAACTTTCACTCTG 3') was located in the 5' region of the first exon for *Ruk*$_l$, *Ruk*$_{xl}$ and *Ruk*$_{ml}$, while oligonucleotide M1' (5' GTGGAAAATGACTTCCTGCC 3') is located in Exon 8, the exon that is specific to the *Ruk*$_{xl}$ transcript. The oligonucleotide M2

(5' CACAGAATGGAGCTTTCTGC 3') is located in the $Ruk_{\Delta A}$ specific exon that is 3' to Exon 2 that encodes SH3A. M3 (5' GGATTTCAGGGTAGTTCTGG 3') is located in Exon 10, the most upstream exon for Ruk_{m1}, Ruk_{m3} and Ruk_s, and M4 (5' TGAATCTGTTTCGGCAGACC 3') in Exon 18 is specific for Ruk_t. M5 (5' TACAGAACAGAGGGACATCC 3') is contained in a region specific for the Ruk_h transcripts. The reverse primers are contained in Exon 9, MM (5' GGCAGGAAGTCATTTTCCAC 3'), which is 3' to the exons encoding SH3B and in Exon 24, MC (5' TTCACTTCCATCTGCAACCG 3'), 3' to the exons encoding the CCD. The oligonucleotides used as primers for amplification were specifically chosen to detect and discriminate most of the alternatively spliced Ruk transcripts (see Section 2.15.1 for PCR programme). The standard L27 primers were used as a control to ensure equal amounts of cDNA for each sample.

3.2.2.1 Adult samples

Three adult tissue samples were used to extract RNA from; these samples were the skin, testis and thymus. The results of the RT-PCR amplification showed that the adult skin sample lacked all *Ruk* transcripts except for a very faint, almost undetectable amount of $Ruk_{\Delta A}$ (Figure 3.4C). The size of the transcript found in the adult skin sample was approximately 600 bp, which is similar to the predicted size (612 bp) of the portion of $Ruk_{\Delta A}$ amplified by M2 and MM. The adult testis sample amplified two splice variants (Figure 3.4F). The Ruk_t was found at the 700 bp marker, which corresponds to the predicted size of 694 bp, while the other transcript amplified, Ruk_{h2} was at the expected size of approximately 650 bp (predicted size is 643 bp). Finally, the adult thymus also amplified $Ruk_{\Delta A}$ as well as Ruk_{xl} which could

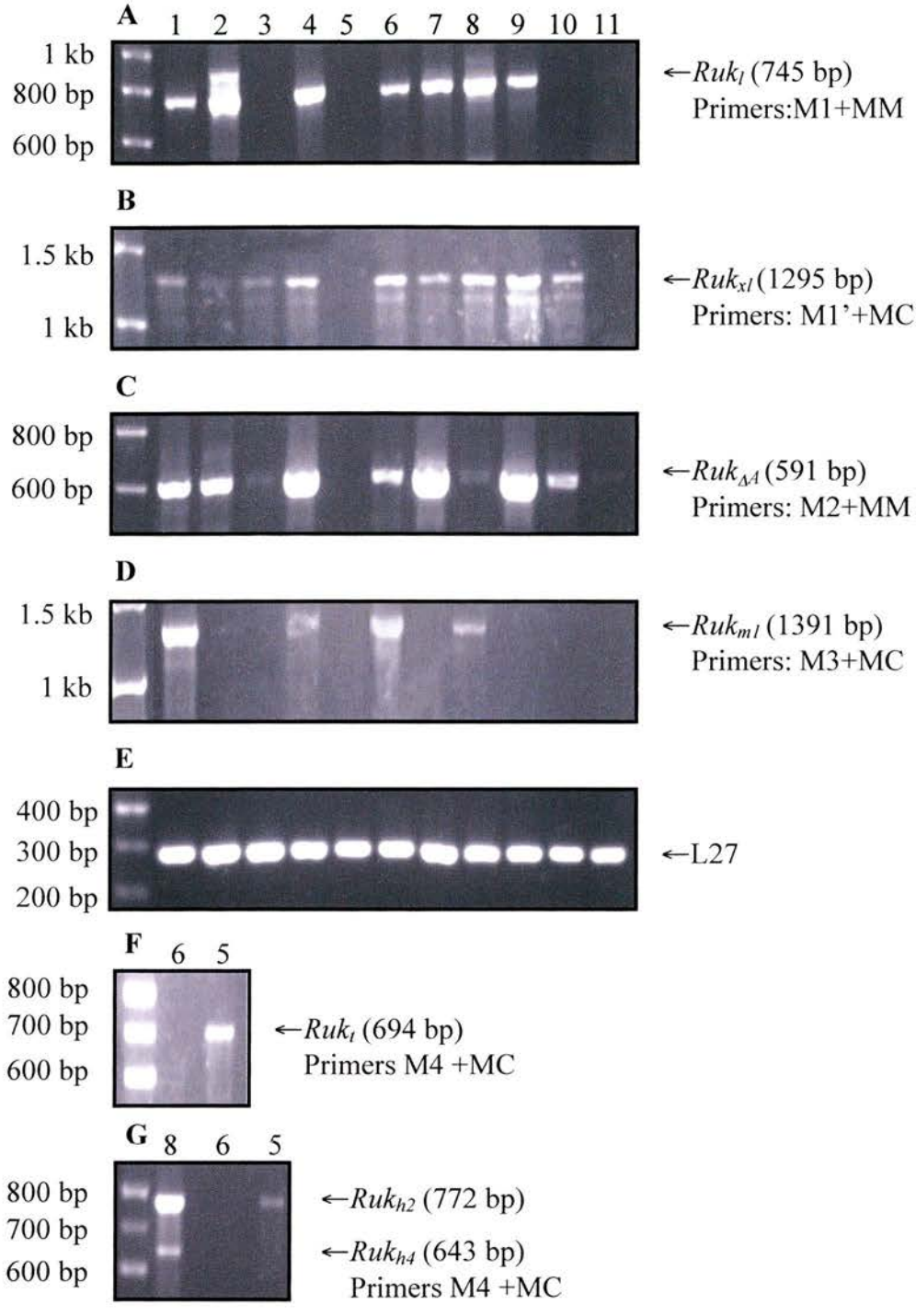

Figure 3.4: The expression patterns of (A) Ruk_1, (B) Ruk_{xl}, (C) $Ruk_{\Delta A}$, (D) Ruk_{m1} (F) Ruk_t and (G) Ruk_{h2} and Ruk_{h4}. The location of the primers can be found in Figure 12 and the actual primer sequences can be found in Section 2.14. The samples are: (1) P8 skin, (2) P8 brain, (3) P8 lung, (4) P8 kidney, (5) adult testis, (6) P8 testis, (7) P8 spleen, (8) P8 heart, (9) P8 thymus, (10) adult thymus, (11) adult skin. (E) The L27 control PCR can also be seen. The basic expression pattern is developmental downregulation, except in the case of Ruk_t and Ruk_{h2} which were upregulated in the adult testis. Adapted from Buchman *et al.*, 2002.

be found at the expected size of ~1,200 bp, the actual size was predicted to be 1215 bp (Figure 3.4B).

3.2.2.2 P8 samples

In contrast to the adult skin sample, the four major transcripts (*Ruk$_l$* (Figure 3.4A), *Ruk$_{xl}$* (Figure 3.4B), *Ruk$_{\Delta A}$* (Figure 3.4C) and *Ruk$_{m1}$* (1391 bp; Figure 3.4D) were all amplified from the P8 skin cDNA. All four of these bands were found at approximately the correct size as would be expected from the position of the primers. The P8 testis, kidney and spleen samples also amplified all four of these major transcripts at their expected sizes. These three tissues, P8 testis, kidney and spleen, as well as P8 heart all expressed the *Ruk$_{m1}$* transcript exclusively (Figure 3.4D). The M3 and MC primers that were used for amplification should also have amplified the *Ruk$_s$* and *Ruk$_{m3}$* transcripts but failed to do so.

P8 heart also exhibited the four major transcripts, as well as *Ruk$_{h2}$* (predicted size 772 bp) and *Ruk$_{h4}$* (predicted size 653 bp; Figure 3.4G). These two bands, later designated h2 and h4, were not expected from previously available experimental data (cDNA and EST clones, sequencing) in contrast to the other bands. Therefore, in order to confirm the identity of the *Ruk$_h$* splice variants, the two transcripts were individually subcloned and sequenced. When the sequences were compared to the sequence of the mouse genomic *Ruk* locus, *Ruk$_{h2}$* and *Ruk$_{h4}$* were identified as two new *Ruk* splice variants. The *Ruk$_{h4}$* splice variant was the most tissue specific as it was only found in the P8 heart sample. The *Ruk$_{h2}$* transcript was found only in the P8 heart sample and the adult testis sample (Figure 3.4F), making it and the *Ruk$_t$* transcript the only two transcripts to be developmentally upregulated.

The P8 thymus sample expressed only three of the transcripts, *Ruk$_l$*, *Ruk$_{xl}$* and *Ruk$_{\Delta A}$*. There was a marked increase in expression of the *Ruk$_{\Delta A}$* and *Ruk$_{xl}$* transcripts over the adult thymus expression levels showing that these transcripts are definitely down regulated in adult thymus but are not completely inhibited.

The P8 lung was unique out of all the P8 samples because it had the lowest expression levels out of all the tissues sampled. There was barely detectable amplification of *Ruk$_{xl}$* and *Ruk$_{\Delta A}$*; the amount of *Ruk$_{\Delta A}$* that was expressed was so small that it was comparable to that found in adult skin. The amount of *Ruk$_{xl}$* found in P8 lung was equal to the amount found in P8 brain and together the two samples had the lowest amount of *Ruk$_{xl}$* out of all the tissues sampled.

3.3 The expression pattern of Ruk isoforms was determined

The different Ruk isoforms share a common CCD, therefore an antibody to this domain was developed and used to detect the various Ruk isoforms present in different tissue samples (see Section 2.61). These protein samples were extracted from P8 skin, brain, kidney, spleen, heart and thymus tissues as well as adult testis. The Western blotting of these tissues revealed a complex pattern of protein expression, as can be seen in Figure 3.5.

Ruk$_l$ was expressed in all the P8 samples to varying degrees. The highest expression was in the thymus, with almost equal amounts being expressed in the skin, brain and spleen. A very low amount of Ruk$_l$ was expressed in the kidney and heart. Ruk$_{\Delta A}$ was highly expressed in almost equal amounts in the skin and spleen samples and in lower amounts in the thymus and adult testis samples. An almost negligible amount of Ruk$_{\Delta A}$ was found in the kidney and heart samples. Only three samples showed translation of Ruk$_m$; the isoform was found in the skin, spleen and

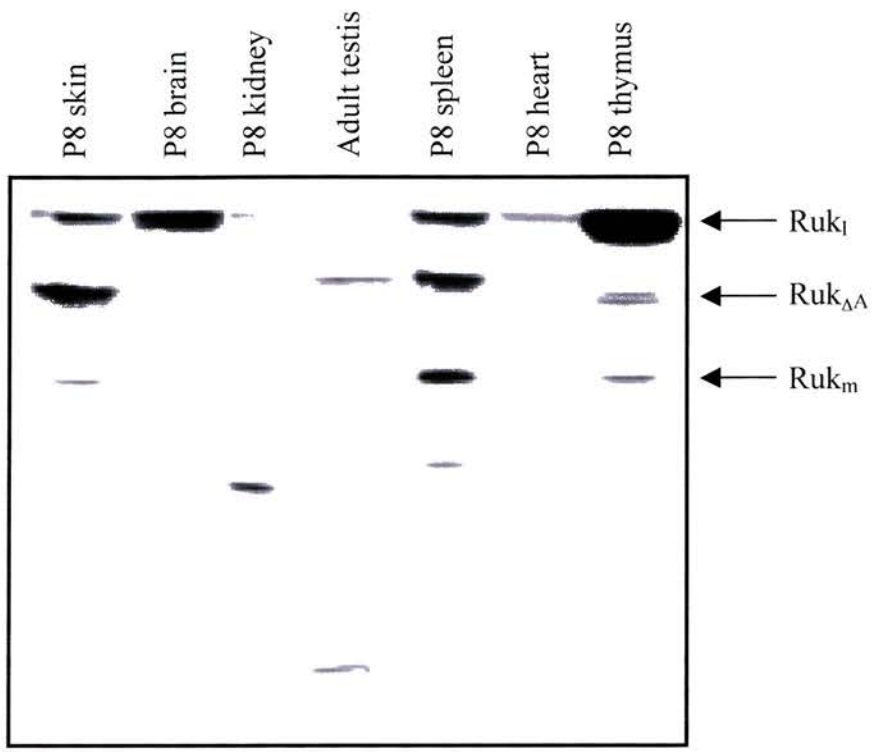

Figure 3.5: The expression pattern of Ruk proteins in various tissues samples. Samples were taken from skin, brain, kidney, spleen, heart and thymus from P8 mice or adult testis. Positions of the different isoforms are shown on the right. Adapted from Buchman *et al.*, 2002.

thymus samples, with the highest amount found in the spleen. Four samples (skin, kidney, spleen and thymus) exhibited the Ruk_s isoform. The highest amount was found in the kidney, while a lesser amount was found in the spleen and an almostnegligible amount was found in the skin and thymus.

The isoforms seemed to be found at slightly different sizes than would be expected, possibly due to posttranslational modification. For instance, Ruk_l migrated at 85 kDa while its molecular weight can be calculated at only 73 kDa. Furthermore, the smaller isoforms of Ruk_h and Ruk_t were not detected, possibly because they exist in forms that did not allow effective extraction by the methods used in this study

Chapter 4:
Conditional inactivation of Ruk isoforms

4.1 LoxP-Cre strategy for conditional inactivation of *Ruk* gene

4.1.1 Why conditional inactivation

The classical method of inactivating a protein by deleting all or a crucial part of its gene has several limitations such as the possibility of embryonic lethality if the gene in question is critically important for development. Alternatively, the protein may play distinct roles from tissue to tissue, and thus the general 'knocking out' of the gene would cause a confusing phenotype and tissue specific functions would be indistinguishable from one another. It soon became obvious to researchers that a method to remove genes only if certain conditions were met, such as age of the organism or tissue specificity, was needed. Soon the potential of Cre recombinase was realized and today one of the most commonly used methods to achieve conditional knocking out is through the Cre recombinase system called Cre-loxP.

The Cre recombinase protein is endogenous to bacteriophage P1 and mediates a site-specific recombination of the DNA sequence that is situated between sites of a specific sequence called loxP, such a sequences is said to be floxed (Nagy, 2000). The result of Cre mediated recombination of floxed sequences is either excision of sequences floxed by similarly orientated loxP sequences or inversion of sequences flanked by opposite orientated loxP sequences (Nagy, 2000). The breakthrough in using the Cre-loxP system to mediate conditional inactivation of genes *in vivo* came when it was confirmed that Cre recombinase mediated recombination occurs in all cellular environments and in all types of DNA, allowing an almost limitless potential for this protocol (Nagy, 2000). The application of this protocol is also assisted by the fact that natural loxP sites are very rare, allowing

exogenous loxP sites to be introduced without the possibility of unwanted excision or inversion in the genome (Nagy, 2000).

Once the loxP sites are introduced to ES cells, there are two ways to inactivate the floxed gene. One method is to transiently express Cre recombinase in the ES cells and produce a traditional knock out mouse, and the other is to produce a line of mice that contain the floxed sequence and cross breed that line to a mouse line expressing Cre recombinase under tissue specific promoters. Due to the versatility of the Cre-loxP system, several mouse lines expressing tissue specific Cre recombinase are now widely available (see http://www.mshri.on.ca/nagy/ for a list and contact information). By crossing a floxed mouse line to a tissue specific Cre recombinase line, the gene of interest will be inactivated in a tissue specific manner and only one floxed mouse line would be needed to investigate several different aspects of the gene's inactivation.

Taking into consideration the fact that the exact function of Ruk isoforms are almost unknown outside of the role of Ruk_1 in endocytosis and PI3K inhibition, it was decided to take a conservative approach to the inactivation of Ruk isoforms. As is detailed above in Chapter 1, among the known pathways that Ruk isoforms are involved in are several key physiological pathways whose impairment would possibly lead to several possible phenotypes. Another factor was that as discussed in Chapter 3, Ruk isoforms are widespread in development leading to the possibility that they play a role in development and that inactivation may cause embryonic lethality. One of the most important reasons for using the loxP-Cre system was that the *Ruk* gene is located on the X chromosome allowing complete inactivation of *Ruk* in the mouse ES cells that are exclusively male. For all these reasons it was decided

to use the Cre-loxP system to conditionally inactivate *Ruk* in a tissue specific manner by crossing mice that had part of the *Ruk* gene floxed with mice lines expressing Cre recombinase under tissue specific promoters.

4.1.2 CCD dimerises isoforms

Because other proteins homodimerise through their CCDs (coiled-coil domain), it has always been hypothesized that Ruk isoforms would also be able to dimerise through their common CCD. Recently this hypothesis was proved when the dimerisation of Ruk isoforms through the CCD was confirmed using both yeast two-hybrid studies and GST-fusion proteins (Borthwick *et al.*, 2004) and co-immunoprecipitation studies (Watanabe *et al.*, 2000). This dimerisation could be either homodimerisation between the same isoform or heterodimerisation between different isoforms and may lead to the formation of large, multi-protein complexes based on Ruk proteins. Ruk_1 based multi-protein complexes are thought to act as linker between various signalling pathways and bring about the diverse responses that are the result of extracellular stimuli. For instance, Ruk_1 is found in multi-protein complexes that connect the actin machinery and RTK (receptor tyrosine kinase) endocytosis leading to CCV (clathrin coated vesicle) formation and movement (Kowanetz *et al.*, 2004). Each Ruk isoform may bring different binding partners to these complexes thereby increasing the combinatorial possibilities and producing different response to stimuli. However, the role of Ruk dimerisation in multi-protein complexes has only been hypothesized as there is not much direct evidence that it occurs.

4.1.3 The CCD was chosen for inactivation

As can be seen from Section 3.2.1 and Figure 3.2, all 11 different *Ruk* transcripts have three exons in common, Exons 22, 23 and 24. These exons encode the only domain that all isoforms share, the CCD that enables dimerisation of Ruk isoforms. Due to the size and difficulty of removing the entire gene, the conditional inactivation construct was focused on these last three exons of *Ruk*, in the hopes that the removal of the CCD would affect the functions of the various Ruk isoforms.

The CCD may play a greater role than mere dimerisation, as there is the possibility that the CCD mediates unknown Ruk isoform interactions. This possibility will be seen during the removal of the CCD in tissues expressing the smaller Ruk isoforms such as Ruk_s, Ruk_t and Ruk_h that are mainly composed of the CCD. When the CCD of these isoforms is disrupted, it may be possible to deduce which proteins are no longer able to interact with these smaller isoforms.

4.2 An ES cell line containing the floxed *Ruk* gene was generated

4.2.1 A conditional inactivation construct was created

As can been seen from Figure 3.1, Exon 22 of *Ruk* encodes the C terminal portion of the serine rich domain and the N terminal portion of the CCD. The deletion of Exon 22 will also create a splice between Exons 21 and 23 that will cause the sequences of Exon 23 and 24 to move out of frame with upstream sequences. This will create a truncation after Exon 21 and the complete absence of the CCD in all of the isoforms. For these reasons Exon 22 was targeted for floxing and eventual excision from the genome. Through the inactivation of the CCD, the importance of dimerisation and other CCD dependent interactions in respect to Ruk functions could be evaluated.

Genomic clone λ11 was previously identified as containing the 3' end of *Ruk* genomic sequence, which encompassed Exons 22, 23 and 24 and the surrounding intronic sequence. During the process of identifying its genomic inserts, a comprehensive map of the restriction digest sites was created and large portions of the clone had been sequenced (Figure 4.1). Portions of this clone were used as the basis for the genomic construct that was introduced into mouse ES cells.

An approximately 7.0 kb EcoR I-Sal I fragment of genomic clone λ11 which contained Exon 22 and its surrounding intronic sequence, was ligated into the pGem 3Z vector MCS (Figure 4.2). The identity of the insert was confirmed by restriction digestion with Sal I and EcoR I, HinD III, Nco I and Apa LI (Figure 4.3) as well as sequencing both of its ends. An approximately 1.3 kb fragment containing a Neomycin resistance cassette and a flanking 5' loxP site was excised from the pLoxP plasmid (gift of Dr. A Medvinsky, Institute of Stem Cell Research, University of Edinburgh) by Avr II and Xba digestion. An adaptor oligonucleotide (CTAGGTAC) was used to introduce the loxP/Neomycin resistance cassette into the Kpn I site that is found in the 5' intron of Exon 22 (Figure 4.4). The adaptor oligonucleotide was added into the ligation mixture (see Section 2.3) and the resulting plasmid contained the Avr II and Kpn I site while but not the Xba I site at the other end (Figure 4.5). The presence of the insert was confirmed through enzymatic digestion with Kpn I; its orientation was confirmed with EcoR I digestion (Figure 4.6). The plasmid was then partially enzymatically digested with EcoR I and ApaL I (described in Section 2.5) to obtain the approximately 6.5 kb EcoR I/ApaL I fragment that contained both Exon 22 and the Neomycin resistance cassette (Figure 4.7). The ends of the fragment were blunted as described in Section 2.8.2 which destroyed both the EcoR I and ApaL I

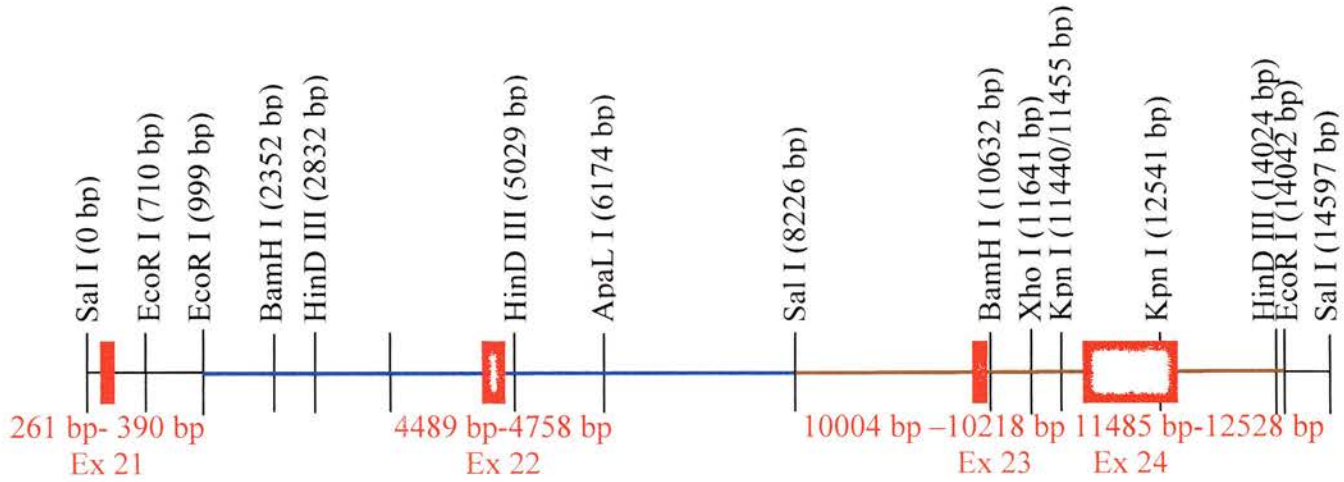

Figure 4.1: A map of λ11 showing the restriction sites and exons. The screening of genomic clones showed that λ11 contained Exons 21-24 and surround introns. This genomic clone was used to create the construct that was electroporated into mouse ES cells. The dark blue indicates the sequence that became the 5' portion of the final construct and the brown indicates the sequence that became the 3' portion of the final construct.

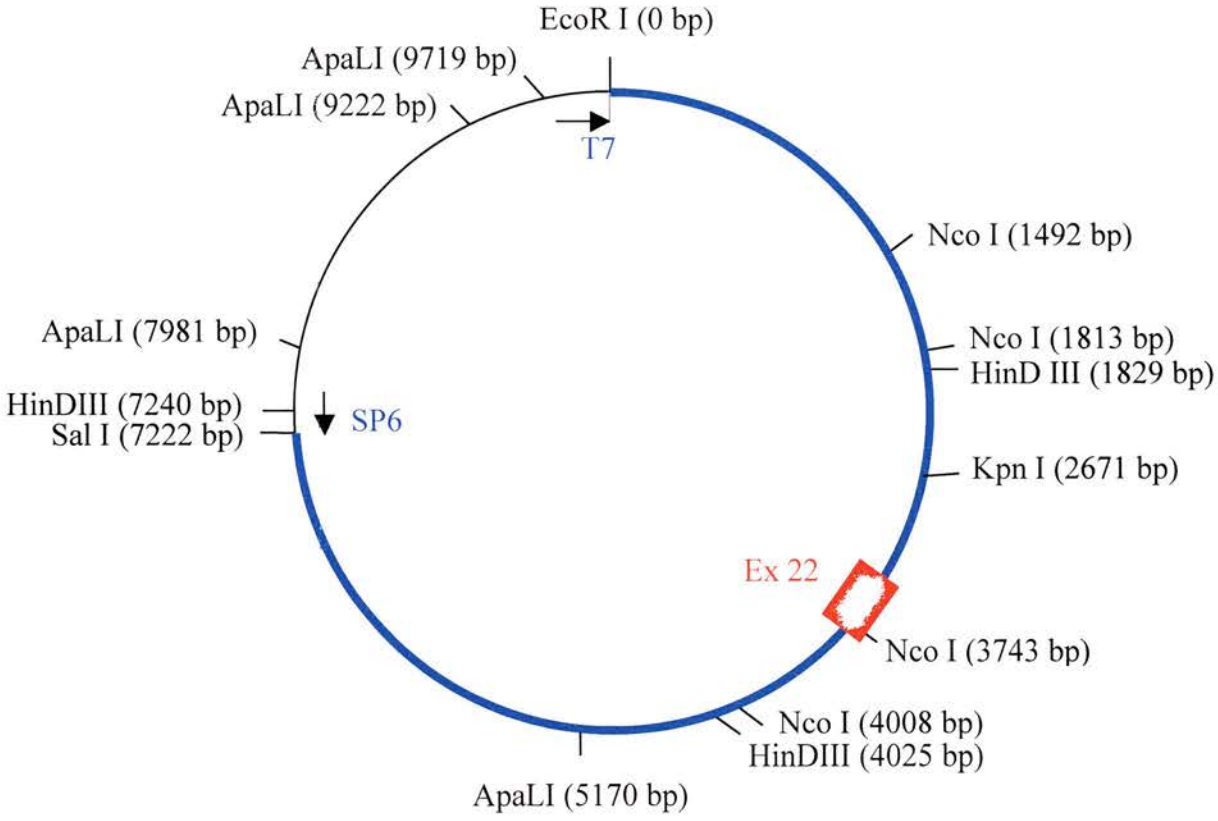

Figure 4.2: A plasmid map of the ~7.0 kb Sal I/EcoR I fragment of genomic DNA that was ligated into pGem 3Z. The blue area indicates the genomic sequence inserted into the plasmid. Also shown are the standard primers that were used to confirm the orientation of the insert. The sole Kpn 1 site (2671 bp) was used to open this plasmid and insert a Neo^R/loxP fragment.

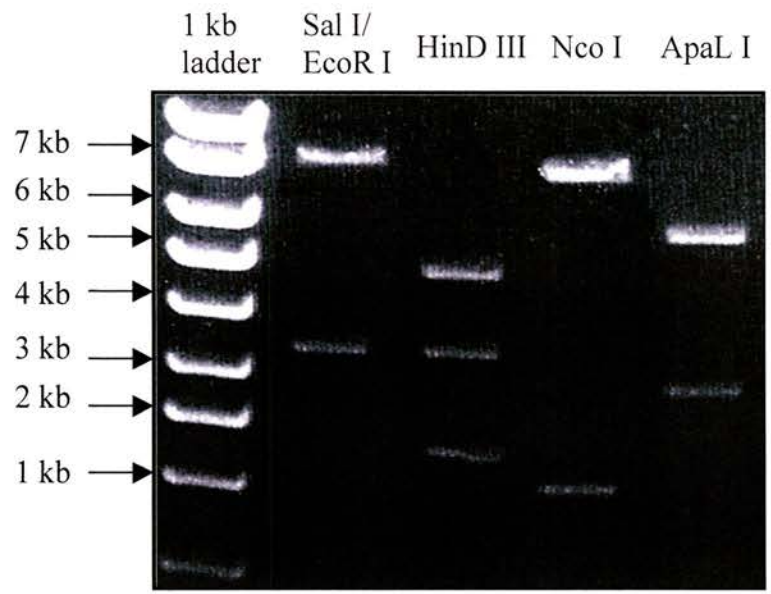

Figure 4.3: The pGem 3Z plasmid containing the ~7.0 kb genomic Sal I/EcoR I fragment was digested with Sal I and EcoR I, HinD III, Nco I and Apa LI in order to confirm the identity and orientation of the insert. As expected, the Sal I/EcoR I digest produced fragments at 7 kb and 3 kb, while the HinD III digest produced fragments at 5 kb, 3 kb and 1.2 kb. Also as expected, Nco I digestion resulted in two bands (7 kb and 1 kb) as did ApaL I (5 kb and 3 kb). The ApaL I ~1.0 kb and ~0.5 kb fragments that were also expected did not cut for an unknown reason. Further confirmation was acheived through sequence analysis using the standard T7 and T3 primers contained in the pGem 3Z vector.

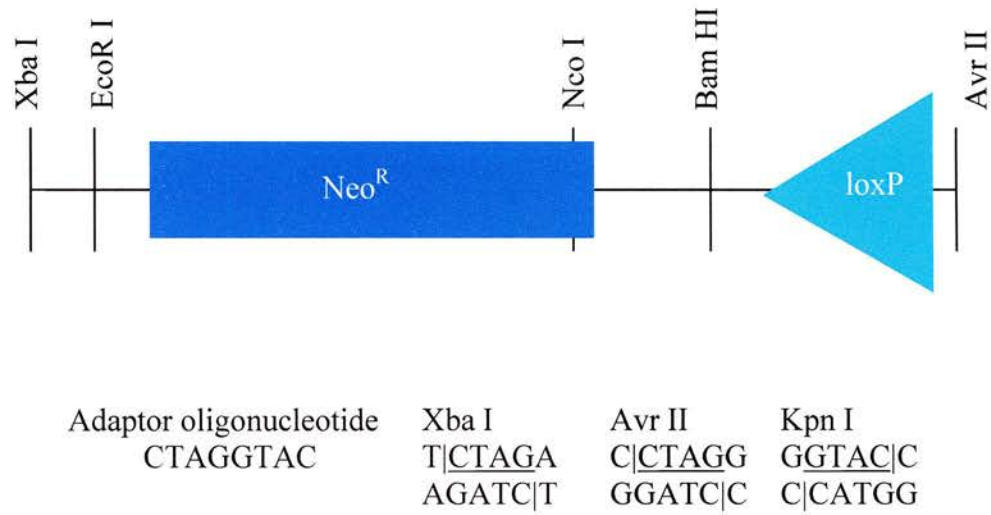

Figure 4.4: A 1.3 kb fragment was excised from the ploxP plasmid using Xba I and Avr II. This fragment containing the Neomycin resistance cassette (Neo^R) and the loxP site. Also shown are the adaptor oligonucleotide and the restriction enzyme sites used to ligate the fragment into the Kpn I site of the plasmid shown in Figure 17.

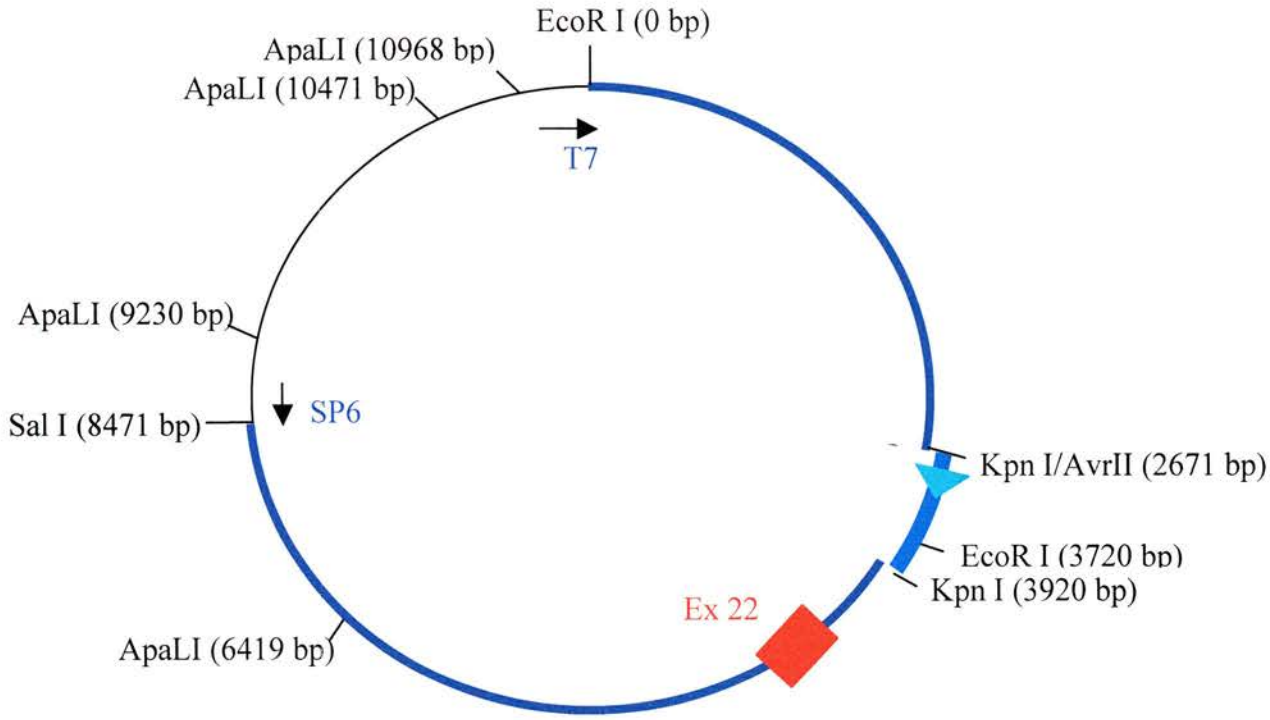

Figure 4.5: A map of the plasmid resulting from the addition of the ~1.3 kb Neo^R/loxP fragment into Kpn I site of the plasmid shown in Figure 4.3. The parent vector is pGem 3ZThis ligation created a plasmid containing the Neo^R cassette and loxP in the intronic sequence 5' to Exon 22. The identity and orientation of the insert was confirmed by restriction digests using Kpn I and EcoR I.

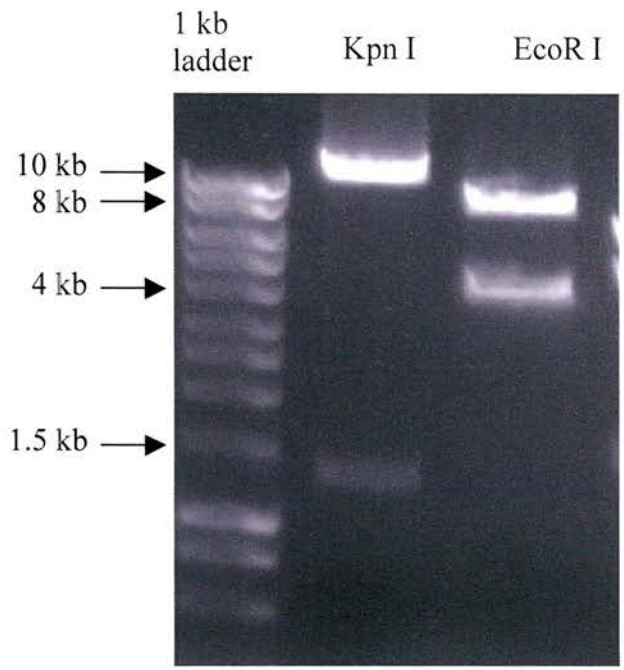

Figure 4.6: The plasmid shown in Figure 4.5 was digested using Kpn I and EcoR I to confirm the orientation and identity of the Neo^R/loxp insert. As expected, digestion with Kpn I produced a >10 kb fragment and an ~1.2 kb fragment. EcoR I produced two large fragments at ~8 kb and ~4 kb.

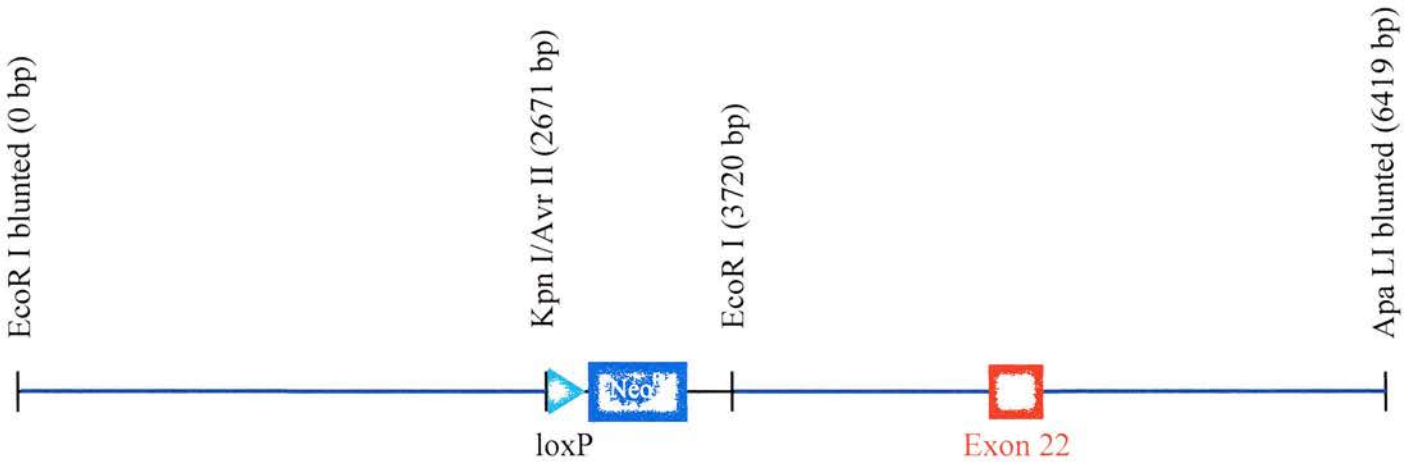

Figure 4.7: The pGem 3Z plasmid containing Exon 22 and the loxP/Neo^R cassette (Figure 4.6) was partially digested by EcoR I and ApaL I to generate an approximately 6.5 kb fragment. The EcoR I/ Apa LI fragment (~6.5 kb) was blunted after digestion; it contained the loxP site, Neo cassette and Exon 22 and was devoid of any vector sequence.

sites at the ends of this fragment in the final construct.

At the same time, a loxP site was generated by annealing two oligonucleotides (loxP RIA and loxP RIB) together (Figure 4.8). The resulting short, double stranded loxP site-containing fragment was placed upstream of a Puromycin resistance cassette at an EcoR I site in the pLoxM plasmid (gift of Dr. A Medvinsky, Institute of Stem Cell Research, University of Edinburgh). The oligonucleotides were generated in such a manner as to have EcoR I sites on either end of the loxP site and were ligated into the plasmid using the EcoR I site in the MCS (Figure 4.9). The orientation of the insert was confirmed using digestion with Xba I and sequencing (Figure 4.10). The Puromycin resistance cassette and loxP were excised from the plasmid using Sbf I and Pme I and blunted for ligation; the blunting step destroyed both the Sbf I and Pme I sites at the ends of this fragment in the final plasmid construct.

The approximately 6.0 kb Sal I/EcoR I fragment of genomic sequence that contained Exon 23 and Exon 24 was excised from genomic clone λ11 and ligated into a pBS SK^+ plasmid using the Sal I and EcoR I sites found in the MCS (Figure 4.11). The orientation and identity of the insert was confirmed using enzymatic digestion with Xho I and Kpn as well as sequence analysis (Figure 4.12). This plasmid contained two Bam HI sites, one in the intronic sequence 3' to Exon 23 and another in the MCS of pBS SK^+ (Figure 4.13). Exon 24 was removed from the plasmid by digestion with Bam HI and the remaining plasmid was circularized by self-ligation. The vector was prepared from the resulting plasmid by digestion with Sal I and blunting with the Klenow fragment thereby destroying the Sal I site in the final plasmid construct.

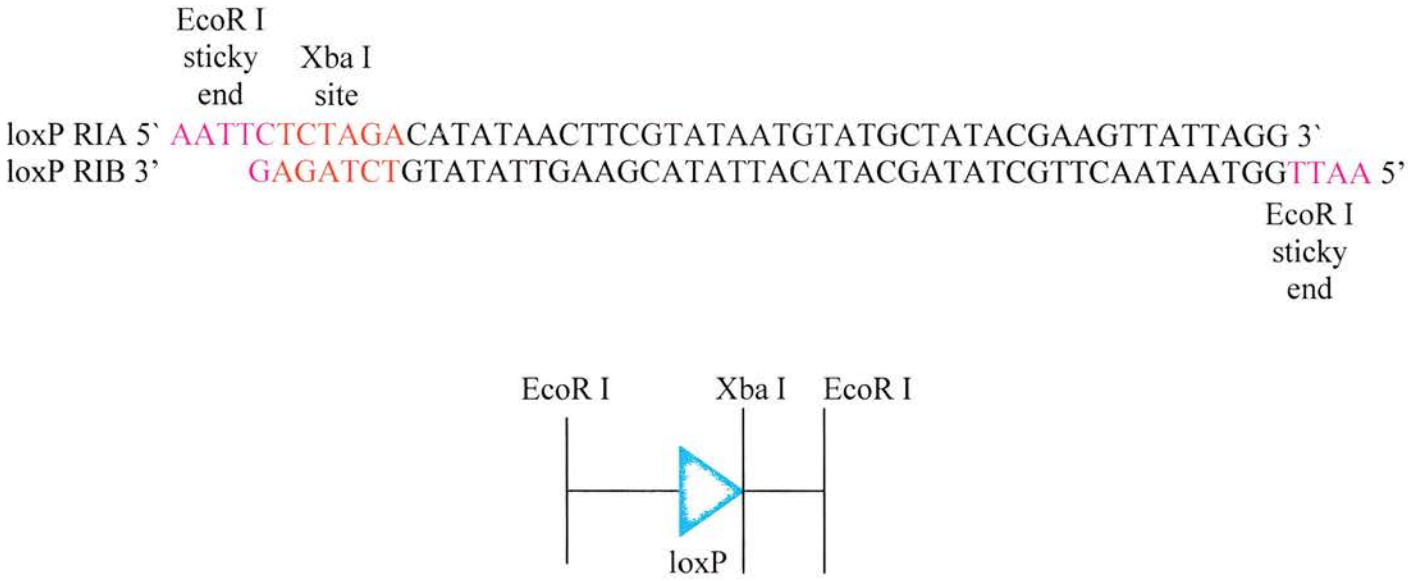

Figure 4.8: Two oligonucleotides were annealed together to create a loxP site for introduction in to the EcoR I site in the pLoxM plasmid. These oligonucleotides were designed so that they created a Xba I site and two EcoR I sticky ends.

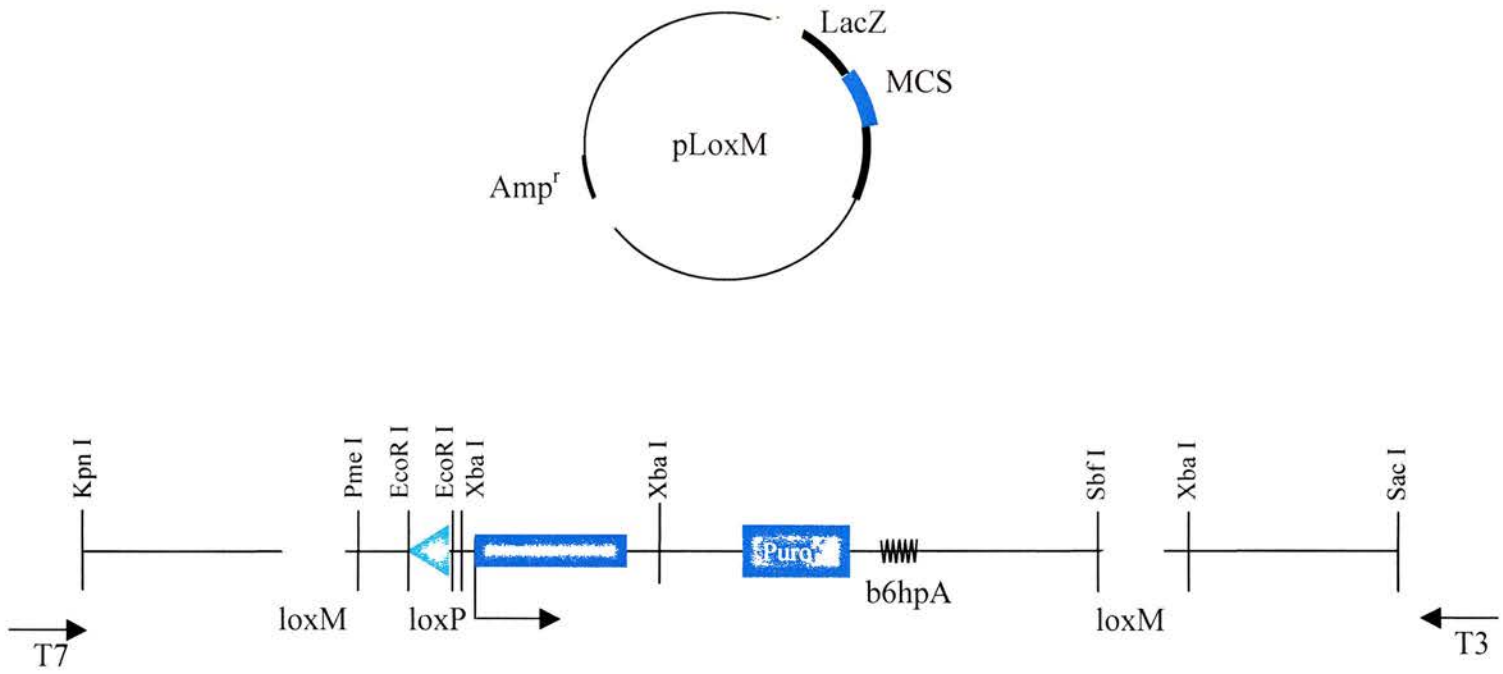

Figure 4.9: The annealed oligonucleotides were introduced into the EcoR I site of the MCS of pLoxM. The loxP was placed between the forward loxM and the Puro^R cassette, and its orientation was confirmed using an Xba I digest. A fragment containing the loxP and Puro^R cassette was excised using Pme I and Sbf I.

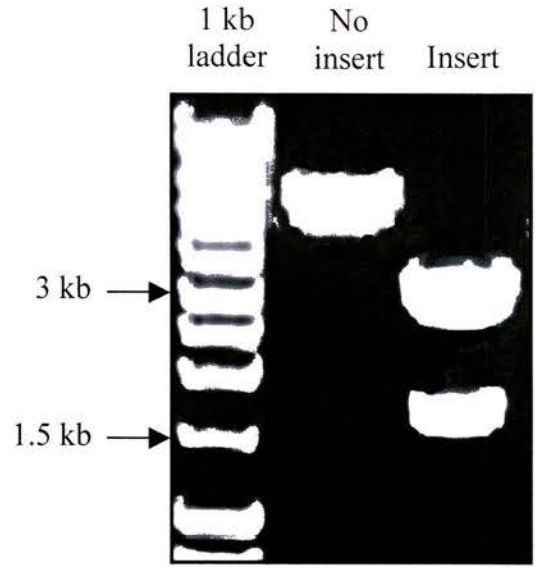

Figure 4.10: The insertion of the loxP site into pLoxM was confirmed through digestion with Xba I. When no insert was present, only one large band was present , and when the loxP site was inserted two bands (1.5 kb and 3 kb) were generated due to the design of the oligonucleotides. While this showed the insert to be present, the orientation had to be confirmed through sequencing by T7.

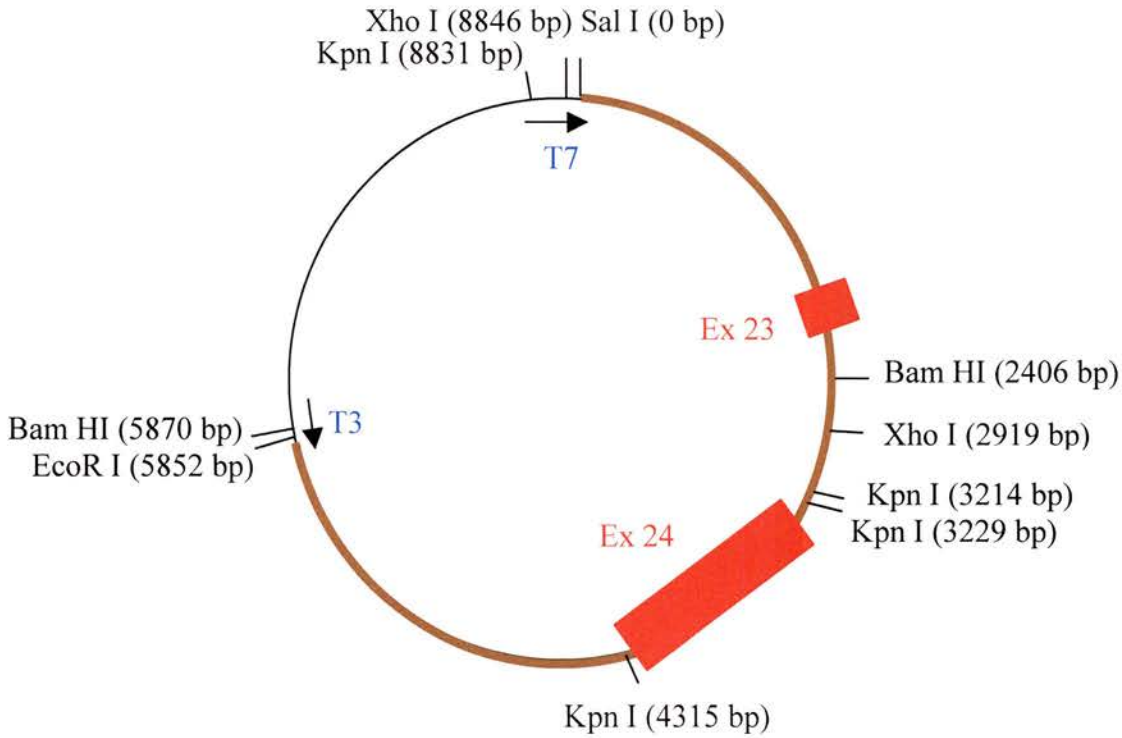

Figure 4.11: An approximately 6.0 kb Sal I/EcoR I fragment of genomic DNA was ligated into pBS SK^{+}. This fragment included Exons 23 and 24 and the intronic sequence surrounding the two exons. The insert and its orientation were confirmed using restriction digest with Xho I and Kpn I and sequencing of the insert by T7 and T3.

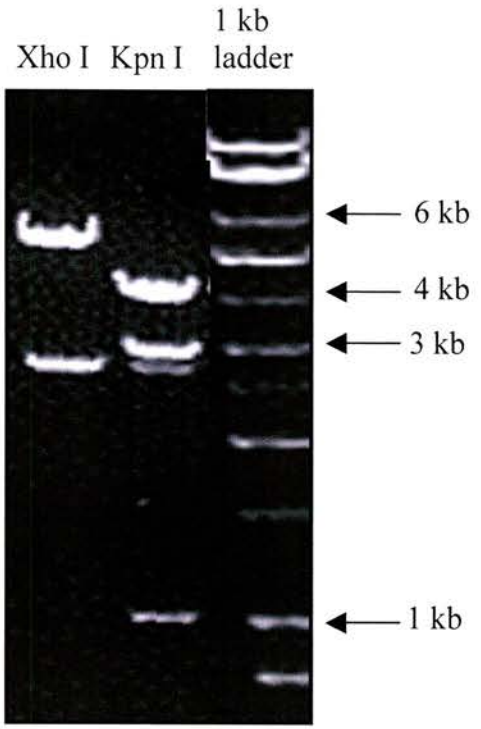

Figure 4.12: The presence of the ~6.0 kb genomic fragment in pBS SK$^+$ was confirmed through enzymatic digestion with Xho I and Kpn I. As expected, Xho I digestion produced two bands (~5.5 kb and ~3 kb) while the Kpn I digest resulted in three fragments (~4 kb, ~3 kb and ~1 kb). Further confirmation of the insert was achieved through sequencing with T7 and T3 that are found in the vector.

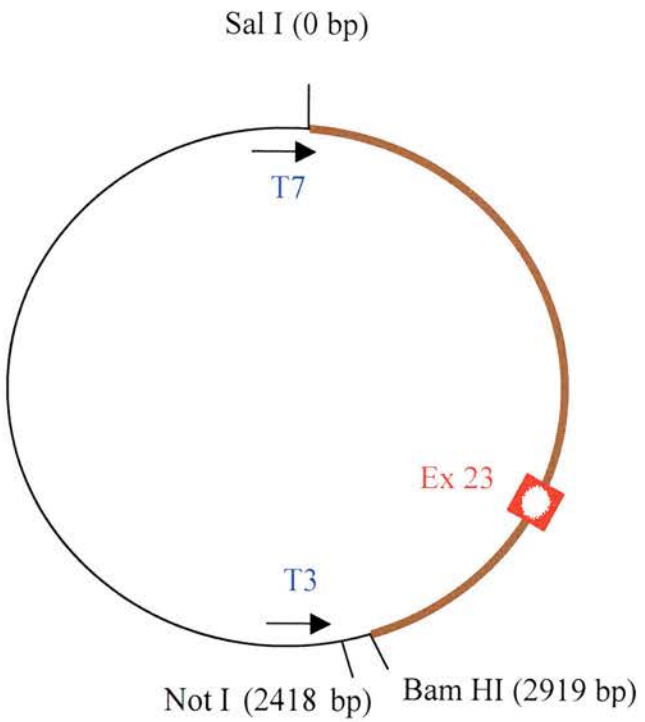

Figure 4.13: Exon 24 was excised from the pBS SK$^+$ plasmid pictured in Figure 4.11 by digesting the plasmid with Bam HI and religating it to itself.

This blunt-ended vector was then ligated with the Sbf I/Pme I fragment containing the Puromycin resistance cassette and loxP (Figure 4.14). This resulted in the Puromycin resistance cassette being placed 5' to Exon 23 with the loxP site facing Exon 23 and between the exon and resistance cassette. The correct insertion of the Sbf I/Pme I fragment was confirmed by enzymatic digestion with Bam HI/Sal I, Bgl II, Xba I and Xho I as well as partial sequencing (Figure 4.15).

The resulting plasmid was digested with Kpn I, an MCS site that was 5' to the Puromycin resistance cassette and blunted with the Klenow fragment. The vector was ligated with the EcoR I/ApaL I fragment containing Exon 22 and the Neomycin resistance cassette, thereby creating the final construct (Figure 4.16).

The orientation of this insert in the final construct was tested using enzymatic digests. The EcoR I digest confirmed the orientiation with bands appearing at 4.0 kb and 9.1 kb, while the Bam HI digest showed bands as predicted at 7.5 kb, 1.4 kb and 4.3 kb (Figure 4.17). The DNA found in the construct was verified by sequencing the genomic DNA, the antibiotic resistance cassettes and the loxP sites. DNA sequences obtained by using standard plasmid primers showed a match to the genomic DNA from the expected restriction enzyme sites onwards. Both loxP sites were orientated 5' to 3' and surrounded Exon 22 as well as both Neomycin and Puromycin resistance cassettes. The construct was linearised by digestion with Not I and used for electroporation into mouse ES cells, as described in Materials in Methods (2.38-2.40).

4.2.2 Screening the ES clones

The resulting ES cell colonies were selected using either Neomycin alone or both Puromycin and Neomcyin, the process is described in Section 2.41. The DNA

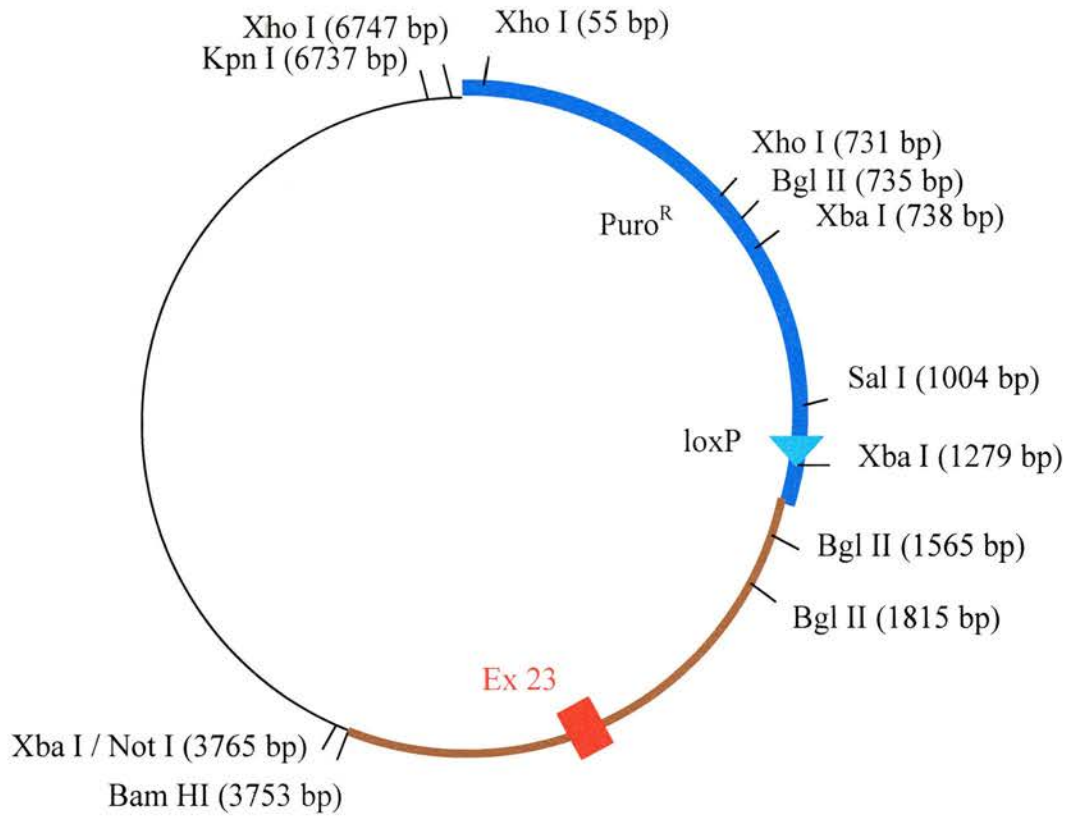

Figure 4.14: The Sbf I/Pme I fragment containing the loxP/Puro^R cassette was ligated into the pBS SK$^+$ plasmid containing Exon 23, shown in Figure 4.13. The fragment was blunt ligated into the Sal I site, abolishing the Sal I, Sbf I and Pme I sites. The orientation and identity of the insert was confirmed through ezymatic digest with Bam HI and Sal I, Bgl II, Xba I and Xho I as well as sequencing with T7.

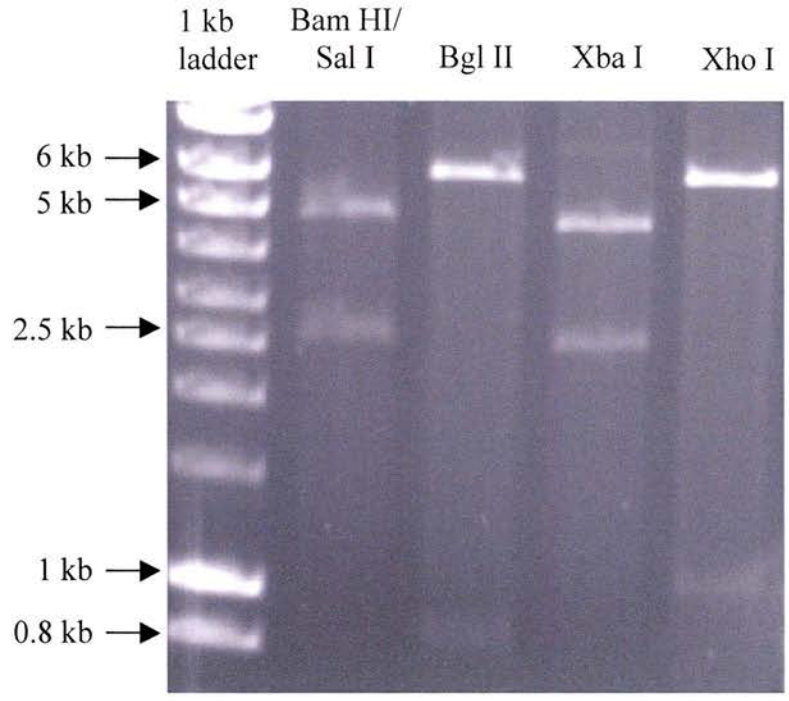

Figure 4.15: The identity and orientation of the Puro^{R}/loxP insert in the intronic sequence 5' to Exon 23 was confirmed using ezymatic digestion with Bam HI and Sal I, Bgl II, Xba I and Xho I. As expected from the plasmid map, the Bam HI/Sal I digest created two bands at ~5 kb and ~2.5 kb, and the Xba I digest created two bands at ~6 kb and 1 kb. The Bgl II digest resulted in two bands at ~6 kb and ~0.8 kb, another expected band at ~3 kb is missing for an unknown reason. Xba I was also supposed to create three bands at ~2.5 kb, ~4 kb and ~5 kb, but the 4 kb band did not appear. Further confirmation of the insert was acheived through sequencing using the T7 promoter.

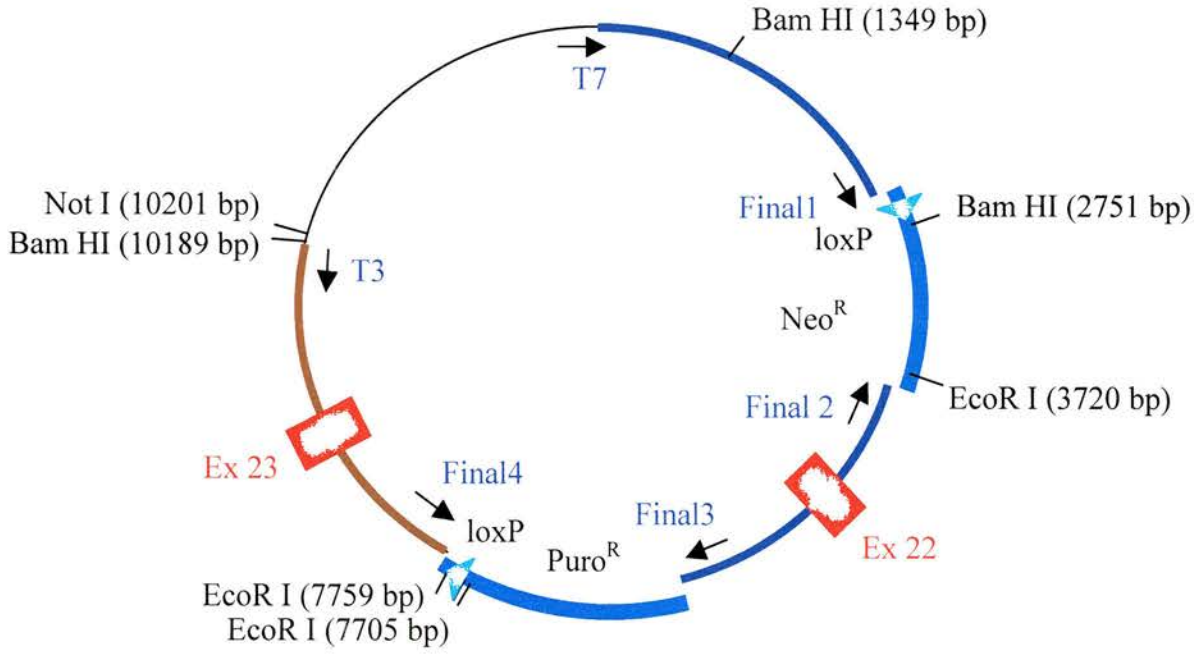

Figure 4.16: A plasmid map of the final construct in Pbs SK$^+$. Neo^R is 5' to Exon 22 which is then followed by Puro^R; all three are flanked by loxP sites. The exonic DNA is highlighted in red, the cassettes are shown in light blue. The intronic DNA is highlighted in dark blue and brown, and corresponds to λ11 portions highlighted in the same colours in Figure 4.1. The position of the primers used to sequence this construct and position of the restriction enzymes (Bam HI and EcoR I) that were used to confirm all the inserts are also shown. This plasmid was linearised by digestion with Not I for electroporation.

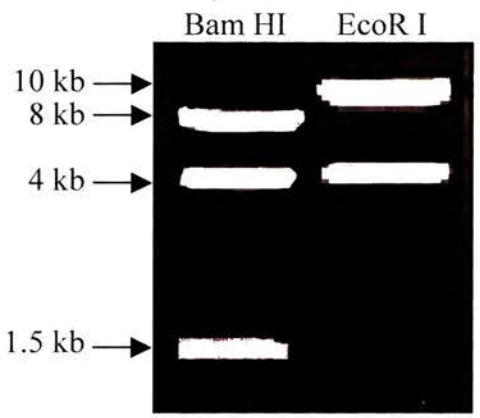

Figure 4.17: DNA from the plasmid pictured in Figure 4.16 was digested with Bam HI and EcoR I, confirming that the Neomycin and Puromycin resistance cassettes along with the loxP sites had integrated correctly into genomic sequence surround Exon 22. As expected, the Bam HI digest created three bands at ~7kb, ~4 kb and ~1.5 kb, and the EcoR I digest resulted in two bands on at ~10 kb and another at ~4 kb. Further confirmation was achieved through sequence analysis using the primers indicated in Figure 4.16.

from the ES cells was isolated (see Section 2.46) and initially screened using PCR (see Section 2.15.2). *Ruk* is found on the X chromosome and the ES cells used in this project are of male origin (e.g. have only one *Ruk* locus) so the primers used were designed to amplify the site where the loxP/Neomycin resistance cassette was placed. The forward primer (NeoF: GGTATACCCTCTCAGCTATC) was designed from the sequence 5' to the most 5' loxP, while the reverse primer (NeoR: ACACTACCCACTGTCAGGGA) was chosen from the sequence 3' to the Neomycin resistance cassette (Figure 4.18). Genotyping of ES cell clones using PCR with these two primers produced two bands (1.5 kb and 0.2 kb) in the clones with the targeting plasmid randomly integrated into the genome, "negatives", while a single 1.5 kb band should have been detected in clones with proper homologous recombination in the *Ruk* locus, "positives" (Figure 4.19). "Positives" had the *Ruk* locus disrupted by the targeting plasmid and could only amplify the 1.5 kb band. Out of the 394 clones screened with this PCR, 210 were clearly negative, and the remaining 184 clones were further checked for homologous recombination by Southern hybridisation.

For Southern hybridisation, genomic DNA from each clone was digested with EcoR I or HinD III, transferred to nylon membranes and hybridized with a ^{32}P labeled specific probe which was a 1.1 kb fragment that encompasses Exon 24 (Figure 4.20, described in Section 2.26). This probe hybridized with a large (>20 kb) fragment originated from EcoR I-digested wild-type *Ruk* locus, but a much shorter 6.0 kb EcoR I fragment in clones with homologous recombination within the *Ruk* locus. Digestion with HinD III produces either a 9.0 kb band (wild-type locus) or a 6.5 kb band (locus with homologous recombination) that hybridizes to the probe

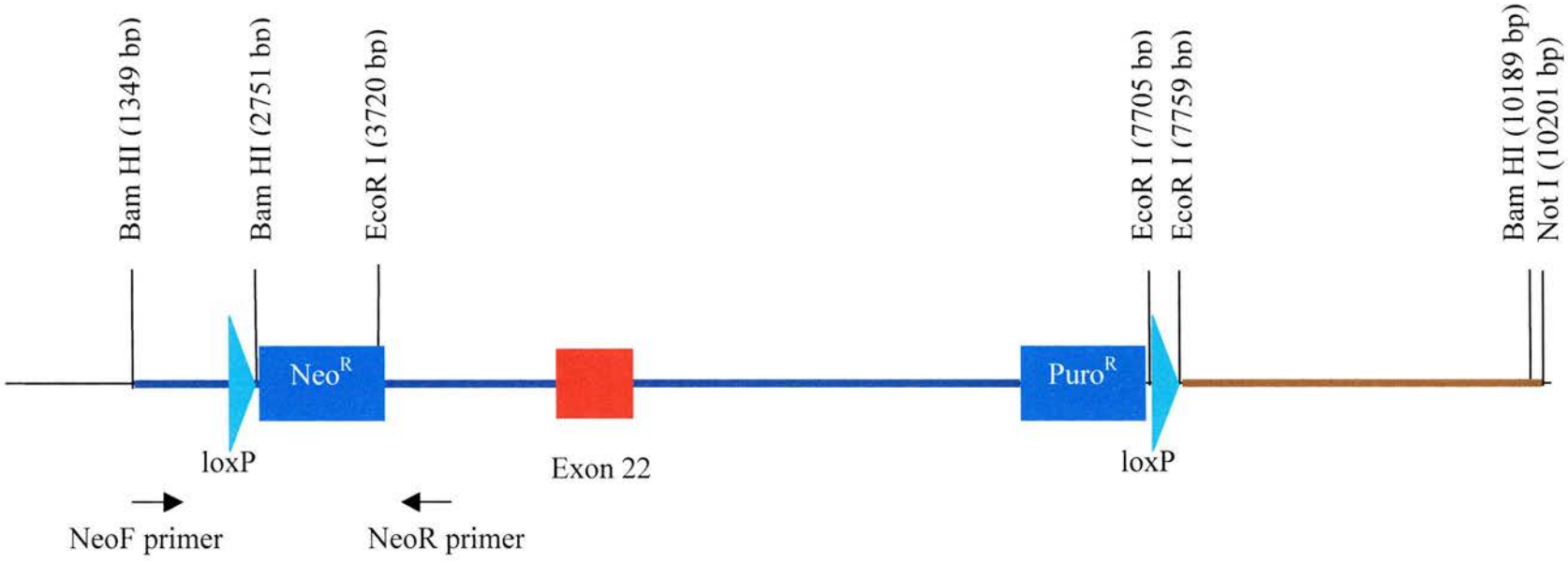

NeoF primer	GGTATACCCTCTCAGCTATC
NeoR primer	ACACTACCCACTGTCAGGGA

Figure 4.18: A linearised representation of the construct created for the introduction into the genome. The position of the primers and their sequences used in the PCR analysis of the clones are also shown. The placement of the Neomycin and Puromycin resistance cassettes and the loxP sites were confirmed by restriction digests using EcoR I and Bam HI.

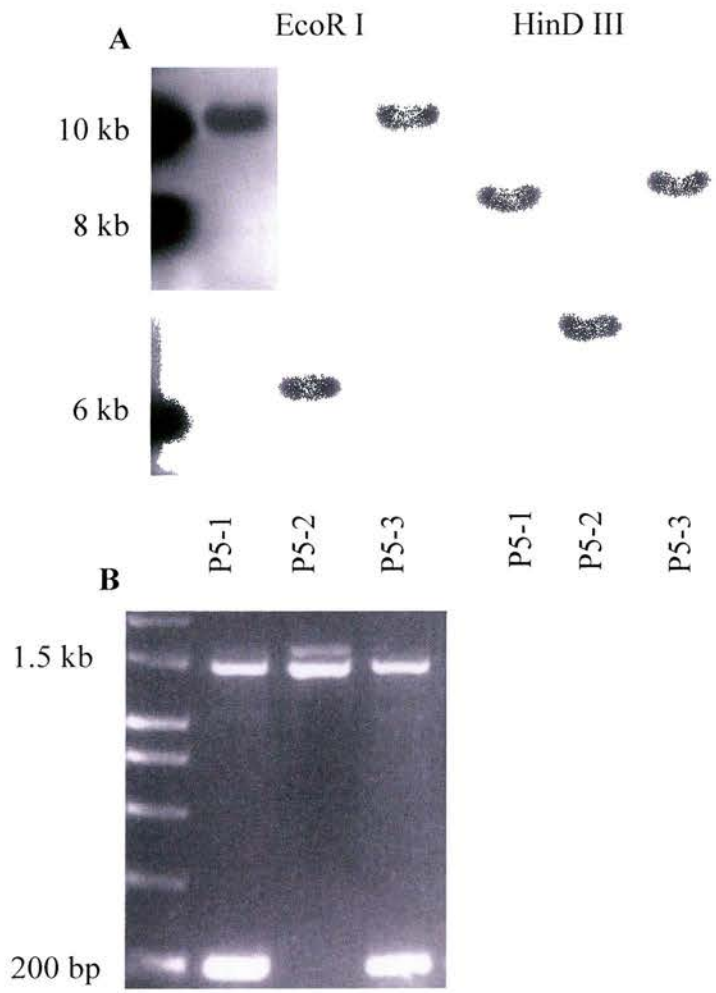

Figure 4.19: (A) The Southern hybridisation of genomic DNA from ES clones P5-1, P5-2 and P5-3 digested with EcoR I and Sal I. The probe used was created from Exon 24 and hybridized to a 6.0 kb fragment in the EcoR I digest of P5-2 and a 6.5 kb fragment in the HinD III digest of P5-2. This confirmed that P5-2 contained the correctly homologous recombined DNA. (B) PCR of the same genomic DNA using NeoFor and NeoRev primers that amplified a portion of the Neomycin resistance casette. This PCR provided the initial proof that P5-2 contained the properly recombined DNA by showing only the 1.5 kb band in that sample.

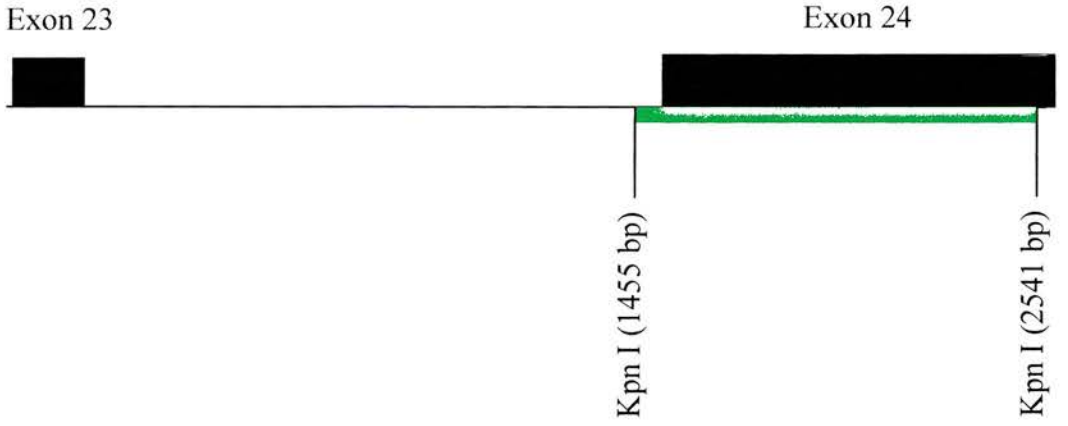

Figure 4.20: A schematic representation of *Ruk* sequence showing the 1.1 kb fragment (highlighted in green) encompassing the majority of Exon 24 that was used as probe for Southern hybridisation analysis of ES clones. Map is not to scale.

(Figure 4.19). From the 184 analysed clones, only a single clone (P5-2) was actually confirmed as positive for the insert by both methods. The PCR-based method demonstrated that correct recombination took place at the left junction of the *Ruk* locus/targeting construct while the Southern hybridisation confirmed the correct orientation at the right junction. Together the two analyses showed that both junctions were correctly recombined in clone P5-2.

P5-2 was karyotyped (see Sections 2.49) to determine if its chromosomal number had not been compromised during *in vitro* cultivation. Out of 20 metaphase plates counted, 14 had 40 chromosomes, 2 had 39 chromosomes and 4 had 38 or less (Figure 4.21). Since over half of the cells counted had the proper number of chromosomes, it was decided that the number of chromosomes was unaffected by the process and the clone could be used for production of chimeric mice.

4.2.3 Chimeric animals were produced

So far, the P5-2 clone has been microinjected into a limited number of blastocysts (see Sections 2.50-2.54); only two chimeric mice were generated and neither of them were capable of transferring the ES cell genotype through the germ line. A more extensive microinjection programme (planned for the nearest future) will be carried out to generate more and better chimeric mice and achieve germ-line transfer.

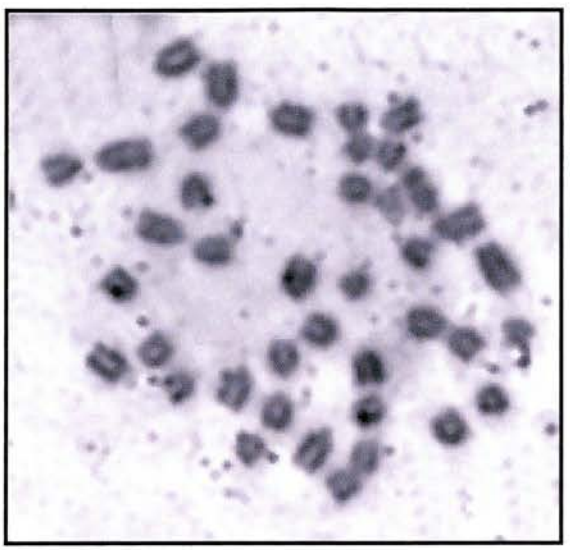

Figure 4.21: A representative chromosomal smear of ES clone P5-2, showing 40 chromosomes. The cells were burst with an hypotonic solution, fixed to the slide with Acetic acid and Methanol and the chromosomes were stained with Geimsa stain. The chromosomes were visualized and counted under bright field microscopy.

Chapter 5:
Ruk based interactions between isoforms and p85α

5.1 Ruk$_I$ is a multi-domain adaptor protein

The longest Ruk isoform, Ruk$_I$, contains several different binding domains including three SH3 domains, a PRD (proline rich domain) and a CCD (coiled-coil domain). While it was thought that the CCD acts to dimerise the different isoforms, it was also hypothesized that another dimerisation mechanism exists between the SH3A and the PRD (Kowanetz *et al.*, 2003a). In addition to dimerising, the various SH3 domains are also known to interact with a wide variety of PRD containing proteins, which allows the Ruk isoforms to act in a diversity of pathways. Conversely, the PRD of the Ruk isoforms is simultaneously able to bind SH3 domain containing proteins. Through these multiple simultaneous interactions Ruk isoforms hetero- and homo-dimerise to form multi-protein complexes that bridge different pathways.

One of the most interesting Ruk$_I$-based interactions was that discovered between Ruk$_I$ and p85α, the regulatory subunit of PI3K (Gout *et al.*, 2000). It was initially supposed that the p85α SH3 domains interacted with the PRD of Ruk isoforms, however the exact nature of the interaction was unknown.

Due to its importance, it was decided to investigate the interaction between Ruk$_I$ and p85α in detail. Several methods of analysis were used to clarify the relationship between the two proteins, including *in vitro* GST pull-down studies and co-immunoprecipitation of proteins expressed in HEK293 cells. These studies not only illuminated the relationship between the Ruk isoforms and p85α, they also confirmed the importance of the SH3A-PRD inter-Ruk$_I$ interaction. The results presented here show that Ruk$_I$ dimerises through the CCD, and other intermolecular interactions are inhibited by the presence of the SH3A-PRD binding that closes the

dimer to other interactions. The p85α subunit exists as a dimer and binds to the Ruk_l dimer through both the interactions between each dimer's SH3 domains and PRDs. Presumably, other relatively high affinity interactions, such as that between Ruk_l and Cbl, also "break open" the dimer allowing it to interact with other proteins and forming multi-protein complexes.

5.2 Ruk_l and p85α interact using SH3 domains and PRDs

5.2.1 Interaction of Ruk proteins with p85α and ΔSH3-p85α in HEK293 cells

The cDNAs encoding various isoforms of Ruk, Ruk_l, ΔA-Ruk, Ruk_m, Ruk_h and Ruk_s were subcloned into pCMV5 expression vectors and transiently expressed in HEK293 cells as described in Section 2.55. Additionally, several deletion mutants, ΔC-Ruk, ΔSH3-Ruk, Ruk_e, ΔCterm-Ruk, ABC-Ruk, ΔPro-Ruk, were also generated (see Section 2.15.4) and expressed in this manner; a FLAG tag was added to all the Ruk cDNAs during the subcloning process and the resulting proteins are illustrated in Figure 5.1. In addition to two variants of triple-myc-tagged p85α (p85α and ΔSH3-p85α), described earlier (Borthwick *et al.*, 2004) and kindly provided by Peter Shepherd, a third variant with a deletion of the region that included both Pro-rich and BH domains has been generated (ΔBH/Pro-p85α; Figure 5.1). The Ruk and p85α expression plasmids were co-transfected into HEK293 cells and the Ruk proteins were immunoprecipitated from cell lysates using immobilised anti-FLAG antibody (see Section 2.63). The presence of p85α or its mutant forms in cell lysates and immunoprecipitates was assessed by Western blotting, the results of which are shown in Figure 5.2.

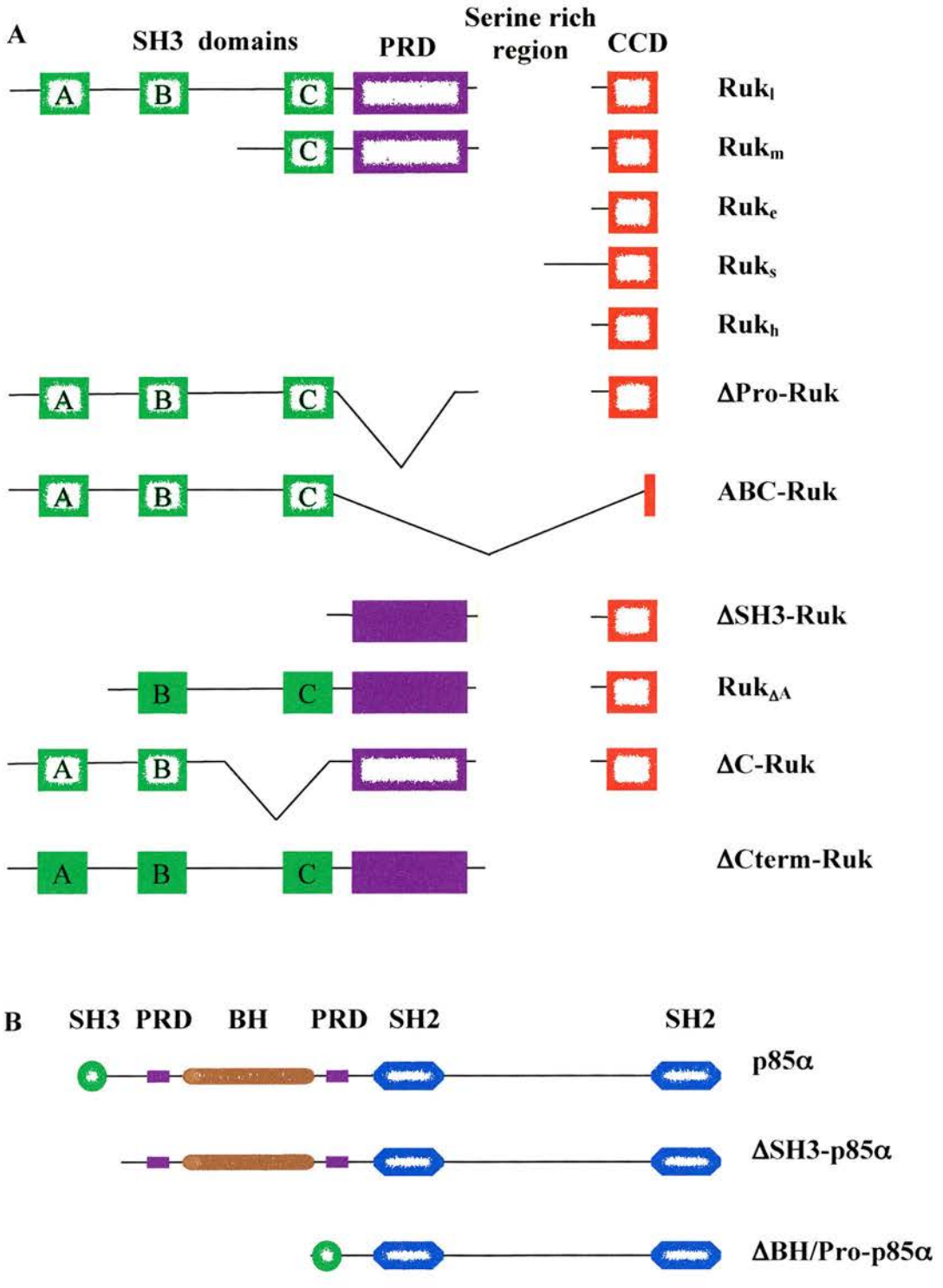

Figure 5.1: The Ruk isoforms and deletion mutants that were Flag tagged and transiently expressed in Hek293 cells in order to study interactions between Ruk$_l$ and p85α and ΔSH3-p85α (A). The full length p85α, ΔSH3-p85α and ΔBH/Pro-p85α (B). Reproduced with the permission of E. Borthwick.

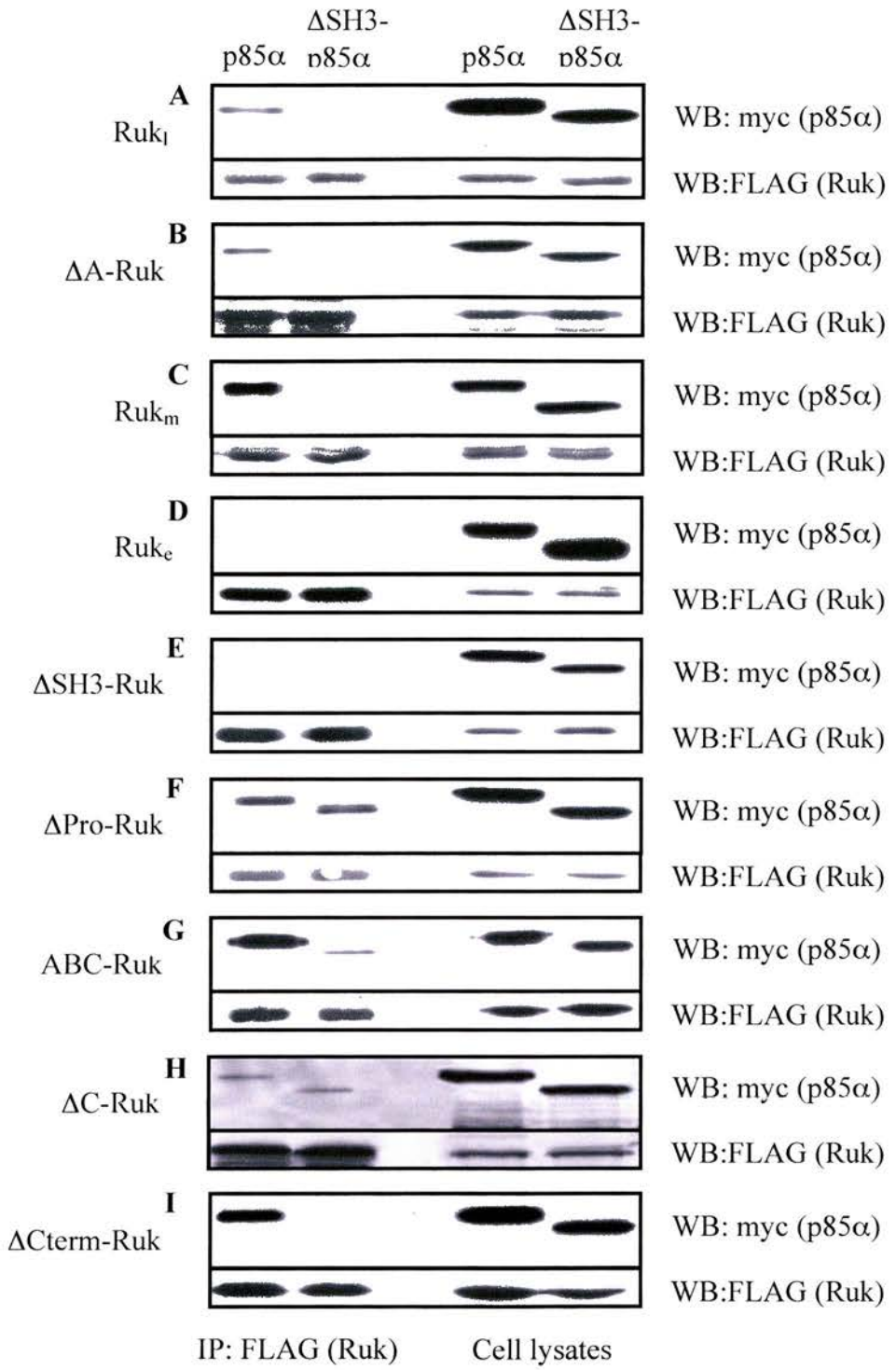

Figure 5.2: Interaction of FLAG-tagged Ruk proteins with myc-tagged p85α and ΔSH3-p85α in HEK293 cells. Total cell lysates and proteins immunoprecipitated with anti-FLAG antibody were analysed by Western blotting using anti-myc antibody to detect p85α proteins and anti-Ruk or anti-FLAG (for ΔCterm-Ruk and ABC-Ruk isoforms) antibody to detect Ruk proteins. Adapted from Borthwick *et al.*, 2004.

In mammalian cells, both Ruk_l and $Ruk_{\Delta A}$ were able to co-immunoprecipitate p85α but were unable to co-immunoprecipitate ΔSH3-p85α. Likewise, Ruk_m retained the ability to co-immunoprecipitate p85α while being unable to interact with ΔSH3-p85α. However, quantification using normalised Western blots showed that the amount of p85α co-immunoprecipitated by Ruk_m was approximately five times less than the amount co-immunoprecipitated by Ruk_l or $Ruk_{\Delta A}$. A mutant lacking SH3C, ΔC-Ruk, weakly interacted with both p85α variants.

Smaller N-terminally truncated Ruk proteins, such as ΔSH3-Ruk that lacks all three SH3 domains, Ruk_e, consisting of only the serine rich region and CCD, and the shortest isoforms Ruk_h and Ruk_s, comprised of only the CCD, failed to interact with either of the p85α variants (data not shown). In contrast, two mutants with all three SH3 domains but without the PRD, ABC-Ruk and ΔPro-Ruk, co-immunoprecipated both p85α and ΔSH3-p85α. C-terminally truncated Ruk that lacks the CCD, ΔCterm-Ruk, was also able to co-immunoprecipitate both p85α variants, although it bound ΔSH3-p85α with very low efficiency.

5.2.2 Interaction of Ruk proteins with ΔBH/Pro-p85α in HEK293 cells

A myc-tagged p85α isoform was created that was unable to dimerase due to its lack of PRD and BH domains. Either this ΔBH/Pro-p85α isoform or full-length p85α was co-expressed in HEK293 cells with FLAG-tagged Ruk proteins (Ruk_l, ΔSH3-Ruk or ABC-Ruk) and the ability of the proteins to interact with one another were assessed by co-immunoprecipitation as described in Section 2.63. As can be seen in Figure 5.3, Ruk_l was able to co-immunoprecipitate both full length p85α and

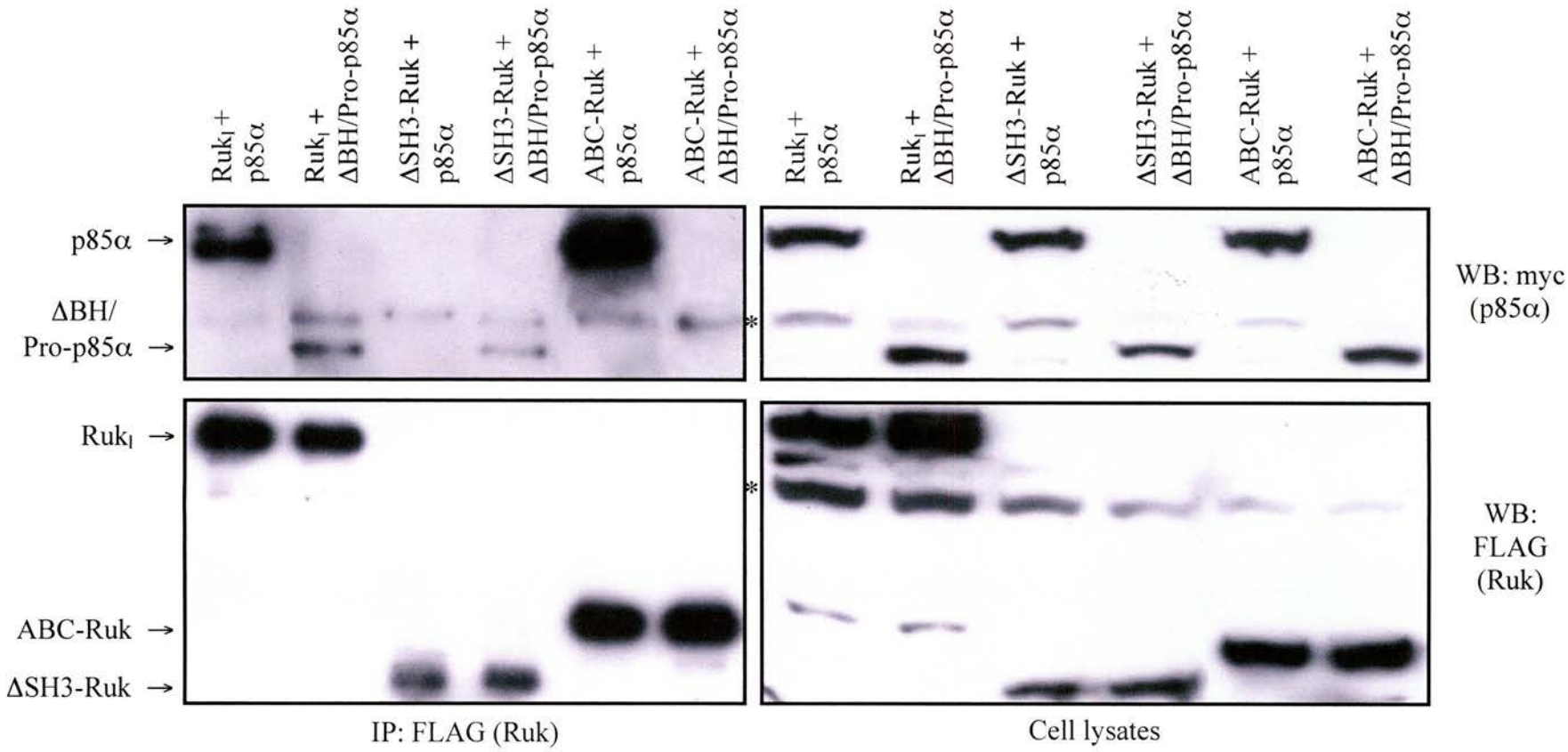

Figure 5.3: The interaction between certain FLAG-tagged Ruk proteins, Ruk$_I$, ΔSH3-Ruk or ABC-Ruk with my-tagged p85α and ΔBH/Pro-p85α. Total cell lysates and proteins immunoprecipitated with anti-FLAG antibody were analysed by Western blotting using anti-myc antibody to detect p85α proteins and anti-FLAG antibody to detect Ruk proteins. Non-specific bands are indicated by asterixs. Adapted from Borthwick *et al.*, 2004.

ΔBH/Pro-p85α. Consistent with the results described in Section 5.2.1, ΔSH3-Ruk was able to co-immunoprecipitate ΔBH/Pro-p85α but not full length p85α. Also consistent with the previous results, ABC-Ruk co-immunoprecipitated p85α while not interacting with ΔBH/Pro-p85α.

5.2.3 Interaction of p85α and Ruk isoforms with separate domains of Ruk in vitro

The individual SH3 domains and Ruk_s isoform, consisting of CCD, were cloned into bacterial expression plasmids in frame with a GST tag (see Section 2.15.3). The fusion proteins were expressed in BL21 cells in the empirically determined optimal conditions, purified (see Sections 2.64-2.67) and used in "pulldown" studies with different Ruk isoforms and p85α proteins from HEK293 cell lysates (see Section 2.68).

Aliquots of lysate from HEK293 cells transiently transfected with p85α expression plasmid were incubated with immobiliased GST-tagged SH3A, SH3B, SH3C or Ruk_s to test for interactions. The resulting Western blot was probed with anti-p85α antibody (see Section 2.61) to show the ability of p85α to interact with some of the GST-SH3 proteins. As seen in Figure 5.4A, both GST-SH3A and SH3B bound p85α, but SH3B did not bind as much p85α as GST-SH3A did. However, both GST-SH3C and Ruk_s were unable to bind p85α in this assay.

The same technique was used with FLAG-tagged Ruk isoforms that were expressed in HEK293 cells and the subsequent Western blots were analysed with an anti-FLAG antibody. The four FLAG-tagged isoforms used in this study were Ruk_l, Ruk_m, Ruk_h and ΔPro-Ruk and the results are found in Figure 5.4B-E. All four of

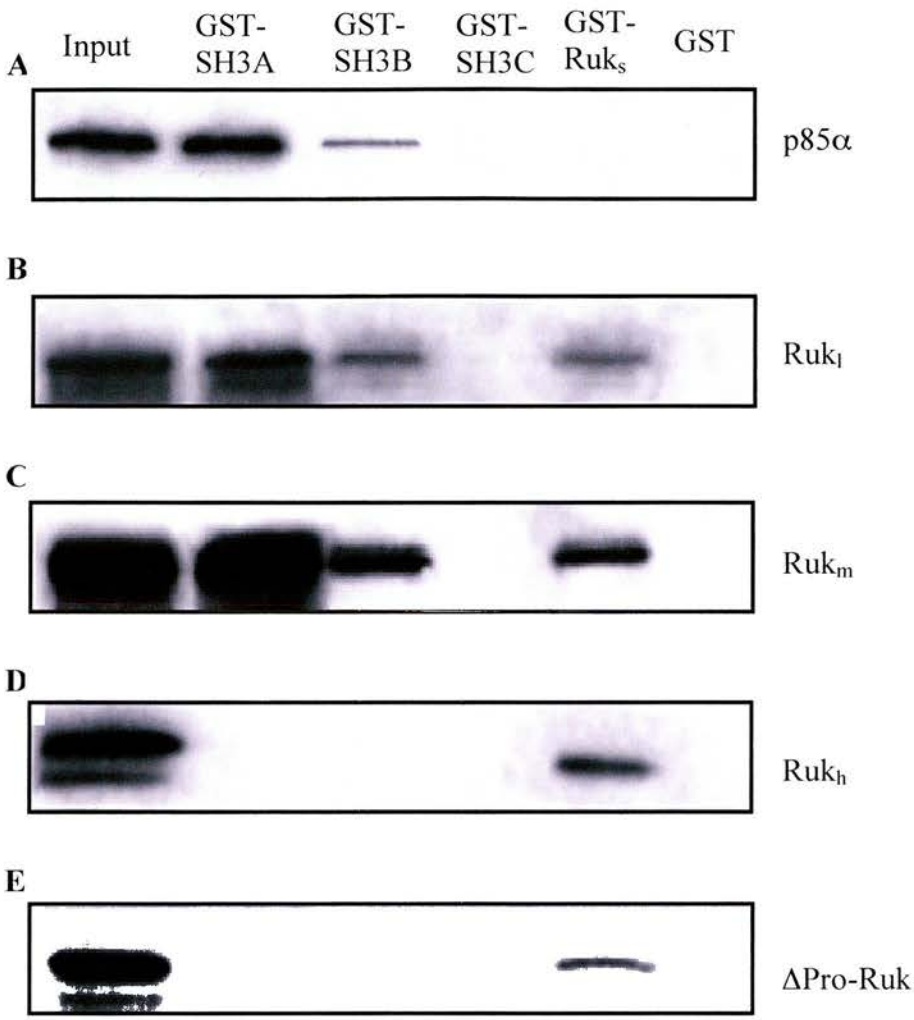

Figure 5.4: The interaction between GST-tagged Ruk SH3 domains and GST-Ruk$_s$ with myc tagged-p85α and FLAG tagged-Ruk proteins. Individual SH3 domains and Ruk$_s$ interacting with p85α (A), Ruk$_l$-FLAG (B), Ruk$_m$-FLAG (C), Ruk$_h$-FLAG (D) or ΔPro-Ruk-FLAG (E). The GST-SH3 domains and Ruk$_s$ were immobilized onto Glutathione Sepharose beads as described in Section 2.67 and the resulting Western blots were probed with anti-myc Ab (p85α) or anti-FLAG Ab (Ruk isoforms). Adapted from Borthwick *et al.*, 2004.

these proteins were effectively pulled down by GST-Ruk$_s$ with approximately equal affinity for all isoforms. However, the GST-SH3C fusion protein did not interact with any of four Ruk proteins. GST-SH3A and GST-SH3B were both able to interact with Ruk$_l$ and Ruk$_m$ but not those lacking the PRD, ΔPro-Ruk or Ruk$_h$. GST-SH3A did have a higher affinity for Ruk$_l$ and Ruk$_m$ than GST-SH3B.

Chapter 6:
Discussion

6.1 The *Ruk* gene structure

As shown in Section 3.2, a 129Ola genomic library contained in λ phages was screened using probes derived from the known cDNA of Ruk_l, Ruk_m and Ruk_s. Seven consecutive screenings occurred with various probes; these screenings showed that *Ruk* is a relatively large gene that encompasses over 320 kb, and it is somewhat complex with 24 exons and 5 different promoters (Figures 3.1 and 3.2). Three of these exons were not isolated from the screenings instead they were identified through analysis of the mouse EST database.

The 24 exons of *Ruk* come together in various ways to create 12 different splice variants, which are then translated into the 7 different isoforms of Ruk shown in Figure 3.3. The 12 *Ruk* transcripts vary from one another in their 5' end, and some of the exons of the *Ruk* gene are limited to specific subsets of transcripts. As can be seen from Figure 3.3, the different isoforms translated from the *Ruk* transcripts vary greatly from one another but are mainly N truncated forms of the template, Ruk_l. Figure 3.2 shows that the only common domain between all the isoforms is the CCD (coiled-coil domain) that is encoded by Exon 22, 23 and 24.

Unfortunately, the different isoforms make immunohistochemical based expression studies of specific Ruk isoforms very hard. Isoform specific antibodies could be produced, but the cost and time involved are almost prohibitive when the number of isoforms is taken into consideration. Thus, the genomic approach described in Section 3.2 was taken to resolve the developmental expression patterns of *Ruk* transcripts.

6.2 Seven *Ruk* splice variants were discovered

The RT-PCR process described in Section 3.2.2 was performed to amplify

specific *Ruk* transcripts from the RNA of different tissue samples taken from adult and P8 mice. For the RT-PCR done on these samples, primers were designed that would amplify only certain *Ruk* splice variants that are distinguishable from one another due to their size variance as can be seen in Figure 3.4.

6.2.1 The Ruk_{xl} and Ruk_{l} transcripts and Ruk_{l} protein

Ruk_{xl} varies from Ruk_{l} only in the presence or absence of Exons 7 and 8 that encode a linker region between SH3B and SH3C (see Section 3.2.1 and Figure 3.2). However, there is a marked preference for the Ruk_{l} transcript in certain tissues, which may be due to the dominance of a splicing event that cut out Exons 7 and 8 in these tissues as a promoter for both transcripts is the same.

The Ruk_{l} isoform is the second longest of the Ruk family and is comprised of three SH3 domains followed by a PRD, a serine rich region and a CCD (Figure 3.3; Buchman *et al.*, 2000; Take *et al.*, 2000; Borinstein *et al.*, 2000). This isoform is the most studied isoform and most of the interactions that Ruk isoforms are known to perform in, are mediated through Ruk_{l}. However, it is likely that Ruk_{l} acts as a dimer with the other Ruk isoforms and has a larger role in cellular physiology than is currently known.

6.2.2 The $Ruk_{\Delta A}$ transcript and protein

The $Ruk_{\Delta A}$ transcript differs from Ruk_{l} by the lack of Exons 1 and 2, instead it is primed from Exon 3 (see Section 3.2.1 and Figure 3.2). Exon 2 is the main coding exon for SH3A, and therefore, the protein encoded by $Ruk_{\Delta A}$ lacks the SH3A domain and both the splice variant and protein are named after this loss (Figure 3.3). Exon 3 is specific to $Ruk_{\Delta A}$, it is not found in any of the other transcripts, while the 5' region

of Exon 3 probably contains the $Ruk_{\Delta A}$ promoter, the 3' region contains a start codon and a small coding region that specifies an N-terminal sequence that is unique to $Ruk_{\Delta A}$ protein. While $Ruk_{\Delta A}$ is fairly well expressed in the P8 mouse tissues sampled, there is a preference for it in some tissues that can be attributed to the emphasis and necessity of $Ruk_{\Delta A}$ over other Ruk isoforms.

The SH3A domain absent in $Ruk_{\Delta A}$ does mediate some Ruk_I interactions, and current thinking places $Ruk_{\Delta A}$ as a negative inhibitor of Ruk_I and CD2AP/CMS. $Ruk_{\Delta A}$ functions through binding similar partners to CD2AP/CMS without eliciting the same responses (Section 1.3.6.2; Tibaldi and Reinherz, 2003). It is also possible that $Ruk_{\Delta A}$ acts independently of Ruk_I and CD2AP/CMS to produce its own signalling cascade (Section 1.4) which may account for the preference that some tissues have for $Ruk_{\Delta A}$. However, it remains to be seen if there are unique $Ruk_{\Delta A}$ bidning partners, but it is distinctly possible there are some due to the preference that some tissues have for the transcript.

6.2.3 The $Ruk_{\Delta CP}$ transcript and protein

$Ruk_{\Delta CP}$ is similar to Ruk_I, except that it lacks the exons between Exon 13 and Exon 22 that are normally translated into the SH3C, PRD (proline rich domain) and serine rich regions (see Section 3.2.1 and Figure 3.2). Hence, the designation for the transcript indicates that the SH3C and PRD are lacking in the protein (Figure 3.3). The $Ruk_{\Delta CP}$ promoter is the same as that for Ruk_I and Ruk_{xI}, and is probably contained in front of Exon 1. The existance of this transcript is suggested by the presence of a clone in the EST database (Buchman *et al.*, 2004). However, neither RT-PCR nor protein expression studies have shown $Ruk_{\Delta CP}$ or its translated protein to actually

exist in the tissues so far sampled.

The lack of the middle domains in $Ruk_{\Delta CP}$ means that there are severe limitations to the number of binding partners for the isoform. $Ruk_{\Delta CP}$ will most likely be able to interact with proteins that bind Ruk SH3A and B, such as ARAP3, CAMGAP1 and AIP1/Alix (Kowanetz *et al.,* 2004; Sakakibara *et al.,* 2004; Bogler *et al.,* 2000). There may also be $Ruk_{\Delta CP}$ binding partners and functions that are currently unknown due to the lack of research into this isoform. The lack of a PRD would prevent $Ruk_{\Delta CP}$ from playing a direct role in many of the Ruk_I processes such as FA (focal adhesion) formation and endocytosis, as it would be unable to bind endophilins, $p130^{Cas}$ and other proteins (Petrelli *et al.*, 2002; Soubeyran *et al.*, 2002; Watanabe *et al.,* 2000; Hutchings *et al.,* 2003).

$Ruk_{\Delta CP}$ may be able to interact with CAPZ and thus play a role in actin rearrangements. $Ruk_{\Delta CP}$ may act as a negative inhibitor of Ruk_I function by binding to CAPZ without binding to CD2 in a manner the opposite to how $Ruk_{\Delta A}$ is thought to inhibit Ruk_I and CD2AP/CMS function in T cells (Tibaldi and Reinherz, 2003). Alternatively, $Ruk_{\Delta CP}$ may inhibit Ruk_I, CD2AP/CMS and $Ruk_{\Delta A}$ functions through dimerisation with these isoforms. The dimerisation would inhibit the formation of multi-protein complexes and prevent the larger isoforms from acting as a scaffolding protein that bridges multiple cellular pathways.

6.2.4 Ruk_m transcripts and protein

Two versions of Ruk_m transcripts were found in rat skin previously, Ruk_{m1} and Ruk_{m3}. Analysis of the mouse *Ruk* locus has shown that both Ruk_{m1} and Ruk_{m3} are transcribed from the promoter located upstream of Exon 10 that also contains a very small coding region in its 3' end and these transcripts are the same except for

the presence of Exon 11 in *Ruk$_{m1}$* (see Section 3.2.1 and Figure 3.2). Exon 11 does not change the overall structure of the transcripts as it merely serves to extend the N terminal region of Ruk$_m$ that does not belong to any specific binding domain. *Ruk$_{m1}$* and *Ruk$_{m3}$* are transcribed into two distinct proteins due to the different start codons are used, but this difference is so insignificant that both proteins can be considered to be Ruk$_m$.

The Ruk$_m$ protein is a truncated form of Ruk$_l$ that is missing the two most N terminal SH3 domains; Ruk$_m$ is comprised of the SH3C, PRD, serine rich region and CCD (Figure 3.3). While *Ruk$_{m3}$* was not amplified during the RT-PCR study, *Ruk$_{m1}$* was and the study shows that its expression is restricted to a small number of tissues with the developmental downregulation similar to certain other *Ruk* transcripts.

The Ruk$_m$ isoform, similarly to most of the smaller isoforms, has not been studied extensively. It is known to interact with Ruk$_l$ and become ubiquitinated during the endocytic process through the Ruk$_l$-Cbl interaction (Verdier *et al.*, 2002). However, the result of this ubiquitination is not known and there are no known Ruk$_m$ specific binding partners. Theoretically, Ruk$_m$ would be able to interact with proteins such as endophilin, Crk, p130^{Cas} and CAPZ that are thought to interact with the PRD and serine rich regions of Ruk$_l$ (Petrelli *et al.*, 2002; Soubeyran *et al.*, 2002; Watanabe *et al.*, 2000; Hutchings *et al.*, 2003). Through these interactions, Ruk$_m$ may inhibit other Ruk isoforms by binding to only a certain subset of Ruk$_l$ interactors without binding others and eliciting the same responses. Additionally, Ruk$_m$ should dimerise with the other Ruk isoforms and through this interaction may inhibit the functions of Ruk$_l$ and other isoforms. Ruk$_m$ may dimerise with Ruk$_l$,

CD2AP/CMS and $Ruk_{\Delta A}$ and prevent the formation of multi-protein complexes that are critical to various pathways in a manner similar to $Ruk_{\Delta CP}$ inhibition.

6.2.5 Ruk_s transcript and protein

Exons 10 and 11 are found in only three transcripts: the two *Ruk_m* transcripts and *Ruk_s*. *Ruk_s* is composed of Exons 10, 11, the 5' portion of Exon 12 and the common Exons 22 (only the 3' portion) through to 24 (see Section 3.2.1 and Figure 3.2). When translated, the Ruk_s protein contains the N terminal linker region that it has in common with Ruk_m and the CCD, making it the smallest isoform with only a single binding domain for interactions (Figure 3.3). Previous work has shown it is expressed in newborn and adult rat skin (Gout *et al.*, 2000). However, although one would expect amplification of a *Ruk_s* band at 440 bp with M3 and MC primers in tissues expressing Ruk_s, these primers efficiently amplified the much longer fragment corresponding to *Ruk_{m3}* (Figure 3.4. discussed in Section 6.3).

The CCD found in Ruk_s allows this isoform to dimerise with the other longer isoforms and influence their functions. For instance, Ruk_s is ubiquitinated by Cbl during endocytosis because of the dimerisation of the Ruk_l and Ruk_s isoforms (Verdier *et al.*, 2002). Through this dimerisation, Ruk_s may inhibit Ruk_l, CD2AP/CMS and $Ruk_{\Delta A}$ function in multi-protein complexes in a manner similar to the possible inhibitory effects of $Ruk_{\Delta CP}$. There may also be Ruk_s specific interactions that occur, but as of yet no unique binding partners have been identified.

6.2.6 Ruk_h transcripts and protein

There are four distinct *Ruk_h* transcripts, which are among the smallest transcripts derived from the *Ruk* gene. The *Ruk_h* transcription is promoted by

sequences upstream of Exon 19, which also contains a portion encoding the N-terminus of the serine rich domain in its 3' end and contains, in addition to Exon 19 and 21 as disccused below, Exons 20, 22, 23 and 24 (see Section 3.2.1 and Figure 3.2). However, each *Ruk*$_h$ isoform is slightly different from the others based on the presence or absence of the middle region of Exon 19 and the entirety of Exon 21. *Ruk*$_{h1}$ contains the entirety of both Exon 19 and Exon 21, *Ruk*$_{h2}$ contains all of Exon 21 but lacks the middle portion of Exon 19, while *Ruk*$_{h3}$ has the entire Exon 19 but lacks the entire Exon 21. *Ruk*$_{h4}$ lacks both the middle portion of Exon 19 and the entire Exon 21. The middle portion of Exon 19 contains only the 5' untranslated sequences for *Ruk*$_h$ and may affect *Ruk*$_h$ expression, while Exon 21 encodes a portion of the serine rich region in other Ruk proteins.

It should be noted that there is no in-frame start codon in any of the *Ruk*$_h$ transcripts upstream of the ATG found in Exon 22. Therefore, the four *Ruk*$_h$ transcripts are all translated into a single protein, Ruk$_h$. Ruk$_h$ is a relatively small isoform consisting of a portion of the serine rich region and the CCD (Figure 3.3). This limits the known interactions that Ruk$_h$ is able to participate in to CAPZ binding and dimerisation. Much like the smaller isoforms of Ruk, such as Ruk$_{\Delta CP}$, Ruk$_h$ should be able to inhibit the formation of Ruk-based multi-protein complexes by dimerising Ruk$_l$ and Ruk$_{\Delta A}$. This would also prevent multi-protein complexes based around CD2AP from forming.

While it was possible to specifically amplify *Ruk*$_{h2}$ and *Ruk*$_{h4}$ with the help of primers used in the RT-PCR study, this was not possible for *Ruk*$_{h1}$ and *Ruk*$_{h3}$ that contain Exon 19 in its entirety. One possible explanation of this phenomenon is a higher abundance of *Ruk*$_{h2}$ and *Ruk*$_{h4}$ than of *Ruk*$_{h1}$ and *Ruk*$_{h3}$ transcripts in the

mouse tissues used in this study. Another explaination is that *Ruk*$_{h1}$ and *Ruk*$_{h3}$ are found in samples not taken, such as the adult heart. It is also possible that Exon 19 produces a 2° cDNA structure somehow disrupts the RT-PCR process. The *Ruk*$_h$ transcripts are mainly found in the heart (hence their name) and the dimerisation/inhibition of other Ruk isoforms or other undiscovered Ruk$_h$-specific interactors may be crucial to the proper development and function of the heart.

6.2.7 Ruk$_t$ transcript and protein

The final *Ruk* transcript is *Ruk$_t$*, a testis specific form (hence its designation) that has a unique exon, Exon 18. A region upstream of this exon probably contains a *Ruk$_t$* specific promoter and the exon itself encodes the 3' UTR, start codon and a short stretch of coding region that does not belong to any domain. The *Ruk$_t$* transcript is very similar to *Ruk*$_{h2}$, except that it swaps the *Ruk*$_h$ promoter for Exon 18. It contains the 3' portion of Exon 19 and Exon 21 along with all the downstream exons that encode the CCD (Exons 22-24; see Section 3.2.1 and Figure 3.2).

This means that the translated protein, Ruk$_t$, contains a non-domain region in its N-terminus but is mainly composed of the serine rich region and CCD (Figure 3.3). Much like for Ruk$_h$ the known interactions are limited to CAPZ and dimerisation with other Ruk isoforms (Verdier *et al.*, 2002). While it is theoretically possible for Ruk$_t$ to dimerise with the other isoforms, the only other *Ruk* transcript expressed with in adult testis *Ruk$_t$* is *Ruk*$_{h2}$ (see Section 6.3.5). It is unknown why they are developmentally upregulated in the mouse adult testis but the upregulation does indicate a possible role for Ruk$_t$ and Ruk$_h$ in male sexual maturity. There may be Ruk$_t$-specific interactors but currently none are known.

6.3 Ruk transcripts are developmentally down regulated

The RT-PCR study allowed an expression pattern to be developed, which showed that every *Ruk* transcript, with the exception of Ruk_l, is developmentally downregulated in the adult mouse; when the same P8 and adult tissue samples were used, there was a marked decrease in transcript amplification as seen in Figure 3.4. This shows that there is a direct correlation between development and the inhibition of *Ruk* transcription in certain tissues, thus implicating Ruk isoforms in mammalian development. This hypothesis is also based on the current research that points to a role for Ruk isoforms in cellular proliferation, largely due to the role of Ruk_l in endocytosis and PI3K inhibition. It may be that Ruk downregulation results in changes in signal transduction regulation, leading to a decrease in cellular proliferation and indicating the onset of adulthood.

6.3.1 Ruk transcripts in skin

As shown in Figure 3.4, $Ruk_{\Delta A}$ and Ruk_{ml} are amplified prominently from the P8 skin sample, with Ruk_l and Ruk_{xl} being only slightly less amplified. This expression pattern corresponds to the protein samples taken from P8 skin, which showed that Ruk_l, $Ruk_{\Delta A}$, Ruk_m and Ruk_s are all translated (Figure 3.5). There was a high amount of $Ruk_{\Delta A}$ with a lesser amount of Ruk_l translation and almost negligible amounts of Ruk_m and Ruk_s. The adult mouse skin sample showed no amplification of any splice variants indicating the developmental downregulation of all *Ruk* transcripts.

Previous research using immature rat skin samples showed that the Ruk_l, Ruk_m and Ruk_s transcripts are detectable (Gout *et al.*, 2000). Possibly through a slight difference of expression in rat tissues, adult rat skin has been shown to express

Ruk_l and Ruk_m (Gout *et al.*, 2000). The level of expression of these proteins in adult rat skin is very slight when compared to the immature skin samples so this does not contradict the pattern of developmental downregulation seen in mouse tissues.

The developmental inhibition of *Ruk* transcription could be interpreted as meaning that Ruk isoforms do not play a crucial role in maintaining mature skin despite the constant turnover of epidermal cells. Instead, it seems that most of the Ruk isoforms are important to developing skin, possibly through their roles in pathways leading to cell growth and proliferation, such as RTK endocytosis and cellular responses to growth factors (see Section 1.3.1). The appearance of several different *Ruk* transcripts and isoforms in immature skin indicates that the isoforms probably interact with one another to regulate their actions. The combinatorial possibilities when Ruk isoforms dimerise lead to either bridging of different cellular pathways (eg: Ruk_l homodimerisation) or the inhibition of multi-protein complexes and the attenuation of signalling (eg: Ruk_l heterodimerisation with Ruk_s or Ruk_m).

6.3.2 Ruk transcripts in brain

The P8 brain sample showed a prominent amplification of Ruk_l and $Ruk_{\Delta A}$ with a slight amplification of Ruk_{xl} (see Section 3.2 and Figure 3.4). This corresponds to the protein expression profile that shows a fairly high amount of Ruk_l translation in P8 brain samples (see Section 3.3 and Figure 3.5). This does conflict with previous studies that showed that the newborn rat brain contains only Ruk_l mRNA, but the difference might be due to either the species or techniques used (Gout *et al.*, 2000). It may be that $Ruk_{\Delta A}$ is not translated in premature tissues as none was found in the protein expression study. While an adult brain sample was not used in any of these studies, Bogler *et al.* (2000) showed that adult brain tissues

showed barely detectable levels of $Ruk_{\Delta A}$ expression. Gout *et al.* (2000) have also shown that the Ruk_I isoform is primarily expressed in adult rat brain samples, but there are no juvenile rat brain samples to directly compare with the adult samples. Therefore, it cannot be said if Ruk isoforms are developmentally downregulated in brain samples as they are in other tissues.

However, much like in other tissues, it is probable that Ruk isoforms are necessary for the neuronal development and proliferation that does occur thoughout development. Since Ruk_I acts in many different known pathways and with the possibility that there are undiscovered pathways that Ruk isoforms act in, it is hard to say what exact function they perform in the brain. The indications are that Ruk isoforms are limited to dividing cells, a theory that is supported by the fact that $Ruk_{\Delta A}$ expression in adult brain cells is limited to cancerous cells and can be found in half of the human gliomas so far tested (Bogler *et al.*, 2000; Borinstein *et al.*, 2000). The re-expression of $Ruk_{\Delta A}$ is one of the hallmarks of brain tumours, and its re-expression may help the normally senescent neuronal cells to begin dividing again.

6.3.3 Ruk transcripts in lung

P8 lung showed negligible expression levels of Ruk_{xI} and $Ruk_{\Delta A}$, with no other transcript being expressed (see Section 3.2 and Figure 3.4). This concurs with previous reports, prior to the discovery of $Ruk_{\Delta A}$, that only the mRNA for Ruk_I was detected in newborn rat tissues (Gout *et al.*, 2000). These results indicate that only small amounts of Ruk_I and $Ruk_{\Delta A}$ are translated in the developing lung and, therefore, it can be said that Ruk isoforms play an unimportant role in lung development at this post-natal stage. It should be noted that the Ruk_I isoform was found in rat adult lung samples in a previous study, but there were no early postnatal

samples to compare the expression amount to and the amount could be described as negligible (Gout *et al.*, 2000).

Previous research has shown that EGFR is crucial to embryonic lung development and bronchial branching (Warburton *et al.*, 1992; Seth *et al.*, 1993), meaning that *Ruk* transcripts may be downregulated sooner in the lung than in other tissues, possibly at the late embryonic stages. One of the main functions of Ruk_I is to regulate RTK endocytosis and modulate cellular responses, and the transcription of the two proteins may be tied to one another. Therefore, once EGFR and other RTKs are no longer necessary to post-natal lung development neither are the Ruk isoforms, and the low levels of Ruk_{xl} and $Ruk_{\Delta A}$ that are seen in the P8 lung may be vestigial traces of a much higher level of expression found in fetal lungs.

It is interesting to note that only P8 lung and thymus samples show a marked preference for the Ruk_{xl} transcript, as all of the other samples amplified Ruk_l to a higher or equal degree (Figure 3.4A and 3.4B). It is currently unknown why some tissues favour Ruk_{xl}, since both transcripts vary only by the presence of Exons 7 and 8 in Ruk_{xl}, as previously described. Perhaps the presence of Exons 7 and 8 in Ruk_{xl} is preferred in certain tissues for an unknown reason.

6.3.4 Ruk transcripts in kidney

As would be expected by the similarities between CD2AP/CMS and Ruk_I structure and function and the importance of CD2AP/CMS to kidney architecture, all four of the main transcripts (Ruk_l, Ruk_{xl}, $Ruk_{\Delta A}$ and Ruk_{ml}) were amplified from the P8 kidney sample (see Section 3.2 and Figure 3.4). The high amplification of $Ruk_{\Delta A}$, equal to the highest expression in the samples used, shows that the $Ruk_{\Delta A}$ isoform must perform some role in kidney development (Figure 3.4C). Curiously enough,

protein samples taken from the mouse P8 lung showed very slight expression of Ruk_l and Ruk_s; no other isoform was translated in this tissue (see Section 3.3 and Figure 3.5).

As has been previously stated in Section 1.3.6.2, it has been hypothesized that $Ruk_{\Delta A}$ is a negative regulator of CD2AP/CMS and Ruk_l in T cells (Tibaldi and Reinherz, 2003). Therefore is possible that $Ruk_{\Delta A}$ and Ruk_l act in a similar manner in kidney cells and together subtly attenuate the function of CD2AP/CMS in kidney architecture and function as elucidated in Section 1.7.3.

6.3.5 Ruk transcripts in testis

The two exceptions to the overall developmental down-regulation of *Ruk* transcripts are *Ruk$_t$* and *Ruk$_{h2}$* (see Section 3.2 and Figure 3.4). Strangely, these *Ruk* transcripts are up regulated specifically in the adult testis (Figure 3.4F), a fact that indicates a possible function of Ruk_t and Ruk_h in sexual development and maturation. The expression of Ruk_t and Ruk_h could not be confirmed through protein expression studies using adult testis samples, possibly due to post-translational modifications that do not allow their effective extraction with the methods used in the study (see Section 3.3 and Figure 3.5). While the *Ruk$_t$* and *Ruk$_{h2}$* transcripts are basically similar, they do differ in their most 5' exon and their promoters. Due to their developmental upregulation, it can be hypothesised that these promoters are under the control of the same factors that regulate expression of other proteins involved in sexual maturity.

If both isoforms are translated in adult testis, they may be able to dimerise via their CCDs. While, no binding partners for either isoform have been discovered, Ruk_t and Ruk_h are likely able to interact with CAPZ and thereby influence actin

rearrangements. Possibly, the continual *Ruk$_t$* transcription in adult testis is an indication that the Ruk$_t$ isoform is necessary for spermatogenesis. The P8 testis sample, in contrast to the adult testis, shows an almost universal expression of *Ruk* transcripts. *Ruk$_l$*, *Ruk$_{xl}$*, *Ruk$_{\Delta A}$* and *Ruk$_{ml}$* are prominently expressed and are all downregulated in the adult testis which expresses none of these transcripts (Figure 3.4). Strangely, a relatively small amount of Ruk$_{\Delta A}$ is translated in the adult testis according to the protein expression profile (Figure 3.5). It is unknown why the transcript was not found in the RT-PCR, although the protein found in the Western blot may be another, unknown Ruk, isoform that travels at the same electrophoretic mobility of Ruk$_{\Delta A}$.

Recent work has discovered a testis-specific form of the PI3K functional antagonist PTEN, which was named PTEN 2 and acts as a 3' phosphatase with a preference for PtdIns(3,4,5)P_3 and PtdIns(3,5)P_2 (Wu *et al.*, 2001). PTEN 2 is believed to play a role in the terminal differentiation of sperm and is expressed with the onset of sexual maturity, similarly to *Ruk$_t$* and *Ruk$_{h2}$* (Wu *et al.*, 2001). It is possible that the various isoforms of Ruk act in concert to "fine-tune" PI3K function prior to sexual maturity when there is no PTEN 2 expression. The longer transcripts are then downregulated in favour of Ruk$_t$ and Ruk$_h$ when sexual maturity is reached, thereby allowing PI3K to produce the substrates preferred by PTEN2, and beginning the signalling cascades that result in sperm development.

6.3.6 Ruk transcripts in spleen and thymus

Among other isolations of Ruk$_l$, Take *et* al. (2000) and Watanabe *et al.* (2000) both reported isolating Ruk$_l$ using a yeast two-hybrid screen based on a B lymphocyte library. Tibaldi and Reinherz (2003) also reported cloning both *Ruk$_l$* and

Ruk$_{\Delta A}$ from a T lymphocyte library, and Gout *et al.* (2000) showed that Ruk$_{I}$ is expressed in adult rat spleen samples. Additionally, Ruk$_{I}$ is thought to play a role in both B and T lymphocyte activation and maturity (see Section 1.3.5 and 1.3.6).

Taken together this research indicates that both transcripts should be found in the immune system organs. Therefore, it is no surprise that *Ruk*$_{I}$, *Ruk*$_{xI}$ and *Ruk*$_{\Delta A}$ transcripts have been found in a P8 spleen sample by RT-PCR (see Section 3.2 and Figure 3.4). In fact, the *Ruk*$_{\Delta A}$ transcript is among the most highly expressed in all the tissue samples used. This means that three distinct isoforms (Ruk$_{xI}$, Ruk$_{I}$ and Ruk$_{\Delta A}$) may be translated in the developing spleen; indeed equal amounts of Ruk$_{I}$, Ruk$_{\Delta A}$, Ruk$_{m}$ and a lesser amount of Ruk$_{s}$ are found in protein samples taken from mouse P8 spleen tissues (see Section 3.3 and Figure 3.5).

While no adult spleen sample was taken, an adult thymus sample was taken, thereby allowing a direct comparison between the immature and mature thymus. In the immature thymus, there is a high level of *Ruk*$_{\Delta A}$ expressed (it is an equally highest amount of all the samples used), with lower levels of *Ruk*$_{I}$ and *Ruk*$_{xI}$. The *Ruk*$_{xI}$ transcript has the highest amount of expression in the P8 thymus out of all the tissues sampled, as can be seen in Figure 3.4. The isoforms translated from these transcripts are found in similar amounts in Figure 3.5; Ruk$_{I}$ is the highest expressed with lesser amounts of Ruk$_{\Delta A}$ and Ruk$_{m}$ being expressed. An almost negligible amount of Ruk$_{s}$ was also detected in the Western blot. This adolescent expression pattern is carried over to the adult thymus; there is decreased expression of *Ruk*$_{xI}$ and *Ruk*$_{\Delta A}$, and a complete abrogation of *Ruk*$_{I}$. A study using rat adult thymus showed a slightly different expression pattern with no Ruk $_{\Delta A}$ being expressed and with Ruk$_{I}$ as

the primary isoform expressed and possibly being derived from *Ruk$_{xl}$* (Gout *et al.*, 2000).

The continued expression of *Ruk$_{xl}$* and *Ruk$_{\Delta A}$* in the adult thymus indicates that these proteins are necessary for its function, probably due to their roles in T cell development and activation. Current research makes a compelling argument that Ruk isoforms act in T cells through a variety of mechanisms, as discussed in Section 1.3.6. In T cells Ruk$_{\Delta A}$ is known to bind the same proteins (eg: CD2) as CD2AP/CMS without producing the same responses (eg: p130^{Cas}), thereby inhibiting CD2AP/CMS function (Tibaldi and Reinherz, 2003). Also in T cells, Ruk$_l$ is known to weakly bind p130^{Cas} and CD2 and elicit responses similar to, but to a lesser extent, than CD2AP/CMS does, thereby subtly attenuating CD2AP/CMS-based signalling (Tibaldi and Reinherz, 2000). Ruk$_l$ may also play a role in attenuating signals from the TCR as it binds the TCR inhibitors c-Cbl and Cbl-b. Other T cell specific, Ruk$_l$ interactions are known to occur placing Ruk isoforms in the pathways that control T cell development, proliferation and antibody specificity.

Less is known of Ruk$_l$ and Ruk$_{\Delta A}$ function in B cells (Section 1.3.5), but the general method of interaction is probably the same, in that both bind to the same proteins without Ruk$_{\Delta A}$ causing the same downstream responses as Ruk$_l$. In both T and B cells, there is the possibility that the Ruk isoforms dimerise to produce unique multi-protein complexes that act separately from CD2AP/CMS functions.

6.3.7 Ruk transcripts in heart

The P8 heart sample showed an amplification of all four major transcripts, *Ruk$_l$*, *Ruk$_{xl}$*, *Ruk$_{\Delta A}$* and *Ruk$_{m1}$*, as well as the smaller transcripts *Ruk$_{h2}$* and *Ruk$_{h4}$* (see Section 3.2 and Figure 3.4). Out of these transcripts expressed, only *Ruk$_{h4}$* was truly

heart specific as *Ruk*$_{h2}$ is also found in the adult testis sample. A small amount of Ruk$_{l}$ and a negligible amount of Ruk$_{\Delta A}$ were translated, as shown in the protein expression profile (see Section 3.3 and Figure 3.5). The smaller Ruk$_{h}$ isoform may not have been detected in this Western blot due to the post-translational modifications which are thought to occur and which make this isoform harder to extract with the methods used in the study.

It is theorized that Ruk$_{h}$ has a unique role in the heart, but no binding partners for Ruk$_{h}$ in heart have yet been found and its role is largely unknown. Theoretically, it could be possible for Ruk$_{h}$ to bind CAPZ and play a role in actin cytoskeleton reorganization as well as dimerising with Ruk$_{l}$ and Ruk$_{\Delta A}$. The Ruk$_{l}$ and Ruk$_{\Delta A}$ isoforms that can be found in the heart are likely to perform the same function as in other tissues that leads to cell growth, division and proliferation in order to develop the heart to adult size.

6.3.8 Future work to clarify expression patterns

While the expression pattern of *Ruk* transcripts is enlightening, more research will need to be done in order to better understand why *Ruk* transcription is developmentally downregulated and to elucidate the expression pattern of some transcripts that were not amplified by the RT-PCR. Two additional transcripts (*Ruk*$_{s}$ and *Ruk*$_{m3}$) that are known to exist were not amplified by the RT-PCR for some unknown reason. Previous work has shown that *Ruk*$_{s}$ and *Ruk*$_{m3}$ can be found in newborn and adult rat skin (Gout *et al.*, 2000). It is interesting that *Ruk*$_{m1}$ is amplified and contains Exon 11 that is lacking in *Ruk*$_{m3}$ but present in *Ruk*$_{s}$; therefore, there is no common factor in *Ruk*$_{m3}$ and *Ruk*$_{s}$ that would account for their inability to be amplified.

Another transcript that was expected from the sequence analysis of *Ruk* was $Ruk_{\Delta CP}$, this transcript should have been amplified by the M1' and MC primers that did amplify Ruk_I. Other assays have yet to determine the existence of $Ruk_{\Delta CP}$ or the corresponding protein, and no $Ruk_{\Delta CP}$ specific interactors have been identified. The existence of every other transcript and isoform has been confirmed by either cloning the cDNA or through protein expression studies, making $Ruk_{\Delta CP}$ an interesting unknown factor in Ruk functions.

Two of the Ruk_h transcripts also failed to amplify for an unknown reason. The RT-PCR using the P8 heart sample and M5 and MC primers did amplify Ruk_{h2} and Ruk_{h4} and should also have amplified Ruk_{h1} and Ruk_{h3}. However, these two Ruk_h transcripts failed to amplify, an occurrence that can be attributed to the slight difference between the two pairs of transcripts. Ruk_{h1} and Ruk_{h3} contain the whole of Exon 19 while Ruk_{h2} and Ruk_{h4} lack the middle portion of this exon. Possibly, this middle portion causes a mRNA secondary structure that is unique to Ruk_{h1} and Ruk_{h3} and interferes in the RT-PCR. Alternatively, Ruk_{h1} and Ruk_{h3} are developmentally upregulated specifically in the adult heart and this tissue was not sampled in these experiments.

6.4 The Ruk-loxP construct

The *Ruk* gene is large, complex and produces many different mRNA by alternative splicing and differential promoter usage. All known transcripts have only the three most 3' Exons (22, 23 and 24) in common; these exons encode the CCD and the 3' UTR (Figure 3.2). Therefore, Exon 22 was targeted for the conditional inactivation construct using the Cre-loxP system for a variety of reasons that are explained in Section 3.1. As discussed in Section 4.2.1, a Puromycin resistance

cassette and loxP sequence were placed 3' to Exon 22 while another loxP sequence and a Neomycin resistance cassette were placed 5' to the Exon 22 (Figures 4.18 and 6.1B). When Cre recombinase is expressed, Exon 22 and both antibiotic resistance cassettes will be excised leaving a single loxP site (Figure 6.1C). As a result, the common CCD will not be translated in any Ruk isoform because the splicing of Exon 21 and 23 will result in a frame-shift that will disrupt the translation of the entire CCD (Figure 6.1D). It has been theorized that the lack of the CCD will affect the ability of Ruk isoforms to dimerise, an ability that is thought to play a role in Ruk protein functions.

6.4.1 The mouse model will help to elucidate the role of Ruk isoforms in various pathways

6.4.1.1 Lack of dimerisation may affect RTK endocytosis

Recent work has shown that some Ruk isoforms interact with one another during the endocytic process, as evidenced by the fact that the Ruk_m and Ruk_s, neither of which directly interacts with Cbl, are ubiquitinated through the Ruk_l-Cbl interaction (Verdier *et al.*, 2002). A role for dimerisation is further confirmed by the inability of Ruk_l lacking the CCD to participate in endocytosis (Kowanetz *et al.*, unpublished observation). This mutant does not localize to vesicular membranes, making it distinctly possible that dimerisation with Ruk_m or Ruk_s is acts in localizing Ruk_l to plasma membranes. Inactivation of the CCD will confirm the importance of hetero-dimerisation of Ruk_l to endocytosis.

In addition to localizing Ruk_l to the membrane and promoting endocytic machinery clutering (Kowanetz *et al.*, 2004), dimerisation may also influence Ruk-based interactions that help to form and move CCVs (clathrin coated vesicles). Most

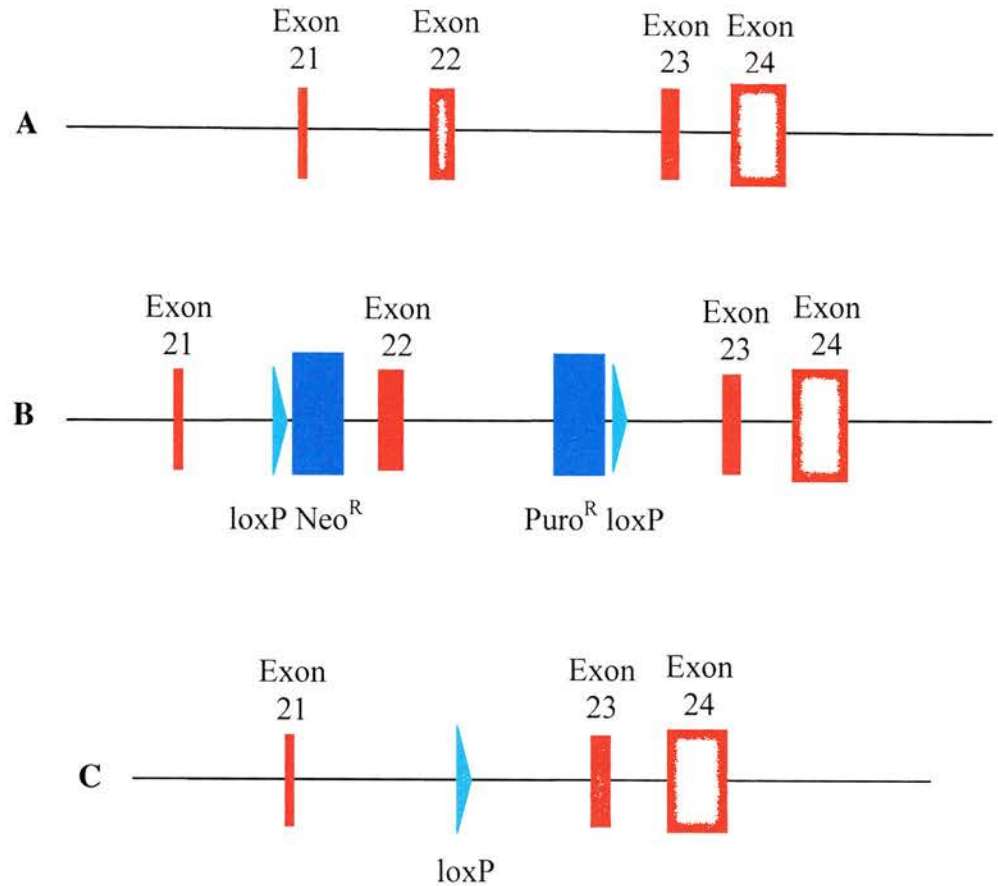

Figure 6.1: (A) The last four exons of *Ruk* and (B) the placement of the Neomycin resistance cassette, Puromycin resistance cassette and loxP sequences when homologous recombination occurs. (C) When *Cre recombinase* is expressed, Exon 22 will be spliced out of the genome leaving a single loxP site. Exon 22 encodes the majority of the CCD and its loss will disrupt the translation of the CCD.

of these interactions are theorized to occur in multi-protein complexes based around Ruk_I dimers and their multiple binding domains (see Section 1.3.1). These Ruk_I-based multi-protein complexes are composed of low affinity interactions that allow the proteins to be rapidly exchanged for one another. One of these complexes likely involves the early endocytic proteins that are also ABPs (Hip1R, Dab-2 and CAPZ; Kowanetz *et al.*, 2003a) working in conjunction to produce actin's various effects on endocytosis including CCP (clathrin coated pit) targeting and CCV movement (see Section 1.3.1.3). Another of these Ruk_I dimer based complexes may be comprised of the endocytic proteins such as endophilin and Cbl (see Section 1.3.1.2; Watanabe *et al.*, 2000; Take *et al.*, 2000). Ruk_I dimers might also play a role in targeting the activated RTK to the CCP by binding proteins such as synaptojanin2 and Cbl (Kowanetz *et al.*, 2003a).

Therefore, the inactivation of the Ruk CCD and the subsequent effect on dimerisation will help to elucidate the role of Ruk dimerisation in endocytosis. With the animal model that will be eventually produced, it will be possible to see how much of a role dimerisation plays in endocytic multi-protein complexes and if endocytosis will be greatly impaired. Since most of the Ruk_I interactors discovered so far interact via SH3-PRD interactions, it may be possible that some of the Ruk isoforms have redundant functions to Ruk_I in endocytosis. This question will eventually be answered with the help of the mouse model that will be produced.

6.4.1.2 Lack of dimerisation may affect FAs

As detailed in Section 1.3.3, Ruk_I is known to play a role in FA (focal adhesion) formation and maintenance, through its role as a scaffolding protein for multi-protein complexes. Current research points to the hypothesis that Ruk_I

interactors such as $p130^{Cas}$, Crk and AIP1/Alix draw it to the FAs without an intrinsic ability of Ruk_I to localize to them (Schmidt *et al.*, 2003a). It is possible that Ruk_I forms a complex with $p130^{Cas}$ and Crk that has an effect on their binding of other proteins and FA mediated signal transduction. The overexpression of Ruk_I has been shown to have pro-adhesive effects, probably through an increased inhibition of AIP1/Alix and p85α functions (see Section 1.3.3.4; Schmidt *et al.*, 2003a). It is possible that in a manner similar to their roles in other pathways, the smaller Ruk isoforms act to negatively regulate Ruk_I and release its inhibitory effects.

The mouse model will show if Ruk_I interactions are actually inhibited by the smaller isoforms in FAs. The removal of dimerising ability may affect cellular adhesion and have unknown ramifications in FA based signalling transduction. It is hoped that the mouse model will help to a greater understanding of the role of Ruk isoforms in FA formation and maintanence.

6.4.1.3 Lack of dimerisation may affect B cells

Several Ruk_I interactors are known to play key roles in B cells, and it seems plausible that Ruk isoforms play a role in B cell activation and maturation through these interactors (see Section 1.3.5). Ruk isoforms act in a manner similar to their role in endocytosis by forming multi-protein complexes where different pathways intersect with one another. For instance, Ruk_I, via binding to BLNK (Watanabe *et al.*, 2000), provides a link between the PI3K pathway and Ca^{2+} influx. Since PI3K is activated earlier in the BCR pathway than BLNK (Fruman *et al.*, 1997), Ruk_I binding to BLNK could serve as a signal for Ruk_I to attenuate PI3K signalling and prevent over-signalling from occurring. Ruk_I interacts with several proteins that attenuate BCR signalling, including c-Cbl (Watanabe *et al.*, 2000; Take *et al.*, 2000) and

SHIP1 (Kowanetz *et al.*, 2004) and it interacts with an unknown effect on STAP-1/BRDG1 (Kowanetz *et al.*, 2004) and Crk. It is interesting to note that SHIP1, a Ruk_I interactor, hydrolyses PtdIns(3,4,5)P_3 to PtdIns(3,4)P_2 while Ruk_I also inhibits PI3K production of PtdIns(3,4,5)P_3; thus Ruk isoforms may provide a mechanism for PI3K activity to reflect and respond to SHIP1 activity.

As can be seen, the current data points to a negative role for Ruk_I in B cells, and the only other isoform found in P8 spleen is $Ruk_{\Delta A}$. $Ruk_{\Delta A}$ may dimerise with Ruk_I to play a negative inhibitory role and attenuate Ruk_I action. Alternatively, $Ruk_{\Delta A}$ may bind to Ruk_I interactors without provoking the same response as Ruk_I due to the lack of SH3A or it play an independent role leading to B cell activation.

All of these hypotheses will be tested in the predicted mouse model by conditionally inactivating the Ruk CCD in B cells. If dimerisation is playing a role in these cells, the lack of CCD and Ruk_I dimerisation may lead to impaired B cell development and a greater understanding of the role of Ruk isoforms in this process. As the scaffolding ability of Ruk will be greatly decreased in the mouse model, it will be interesting to see how and why the cellular physiology changes.

6.4.1.4 Lack of dimerisation may affect T cells

Much like in B cells, Ruk isoforms play a role in T cell activation and maturation, particularly through their interaction with CD2 (see Section 1.3.6). Among other T cell specific interactions, Ruk_I bridges T cell activation (via CD2) to actin rearrangements (via CAPZ; Hutchings *et al.*, 2003; Tibaldi and Reinherz, 2003), while simultaneously inhibiting the activation of proteins downstream of the TCR through Ruk_I's inhibition of PI3K (Gout *et al.*, 2000). It is thought that both Ruk_I and $Ruk_{\Delta A}$ play inhibitory roles in CD2 activation by binding to CD2 without

eliciting the same downstream response as the main CD2 interactor, CD2AP (Hutchings *et al.*, 2003; Tibaldi and Reinherz, 2003). It is thought that Ruk_I produces some of the responses as CD2AP to only slightly inhibit CD2, whereas $Ruk_{\Delta A}$ does not provoke any of the responses and completely inhibits CD2 action. However, Ruk_I may even play a direct role in inhibiting TCR activation through its interactions with c-Cbl and Cbl-b, which inhibit TCR through endocytosis and inhibition of Vav1, respectively (Wang *et al.*, 2001; Chiang *et al.*, 2000).

Once again, whether or not Ruk dimerisation plays a role in T cell activation is questionable. However, inactivation of the CCD will be especially interesting in T cells due to the possibility that Ruk isoforms are able to dimerise with CD2AP. It has been predicted that the similarities in their CCDs would allow CD2AP and Ruk isoforms to dimerise with one another and CD2AP has a well-defined role in T cell activation. The end result of the conditional inactivation of the CCD of Ruk_I in T cells will most likely be a compromised immune system due to the inability of Ruk_I to dimerise with either itself or CD2AP/CMS.

6.4.1.5 Lack of dimerisation may affect PI3K activity

As explained in Section 1.3.4, Ruk isoforms, specifically Ruk_I, are known to inhibit PI3K function through direct binding to p85α. Ruk_I is the only known negative regulator of PI3K and inter-isoform dimerisation is thought to attenuate the inhibition by Ruk_I of the p85α subunit (Gout *et al.*, 2000). The PtdIns(3,4,5)P_3 product of PI3K activates a variety of pathways leading to cell survival, proliferation and growth. Several of the pathways that PtdIns(3,4,5)P_3 triggers are perturbed in cancerous phenotypes leading to the possibility that Ruk isoforms have a direct impact on cancer through their inhibition of PI3K. Additionally, p85α acts

independently of the PI3K holoenzyme in stress fiber formation and in p53-mediated apoptosis due to oxidative stress (see Section 1.3.3.5; Yin *et al.*, 1998; Jimenez *et al.*, 2000). Ruk_I probably affects both of these PI3K independent functions of p85α, although this suggestion has not been substantiated.

It has been suggested that an interaction between Ruk_I and certain smaller isoforms of Ruk is able to modify the effect that Ruk_I has on PI3K activity. For instance, when co-injected with Ruk_I, Ruk_m decreases the toxic effect of Ruk_I on cultured neurons in a PI3K dependent manner (Gout *et al.*, 2000). Since Ruk isoforms are thought to interact through their CCD, one possible outcome of the removal of the CCD may be a decrease in PI3K activity and PtdIns(3,4,5)P_3 levels. The downstream signalling affects of a lessened amount of PtdIns(3,4,5)P_3 will be decreased cell size and a lack of cellular proliferation. This hypothesis is supported by recent work that shows that a constitutively inactivated form of PI3K caused a decrease in myocardial cell size (Shioi *et al.*, 2000). Only the *in vivo* de-activation of the CCD will show if this will actually occur.

Since Ruk_I affects PI3K activity and PtdIns(3,4,5)P_3 levels through a variety of interactors, it will take the de-activation of the Ruk CCD in order to fully understand the affect of Ruk isoforms on PtdIns(3,4,5)P_3. Due to the fact that Ruk isoforms interact with so many different kinases, phosphates and PtdIns interactors it will be very interesting to see what the overall effect of the lack of Ruk dimersation will have on the animal model.

6.4.1.6 Lack of dimerisation may affect other pathways

One of the more interesting effects that may be seen is the conditional

inactivation of the CCD in murine sexual organs. There are two isoforms, Ruk_t and Ruk_h that are found exclusively in the adult testis. Ruk_t is composed of a serine rich region followed by a CCD and is the only Ruk isoform to be developmentally upregulated (see Sections 6.2.7 and 6.3.5). The loxP targeting construct was created in such a method as to incapacitate the entire CCD when Exon 22 was removed, and therefore, will drastically affect both the Ruk_t and Ruk_h isoforms. One of the most probable outcomes will be an effect on sexual maturation; the sexual maturation of the male animals used in these experiments may be retarded as it seems that Ruk_t and Ruk_h are the only transcripts developmentally upregulated in an adult tissue and may therefore play a role in male sexual maturity. Ruk_t and Ruk_h may also act in spermatogenesis and the lack of a CCD may affect reproductive abilities of the animal models. There is also a possibility that the N-terminal half of the serine rich region is able to mediate some interactions that will become apparent when the CCD and is deactivated.

Both Ruk_t and Ruk_h will also be incapacitated in their entirety when the CCD is specifically excised in heart tissues. This approach will show what function these smaller isoforms play in heart development and possibly the adult organ. Hopefully, much like in the testis, any interactions unique to the N-terminal half of the serine rich region will be uncovered in this process as well.

6.4.2 Future work on conditional inactivation of Ruk isoforms

The only ES clone to be identified as containing a floxed Exon 22 was clone P5-2 (see Section 4.2.2). In the near future, *Cre recombinase* will be transiently expressed in this cell line in order to observe the effect of the lack of the CCD in ES

cells. It is hoped that morphological changes will help to elucidate the function of Ruk isoform interactions.

Due to the fact that no chimeras were produced at this time, future work will concentrate on developing the floxed *Ruk* mouse line (see Section 4.2.3). Once the floxed line is created, it will be crossed with different lines expressing the Cre recombinase protein under tissue specific promoters; this will result in the inactivation of the CCD only in the tissues of interest. One of the first Cre recombinase lines used will be a neuron specific line that will help elucidate the effects of dimerisation in the brain. Further work will be done on crossing the floxed line with heart and testis specific Cre recombinase. These tissue specific inactivated lines will be produced simultaneously to reduce the amount of animals and time involved in the study.

The size of the gene makes a knockout mouse model very hard to generate. However, it is known that one group is trying a conditional inactivation of the entire gene (I. Dikic, personal communication to V. Buchman). This approach may prove useful, but will not be able to distinguish the effects of different isoforms, which would be especially interesting. It may be that in the future each isoform will have to be specifically inactivated, either through siRNA or other techniques, in order to fully understand what their physiological roles are. It seems likely that each isoform plays a specific role in the many pathways that Ruk_I is involved in, possibly helping to attenuate Ruk_I and $Ruk_{\Delta A}$ activity or through isoform specific interactions.

6.5 Ruk_I interacts with p85α

It has previously been demonstrated that Ruk_I is able to interact with p85α,

the regulatory subunit of PI3K, in both mammalian and insect cell lines (Gout *et al.*, 2000). This study also showed that the deletion of the SH3 domain of p85α abolished the interaction between p85α and Ruk_l, thereby implying that this SH3 domain bound to the PRD of Ruk_l. However, the exact mechanism of the interaction between these two proteins was unclear due to the presence of SH3 domains and PRDs in both proteins. Therefore, the interaction between mutants/isoforms of Ruk lacking key domains and either full-length p85α or ΔSH3-p85α was studied in HEK293 cells. Further research on the nature of the p85α-Ruk interaction and the dimerisation of Ruk_l was done using GST-fusion proteins.

6.5.1 Ruk_l and p85α interact primarily through the Ruk SH3-p85α PRD

These studies showed that in Hek293 cells, Ruk proteins with atleast the PRD, CCD and one SH3 domain are able to bind full lenth p85α but not ΔSH3-p85α (Figure 5.2). However, the two most C-terminal domains, the serine rich region and CCD, are not directly involved in the interaction with p85α, as evidenced by the inability of Ruk_c, which is comprised of the serine rich region and CCD, to interact with either p85α or ΔSH3-p85α (Figure 5.2 D). These results would indicate that the interaction is dependent on the SH3 domain of p85α and the PRD of Ruk_l, as is confirmed in the co-immunoprecipitation of both full length Ruk_l and ΔSH3-Ruk with ΔBH/Pro-p85α (Figure 5.3). However, some of the results presented in Figures 5.2 and 5.3 contradict even the necessity of the Ruk_l PRD; it seems that the interaction between p85α and Ruk_l is flexible depending on the circumstances.

This flexibility in binding is seen in the fact that ΔPro-Ruk was able to interact with p85α (Figure 5.2 F). Furthermore, ABC-Ruk was able to co-

immunoprecipitate full-length p85α but not ΔBH/Pro-p85α (Figure 5.3). It seems that binding between the p85α SH3 domain and the Ruk_I PRD is secondary to that between the Ruk SH3 domain and p85α PRD. This theory is confirmed by the fact that ΔSH3-Ruk fails to interact with full-length p85α and ABC-Ruk is unable to co-immunoprecipitate ΔBH/Pro-p85α (Figure 5.3). This would indicate that the Ruk SH3 domains are crucial to the binding of p85α.

The GST-fusion pulldown assays confirmed that isolated SH3 domains were able to interact with p85α. In particular SH3A and to a lesser extent SH3B interacted with p85α while SH3C did not directly interact at all (Figure 5.2 A). The theory that the SH3 domains were key to binding p85α was confirmed by the expression studies in HEK293 studies that showed ABC-Ruk interacted with both p85α and ΔSH3-p85α (Figure 5.2 G). Conversely, ΔSH3-Ruk did not interact with either p85α or ΔSH3-p85α (Figure 5.2 E).

The SH3 domains must bind to one of the proline rich regions found in p85α, and in all likelihood this interaction is based on the first proline rich region. Optimal Ruk SH3 binding is achieved through either Px(P/A)xxR or PxxxPR binding motifs (Kurakin *et al.*, 2003; Kowanetz *et al.*, 2003a); the sequence PTPKPR that is found in the first proline rich region of p85α coincides with either of these (Borthwick *et al.*, 2004).

6.5.2 Ruk_I and p85α both form closed dimers

It has been known for some time that excess p85α exists as a homodimer via SH3 domain/first PRD and BH/BH interactions (Harpur *et al.*, 1999). This dimer form has an intradimeric inhibitory interaction between the SH3 and PRD that

prevents the SH3 domain from interacting with non-specific proteins (Harpur *et al.*, 1999; Figure 6.2A).

Since Ruk_l contains a CCD, it was hypothesized to homo-dimerise and the results presented in Figure 5.4 confirm the ability of Ruk_l domains to interact with one another. The GST pulldown study detailed in Section 5.2.3 shows that Ruk_s, which is comprised mainly of the CCD, interacts with other Ruk isoforms including the deletion mutant ΔPro-Ruk. These results, as well as the yeast two-hybrid work shown in Borthwick *et al.* (2004), confirms that Ruk_l also exists as a dimer (Figure 6.2B). Further GST-fusion work shown in Figure 5.4 indicates that this dimer also has an intradimeric inhibitory interaction in the form of the SH3 domains binding to the PRD (Borthwick *et al.*, 2004; Figure 6.2B). SH3A and, to a lesser extent, SH3B interact with proteins containing the Ruk PRD while SH3C does not interact with these proteins. It can be hypothesised that these interactions help to close the SH3 domains to non-specific interactions when the proteins are dimerised (Figure 6.2B).

Borthwick *et al.* (2004) showed through point mutation studies that the second and third proline-rich blocks of the PRD were especially important for binding p85α. The fourth proline-rich block also played a slight role in the interaction but the first proline-rich block did not affect the interaction at all (Borthwick *et al.*, 2004). This is supported by the finding of a PPKKPR sequence in the third proline-rich block of the Ruk PRD that fits into the PxxxPR proposed by Kowanetz *et al.* (2003a). However, this sequence does not fit into the proposed consensus sequence Px(P/A)xxR described by Kurakin *et al.* (2003). Furthermore, the presence of a single motif does not correlate with the high affinity interaction found between the Ruk SH3 domains and PRD. This could be explained by the

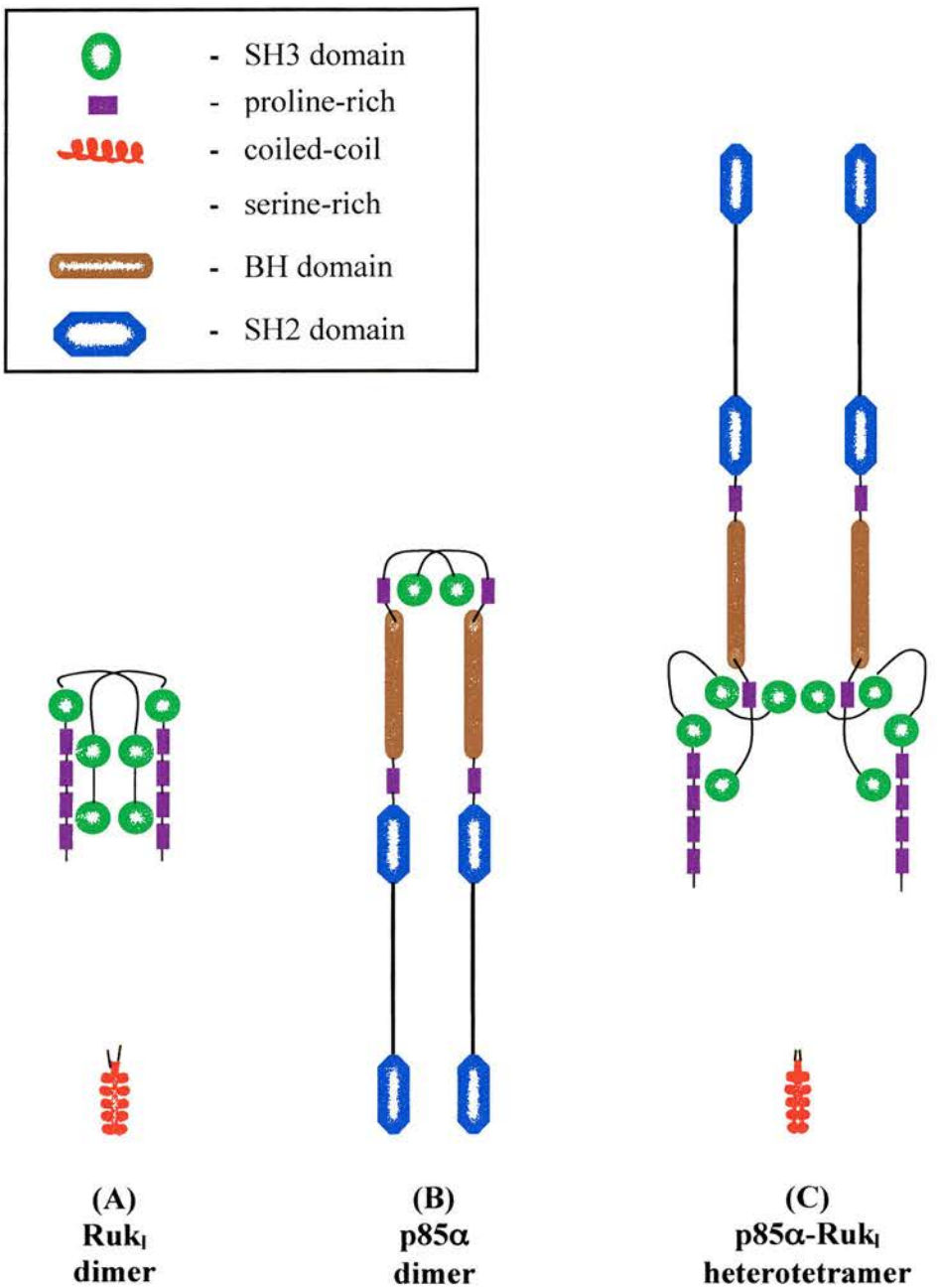

Figure 6.2: Schematic representation of Ruk$_I$-p85α heterotetramerisation. Ruk$_I$ dimerises into a closed conformation due to a PRD-SH3 interaction (A). p85α also dimerises into a closed conformation with a PRD-SH3 interaction (B). The higher affinity p85α-Ruk$_I$ interaction allows both Ruk$_I$ and p85α to form a heterotetrmerisation (C). Adapted from Borthwick *et al.*, 2004.

hypothesis that dimerisation via the CCD creates an allosteric effect allowing a higher affinity interaction between the PRD and SH3 domains.

6.5.3 The Ruk$_l$ and p85α dimers form heterodimers with each other

The evidence presented in Sections 5.2.1 and 5.2.2 as well as in Borthwick *et al* (2004) shows that the Ruk$_l$ and p85α dimers interact with one another to form a heterotetramer (Figure 6.2C). In this scenario, the higher affinity interactions between the Ruk$_l$ SH3 domains and p85α PRD are able to reciprocally oust the intradimeric inhibitions and allow the two dimers to form a heterotetramer. The higher affinity of the Ruk$_l$ SH3 domains for the p85α PRD allows Ruk$_l$ to break open the p85α dimer by displacing the intra-dimeric p85α SH3-PRD interaction and forming a Ruk$_l$ SH3-p85α PRD interaction. p85α SH3 is then free to interact with the Ruk PRD to form a stabilizing interaction. This secondary interaction not only serves to stabilize the dimerisation, it may also act to maintain the specificity of the interaction.

This hypothesis is consistent with the results found in both the HEK 293 expression studies and the GST-fusion protein pulldown assays. Thus, SH3A and SH3B both directly bind p85α, while SH3C stabilizes the interaction and helps to break open the p85α dimer in certain circumstances, as can be seen in Ruk$_m$ binding p85α (Figure 5.4C).

ΔC-Ruk binds both p85α and ΔSH3-p85α showing that the loss of SH3C allows Ruk to interact with both of these proteins (Figure 5.2H). The internal deletion of SH3C changes the distance between interacting domains within the Ruk molecule (e.g. SH3A/B and PRD) and reduces the affinity of SH3A or B to the Ruk

PRD. This lessened affinity causes the dimer to form into a more open configuration, similar to that of ΔPro-Ruk, and allows the Ruk_I dimer to interact with both p85α and ΔSH3-p85α.

The CCD also performs a stabilizing function similar to that of SH3C, probably through its ability to increase the strength of the interaction between Ruk isoforms. The lack of the CCD destabilizes Ruk_I dimers and the intradimeric inhibitory interactions from forming. Thus, Ruk isoforms are still able to bind one another and inhibit SH3 based interactions, but the inhibition is not as strong as that found when Ruk_I dimerises. Therefore, ΔCterm-Ruk is able to interact with p85α and to a much lesser extent ΔSH3-p85α (Figure 5.2 I).

6.5.4 Future work to understand the interaction between Ruk_I and other interactors

While the method of interaction has been greatly elucidated by this work and other experiments, further structural studies will need to be done to confirm the model of interaction proposed here. Further work should also be done to understand how Ruk isoforms interact with other proteins such as Cbl. While the fact that Ruk isoforms interact with various proteins is known, it is largely unknown what effect such dimerisation has on the function of Ruk_I binding partners. It can be theorized that different domain organization of Ruk isoforms will affect its interactors and produce various effects on the cellular processes that Ruk_I is involved. This area of Ruk_I interactions should yield some interesting results that will elucidate the role of Ruk_I in cellular physiology.

Chapter 7:
References

Akagi, T., Shishido, T., Murata, K., and Hanafusa, H. (2000). v-Crk activates the phosphoinositide 3-kinase/AKT pathway in transformation. Proc Natl Acad Sci U S A *97*, 7290-5.

Alessi, D.R., and Downes, C.P. (1998). The role of PI 3-kinase in insulin action. Biochim Biophys Acta *1436*, 151-164.

Aman, M.J., and Ravichandran, K.S. (2000). A requirement for lipid rafts in B cell receptor induced Ca(2+) flux. Curr Biol *10*, 393-396.

Aman, M.J., Tosello-Trampont, A.C., and Ravichandran, K. (2001). Fc gamma RIIB1/SHIP-mediated inhibitory signaling in B cells involves lipid rafts. J Biol Chem *276*, 46371-46378.

Antony, P., Petro, J.B., Carlesso, G., Shinners, N.P., Lowe, J., and Khan, W.N. (2004). B-cell antigen receptor activates transcription factors NFAT (nuclear factor of activated T-cells) and NF-kappaB (nuclear factor kappaB) via a mechanism that involves diacylglycerol. Biochem Soc Trans *32*, 113-115.

Bachmaier, K., Krawczyk, C., Kozieradzki, I., Kong, Y.Y., Sasaki, T., Oliveira-dos-Santos, A., Mariathasan, S., Bouchard, D., Wakeham, A., Itie, A., Le, J., Ohashi, P.S., Sarosi, I., Nishina, H., Lipkowitz, S., and Penninger, J.M. (2000). Negative regulation of lymphocyte activation and autoimmunity by the molecular adaptor Cbl-b. Nature *403*, 211-216.

Benschop, R.J., Brandl, E., Chan, A.C., and Cambier, J.C. (2001). Unique signaling properties of B cell antigen receptor in mature and immature B cells: implications for tolerance and activation. J Immunol *167*, 4172-4179.

Bogler, O., Furnari, F.B., Kindler-Roehrborn, A., Sykes, V.W., Yung, R., Huang, H.J., and Cavenee, W.K. (2000). SETA: a novel SH3 domain-containing adapter molecule associated with malignancy in astrocytes. Neuro-oncol *2*, 6-15.

Bolland, S., Pearse, R.N., Kurosaki, T., and Ravetch, J.V. (1998). SHIP modulates immune receptor responses by regulating membrane association of Btk. Immunity *8*, 509-516.

Borinstein, S.C., Hyatt, M.A., Sykes, V.W., Straub, R.E., Lipkowitz, S., Boulter, J., and Bogler, O. (2000). SETA is a multifunctional adapter protein with three SH3 domains that binds Grb2, Cbl, and the novel SB1 proteins. Cell Signal *12*, 769-779.

Borthwick, E.B., Korobko, I.V., Luke, C., Drel V.R., Fedyshyn Y.Y., Ninkina N., Drobot L.B., Buchman V.L. (2004). Multiple domains of Ruk/CIN85/SETA/CD2BP3 are involved in interaction with p85alpha regulatory subunit of PI 3-kinase. J Mol Biol *343*, 1135-1146.

Bouton, A.H., Riggins, R.B., and Bruce-Staskal, P.J. (2001). Functions of the adapter protein Cas: signal convergence and the determination of cellular responses. Oncogene *20*, 6448-6458.

Brauweiler, A.M., and Cambier, J.C. (2003). Fc gamma RIIB activation leads to inhibition of signalling by independently ligated receptors. Biochem Soc Trans *31*, 281-285.

Brown, F.D., Rozelle, A.L., Yin, H.L., Balla, T., and Donaldson, J.G. (2001). Phosphatidylinositol 4,5-bisphosphate and Arf6-regulated membrane traffic. J Cell Biol *154*, 1007-1017.

Brown, M.T., Andrade, J., Radhakrishna, H., Donaldson, J.G., Cooper, J.A., and Randazzo, P.A. (1998). ASAP1, a phospholipid-dependent arf GTPase-activating protein that associates with and is phosphorylated by Src. Mol Cell Biol *18*, 7038-7051.

Bucci, C., Parton, R.G., Mather, I.H., Stunnenberg, H., Simons, K., Hoflack, B., and Zerial, M. (1992). The small GTPase rab5 functions as a regulatory factor in the early endocytic pathway. Cell *70*, 715-28.

Buchman, V.L., Luke, C., Borthwick, E.B., Gout, I., and Ninkina, N. (2002). Organization of the mouse Ruk locus and expression of isoforms in mouse tissues. Gene *295*, 13-17.

Burnham, M.R., Bruce-Staskal, P.J., Harte, M.T., Weidow, C.L., Ma, A., Weed, S.A., and Bouton, A.H. (2000). Regulation of c-SRC activity and function by the adapter protein CAS. Mol Cell Biol *20*, 5865-5878.

Cantley, L.C. (2002). The phosphoinositide 3-kinase pathway. Science *296*, 1655-1657.

Chamberlain, M.D., Berry, T.R., Pastor, M.C., and Anderson, D.H. (2004). The p85alpha subunit of phosphatidylinositol 3'-kinase binds to and stimulates the GTPase activity of Rab proteins. J Biol Chem *279,* 48607-14.

Chatellard-Causse, C., Blot, B., Cristina, N., Torch, S., Missotten, M., and Sadoul, R. (2002). Alix (ALG-2-interacting protein X), a protein involved in apoptosis, binds to endophilins and induces cytoplasmic vacuolization. J Biol Chem *277*, 29108-29115.

Chen, B., Borinstein, S.C., Gillis, J., Sykes, V.W., and Bogler, O. (2000). The glioma-associated protein SETA interacts with AIP1/Alix and ALG-2 and modulates apoptosis in astrocytes. J Biol Chem *275*, 19275-19281.

Chen, X., and Resh, M.D. (2002). Cholesterol depletion from the plasma membrane triggers ligand-independent activation of the epidermal growth factor receptor. J Biol Chem *277*, 49631-49637.

Chiang, Y.J., Kole, H.K., Brown, K., Naramura, M., Fukuhara, S., Hu, R.J., Jang, I.K., Gutkind, J.S., Shevach, E., and Gu, H. (2000). Cbl-b regulates the CD28 dependence of T-cell activation. Nature *403*, 216-220.

Chikumi, H., Barac, A., Behbahani, B., Gao, Y., Teramoto, H., Zheng, Y., and Gutkind, J.S. (2004). Homo- and hetero-oligomerization of PDZ-RhoGEF, LARG and p115RhoGEF by their C-terminal region regulates their in vivo Rho GEF activity and transforming potential. Oncogene *23*, 233-240.

Cho, S.Y., and Klemke, R.L. (2002). Purification of pseudopodia from polarized cells reveals redistribution and activation of Rac through assembly of a CAS/Crk scaffold. J Cell Biol *156*, 725-736.

Cormont, M., Meton, I., Mari, M., Monzo, P., Keslair, F., Gaskin, C., McGraw, T.E., and Le Marchand-Brustel, Y. (2003). CD2AP/CMS regulates endosome morphology and traffic to the degradative pathway through its interaction with Rab4 and c-Cbl. Traffic *4*, 97-112.

Currie, R.A., Walker, K.S., Gray, A., Deak, M., Casamayor ,A., Downes, C.P., Cohen, P., Alessi, D.R., and Lucocq, J. (1999). Role of phosphatidylinositol 3,4,5-trisphosphate in regulating the activity and localization of 3-phosphoinositide-dependent protein kinase-1. Biochem J *337*, 575-83.

Davis, S.J., Ikemizu, S., Evans, E.J., Fugger, L., Bakker, T.R., and van der Merwe, P.A. (2003). The nature of molecular recognition by T cells. Nat Immunol *4*, 217-224.

Davis, S.J., Ikemizu, S., Wild, M.K., and van der Merwe, P.A. (1998). CD2 and the nature of protein interactions mediating cell-cell recognition. Immunol Rev *163*, 217-236.

Di Fiore, P.P., and De Camilli, P. (2001). Endocytosis and signaling. an inseparable partnership. Cell *106*, 1-4.

Dikic, I. (2002). CIN85/CMS family of adaptor molecules. FEBS Lett *529*, 110-115.

Dikic, I. (2003). Mechanisms controlling EGF receptor endocytosis and degradation. Biochem Soc Trans *31*, 1178-1181.

dos Remedios, C.G., Chhabra, D., Kekic, M., Dedova, I.V., Tsubakihara, M., Berry, D.A., and Nosworthy, N.J. (2003). Actin binding proteins: regulation of cytoskeletal microfilaments. Physiol Rev *83*, 433-473.

D'Souza-Schorey, C., Li, G., Colombo, M.I., and Stahl, P.D. (1995). A regulatory role for ARF6 in receptor-mediated endocytosis. Science *267*, 1175-1178.

Duan, L., Miura, Y., Dimri, M., Majumder, B., Dodge, I.L., Reddi, A.L., Ghosh, A., Fernandes, N., Zhou, P., Mullane-Robinson, K., Rao, N., Donoghue, S., Rogers, R.A., Bowtell, D., Naramura, M., Gu, H., Band, V., and Band, H. (2003). Cbl-mediated ubiquitinylation is required for lysosomal sorting of epidermal growth factor receptor but is dispensable for endocytosis. J Biol Chem *278*, 28950-28960.

Dustin, M.L., Golan, D.E., Zhu, D.M., Miller, J.M., Meier, W., Davies, E.A., and van der Merwe, P.A. (1997). Low affinity interaction of human or rat T cell adhesion molecule CD2 with its ligand aligns adhering membranes to achieve high physiological affinity. J Biol Chem *272*, 30889-98.

Dustin, M.L., Olszowy, M.W., Holdorf, A.D., Li, J., Bromley, S., Desai, N., Widder, P., Rosenberger, F., van der Merwe, P.A., Allen, P.M., and Shaw, A.S. (1998). A novel adaptor protein orchestrates receptor patterning and cytoskeletal polarity in T-cell contacts. Cell *94*, 667-677.

Eitzen, G., Wang, L., Thorngren, N., and Wickner, W. (2002). Remodeling of organelle-bound actin is required for yeast vacuole fusion. J Cell Biol *158*, 669-79.

Engqvist-Goldstein, A.E., and Drubin, D.G. (2003). Actin assembly and endocytosis: from yeast to mammals. Annu Rev Cell Dev Biol *19*, 287-332.

Engqvist-Goldstein, A.E., Warren, R.A., Kessels, M.M., Keen, J.H., Heuser, J., and Drubin, D.G. (2001). The actin-binding protein Hip1R associates with clathrin during early stages of endocytosis and promotes clathrin assembly in vitro. J Cell Biol *154*, 1209-1223.

Engqvist-Goldstein, A.E., Zhang, C.X., Carreno, S., Barroso, C., Heuser, J.E., and Drubin, D.G. (2004). RNAi-mediated Hip1R silencing results in stable association between the endocytic machinery and the actin assembly machinery. Mol Biol Cell *15*, 1666-1679.

Erickson, J.W., and Cerione, R.A. (2004). Structural elements, mechanism, and evolutionary convergence of Rho protein-guanine nucleotide exchange factor complexes. Biochemistry *43*, 837-842.

Escalante, M., Courtney, J., Chin, W.G., Teng, K.K., Kim, J.I., Fajardo, J.E., Mayer, B.J., Hempstead, B.L., and Birge, R.B. (2000). Phosphorylation of c-Crk II on the negative regulatory Tyr222 mediates nerve growth factor-induced cell spreading and morphogenesis. J Biol Chem *275*, 24787-24797.

Fang, D., and Liu, Y.C. (2001). Proteolysis-independent regulation of PI3K by Cbl-b-mediated ubiquitination in T cells. Nat Immunol *2*, 870-875.

Fang, D., Wang, H.Y., Fang, N., Altman, Y., Elly, C., and Liu, Y.C. (2001). Cbl-b, a RING-type E3 ubiquitin ligase, targets phosphatidylinositol 3-kinase for ubiquitination in T cells. J Biol Chem *276*, 4872-4878.

Farsad, K., Ringstad, N., Takei, K., Floyd, S.R., Rose, K., and De Camilli, P. (2001). Generation of high curvature membranes mediated by direct endophilin bilayer interactions. J Cell Biol *155*, 193-200.

Feller, S.M., Knudsen, B., and Hanafusa, H. (1994). c-Abl kinase regulates the protein binding activity of c-Crk. EMBO J *13*, 2341-51.

Feller, S.M. (2001). Crk family adaptors-signalling complex formation and biological roles. Oncogene *20*, 6348-6371.

Feng, Y., Press, B., and Wandinger-Ness, A. (1995). Rab 7: an important regulator of late endocytic membrane traffic. J Cell Biol *131*, 1435-52.

Franco, M., Boretto, J., Robineau, S., Monier, S., Goud, B., Chardin, P., and Chavrier, P. (1998). ARNO3, a Sec7-domain guanine nucleotide exchange factor for ADP ribosylation factor 1, is involved in the control of Golgi structure and function. Proc Natl Acad Sci U S A *95*, 9926-31.

Frauwirth, K.A., Riley, J.L., Harris, M.H., Parry, R.V., Rathmell, J.C., Plas, D.R., Elstrom, R.L., June, C.H., and Thompson, C.B. (2002). The CD28 signaling pathway regulates glucose metabolism. Immunity *16*, 769-777.

Frech, M., Andjelkovic, M., Ingley, E., Reddy, K.K., Falck, J.R., and Hemmings, B.A. (1997). High affinity binding of inositol phosphates and phosphoinositides to the pleckstrin homology domain of RAC/protein kinase B and their influence on kinase activity. J Biol Chem *272*, 8474-81.

Freeburn, R.W., Wright, K.L., Burgess, S.J., Astoul, E., Cantrell, D.A., and Ward, S.G. (2002). Evidence that SHIP-1 contributes to phosphatidylinositol 3,4,5-trisphosphate metabolism in T lymphocytes and can regulate novel phosphoinositide 3-kinase effectors. J Immunol *169*, 5441-5450.

Fruman, D.A. (2004). Phosphoinositide 3-kinase and its targets in B-cell and T-cell signaling. Curr Opin Immunol *16*, 314-320.

Fruman, D.A., Meyers, R.E., and Cantley, L.C. (1998). Phosphoinositide kinases. Annu Rev Biochem *67*, 481-507.

Fruman, D.A., Snapper, S.B., Yballe, C.M., Davidson, L., Yu, J.Y., Alt, F.W., and Cantley, L.C. (1999). Impaired B cell development and proliferation in absence of phosphoinositide 3-kinase p85alpha. Science *283*, 393-397.

Fu, C., Turck, C.W., Kurosaki, T., and Chan, A.C. (1998). BLNK: a central linker protein in B cell activation. Immunity *9*, 93-103.

Fukui, Y., Kornbluth, S., Jong, S.M., Wang, L.H., and Hanafusa, H. (1989). Phosphatidylinositol kinase type I activity associates with various oncogene products. Oncogene Res *4*, 283-92.

Gampel, A. and Mellor, H. (2002). Small interfering RNAs as a tool to assign Rho GTPase exchange-factor function in vivo. Biochem J *366*, 393-8.

Gampel, A., Parker, P.J., and Mellor, H. (1999). Regulation of epidermal growth factor receptor traffic by the small GTPase rhoB. Curr Biol *9*, 955-8.

Gasman, S., Kalaidzidis, Y., and Zerial, M. RhoD regulates endosome dynamics through Diaphanous-related Formin and Src tyrosine kinase. (2003). Nat Cell Biol *5*, 195-204.

Gelkop, S., Babichev, Y., and Isakov, N. (2001). T cell activation induces direct binding of the Crk adapter protein to the regulatory subunit of phosphatidylinositol 3-kinase (p85) via a complex mechanism involving the Cbl protein. J Biol Chem *276*, 36174-36182.

Giuriato, S., Pesesse, X., Bodin, S., Sasaki, T., Viala, C., Marion, E., Penninger, J., Schurmans, S., Erneux, C., and Payrastre, B. (2003). SH2-containing inositol 5-phosphatases 1 and 2 in blood platelets: their interactions and roles in the control of phosphatidylinositol 3,4,5-trisphosphate levels. Biochem J *376*, 199-207.

Gorvel, J.P., Chavrier, P., Zerial, M., and Gruenberg, J. (1991). rab5 controls early endosome fusion in vitro. Cell *64*, 915-25.

Gout, I., Middleton, G., Adu, J., Ninkina, N.N., Drobot, L.B., Filonenko, V., Matsuka, G., Davies, A.M., Waterfield, M., and Buchman, V.L. (2000). Negative regulation of PI 3-kinase by Ruk, a novel adaptor protein. Embo J *19*, 4015-4025.

Haglund, K., Di Fiore, P.P., and Dikic, I. (2003a). Distinct monoubiquitin signals in receptor endocytosis. Trends Biochem Sci *28*, 598-603.

Haglund, K., Ivankovic-Dikic, I., Shimokawa, N., Kruh, G.D., and Dikic, I. (2004). Recruitment of Pyk2 and Cbl to lipid rafts mediates signals important for actin reorganization in growing neurites. J Cell Sci *117*, 2557-2568.

Haglund, K., Sigismund, S., Polo, S., Szymkiewicz, I., Di Fiore, P.P., and Dikic, I. (2003b). Multiple monoubiquitination of RTKs is sufficient for their endocytosis and degradation. Nat Cell Biol *5*, 461-466.

Hahn, W.C., Rosenstein, Y., Calvo, V., Burakoff, S.J., and Bierer, B.E. (1992). A distinct cytoplasmic domain of CD2 regulates ligand avidity and T-cell responsiveness to antigen. Proc Natl Acad Sci U S A *89*, 7179-83.

Harpur, A.G., Layton, M.J., Das, P., Bottomley, M.J., Panayotou, G., Driscoll, P.C., and Waterfield, M.D. (1999). Intermolecular interactions of the p85alpha regulatory subunit of phosphatidylinositol 3-kinase. J Biol Chem *274*, 12323-12332.

Harriague, J. and Bismuth, G. (2002). Imaging antigen-induced PI3K activation in T cells. Nat Immunol *3*, 1090-1096.

Hart, M.J., Jiang, X., Kozasa, T., Roscoe, W., Singer, W.D., Gilman, A.G., Sternweis, P.C., and Bollag, G. (1998). Direct stimulation of the guanine nucleotide exchange activity of p115 RhoGEF by Galpha13. Science *280*, 2112-2114.

Harte, M.T., Hildebrand, J.D., Burnham, M.R., Bouton, A.H., and Parsons, J.T. (1996). p130Cas, a substrate associated with v-Src and v-Crk, localizes to focal adhesions and binds to focal adhesion kinase. J Biol Chem *271*, 13649-13655.

Hill, E., van Der Kaay, J., Downes, C.P., and Smythe, E. (2001). The role of dynamin and its binding partners in coated pit invagination and scission. J Cell Biol *152*, 309-323.

Hilpela, P., Vartiainen, M.K., and Lappalainen, P. (2004). Regulation of the actin cytoskeleton by PI(4,5)P2 and PI(3,4,5)P3. Curr Top Microbiol Immunol *282*, 117-163.

Hinners, I., and Tooze, S.A. (2003). Changing directions: clathrin-mediated transport between the Golgi and endosomes. J Cell Sci *116*, 763-771.

Huang, J., Hamasaki, H., Nakamoto, T., Honda, H., Hirai, H., Saito, M., Takato, T., and Sakai, R. (2002). Differential regulation of cell migration, actin stress fiber organization, and cell transformation by functional domains of Crk-associated substrate. J Biol Chem *277*, 27265-27272.

Huber, T.B., Hartleben, B., Kim, J., Schmidts, M., Schermer, B., Keil, A., Egger, L., Lecha, R.L., Borner, C., Pavenstadt, H., Shaw, A.S., Walz, G., and Benzing, T. (2003). Nephrin and CD2AP associate with phosphoinositide 3-OH kinase and stimulate AKT-dependent signaling. Mol Cell Biol *23*, 4917-4928.

Huber, T.B., Kottgen, M., Schilling, B., Walz, G., and Benzing, T. (2001). Interaction with podocin facilitates nephrin signaling. J Biol Chem *276*, 41543-41546.

Hussain, N.K., Jenna, S., Glogauer, M., Quinn, C.C., Wasiak, S., Guipponi, M., Antonarakis, S.E., Kay, B.K., Stossel, T.P., Lamarche-Vane, N., and McPherson, P.S. (2001). Endocytic protein intersectin-l regulates actin assembly via Cdc42 and N-WASP. Nat Cell Biol *3,* 927-32.

Hutchings, N.J., Clarkson, N., Chalkley, R., Barclay, A.N., and Brown, M.H. (2003). Linking the T cell surface protein CD2 to the actin-capping protein CAPZ via CMS and CIN85. J Biol Chem *278*, 22396-22403.

Huttner, W.B., and Schmidt, A.A. (2002). Membrane curvature: a case of endofeelin'. Trends Cell Biol *12*, 155-158.

Hwang, I.S., Jung, Y.S., and Kim, E. (2002). Interaction of ALG-2 with ASK1 influences ASK1 localization and subsequent JNK activation. FEBS Lett *529*, 183-187.

Hyatt, M.A., Sykes, V.W., Boyer, A.D., Arden, K.C., and Bogler, O. (2000). Assignment of seta to distal mouse X chromosome by radiation hybrid mapping. Cytogenet Cell Genet *89*, 278.

Innocenti, M., Frittoli, E., Ponzanelli, I., Falck, J.R., Brachmann, S.M., Di Fiore, P.P., and Scita, G. (2003). Phosphoinositide 3-kinase activates Rac by entering in a complex with Eps8, Abi1, and Sos-1. J Cell Biol *160*, 17-23.

Innocenti, M., Tenca, P., Frittoli, E., Faretta, M., Tocchetti, A., Di Fiore, P.P., and Scita, G. (2002). Mechanisms through which Sos-1 coordinates the activation of Ras and Rac. J Cell Biol *156*, 125-136.

Inoue, H., Miyaji, M., Kosugi, A., Nagafuku, M., Okazaki, T., Mimori, T., Amakawa, R., Fukuhara, S., Domae, N., Bloom, E.T., and Umehara, H. (2002). Lipid rafts as the signaling scaffold for NK cell activation: tyrosine phosphorylation and association of LAT with phosphatidylinositol 3-kinase and phospholipase C-gamma following CD2 stimulation. Eur J Immunol *32*, 2188-2198.

Insall, R.H., and Weiner, O.D. (2001). PIP3, PIP2, and cell movement--similar messages, different meanings? Dev Cell *1*, 743-747.

Inukai, K., Funaki, M., Ogihara, T., Katagiri, H., Kanda, A., Anai, M., Fukushima, Y., Hosaka, T., Suzuki, M., Shin, B.C., Takata, K., Yazaki, Y., Kikuchi, M., Oka, Y., and Asano, T. (1997). p85alpha gene generates three isoforms of regulatory subunit for phosphatidylinositol 3-kinase (PI 3-Kinase), p50alpha, p55alpha, and p85alpha, with different PI 3-kinase activity elevating responses to insulin. J Biol Chem *272*, 7873-82.

Inukai, K., Funaki, M., Anai, M., Ogihara, T., Katagiri, H., Fukushima, Y., Sakoda, H., Onishi, Y., Ono, H., Fujishiro, M., Abe, M., Oka, Y., Kikuchi, M., and Asano, T. (2001). Five isoforms of the phosphatidylinositol 3-kinase regulatory subunit exhibit different associations with receptor tyrosine kinases and their tyrosine phosphorylations. FEBS Lett *490*, 32-38.

Jiang, X., and Sorkin, A. (2003). Epidermal growth factor receptor internalization through clathrin-coated pits requires Cbl RING finger and proline-rich domains but not receptor polyubiquitylation. Traffic *4*, 529-543.

Jimenez, C., Portela, R.A., Mellado, M., Rodriguez-Frade, J.M., Collard, J., Serrano, A., Martinez, A.C., Avila, J., and Carrera, A.C. (2000). Role of the PI3K regulatory subunit in the control of actin organization and cell migration. J Cell Biol *151*, 249-262.

Joazeiro, C.A., Wing, S.S., Huang, H., Leverson, J.D., Hunter, T., and Liu, Y.C. (1999). The tyrosine kinase negative regulator c-Cbl as a RING-type, E2-dependent ubiquitin-protein ligase. Science *286*, 309-312.

Jones, D.H., Morris, J.B., Morgan, C.P., Kondo, H., Irvine, R.F., and Cockcroft, S. (2000). Type I phosphatidylinositol 4-phosphate 5-kinase directly interacts with ADP-ribosylation factor 1 and is responsible for phosphatidylinositol 4,5-bisphosphate synthesis in the golgi compartment. J Biol Chem *275*, 13962-6.

Jorge, R., Zarich, N., Oliva, J.L., Azanedo, M., Martinez, N., de la Cruz, X., and Rojas, J.M. (2002). HSos1 contains a new amino-terminal regulatory motif with specific binding affinity for its pleckstrin homology domain. J Biol Chem *277*, 44171-44179.

Jung, Y.S., Kim, K.S., Kim, K.D., Lim, J.S., Kim, J.W., and Kim, E. (2001). Apoptosis-linked gene 2 binds to the death domain of Fas and dissociates from Fas during Fas-mediated apoptosis in Jurkat cells. Biochem Biophys Res Commun *288*, 420-426.

Kandel, E.S. and Hay, N. (1999). The regulation and activities of the multifunctional serine/threonine kinase Akt/PKB. Exp Cell Res *253*, 210-29.

Kane, L.P., and Weiss, A. (2003). The PI-3 kinase/Akt pathway and T cell activation: pleiotropic pathways downstream of PIP3. Immunol Rev *192*, 7-20.

Katoh, K., Shibata, H., Hatta, K., and Maki, M. (2004). CHMP4b is a major binding partner of the ALG-2-interacting protein Alix among the three CHMP4 isoforms. Arch Biochem Biophys *421*, 159-165.

Katoh, K., Shibata, H., Suzuki, H., Nara, A., Ishidoh, K., Kominami, E., Yoshimori, T., and Maki, M. (2003). The ALG-2-interacting protein Alix associates with CHMP4b, a human homologue of yeast Snf7 that is involved in multivesicular body sorting. J Biol Chem *278*, 39104-39113.

Khan, A.H., and Pessin, J.E. (2002). Insulin regulation of glucose uptake: a complex interplay of intracellular signalling pathways. Diabetologia *45*, 1475-1483.

Kirchhausen, T. (2000). Three ways to make a vesicle. Nat Rev Mol Cell Biol *1*, 187-198.

Kirsch, K.H., Georgescu, M.M., Ishimaru, S., and Hanafusa, H. (1999). CMS: an adapter molecule involved in cytoskeletal rearrangements. Proc Natl Acad Sci U S A *96*, 6211-6216.

Kirsch, K.H., Georgescu, M.M., Shishido, T., Langdon, W.Y., Birge, R.B., and Hanafusa, H. (2001). The adapter type protein CMS/CD2AP binds to the proto-oncogenic protein c-Cbl through a tyrosine phosphorylation-regulated Src homology 3 domain interaction. J Biol Chem *276*, 4957-4963.

Klemke, R.L., Leng, J., Molander, R., Brooks, P.C., Vuori, K., and Cheresh, D.A. (1998). CAS/Crk coupling serves as a "molecular switch" for induction of cell migration. J Cell Biol *140*, 961-72.

Kowanetz, K., Szymkiewicz, I., Haglund, K., Kowanetz, M., Husnjak, K., Taylor, J.D., Soubeyran, P., Engstrom, U., Ladbury, J.E., and Dikic, I. (2003a). Identification of a novel proline-arginine motif involved in CIN85-dependent clustering of Cbl and down-regulation of epidermal growth factor receptors. J Biol Chem *278*, 39735-39746.

Kowanetz, K., Terzic, J., and Dikic, I. (2003b). Dab2 links CIN85 with clathrin-mediated receptor internalization. FEBS Lett *554*, 81-87.

Kowanetz, K., Husnjak, K., Holler, D., Kowanetz, M., Soubeyran, P., Hirsch, D., Schmidt, M.H., Pavelic, K., De Camilli, P., Randazzo, P.A., and Dikic, I. (2004). CIN85 Associates with Multiple Effectors Controlling Intracellular Trafficking of Epidermal Growth Factor Receptors. Mol Biol Cell *15*, 3155-3166.

Krawczyk, C., Bachmaier, K., Sasaki, T., Jones, G.R., Snapper, B.S., Bouchard, D., Kozieradzki, I., Ohashi, S.P., Alt, W.F., and Penninger, M.J. (2000). Cbl-b is a negative regulator of receptor clustering and raft aggregation in T cells. Immunity *13*, 463-473.

Krugmann, S., Anderson, K.E., Ridley, S.H., Risso, N., McGregor, A., Coadwell, J., Davidson, K., Eguinoa, A., Ellson, C.D., Lipp, P., Manifava, M., Ktistakis, N., Painter, G., Thuring, J.W., Cooper, M.A., Lim, Z.Y., Holmes, A.B., Dove, S.K., Michell, R.H., Grewal, A., Nazarian, A., Erdjument-Bromage, H., Tempst, P., Stephens, L.R., and Hawkins, P.T. (2002). Identification of ARAP3, a novel PI3K effector regulating both Arf and Rho GTPases, by selective capture on phosphoinositide affinity matrices. Mol Cell *9*, 95-108.

Kruljac-Letunic, A., Moelleken, J., Kallin, A., Wieland, F., and Blaukat, A. (2003). The tyrosine kinase Pyk2 regulates Arf1 activity by phosphorylation and inhibition of the Arf-GTPase-activating protein ASAP1. J Biol Chem *278*, 29560-29570.

Kurakin, A.V., Wu, S., and Bredesen, D.E. (2003). Atypical recognition consensus of CIN85/SETA/Ruk SH3 domains revealed by target-assisted iterative screening. J Biol Chem *278*, 34102-34109.

Kurosaki, T., Maeda, A., Ishiai, M., Hashimoto, A., Inabe, K., and Takata, M. (2000). Regulation of the phospholipase C-gamma2 pathway in B cells. Immunol Rev *176*, 19-29.

Lafer, E.M. (2002). Clathrin-protein interactions. Traffic *3*, 513-520.

Lai, E.C. (2003). Lipid rafts make for slippery platforms. J Cell Biol *162*, 365-370.

Lamaze, C., Chuang, T.H., Terlecky, L.J., Bokoch, G.M., and Schmid, S.L. (1996). Regulation of receptor-mediated endocytosis by Rho and Rac. Nature *382*, 177-9.

Leevers, S.J., Vanhaesebroeck, B., and Waterfield, M.D. (1999). Signalling through phosphoinositide 3-kinases: the lipids take centre stage. Curr Opin Cell Biol *11*, 219-225.

Lehtonen, S., Ora, A., Olkkonen, V.M., Geng, L., Zerial, M., Somlo, S., and Lehtonen, E. (2000). In vivo interaction of the adapter protein CD2-associated protein with the type 2 polycystic kidney disease protein, polycystin-2. J Biol Chem *275*, 32888-32893.

Li, C., Ruotsalainen, V., Tryggvason, K., Shaw, A.S., and Miner, J.H. (2000). CD2AP is expressed with nephrin in developing podocytes and is found widely in mature kidney and elsewhere. Am J Physiol Renal Physiol *279*, F785-792.

Lucas, J.A., Miller, A.T., Atherly, L.O., and Berg, L.J. (2003). The role of Tec family kinases in T cell development and function. Immunol Rev *191*, 119-138.

Lynch, D.K., Winata, S.C., Lyons, R.J., Hughes, W.E., Lehrbach, G.M., Wasinger, V., Corthals, G., Cordwell, S., and Daly, R.J. (2003). A Cortactin-CD2-associated protein (CD2AP) complex provides a novel link between epidermal growth factor receptor endocytosis and the actin cytoskeleton. J Biol Chem *278*, 21805-21813.

Malbec, O., Schmitt, C., Bruhns, P., Krystal, G., Fridman, W.H., and Daeron, M. (2001). Src homology 2 domain-containing inositol 5-phosphatase 1 mediates cell cycle arrest by FcgammaRIIB. J Biol Chem *276*, 30381-30391.

Malecz, N., McCabe, P.C., Spaargaren, C., Qiu, R., Chuang, Y., Symons, M. (2000). Synaptojanin 2, a novel Rac1 effector that regulates clathrin-mediated endocytosis. Curr Biol *10* 1383-6.

Manser, E., Leung, T., Salihuddin, H., Tan, L., and Lim L. (1993). A non-receptor tyrosine kinase that inhibits the GTPase activity of p21cdc42. Nature. *363* 364-7.

March, M.E., and Ravichandran, K. (2002). Regulation of the immune response by SHIP. Semin Immunol *14*, 37-47.

Marshall, A.J., Niiro, H., Yun, T.J., and Clark, E.A. (2000). Regulation of B-cell activation and differentiation by the phosphatidylinositol 3-kinase and phospholipase Cgamma pathway. Immunol Rev *176*, 30-46.

Martin-Serrano, J., Yarovoy, A., Perez-Caballero, D., and Bieniasz, P.D. (2003). Divergent retroviral late-budding domains recruit vacuolar protein sorting factors by using alternative adaptor proteins. Proc Natl Acad Sci U S A *100*, 12414-12419.

Masuhara, M., Nagao, K., Nishikawa, M., Sasaki, M., Yoshimura, A., and Osawa, M. (2000). Molecular cloning of murine STAP-1, the stem-cell-specific adaptor protein containing PH and SH2 domains. Biochem Biophys Res Commun *268*, 697-703.

Matsuda, M., Tanaka, S., Nagata, S., Kojima, A., Kurata, T., and Shibuya, M. (1992). Two species of human CRK cDNA encode proteins with distinct biological activities. Mol Cell Biol *12*, 3482-9.

Matsuo, H., Chevallier, J., Mayran, N., Le Blanc, I., Ferguson, C., Faure, J., Blanc, N.S., Matile, S., Dubochet, J., Sadoul, R., Parton, R.G., Vilbois, F., and Gruenberg, J. (2004). Role of LBPA and Alix in multivesicular liposome formation and endosome organization. Science *303*, 531-534.

Minegishi, Y., Rohrer, J., Coustan-Smith, E., Lederman, H.M., Pappu, R., Campana, D., Chan, A.C., and Conley, M.E. (1999). An essential role for BLNK in human B cell development. Science *286*, 1954-1957.

Mishra, S.K., Keyel, P.A., Hawryluk, M.J., Agostinelli, N.R., Watkins, S.C., and Traub, L.M. (2002). Disabled-2 exhibits the properties of a cargo-selective endocytic clathrin adaptor. Embo J *21*, 4915-4926.

Missotten, M., Nichols, A., Rieger, K., and Sadoul, R. (1999). Alix, a novel mouse protein undergoing calcium-dependent interaction with the apoptosis-linked-gene 2 (ALG-2) protein. Cell Death Differ *6*, 124-129.

Mousavi, S.A., Malerod, L., Berg, T., and Kjeken, R. (2004). Clathrin-dependent endocytosis. Biochem J *377*, 1-16.

Murphy, C., Saffrich, R., Grummt, M., Gournier, H., Rybin, V., Rubino, M., Auvinen, P., Lutcke, A., Parton, R.G., and Zerial, M. (1996). Endosome dynamics regulated by a Rho protein. Nature. *384* 427-32.

Murphy, M.A., Schnall, R.G., Venter, D.J., Barnett, L., Bertoncello, I., Thien, C.B., Langdon, W.Y., and Bowtell, D.D. (1998). Tissue hyperplasia and enhanced T-cell signalling via ZAP-70 in c-Cbl-deficient mice. Mol Cell Biol *18*, 4872-4882.

Nagy, A. (2000). Cre recombinase: the universal reagent for genome tailoring. Genesis *26*, 99-109.

Nakamoto, T., Sakai, R., Ozawa, K., Yazaki, Y., and Hirai, H. (1996). Direct binding of C-terminal region of p130Cas to SH2 and SH3 domains of Src kinase. J Biol Chem *271*, 8959-8965.

Naramura, M., Kole, H.K., Hu, R.J., and Gu, H. (1998). Altered thymic positive selection and intracellular signals in Cbl-deficient mice. Proc Natl Acad Sci U S A *95*, 15547-15552.

Narita, T., Amano, F., Yoshizaki, K., Nishimoto, N., Nishimura, T., Tajima, T., Namiki, H., and Taniyama, T. (2001). Assignment of SH3KBP1 to human chromosome band Xp22.1-->p21.3 by in situ hybridization. Cytogenet Cell Genet *93*, 133-134.

Neves, S.R., Ram, P.T., and Iyengar, R. (2002). G protein pathways. Science *296*, 1636-1639.

Nie, Z., Hirsch, D.S., and Randazzo, P.A. (2003). Arf and its many interactors. Curr Opin Cell Biol *15*, 396-404.

Nimnual, A., and Bar-Sagi, D. (2002). The two hats of SOS. Sci STKE *2002*, PE36.

Norman, J.C., Jones, D., Barry, S.T., Holt, M.R., Cockcroft, S., and Critchley, D.R. (1998). ARF1 mediates paxillin recruitment to focal adhesions and potentiates Rho-stimulated stress fiber formation in intact and permeabilized Swiss 3T3 fibroblasts. J Cell Biol *143*, 1981-95.

Ohya, K., Kajigaya, S., Kitanaka, A., Yoshida, K., Miyazato, A., Yamashita, Y., Yamanaka, T., Ikeda, U., Shimada, K., Ozawa, K., and Mano, H. (1999). Molecular cloning of a docking protein, BRDG1, that acts downstream of the Tec tyrosine kinase. Proc Natl Acad Sci U S A *96*, 11976-11981.

Okada, T., Maeda, A., Iwamatsu, A., Gotoh, K., and Kurosaki, T. (2000). BCAP: the tyrosine kinase substrate that connects B cell receptor to phosphoinositide 3-kinase activation. Immunity *13*, 817-827.

Okkenhaug, K., and Vanhaesebroeck, B. (2001). New responsibilities for the PI3K regulatory subunit p85 alpha. Sci STKE *2001*, PE1.

Okkenhaug, K., and Vanhaesebroeck, B. (2003). PI3K in lymphocyte development, differentiation and activation. Nat Rev Immunol *3*, 317-330.

Pappu, R., Cheng, A.M., Li, B., Gong, Q., Chiu, C., Griffin, N., White, M., Sleckman, B.P., and Chan, A.C. (1999). Requirement for B cell linker protein (BLNK) in B cell development. Science *286*, 1949-1954.

Parsons, J.T. (2003). Focal adhesion kinase: the first ten years. J Cell Sci *116*, 1409-1416.

Pearse, R.N., Kawabe, T., Bolland, S., Guinamard, R., Kurosaki, T., and Ravetch, J.V. (1999). SHIP recruitment attenuates Fc gamma RIIB-induced B cell apoptosis. Immunity *10*, 753-760.

Petit, V., and Thiery, J.P. (2000). Focal adhesions: structure and dynamics. Biol Cell *92*, 477-494.

Petrelli, A., Gilestro, G.F., Lanzardo, S., Comoglio, P.M., Migone, N., and Giordano, S. (2002). The endophilin-CIN85-Cbl complex mediates ligand-dependent downregulation of c-Met. Nature *416*, 187-190.

Petro, J.B., and Khan, W.N. (2001). Phospholipase C-gamma 2 couples Bruton's tyrosine kinase to the NF-kappaB signaling pathway in B lymphocytes. J Biol Chem *276*, 1715-1719.

Pike, L.J. (2004). Lipid rafts: heterogeneity on the high seas. Biochem J *378*, 281-292.

Pike, L.J., and Casey, L. (2002). Cholesterol levels modulate EGF receptor-mediated signaling by altering receptor function and trafficking. Biochemistry *41*, 10315-10322.

Polte, T.R., and Hanks, S.K. (1995). Interaction between focal adhesion kinase and Crk-associated tyrosine kinase substrate p130Cas. Proc Natl Acad Sci U S A *92*, 10678-10682.

Qiu, Y., and Kung, H.J. (2000). Signaling network of the Btk family kinases. Oncogene *19*, 5651-5661.

Qualmann, B., and Mellor, H. (2003). Regulation of endocytic traffic by Rho GTPases. Biochem J *371*, 233-241.

Rameh, L.E., Chen, C.S., and Cantley, L.C. (1995). Phosphatidylinositol (3,4,5)P3 interacts with SH2 domains and modulates PI 3-kinase association with tyrosine-phosphorylated proteins. Cell *83*, 821-30.

Randazzo, P.A., Andrade, J., Miura, K., Brown, M.T., Long, Y.Q., Stauffer, S., Roller, P., and Cooper, J.A. (2000a). The Arf GTPase-activating protein ASAP1 regulates the actin cytoskeleton. Proc Natl Acad Sci U S A *97*, 4011-4016.

Randazzo, P.A., Nie, Z., Miura, K., and Hsu, V.W. (2000b). Molecular aspects of the cellular activities of ADP-ribosylation factors. Sci STKE *2000*, RE1.

Rao, R.V., Poksay, K.S., Castro-Obregon, S., Schilling, B., Row, R.H., del Rio, G., Gibson, B.W., Ellerby, H.M., and Bredesen, D.E. (2004). Molecular components of a cell death pathway activated by endoplasmic reticulum stress. J Biol Chem *279*, 177-187.

Rathmell, J.C., Elstrom, R.L., Cinalli, R.M., and Thompson, C.B. (2003). Activated Akt promotes increased resting T cell size, CD28-independent T cell growth, and development of autoimmunity and lymphoma. Eur J Immunol *33*, 2223-2232.

Reynolds, L.F., de Bettignies, C., Norton, T., Beeser, A., Chernoff, J., and Tybulewicz, V.L. (2004). Vav1 transduces T cell receptor signals to the activation of the Ras/ERK pathway via LAT, Sos, and RasGRP1. J Biol Chem *279*, 18239-18246.

Rodal, S.K., Skretting, G., Garred, O., Vilhardt, F., van Deurs, B., and Sandvig, K. (1999). Extraction of cholesterol with methyl-beta-cyclodextrin perturbs formation of clathrin-coated endocytic vesicles. Mol Biol Cell *10*, 961-974.

Rusk, N., Le, P.U., Mariggio, S., Guay, G., Lurisci, C., Nabi, I.R., Corda, D., and Symons, M. (2003). Synaptojanin 2 functions at an early step of clathrin-mediated endocytosis. Curr Biol *13*, 659-663.

Saito, K., Tolias, K.F., Saci, A., Koon, H.B., Humphries, L.A., Scharenberg, A., Rawlings, D.J., Kinet, J.P., and Carpenter, C.L. (2003). BTK regulates PtdIns-4,5-P2 synthesis: importance for calcium signaling and PI3K activity. Immunity *19*, 669-678.

Sakakibara, T., Nemoto, Y., Nukiwa, T., and Takeshima, H. (2004). Identification and characterization of a novel Rho GTPase activating protein implicated in receptor-mediated endocytosis. FEBS Lett *566*, 294-300.

Salim, K., Bottomley, M.J., Querfurth, E., Zvelebil, M.J., Gout, I., Scaife, R., Margolis, R.L., Gigg, R., Smith, C.I., Driscoll, P.C., Waterfield, M.D., and Panayotou, G. (1996). Distinct specificity in the recognition of phosphoinositides by the pleckstrin homology domains of dynamin and Bruton's tyrosine kinase. EMBO J *15*, 6241-50.

Sambrook, J., and Russell, D.W. (2001). Molecular Cloning: A Laboratory Manual. Cold Spring Harbour Laboratory Press.

Santy, L.C., and Casanova, J.E. (2002). GTPase signaling: bridging the GAP between ARF and Rho. Curr Biol *12*, R360-362.

Sastry, S.K., and Burridge, K. (2000). Focal adhesions: a nexus for intracellular signaling and cytoskeletal dynamics. Exp Cell Res *261*, 25-36.

Sattler, M., Verma, S., Pride, Y.B., Salgia, R., Rohrschneider, L.R., and Griffin, J.D. (2001). SHIP1, an SH2 domain containing polyinositol-5-phosphatase, regulates migration through two critical tyrosine residues and forms a novel signaling complex with DOK1 and CRKL. J Biol Chem *276*, 2451-2458.

Scaife, R.M., Courtneidge, S.A., and Langdon, W.Y. (2003). The multi-adaptor proto-oncoprotein Cbl is a key regulator of Rac and actin assembly. J Cell Sci *116*, 463-473.

Schafer, D.A., D'Souza-Schorey, C., and Cooper, J.A. (2000). Actin Assembly at Membranes Controlled by ARF6. Traffic *1*, 896-907.

Schmidt, A., Wolde, M., Thiele, C., Fest, W., Kratzin, H., Podtelejnikov, A.V., Witke, W., Huttner, W.B., and Soling, H.D. (1999). Endophilin I mediates synaptic vesicle formation by transfer of arachidonate to lysophosphatidic acid. Nature *401*, 133-141.

Schmidt, M.H., Chen, B., Randazzo, L.M., and Bogler, O. (2003a). SETA/CIN85/Ruk and its binding partner AIP1 associate with diverse cytoskeletal elements, including FAKs, and modulate cell adhesion. J Cell Sci *116*, 2845-2855.

Schmidt, M.H., Furnari, F.B., Cavenee, W.K., and Bogler, O. (2003b). Epidermal growth factor receptor signaling intensity determines intracellular protein interactions, ubiquitination, and internalization. Proc Natl Acad Sci U S A *100*, 6505-6510.

Schmidt, M.H., Hoeller, D., Yu, J., Furnari, F.B., Cavenee, W.K., Dikic, I., and Bogler, O. (2004) Alix/AIP1 Antagonizes Epidermal Growth Factor Receptor Downregulation by the Cbl-SETA/CIN85 Complex. Mol Cell Biol 24, 8981-93.

Schuske, K.R., Richmond, J.E., Matthies, D.S., Davis, W.S., Runz, S., Rube, D.A., van der Bliek, A.M., and Jorgensen, E.M. (2003). Endophilin is required for synaptic vesicle endocytosis by localizing synaptojanin. Neuron *40*, 749-762.

Scita, G., Tenca, P., Areces, L.B., Tocchetti, A., Frittoli, E., Giardina, G., Ponzanelli, I., Sini, P., Innocenti, M., and Di Fiore, P.P. (2001). An effector region in Eps8 is responsible for the activation of the Rac-specific GEF activity of Sos-1 and for the proper localization of the Rac-based actin-polymerizing machine. J Cell Biol *154*, 1031-1044.

Seth, R., Shum, L., Wu, F., Wuenschell, C., Hall, F.L., Slavkin, H.C., and Warburton, D. (1993). Role of epidermal growth factor expression in early mouse embryo lung branching morphogenesis in culture: antisense oligodeoxynucleotide inhibitory strategy. Dev Biol *158*, 555-559.

Sheff, D.R., Daro, E.A., Hull, M., and Mellman, I. (1999). The receptor recycling pathway contains two distinct populations of early endosomes with different sorting functions. J Cell Biol *145*, 123-39.

Shibata, H., Yamada, K., Mizuno, T., Yorikawa, C., Takahashi, H., Satoh, H., Kitaura, Y., and Maki, M. (2004). The penta-EF-hand protein ALG-2 interacts with a region containing PxY repeats in Alix/AIP1, which is required for the subcellular punctate distribution of the amino-terminal truncation form of Alix/AIP1. J Biochem (Tokyo) *135*, 117-128.

Shih, N.Y., Li, J., Karpitskii, V., Nguyen, A., Dustin, M.L., Kanagawa, O., Miner, J.H., and Shaw, A.S. (1999). Congenital nephrotic syndrome in mice lacking CD2-associated protein. Science *286*, 312-315.

Shioi, T., Kang, P.M., Douglas, P.S., Hampe, J., Yballe, C.M., Lawitts, J., Cantley, L.C., and Izumo, S. (2000). The conserved phosphoinositide 3-kinase pathway determines heart size in mice. Embo J *19*, 2537-2548.

Sini, P., Cannas, A., Koleske, A.J., Di Fiore, P.P., and Scita, G. (2004). Abl-dependent tyrosine phosphorylation of Sos-1 mediates growth-factor-induced Rac activation. Nat Cell Biol *6*, 268-274.

Sly, L.M., Rauh, M.J., Kalesnikoff, J., Buchse, T., and Krystal, G. (2003). SHIP, SHIP2, and PTEN activities are regulated in vivo by modulation of their protein levels: SHIP is up-regulated in macrophages and mast cells by lipopolysaccharide. Exp Hematol *31*, 1170-1181.

Sohn, H.W., Gu, H., and Pierce, S.K. (2003). Cbl-b negatively regulates B cell antigen receptor signaling in mature B cells through ubiquitination of the tyrosine kinase Syk. J Exp Med *197*, 1511-1524.

Somsel Rodman, J. and Wandinger-Ness, A. (2000). Rab GTPases coordinate endocytosis. J Cell Sci *113 Pt 2*, 183-92.

Soubeyran, P., Kowanetz, K., Szymkiewicz, I., Langdon, W.Y., and Dikic, I. (2002). Cbl-CIN85-endophilin complex mediates ligand-induced downregulation of EGF receptors. Nature *416*, 183-187.

Stamenova, S.D., Dunn, R., Adler, A.S., and Hicke, L. (2004). The Rsp5 ubiquitin ligase binds to and ubiquitinates members of the yeast CIN85-endophilin complex, Sla1-Rvs167. J Biol Chem *279*, 16017-16025.

Strack, B., Calistri, A., Craig, S., Popova, E., and Gottlinger, H.G. (2003). AIP1/ALIX is a binding partner for HIV-1 p6 and EIAV p9 functioning in virus budding. Cell *114*, 689-699.

Subtil, A., Gaidarov, I., Kobylarz, K., Lampson, M.A., Keen, J.H., and McGraw, T.E. (1999). Acute cholesterol depletion inhibits clathrin-coated pit budding. Proc Natl Acad Sci U S A *96*, 6775-6780.

Szymkiewicz, I., Kowanetz, K., Soubeyran, P., Dinarina, A., Lipkowitz, S., and Dikic, I. (2002). CIN85 participates in Cbl-b-mediated down-regulation of receptor tyrosine kinases. J Biol Chem *277*, 39666-39672.

Take, H., Watanabe, S., Takeda, K., Yu, Z.X., Iwata, N., and Kajigaya, S. (2000). Cloning and characterization of a novel adaptor protein, CIN85, that interacts with c-Cbl. Biochem Biophys Res Commun *268*, 321-328.

Takesono, A., Finkelstein, L.D., and Schwartzberg, P.L. (2002). Beyond calcium: new signaling pathways for Tec family kinases. J Cell Sci *115*, 3039-3048.

Takino, T., Tamura, M., Miyamori, H., Araki, M., Matsumoto, K., Sato, H., and Yamada, K.M. (2003). Tyrosine phosphorylation of the CrkII adaptor protein modulates cell migration. J Cell Sci *116*, 3145-3155.

Tan, J.E., Wong, S.C., Gan, S.K., Xu, S., and Lam, K.P. (2001). The adaptor protein BLNK is required for b cell antigen receptor-induced activation of nuclear factor-kappa B and cell cycle entry and survival of B lymphocytes. J Biol Chem *276*, 20055-20063.

Teo, M., Tan, L., Lim, L., and Manser, E. (2001). The tyrosine kinase ACK1 associates with clathrin-coated vesicles through a binding motif shared by arrestin and other adaptors. J Biol Chem *276*, 18392-8

Terauchi, Y., Tsuji, Y,. Satoh, S., Minoura, H., Murakami, K., Okuno, A., Inukai, K., Asano, T., Kaburagi, Y., Ueki, K., Nakajima, H., Hanafusa, T., Matsuzawa, Y., Sekihara, H., Yin, Y., Barrett, J.C., Oda, H., Ishikawa, T., Akanuma, Y., Komuro, I., Suzuki, M., Yamamura, K., Kodama, T., Suzuki, H., and Kadowaki, T. (1999). Increased insulin sensitivity and hypoglycaemia in mice lacking the p85 alpha subunit of phosphoinositide 3-kinase. Nat Genet *21*, 230-5.

Thien, C.B., and Langdon, W.Y. (2001). Cbl: many adaptations to regulate protein tyrosine kinases. Nat Rev Mol Cell Biol *2*, 294-307.

Tibaldi, E.V., and Reinherz, E.L. (2003). CD2BP3, CIN85 and the structurally related adaptor protein CMS bind to the same CD2 cytoplasmic segment, but elicit divergent functional activities. Int Immunol *15*, 313-329.

Tolias, K.F., Cantley, L.C., Carpenter, C.L. (1995). Rho family GTPases bind to phosphoinositide kinases. J Biol Chem *270*, 17656-9.

Trioulier, Y., Torch, S., Blot, B., Cristina, N., Chatellard-Causse, C., Verna, J.M., and Sadoul, R. (2004). Alix, a protein regulating endosomal trafficking, is involved in neuronal death. J Biol Chem *279*, 2046-2052.

Ueki, K., Fruman, D.A., Brachmann, S.M., Tseng, Y.H., Cantley, L.C., and Kahn, C.R. (2002). Molecular balance between the regulatory and catalytic subunits of phosphoinositide 3-kinase regulates cell signaling and survival. Mol Cell Biol *22*, 965-977.

van der Sluijs, P., Hull, M., Zahraoui, A., Tavitian, A., Goud, B., and Mellman, I. (1991). The small GTP-binding protein rab4 is associated with early endosomes. Proc Natl Acad Sci U S A *88*, 6313-7.

van der Sluijs, P., Hull, M., Webster, P., Male, P., Goud, B., and Mellman, I. (1992). The small GTP-binding protein rab4 controls an early sorting event on the endocytic pathway. Cell *70*, 729-40.

Vanhaesebroeck, B., and Waterfield, M.D. (1999). Signaling by distinct classes of phosphoinositide 3-kinases. Exp Cell Res *253*, 239-254.

Verdier, F., Valovka, T., Zhyvoloup, A., Drobot, L.B., Buchman, V., Waterfield, M., and Gout, I. (2002). Ruk is ubiquitinated but not degraded by the proteasome. Eur J Biochem *269*, 3402-3408.

Verstreken, P., Koh, T.W., Schulze, K.L., Zhai, R.G., Hiesinger, P.R., Zhou, Y., Mehta, S.Q., Cao, Y., Roos, J., and Bellen, H.J. (2003). Synaptojanin is recruited by endophilin to promote synaptic vesicle uncoating. Neuron *40*, 733-748.

Vito, P., Pellegrini, L., Guiet, C., and D'Adamio, L. (1999). Cloning of AIP1, a novel protein that associates with the apoptosis-linked gene ALG-2 in a Ca2+-dependent reaction. J Biol Chem *274*, 1533-1540.

von Schwedler, U.K., Stuchell, M., Muller, B., Ward, D.M., Chung, H.Y., Morita, E., Wang, H.E., Davis, T., He, G.P., Cimbora, D.M., Scott, A., Krausslich, H.G., Kaplan, J., Morham, S.G., and Sundquist, W.I. (2003). The protein network of HIV budding. Cell *114*, 701-713.

Wang, H., and Clarke, S.H. (2003). Evidence for a ligand-mediated positive selection signal in differentiation to a mature B cell. J Immunol *171*, 6381-6388.

Wang, H.Y., Altman, Y., Fang, D., Elly, C., Dai, Y., Shao, Y., and Liu, Y.C. (2001). Cbl promotes ubiquitination of the T cell receptor zeta through an adaptor function of Zap-70. J Biol Chem *276*, 26004-26011.

Warburton, D., Seth, R., Shum, L., Horcher, P.G., Hall, F.L., Werb, Z., and Slavkin, H.C. (1992). Epigenetic role of epidermal growth factor expression and signalling in embryonic mouse lung morphogenesis. Dev Biol *149*, 123-133.

Watanabe, S., Take, H., Takeda, K., Yu, Z.X., Iwata, N., and Kajigaya, S. (2000). Characterization of the CIN85 adaptor protein and identification of components involved in CIN85 complexes. Biochem Biophys Res Commun *278*, 167-174.

Webster, G.A. and Perkins, N.D. (1999). Transcriptional cross talk between NF-kappaB and p53. *Mol Cell Biol* 19, 3485-3495.

Wells, C.D., Liu, M.Y., Jackson, M., Gutowski, S., Sternweis, P.M., Rothstein, J.D., Kozasa, T., and Sternweis, P.C. (2002). Mechanisms for reversible regulation between G13 and Rho exchange factors. J Biol Chem *277*, 1174-1181.

Westover, E.J., Covey, D.F., Brockman, H.L., Brown, R.E., and Pike, L.J. (2003). Cholesterol depletion results in site-specific increases in epidermal growth factor receptor phosphorylation due to membrane level effects. Studies with cholesterol enantiomers. J Biol Chem *278*, 51125-51133.

Wilson, P.D. (2001). Polycystin: new aspects of structure, function, and regulation. J Am Soc Nephrol *12*, 834-845.

Wu, Y., Dowbenko, D., Pisabarro, M.T., Dillard-Telm, L., Koeppen, H., Lasky, L.A. (2001). PTEN 2, a Golgi-associated testis-specific homologue of the PTEN tumor suppressor lipid phsophatase, J Biol Chem *276*, 21745-53.

Wu, W.J., Tu, S., and Cerione, R.A. (2003). Activated Cdc42 sequesters c-Cbl and prevents EGF receptor degradation. Cell *114*, 715-725.

Wymann, M.P., and Pirola, L. (1998). Structure and function of phosphoinositide 3-kinases. Biochim Biophys Acta *1436*, 127-150.

Yamabhai, M., Hoffman, N.G., Hardison, N.L., McPherson, P.S., Castagnoli, L., Cesareni, G., and Kay, B.K. (1998). Intersectin, a novel adaptor protein with two Eps15 homology and five Src homology 3 domains. J Biol Chem *273*, 31401-31407.

Yasuda, T., Maeda, A., Kurosaki, M., Tezuka, T., Hironaka, K., Yamamoto, T., and Kurosaki, T. (2000). Cbl suppresses B cell receptor-mediated phospholipase C (PLC)-gamma2 activation by regulating B cell linker protein-PLC-gamma2 binding. J Exp Med *191*, 641-650.

Yasuda, T., Tezuka, T., Maeda, A., Inazu, T., Yamanashi, Y., Gu, H., Kurosaki, T., and Yamamoto, T. (2002). Cbl-b positively regulates Btk-mediated activation of phospholipase C-gamma2 in B cells. J Exp Med *196*, 51-63.

Yin, Y., Terauchi, Y., Solomon, G.G., Aizawa, S., Rangarajan, P.N., Yazaki, Y., Kadowaki, T., and Barrett, J.C. (1998). Involvement of p85 in p53-dependent apoptotic response to oxidative stress. Nature *391*, 707-710.

Yu, J., Zhang, Y., McIlroy, J., Rordorf-Nikolic, T., Orr, G.A., and Backer, J.M. (1998). Regulation of the p85/p110 phosphatidylinositol 3'-kinase: stabilization and inhibition of the p110alpha catalytic subunit by the p85 regulatory subunit. Mol Cell Biol *18*, 1379-1387.

Zvara, A., Fajardo, J.E., Escalante, M., Cotton, G., Muir, T., Kirsch, K.H., and Birge, R.B. (2001). Activation of the focal adhesion kinase signaling pathway by structural alterations in the carboxyl-terminal region of c-Crk II. Oncogene *20*, 951-961.

Appendix:
Publications

ELSEVIER

Gene 295 (2002) 13–17

GENE
AN INTERNATIONAL JOURNAL ON GENES AND GENOMES

www.elsevier.com/locate/gene

Organization of the mouse *Ruk* locus and expression of isoforms in mouse tissues

Vladimir L. Buchman[a,*], Courtney Luke[a], Emma B. Borthwick[a], Ivan Gout[b], Natalia Ninkina[a]

[a]*Department of Preclinical Veterinary Sciences, University of Edinburgh, Summerhall, Edinburgh, EH9 1QH, UK*
[b]*Ludwig Institute for Cancer Research, 91 Riding House Street, London W1W 7BS, UK*

Received 18 March 2002; received in revised form 10 June 2002; accepted 25 June 2002
Received by E. Sverdlov

Abstract

Ruk is a recently identified gene with a complex pattern of expression in mammalian cells and tissues. Multiple *Ruk* transcripts and several protein isoforms have been detected in various types of cells. Ruk proteins have multidomain organization characteristic of adapter proteins involved in regulation of signal transduction. Interaction of some Ruk isoforms with several signalling proteins, including the p85 regulatory subunit of the Class IA PI 3-kinase, c-Cbl and Grb2, has been demonstrated. Ruk_I, an isoform with three SH3 domains, inhibits lipid kinase activity of the PI 3-kinase in vitro; overexpression of this protein induces apoptotic cell death of primary neurons in culture and changes in membrane trafficking in other cultured cells. However, shorter isoforms of Ruk block pro-apoptotic effect of Ruk_I, suggesting that expression of different combinations of Ruk proteins in cells could be involved in the regulation of their survival and other intracellular processes. To understand the mechanism of differential expression of Ruk proteins we studied organization of the mouse *Ruk* gene and its transcripts. Twenty-four exons of the *Ruk* gene span over 320 kb of the mouse chromosome X. Analysis of cDNA clones, ESTs and products of RT-PCR amplifications with different combinations of primers revealed how alternative splicing and promoter usage generate a variety of *Ruk* transcripts and encoded protein isoforms in different mouse tissues.

Keywords: PI 3-kinase; CIN85; SETA; Sh3kbp1; Adapter protein

1. Introduction

The enzymes known as Class IA PI 3-kinases regulate various aspects of cell physiology acting via their products, PtdIns 3,4 phosphate and PtdIns 3,4,5 phosphate, which are membrane-associated second messengers. As a cross-point of many intracellular signalling pathways Class IA PI 3-kinases require fine regulation of their activity. This regulation is achieved by the interaction of both catalytic (p110) and regulatory (p85 or p55) subunits of the enzyme with different adapter proteins. Most known adapter proteins that interact with the p85 regulatory subunit have a stimulating effect on lipid kinase activity of the holoenzyme. However, recently we identified a protein, Ruk_I, which interacts with the p85α regulatory subunit and by this negatively regulates Class IA PI 3-kinase activity (Gout et al., 2000). This inhibition leads to apoptotic death of PI 3-kinase pathway-dependent cells (Gout et al., 2000; Orike et al., 2001). Ruk_I is a typical adapter protein with multiple domains (three SH3 domains, a Pro-rich region and a C-terminal coiled-coil domain) capable of interacting with other proteins. Not surprisingly, interactions of Ruk_I or its human ortholog, CIN85, with other signalling molecules, including Cbl, Grb2, Crk, Sos and Src-family tyrosine kinases, have been demonstrated in vitro or in cell lines overexpressing these proteins following transfection with expression plasmids (Gout et al., 2000; Take et al., 2000; Borinstein et al., 2000; Watanabe et al., 2000). Recently CIN85/Ruk_I has been found in complexes with endophilin. Activation of receptor tyrosine kinases by ligand binding leads to recruitment of CIN85/Ruk_I-endophilin complexes to the receptor via Cbl and consequent receptor internalization (Soubeyran et al., 2002; Petrelli et al., 2002). These data link Ruk_I with regulation of endocytosis.

Abbreviations: bp, base pairs; cDNA, DNA complementary to RNA; EST, expressed sequence tag; HRP, horse radish peroxidase; kb, kilobase; kDa, kilodalton; mRNA, messenger RNA; ORF, open reading frame; P8, postnatal day 8; PAGE, polyacrylamide gel electrophoresis; PCR, polymerase chain reaction; RT, reverse transcriptase; SDS, sodium dodecil sulphate; UTR, untranslated region

* Corresponding author. Tel.: +44-131-650-6105; fax: +44-131-650-6576.
E-mail address: v.buchman@ed.ac.uk (V.L. Buchman).

0378-1119/02/$ - see front matter.
PII: S0378-1119(02)00821-1

Ruk_l is not the only protein product of the *Ruk* gene. Northern hybridization, direct cDNA cloning and analysis of EST clones in the data banks revealed multiple transcripts of the *Ruk* gene. Some of these transcripts have characteristic tissue-specific or developmentally regulated expression patterns. These results were confirmed by immunoblotting of cell lysates from various tissues with antibody specific to a C-terminal Ruk peptide, common to all known isoforms of Ruk protein (Gout et al., 2000). Most Ruk protein isoforms are either N-terminal truncated versions of Ruk_l or lack certain internal domains, probably because of alternative splicing of internal exons of the gene. However, only cloning of cDNAs encoding isoforms without the first N-terminal SH3 domain (SETA), two N-terminal SH3 domains (Ruk_m), and a short isoform possessing only C-terminal coiled-coil domain (Ruk_s) have been reported (Gout et al., 2000; Borinstein et al., 2000; Chen et al., 2000; Watanabe et al., 2000). The importance of further studies of Ruk isoforms is emphasized by the fact that at least one of the truncated isoforms, Ruk_m, could act as a dominant negative regulator of Ruk_l-induced neuronal apoptosis (Gout et al., 2000). To understand the origin of various transcripts and to be able to use the RT-PCR technique for analysis of complex expression patterns of the *Ruk* gene in different types of cells, information about organization of the *Ruk* gene is essential. It has been reported that the *Ruk* genes are localized on chromosome X in both human and mouse genomes (Hyatt et al., 2000; Narita et al., 2001; and our unpublished FISH data). These results are consistent with data emerging from Human and Mouse Genome Projects. However, at the present time both genome projects lack complete information even about coding exons of *Ruk* genes. Here we present comprehensive data about the organization of the *Ruk* gene in the genome of 129Ola mice. This information facilitated our understanding of how different *Ruk* transcripts, encoding various Ruk protein isoforms, are generated.

2. Materials and methods

2.1. Molecular cloning and analysis of gene structure

Screening of the mouse genomic library in λ FIX II (Stratagene), isolation of lambda genomic clones, subcloning, mapping, Southern hybridization, DNA sequencing and sequence analysis were carried out as described previously (Gout et al., 2000; Mertsalov et al., 2000; Ninkina et al., 2001).

2.2. RT-PCR analysis of Ruk mRNA expression

Total RNA was extracted from mouse tissues as described earlier (Gout et al., 2000). These RNAs were used as templates and oligo$(dT)_{15}$ as a primer for synthesis of a first strand cDNAs by SuperScript reverse transcriptase (Life Technologies). PCR amplifications from these cDNAs were carried out for 35 cycles (25 for L27 and 45 for Ruk_m) of 30 s at 95 °C, 30 s at 58 °C, and 120 s at 72 °C using Taq polymerase from Promega. The following primers were used (for positions of primers see Fig. 1): m1, TTCCGCCAACTTTCACTCTG; m2, CACAGAATGGAGCTTTCTGC; mmn, GGCAGGAAGTCATTTTCCAC; m3, GGATTTCAGGGTAGTTCTGG; m4, TGAATCTGTTTCGGCAGACC; m5, TACAGAACAGAGGGACATCC; mc, TTCACTTCCATCTGCAACCG.

2.3. Analysis of protein expression in mouse tissues

Freshly dissected tissues were homogenized in 50 mM Tris–Cl (pH 7.5), 150 mM NaCl, 1 mM EDTA, and 1% Triton X-100 with Complete protease inhibitors cocktail (Boehringer Mannheim). Homogenates were cleared by centrifugation at $10{,}000 \times g$ and proteins from the supernatant (cytosolic fraction) were analyzed in 12.5% SDS-PAGE. Following transfer to the PVDF membrane Ruk proteins were detected using SK42 antibody, secondary anti-rabbit Ig HRP-conjugated antibody and an ECL detection system from Amersham as described previously (Gout et al., 2000).

3. Results and discussion

3.1. Exon–intron structure of the mouse Ruk gene

Recombinant phage clones (10^6) from the 129Ola mouse genomic library (Stratagene) were screened using fragments of rat *Ruk* cDNA clones as hybridization probes. Seven consecutive screenings were carried out with each hybridization probe shown in Fig. 1. In these screens 27 individual genomic clones were isolated. The majority of isolated clones did not overlap and hybridized with only one of the probes. DNAs of these lambda clones were analyzed by hybridization with specific oligonucleotide primers and hybridizing fragments were subcloned in plasmid vectors. Twenty-two exons and adjacent intronic fragments were sequenced using either universal or specific oligonucleotide primers. These exons contained all sequences corresponding to the longest known *Ruk* mRNA, Ruk_{xl}, and also 5′ sequences of Ruk_m/Ruk_s (exons 10 and 11) and Ruk_h (part of exon 19) mRNAs (Fig. 1). Analysis of mouse EST available in data banks revealed *Ruk* transcripts ($Ruk_{\Delta A}$ and Ruk_t in Fig. 1) with different 5′ sequences, which were absent in our genomic clones. Exons corresponding to these sequences were, however, found in a mouse genomic database and included in the *Ruk* gene structure as exons 3 and 18, respectively.

The sequence and mapping data together with information available from the Mouse Genome Projects showed that 24 exons of the *Ruk* gene spans over 320 kb of mouse genome. Transcription of different *Ruk* transcripts starts from five potential promoters located upstream of exons 1, 3, 10, 18 and 19. Some of these promoters seem to be tissue-

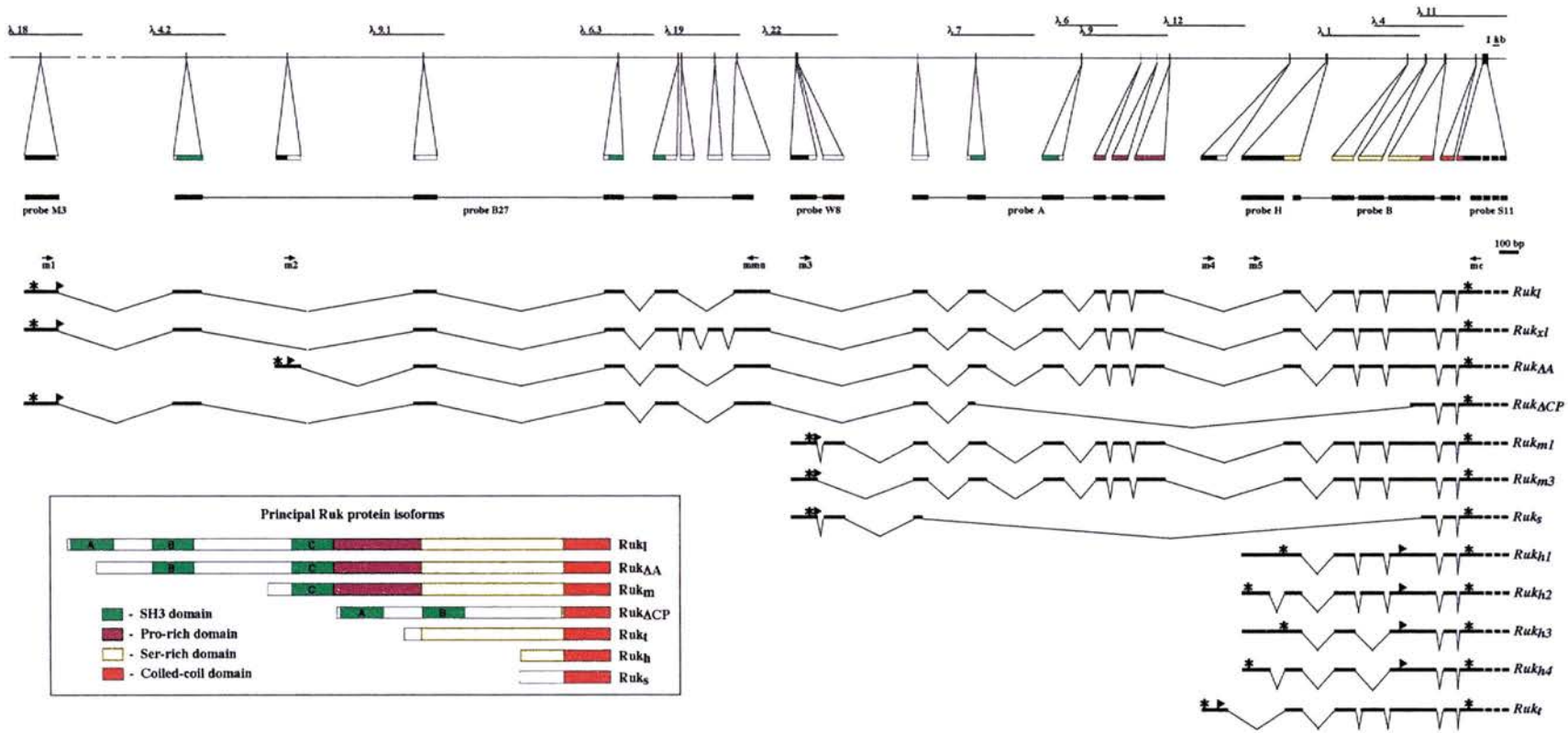

Fig. 1. Mouse *Ruk* locus, transcripts and encoded proteins. A map of the mouse *Ruk* locus was created using information from sequencing and mapping of lambda mouse genomic clones (shown above the map), genomic Southern hybridizations and analysis of available databases from the Mouse Genome Project. All exons (vertical bars on the map, zoomed and numbered below) were completely sequenced. The cDNA fragments used as hybridization probes for genomic library screening and approximate positions of oligonucleotide primers used for RT-PCR are shown. Various transcripts generated from the *Ruk* locus by alternative splicing and promoter usage are shown below. The insert illustrates domain organization of major Ruk protein isoforms. The colour code for zoomed exons is the same as for proteins in the insert and UTRs are shown in black. Sequences of exons of the mouse *Ruk* gene are deposited in GenBank under Accession numbers AF472304–AF472327. Examples of mouse EST clones that represent *Ruk* transcripts: Ruk_l, BB853873; $Ruk_{\Delta A}$, AK004636; Ruk_{m3}, BB611586; $Ruk_{\Delta CP}$, AI428677; Ruk_t, AA145505; Ruk_{h2}, AA500188; Ruk_{h3}, AI593182. Transcripts Ruk_{xl}, Ruk_{m1}, Ruk_s and Ruk_{h1} have not been identified yet in mouse EST databases but were cloned as human and/or rat cDNA (Gout et al., 2000; Borinstein et al., 2000; and our unpublished data).

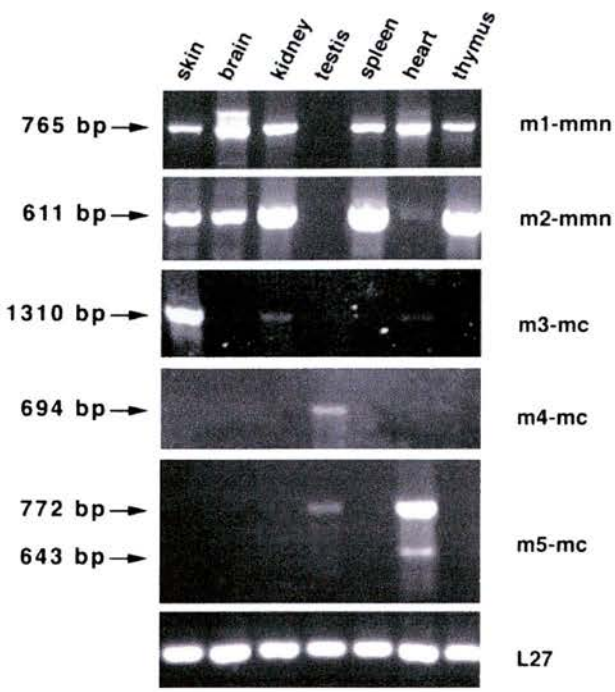

Fig. 2. Expression of Ruk isoforms in mouse tissues. Agarose gel analysis of products of RT-PCR amplification with pairs of primers shown on the right (for positions of primers see Fig. 1; sequences are shown in Section 2.2). Sizes of fragments in bp are shown on the left. RNA was isolated from tissues of P8 mice or adult mouse testis. The lower panel shows amplification of a fragment of housekeeping gene transcript, the ribosomal protein L27 mRNA, as a loading control.

specific while others are active in many types of cells (see below). Sequence data for the region of the human chromosome X, where the *Ruk* gene is located, are not yet complete but available data demonstrate remarkable similarity in the organization of mouse and human *Ruk* genes – not only all the exon–intron junctions but also the sizes of many introns are conserved.

3.2. Expression of Ruk transcripts in mouse tissues

Our previous studies of rat and human cDNA clones revealed several *Ruk* transcripts, which are expressed in different tissues (Gout et al., 2000; and our unpublished data). Similar transcripts as well as additional transcripts were revealed in EST databases (see legend to Fig. 1). Alignment of nucleotide sequences of all these transcripts and exons of the mouse *Ruk* gene demonstrated how alternative splicing generates the diversity of *Ruk* gene products (Fig. 1).

Several oligonucleotide primers (Figs. 1 and 2) were used to study the expression of various *Ruk* transcripts by RT-PCR. RNA templates for RT-PCR were obtained from different tissues of 8-day-old mice (P8) and from adult testis. As illustrated in Fig. 2, different primer combinations amplified fragments corresponding to either a subset or only a single *Ruk* transcript. Using a combination of primers m1 and mmn a 745 bp fragment was revealed, which corresponded to the size of a product of amplification of the Ruk_l transcript. This product was detected in all tissues with the exception of adult testis. In addition, in P8 brain larger fragments were identified (Fig. 2), the largest of them corresponding to amplification products of the Ruk_{xl} transcript (Ruk_l + exons 6 and 7). A transcript designated in Fig. 1 as $Ruk_{\Delta A}$, which is similar to SETA described by Bogler et al. (2000), was revealed using an upstream primer m2 and the downstream primer mmn. The expression pattern of this transcript is similar to the expression pattern of Ruk_l although expression in the heart is substantially lower than in other tissues (Fig. 2).

The expression patterns of three other, smaller, types of mouse *Ruk* transcripts are much more tissue-specific, which is consistent with data of expression of rat *Ruk* transcripts (Gout et al., 2000; and our unpublished data). The first of these was studied using primers m3 and mc (Figs. 1 and 2). Only a 1383 bp fragment corresponding to the Ruk_{m3} transcript was amplified from P8 skin and in a much lesser amount from P8 kidney and P8 heart (Fig. 2). A transcript named Ruk_t was detected using amplification primers m4 and mc exclusively in adult testis (Fig. 2). This is consistent with our previously published results of Northern hybridization, which demonstrated the presence in the rat testis of unique *Ruk* transcript (designated as 3E7 in Akopyan et al., 1996). Several heart-specific transcripts have been identified in rat and human by cDNA cloning or analysis of EST databases (our unpublished observations). In P8 mouse heart, using amplification primers m5 and mc, a major transcript Ruk_{h2} (772 bp fragment, Fig. 2) and minor transcript Ruk_{h4} (643 bp fragment, Fig. 2) were detected. A low level of Ruk_{h2} transcript was also detected in testis. The identity of amplification fragments was verified by sequence analysis. Interestingly, all heart-specific *Ruk* mRNA identified so far in different species (rat, mouse, human) have in-frame stop codons in the 5′ region derived from exon 19. Therefore, all these mRNA encode the same short protein that starts from a Met localized within the Ser-rich domain (Fig. 1).

3.3. Ruk protein isoforms in mouse tissues

All mouse Ruk protein isoforms encoded by transcripts shown in Fig. 1 have a common C-terminal coiled-coil domain. We produced new antiserum, SK42, against the C-terminal peptide of mouse Ruk and affinity purified Ruk-specific antibody on the immobilized peptide column. This affinity purified antibody was used to detect Ruk proteins in different mouse tissues by Western blotting. As illustrated in Fig. 3, the pattern of protein expression revealed by Western blotting is even more complex than the pattern of *Ruk* mRNA expression. This possibly reflects posttranslational modifications of certain Ruk proteins, which could have a substantial effect on their mobility even in SDS-PAGE. For instance, rat, human and mouse Ruk_l proteins migrate in this gel as 85 kDa bands (Gout et

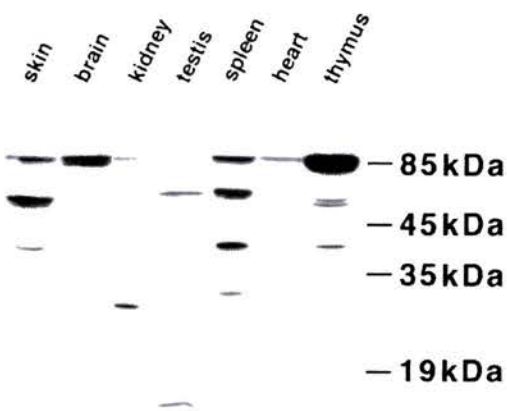

Fig. 3. Ruk proteins in mouse tissues. Western blot analysis of cytosolic proteins extracted from tissues of P8 mice or adult mouse testis. Positions and sizes of protein markers are shown on the right.

al., 2000; Take et al., 2000) (Fig. 3), although their molecular masses calculated from amino acid sequences are only around 73 kDa. On the other hand, we were not able to detect all Ruk proteins by this method; the short Ruk isoforms, Ruk_t in the testis and Ruk_h in the heart, could not be revealed on our Western blots (Fig. 3). Because recombinant Ruk_t and Ruk_h proteins produced in HEK293 cells transfected with corresponding expression plasmids could be effectively detected on Western blots using SK42 antibody (data not shown), it could be suggested that in testis and heart cells these proteins exist in forms which do not allow their effective extraction by the method we used here (see Section 2.3).

In conclusion, the *Ruk* gene comprises 24 exons, which spans over 320 kb of mouse genome. Differential promoter usage and alternative splicing generate a complex tissue-specific pattern of expression of various transcripts and encoded protein isoforms.

Acknowledgements

We thank Julia Wanless and Liz Delaney for technical assistance and the DNA Sequencing Unit of the University of Dundee for excellent service. This work was supported in part by a Research Grant from the Association for International Cancer Research.

References

Akopyan, A.N., Baka, I.D., Chestkov, A.V., Buchman, V.L., Georgiev, G.P., 1996. Cloning of genes differentially expressed in the cerebellum during postnatal rat development. Genetika 32, 886–895.

Bogler, O., Furnari, F.B., Kindler-Roehrborn, A., Sykes, V.W., Yung, R., Huang, H.J., Cavenee, W.K., 2000. SETA: a novel SH3 domain-containing adapter molecule associated with malignancy in astrocytes. Neuro-oncology 2, 6–15.

Borinstein, S.C., Hyatt, M.A., Sykes, V.W., Straub, R.E., Lipkowitz, S., Boulter, J., Bogler, O., 2000. SETA is a multifunctional adapter protein with three SH3 domains that binds Grb2, Cbl, and the novel SB1 proteins. Cell. Signal. 12, 769–779.

Chen, B., Borinstein, S.C., Gillis, J., Sykes, V.W., Bogler, O., 2000. The glioma-associated protein SETA interacts with AIP1/Alix and ALG-2 and modulates apoptosis in astrocytes. J. Biol. Chem. 275, 19275–19281.

Gout, I., Middleton, G., Adu, J., Ninkina, N.N., Drobot, L.B., Filonenko, V., Matsuka, G., Davies, A.M., Waterfield, M., Buchman, V.L., 2000. Negative regulation of PI 3-kinase by Ruk, a novel adaptor protein. EMBO J. 19, 4015–4025.

Hyatt, M.A., Sykes, V.W., Boyer, A.D., Arden, K.C., Bogler, O., 2000. Assignment of seta to distal mouse X chromosome by radiation hybrid mapping. Cytogenet. Cell Genet. 89, 278.

Mertsalov, I.B., Kulikova, D.A., Alimova-Kost, M.V., Ninkina, N.N., Korochkin, L.I., Buchman, V.L., 2000. Structure and expression of two members of the d4 gene family in mouse. Mamm. Genome 11, 72–74.

Narita, T., Amano, F., Yoshizaki, K., Nishimoto, N., Nishimura, T., Tajima, T., Namiki, H., Taniyama, T., 2001. Assignment of SH3KBP1 to human chromosome band Xp22.1-p21.3 by in situ hybridization. Cytogenet. Cell Genet. 93, 133–134.

Ninkina, N.N., Mertsalov, I.B., Kulikova, D.A., Alimova-Kost, M.V., Simonova, O.B., Korochkin, L.I., Kiselev, S.L., Buchman, V.L., 2001. Cerd4, third member of the d4 gene family: expression and organisation of genomic locus. Mamm. Genome 12, 862–866.

Orike, N., Middleton, G., Borthwick, E., Buchman, V., Cowen, T., Davies, A.M., 2001. Role of PI 3-kinase, Akt and Bcl-2-related proteins in sustaining the survival of neurotrophic factor-independent adult sympathetic neurons. J. Cell Biol. 154, 995–1006.

Petrelli, A., Gilestro, G.F., Lanzardo, S., Comoglio, P.M., Migone, N., Giordano, S., 2002. The endophilin-CIN85-Cbl complex mediates ligand-dependent downregulation of c-Met. Nature 416, 187–190.

Soubeyran, P., Kowanetz, K., Szymkiewicz, I., Wallace, Y., Langdon, W.Y., Dikic, I., 2002. Cbl-CIN85-endophilin complex mediates ligand-induced downregulation of EGF receptors. Nature 416, 183–187.

Take, H., Watanabe, S., Takeda, K., Yu, Z., Iwata, N., Kajigaya, S., 2000. Cloning and characterization of a novel adaptor protein, CIN85, that interacts with c-Cbl. Biochem. Biophys. Res. Commun. 268, 321–328.

Watanabe, S., Take, H., Takeda, K., Yu, Z., Iwata, N., Kajigaya, S., 2000. Characterization of the CIN85 adaptor protein and identification of components involved in CIN85 complexes. Biochem. Biophys. Res. Commun. 278, 167–174.

doi:10.1016/j.jmb.2004.08.075 J. Mol. Biol. (2004) 343, 1135–1146

JMB

Available online at www.sciencedirect.com

SCIENCE DIRECT®

ELSEVIER

Multiple Domains of Ruk/CIN85/SETA/CD2BP3 are Involved in Interaction with p85α Regulatory Subunit of PI 3-kinase

Emma B. Borthwick[1], Igor V. Korobko[2], Courtney Luke[1], Victor R. Drel[3] Yaroslav Ya. Fedyshyn[3], Natalia Ninkina[1,2], Ludmila B. Drobot[3] and Vladimir L. Buchman[1]*

[1]*Department of Preclinical Veterinary Sciences, University of Edinburgh, Summerhall Edinburgh EH9 1QH, UK*

[2]*Institute of Gene Biology Russian Academy of Sciences Vavilov Street, 34/5, B334 Moscow, Russia*

[3]*Institute of Cell Biology National Academy of Sciences of Ukraine, 14/16 Drahomanov Street, Lviv 290005, Ukraine*

**Corresponding author*

Ruk/CIN85/SETA/CD2BP3 and CD2AP/CMS/METS-1 comprise a new family of proteins involved in such fundamental processes as clustering of receptors and rearrangement of the cytoskeleton in regions of specialised cell–cell contacts, ligand-activated internalisation and targeting to lysosome degradation pathway of receptor tyrosine kinases, and apoptotic cell death. As typical adapter proteins they execute these functions by interacting with other signalling molecules *via* multiple protein–protein interaction interfaces: SH3 domains, Pro-rich region and coiled-coil domain. It has been previously demonstrated that Ruk is able to interact with the p85α regulatory subunit of PI 3-kinase and that the SH3 domain of p85α is required for this interaction. However, later observations hinted at a more complex mechanism than simple one-way SH3–Pro-rich interaction. Because interaction with p85α was suggested to be important for pro-apoptotic activity of the long isoform of Ruk, Ruk_l/CIN85, we carried out detailed studies of the mechanism of this interaction and demonstrated that multiple domains are involved; SH3 domains of Ruk are required and sufficient for efficient interaction with full-length p85α but the SH3 domain of p85α is vital for their "activation" by ousting them from intramolecular interaction with the Pro-rich region of Ruk. Our data also suggest that homodimerisation *via* C-terminal coiled-coil domain affects both intra- and intermolecular interactions of Ruk proteins.

Keywords: protein–protein interaction; phosphatidylinositol 3-kinase; adaptor protein; SH3 domain; proline-rich region

Introduction

A high degree of structural similarity between two recently identified proteins, CD2AP/CMS/METS-1 and Ruk_l/CIN85/SETA/CD2BP3, allowed them to become founders of a novel protein family.[1] Their structural organisation is typical for adapter proteins: the bulk of the molecule comprises of multiple protein–protein interaction motifs, including three SH3 domains, Pro-rich region and coiled-coil domain. CD2AP/CMS/METS-1 has been implicated in clustering of CD2 receptors and rearrangement of T-cell cytoskeleton in the region of contact with an antigen-presenting cell.[2] Similarly, in podocytes this protein is involved in clustering and anchoring to the cytoskeleton of nephrin, a kidney-specific receptor of the immunoglobulin superfamily.[3–7] Nephrological and immunological phenotypes of CD2AP null mutant mice confirm the suggestion that CD2AP/CMS/METS-1 function is crucial for formation of such specialised types of cell–cell contacts as slit diaphragm and immunological synapse.[4] In the absence of information about the phenotype of null mutant mice, the biological function of Ruk/CIN85/SETA/CD2BP3 is less clear. However, involvement of this protein in several important intracellular processes has been demonstrated in model systems. The best characterised function of

Present address: V. L. Buchman, Cardiff School of Biosciences, Biomedical Sciences Building, Cardiff University, Museum Avenue, Cardiff CF10 3US, UK.

Abbreviations used: GST, glutathione *S*-transferase.

E-mail address of the corresponding author: buchmanvl@cardiff.ac.uk

this protein is down-regulation of receptor tyrosine kinases (RTKs) *via* activation of their internalisation.[8–10] Ruk/CIN85/SETA/CD2BP3 specifically regulates clathrin-dependent endocytosis of ligand-activated receptors and available data suggest that for implementation of this function a direct and simultaneous interaction with two proteins, Cbl and endophilin, is crucial.[1,11,12] Ubiquitin ligases of Cbl family not only interact with but also monoubiquitinate Ruk/CIN85/SETA/CD2BP3.[13] However, such ubiquitination does not play a role of a signal for proteasome degradation[14] but is required for targeting of the protein to the lysosome degradation pathway in trimeric complex with RTK and Cbl proteins.[13] The ability of Ruk/CIN85/SETA/CD2BP3 to interact with other proteins, such as BLNK,[15] SB1, CD2,[16] CAPZ,[17] Grb2, p130Cas,[15,16] FAK and Pyk-2 kinases,[18] and Src family kinases (our unpublished observations) and similarity with CD2AP/CMS/METS-1 (including common binding site in the cytoplasmic segment of CD2[19]) implicates this protein in regulation of B- and T-cell receptor signalling, rearrangements of actin cytoskeleton and cell adhesion. The role of Ruk_l/CIN85/SETA/CD2BP3 and its isoforms in regulation of apoptosis has been demonstrated in two types of cells. In astrocytes, overexpression of SETA protein or its mutants sensitises cells to apoptosis induced by UV irradiation.[20] It has been suggested that this effect depends on the ability of the SH3-B domain of SETA to interact with a proline-rich region of AIP1/Alix protein, an important modulator of apoptosis in glial cells.[20] Apoptosis of peripheral neurons in primary culture could be induced by overexpression of Ruk_l.[21] Because the PI 3-kinase signalling pathway is important for survival of these cells, it is feasible that the negative regulation of PI 3-kinase activity by Ruk_l might trigger apoptotic death. Originally, the effect of Ruk_l on PI 3-kinase activity and neuronal survival was attributed to interaction of its Pro-rich region and the SH3 domain of the p85α regulatory subunit of PI 3-kinase. However, at least one natural isoform of the protein possessing proline-rich region, Ruk_m, does not have pro-apoptotic activity itself and is able to block pro-apoptotic activity of Ruk_l.[21] This suggests that other domains of Ruk and p85α might also be involved, directly or indirectly, in interaction of these two proteins. Due to the complexity of Ruk expression patterns in various types of cells and tissues,[22] two or more isoforms may be expressed in the same cell and modulate each other's signalling abilities. Because of the importance of Ruk interaction with other signalling proteins for cell physiology we decided to scrutinise the role of various Ruk domains in heteromerisation of Ruk isoforms with the p85α regulatory subunit of PI 3-kinase. Our results demonstrate that all three types of protein–protein interaction motifs within the Ruk molecule, SH3 domains, Pro-rich region and coiled-coil domain, affect heteromerisation of two proteins.

Results

Interaction of Ruk proteins with p85α and ΔSH3-p85α in HEK293 cells

For expression in mammalian cells coding regions of cDNAs encoding naturally existing isoforms of Ruk protein, Ruk_l, ΔA-Ruk, Ruk_m, Ruk_h and Ruk_s[21,22] as well as several deletion mutants, ΔC-Ruk, ΔSH3-Ruk, Ruk_e, ΔCterm-Ruk, ABC-Ruk, ΔPro-Ruk, were subcloned into pCMV5

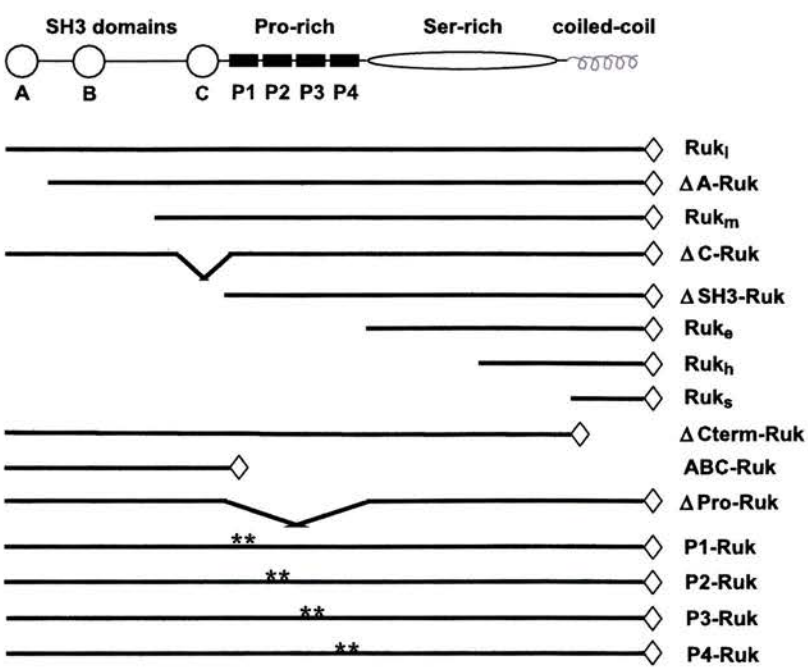

Figure 1. Ruk isoforms and mutants. Domain organisation of Ruk protein molecule and structure of isoforms and mutants used in this study. C-terminal FLAG tags are shown as diamonds and mutated proline-rich blocks as double asterisks.

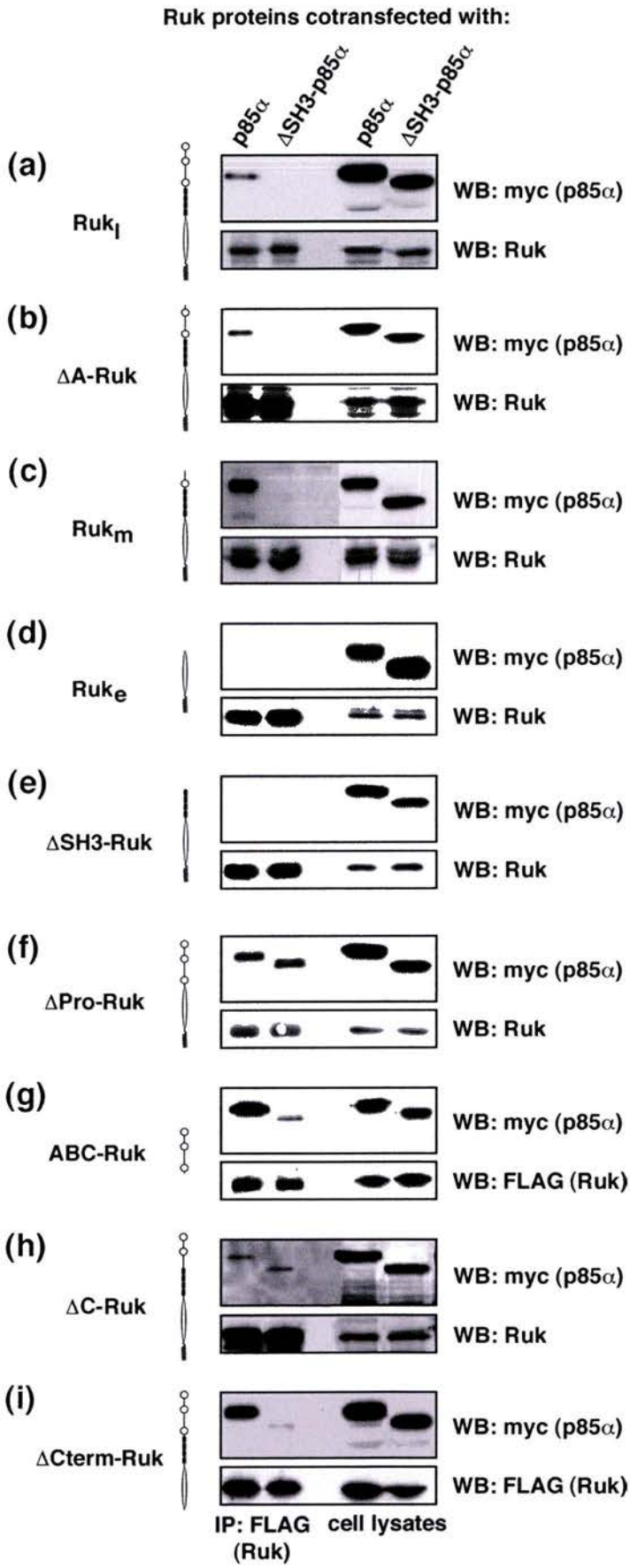

Figure 2. Interaction of Ruk isoforms and mutants with p85α and ΔSH3-p85α in HEK293 cells. Different FLAG-tagged Ruk isoforms and mutants were co-expressed in HEK293 cells with myc-tagged full-length or ΔSH3-p85α. Total cell lysates and proteins immunoprecipitated with anti-FLAG antibody were analysed by Western blotting using anti-myc antibody to detect p85α proteins and anti-Ruk or anti-FLAG (for ΔCterm-Ruk and ABC-Ruk isoforms) antibody to detect Ruk proteins. The upper Ruk$_m$ band in the c is probably a product of posttranslational modification of the protein. To better reveal co-immunoprecipitation of full-length p85α but not ΔSH3-p85α by Ruk$_m$ isoform, the IP parts in c show longer exposure of the Western blot.

expression vector as described in Materials and Methods and illustrated in Figure 1. C-terminal FLAG tag was added to all isoforms and mutant proteins during subcloning. Expression plasmids encoding triple myc-tagged p85α and ΔSH3-p85α mutant were described previously.[23] These plasmids were used for transient transfection of HEK293 cells as described in Materials and Methods. After normalising transfection efficiencies to achieve similar levels of expression for studied proteins in transfected cells, co-transfections of various combinations of Ruk and p85α expression plasmids were carried out. Ruk proteins were immunoprecipitated from cell lysates using immobilised anti-FLAG antibody and the presence of p85α or its mutant forms in cell lysates and immunoprecipitates was assessed by Western blotting. Figure 2(a) demonstrates that in mammalian cells the longest Ruk isoform, Ruk_l, co-immunoprecipitated p85α but was unable to co-immunoprecipitate ΔSH3-p85α. Likewise, the N-terminally truncated Ruk protein, ΔA-Ruk, which lacks the first SH3 domain and is similar to the previously described SETA/CD2BP3 isoform,[19,22,24] co-immunoprecipitated p85α but not ΔSH3-p85α (Figure 2(b)). Ruk_m isoform, which lacks both SH3A and SH3B domains also did not co-immunoprecipitate ΔSH3-p85α and was still able to pull down p85α in these cells (Figure 2(c)), although quantification of normalised Western blots demonstrated that the amount of p85 co-immunoprecipitated by Ruk_m was on average five time less than the amount co-immunoprecipitated by Ruk_l or ΔA-Ruk. Further N-terminally truncated Ruk proteins, ΔSH3-Ruk, lacking all three SH3 domains, Ruk_e, consisting of only the C-terminal Ser-rich region and coiled-coil domain, and the shortest isoforms Ruk_h and Ruk_s[22] were unable to co-immunoprecipitate both p85α variants (Figure 2(d) and (e) and data not shown). In contrast, two mutants with three intact SH3 domains but without a Pro-rich region, ABC-Ruk and ΔPro-Ruk, as well as a mutant lacking only the third SH3 domain, ΔC-Ruk, co-immunoprecipitated both p85α variants (Figure 2(f)–(h)). C-terminally truncated ΔCterm-Ruk was also able to co-immunoprecipitate p85α and, although with very low efficiency, ΔSH3-p85α (Figure 2(i)).

Interaction of Ruk proteins with p85α in the yeast two-hybrid system

To study protein–protein interaction in the yeast two-hybrid system bait and prey plasmids were constructed by subcloning the coding regions of p85α and Ruk isoforms in frame with GAL4 DNA-binding domain (GAL4-BD) or transcription activating domain (GAL4-AD), respectively. Yeast strain Y153 was co-transformed with bait and prey plasmids, transformants were selected by plating on synthetic dextrose leucine and tryptophan dropout plate and *LacZ* reporter gene *trans*-activation was evaluated by filter β-galactosidase assay. Figure 3 shows that *trans*-activation of the reporter gene occurred when GAL4-BD-p85α was co-expressed with GAL4-AD-Ruk_l, GAL4-AD-Ruk_m and GAL4-AD-ΔPro-Ruk but not with GAL4-AD-Ruk_h, suggesting the importance of SH3 domains of Ruk for interaction with p85α.

Interaction of p85α with separate domains of Ruk *in vitro*

Each of three SH3 domains of Ruk and Ruk_s isoform, containing only coiled-coil domain, were subcloned in frame with glutathione-*S*-transferase (GST), expressed in *Escherichia coli*, affinity purified on glutathione-Sepharose and used as baits in pull-down experiments. Aliquots of the cytosolic fraction of lysates of HEK293 cells transiently transfected with p85α expression plasmid were incubated with GST fusion proteins attached to glutathione-Sepharose beads and after thorough washing bound proteins were eluted and analysed by SDS-PAGE followed by Western blotting with anti-p85α antibody. Only GST-fused Ruk SH3 domains A and B but not SH3 domain C or Ruk_s isoform were able to bind p85α in this *in vitro* assay (Figure 4).

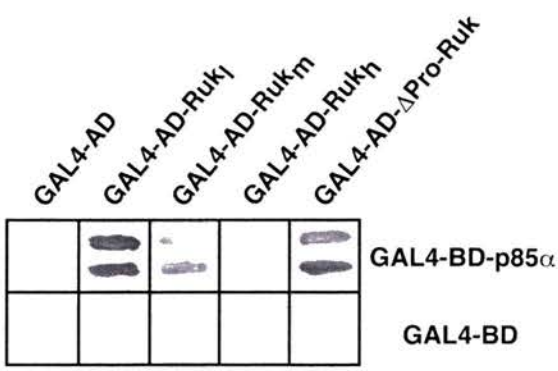

Figure 3. Interaction of Ruk isoforms and mutants with p85α in a yeast two-hybrid system. The filter β-galactosidase assay demonstrates interaction of p85α-GAL4 DNA-binding domain (GAL4-BD) fusion protein with various Ruk-GAL4 transcription activating domain (GAL4-AD) fusion proteins.

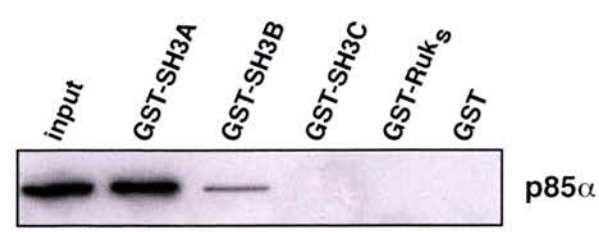

Figure 4. Interaction of separate domains of Ruk with full-length p85α *in vitro*. The full-length p85α expressed in HEK293 cells was incubated with glutathione-Sepharose-immobilised GST-SH3 domains of Ruk or GST-Ruk_s isoform. The presence of p85α in pull-downs was assessed by Western blotting using anti-p85α antibody.

Effect of point mutations in Pro-rich region of Ruk on interaction with p85α in HEK293 cells

Four separate proline-rich blocks (P1–P4) could be identified within the Pro-rich region of the Ruk protein. To assess the effect of each of these blocks on the ability of Ruk to interact with p85α, four expression plasmids encoding mutant proteins were constructed as described in Materials and Methods. Transient transfection of HEK293 cells with each of these plasmids resulted in expression of a Ruk_I protein with several substitutions of proline residues or adjacent charged amino acids to alanine in one of each proline-rich block (Figures 1 and 5(a)). Co-transfections with p85α expression plasmids and co-immunoprecipitation studies were carried out as described above for other Ruk proteins. Like other Ruk proteins, possessing SH3 domains, all four proline-rich block mutant proteins co-immunoprecipitated p85α (Figure 5(b)). No interaction of P1-Ruk with ΔSH3-p85α has been detected but P2-Ruk and P3-Ruk co-immunoprecipitated this protein although with lower than ΔPro-Ruk efficiency (on average 18% and 22% of amount

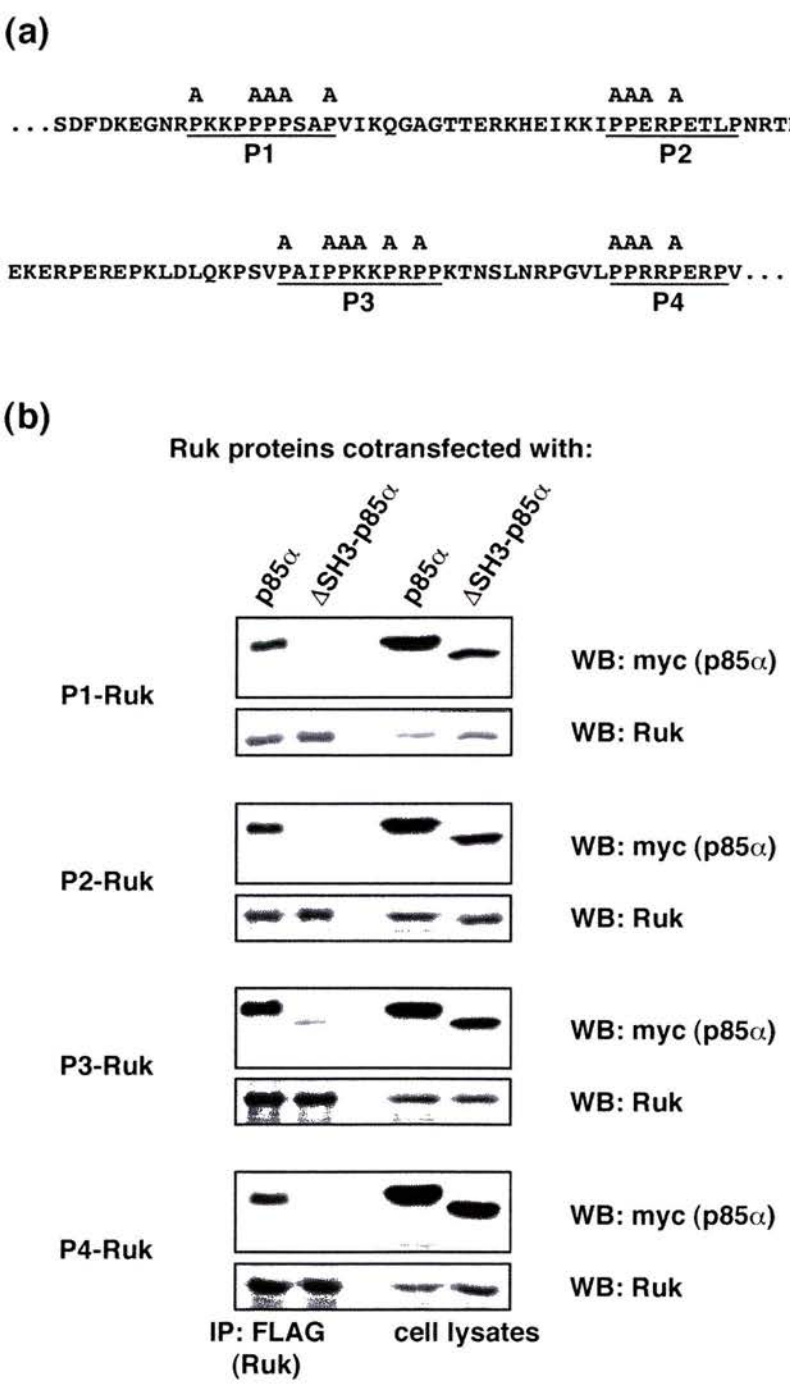

Figure 5. Interaction of Ruk proteins mutated within each of the proline-rich blocks with p85α in HEK293 cells. (a) Alanine substitutions introduced into each of four proline-rich blocks of Ruk_I. (b) Interaction between Ruk proteins bearing mutations in each of the proline-rich blocks (P1–P4) and p85α was assessed by co-immunoprecipitation as described in Materials and Methods and the legend to Figure 2.

co-immunoprecipitated by ΔPro-Ruk in parallel experiments). P4-Ruk showed very weak interaction with ΔSH3-p85α (less than 2% of amount co-immunoprecipitated by ΔPro-Ruk in parallel experiments).

Interaction of Ruk isoforms with separate domains of Ruk *in vitro*

The GST pull-down technique was used to assess interaction between different Ruk domains *in vitro*. FLAG-tagged Ruk proteins were expressed in HEK293 cells, incubated with GST fusion proteins as described above and bound proteins were analysed by Western blotting using anti-FLAG antibody. All four studied Ruk proteins were effectively pulled down by GST-Ruk_s, confirming results of previous studies, which suggested the role of coiled-coil domain in di(oligo)merisation of Ruk proteins.[14,15] GST-SH3C fusion protein did not pull down any of four Ruk proteins, whereas GST-SH3A and, to a lesser extent, GST-SH3B pulled down Pro-rich domain-bearing isoforms Ruk_l and Ruk_m, but not ΔPro-Ruk or Ruk_h (Figure 6).

Interaction between Ruk isoforms in the yeast two-hybrid system

Plasmids for expression of Ruk isoforms or mutant proteins fused with GAL4 DNA-binding domain or transcription activating domain were constructed. Y153 yeast cells were co-transformed with combinations of these bait and prey plasmids and *LacZ* reporter gene *trans*-activation was assessed as described above. Figure 7 shows that in yeast Ruk_l efficiently formed homodimers and interacted with Ruk_m, but only weakly interacted with coiled-coil-only isoform Ruk_h. In contrast, ΔPro-Ruk mutant showed equally strong interaction with all three Ruk isoforms.

Interaction of Ruk proteins with ΔBH/Pro-p85α in HEK293 cells

An additional expression plasmid that encoded a myc-tagged p85α isoform, which was unable to dimerise due to the absence of Pro-rich and BH domains, has been generated as described in Material and Methods. This p85α isoform was co-expressed in HEK293 cells with FLAG-tagged Ruk_l, ΔSH3-Ruk or ABC-Ruk and the ability of co-expressed proteins to interact with each other was assessed by co-immunoprecipitation as described above. Figure 8 shows that not only Ruk_l but also ΔSH3-Ruk co-immuniprecipitate ΔBH/Pro-p85α, although, consistently with results shown in Figure 2(e), ΔSH3-Ruk is not able to co-immunoprecipitate full-length p85α. As expected, the absence of a Pro-rich region in ABC-Ruk and ΔPro-Ruk (data not shown) prevents co-immunoprecipitation of ΔBH/Pro-p85α by these mutants.

Discussion

In the previous study we showed that endogenous Ruk_l, the longest isoform of Ruk/CIN85/SETA/CD2BP3 protein, was able to interact with endogenous p85α regulatory subunit of PI 3-kinase in cell lines expressing both proteins. Ectopically co-expressed Ruk_l and p85α also interacted in insect cells infected with recombinant baculoviruses. Deletion of the SH3 domain of p85α abolished this interaction.[21] This suggested that the single SH3 domain of p85α and one of proline-rich blocks (P1–P4) within a Pro-rich region of Ruk (see Figures 1 and 5(a)) are responsible for interaction of these two proteins.[21] The same results were obtained when Ruk_l and p85α were co-expressed in HEK293 cells (Figure 2(a)). Moreover, in these cells all Ruk proteins bearing a Pro-rich region,

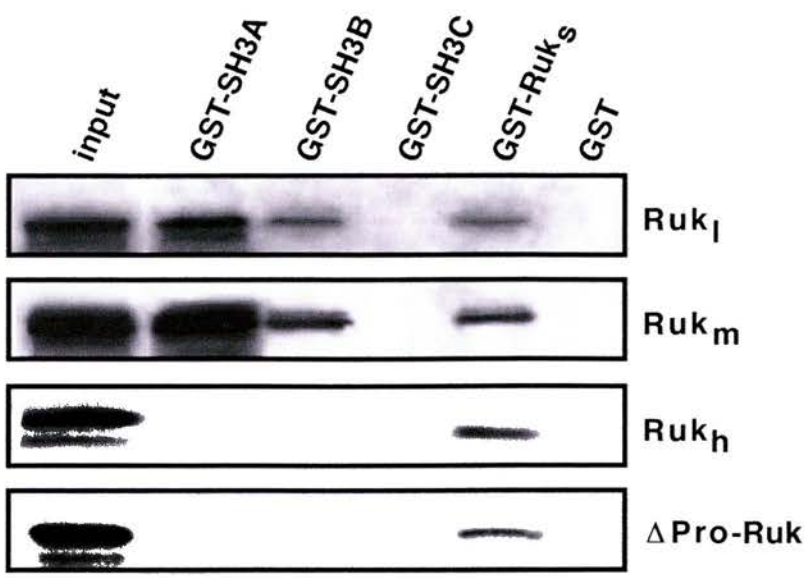

Figure 6. Interaction of separate domains of Ruk with Ruk isoforms and mutants *in vitro*. FLAG-tagged Ruk isoforms and mutants expressed in HEK293 cells were incubated with glutathione-Sepharose-immobilised GST-SH3 domains of Ruk or GST-Ruk_s isoform. The presence of Ruk proteins in pull-downs was assessed by Western blotting using anti-FLAG antibody.

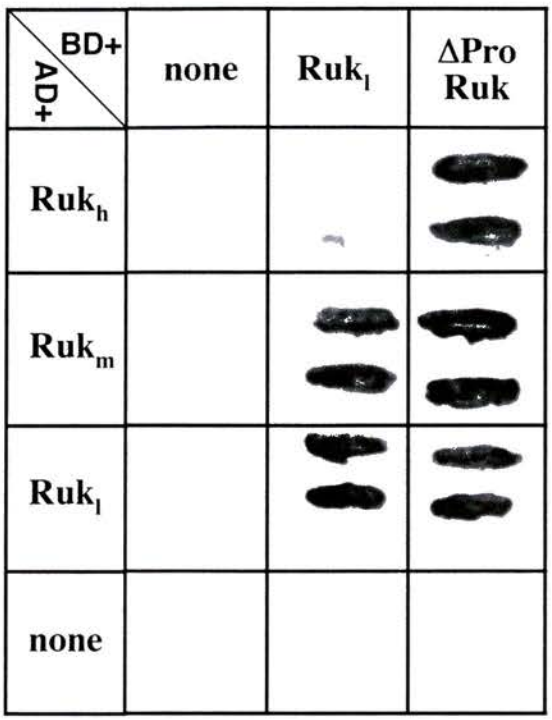

Figure 7. Interaction between various Ruk isoforms and mutants in a yeast two-hybrid system. The filter β-galactosidase assay demonstrates interaction of Ruk-GAL4 DNA-binding domain (BD+) fusion protein with Ruk-GAL4 transcription activating domain (AD+) fusion proteins.

C-terminal coiled coil domain and at least one SH3 domain, SH3C, interacted with full-length p85α but not ΔSH3-p85α (Figure 2(b) and (c)). Short Ruk isoforms did not interact with either of the p85 variants, suggesting that C-terminal Ser-rich and coiled-coil domains are not directly involved in this interaction. Surprisingly, a mutant protein with deletion of the whole Pro-rich region, ΔPro-Ruk, was still able to efficiently interact with p85α (Figure 2(f)). To confirm these observations we studied interaction of full-length p85α and Ruk isoforms or ΔPro-Ruk mutant in a yeast two-hybrid system. Consistently with results obtained in HEK293 cells, in yeast p85α interacted with Ruk$_l$ and Ruk$_m$ isoforms as well as with ΔPro-Ruk mutant but not with Ruk$_h$ (Figure 3). These seemingly controversial results suggested that in different circumstances Ruk and p85α could use different domain combinations to interact with each other. They also clearly demonstrated that interaction between the SH3 domain of p85α and Pro-rich region of Ruk is not absolutely required for heterodimerisation of these two proteins. This raises questions of whether this interaction could be sufficient for dimerisation and if the reciprocal interaction, between SH3 domain(s) of Ruk and Pro-rich region of p85α, was the prerequisite for heterodimerisation. To address these questions we first studied *in vitro* interaction of p85α with GST-fusion SH3 domains of Ruk and demonstrated that the first (SH3A) and to a lesser extent the second (SH3B) SH3 domains of Ruk were able to interact

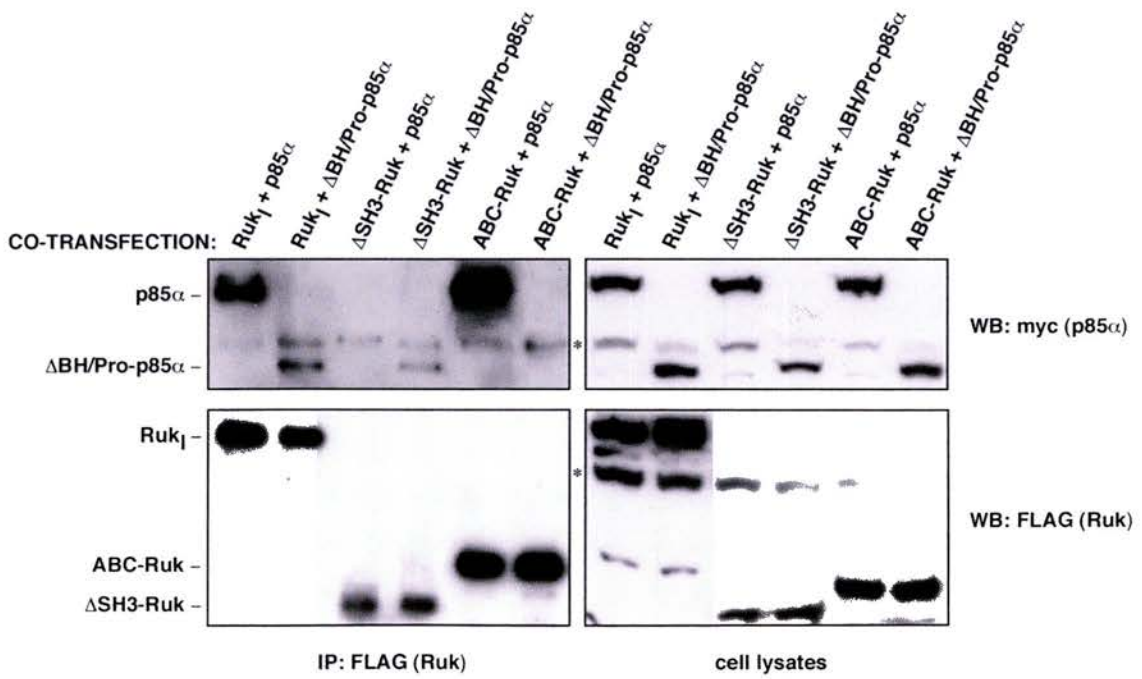

Figure 8. Interaction of Ruk$_l$ and its deletion mutants with ΔBH/Pro-p85α in HEK293 cells. FLAG-tagged Ruk$_l$, ΔSH3-Ruk or ABC-Ruk were co-expressed in HEK293 cells with myc-tagged full-length or ΔBH/Pro-p85α. Total cell lysates and proteins immunoprecipitated with anti-FLAG antibody were analysed by Western blotting using anti-myc antibody to detect p85α proteins and anti-FLAG antibody to detect Ruk proteins. Non-specific bands reacted with these antibodies are marked by asterisks.

with p85α (Figure 4). The third (SH3C) SH3 domain of Ruk did not interact with p85α at all or affinity of their interaction *in vitro* was too low to be detected in GST pull-down experiments. Consistently, when co-expressed in HEK293 cells, a C-terminally truncated Ruk protein, ABC-Ruk, consisting of only three SH3 domains, was able to interact with both p85α proteins (Figure 2(g)). On the contrary, deletion of all three SH3 domains of Ruk in ΔSH3-Ruk protein prevented its interaction with p85α proteins (Figure 2(e)), although the Pro-rich region in this protein was intact and according to the previously proposed model[22] should have been able to secure interaction with full-length p85α. Taken together our new data suggested that SH3 domains of Ruk are required for heterodimerisation with full-length p85α. This is consistent with the presence within the first Pro-rich region of p85α sequence PTPKPR, which perfectly fits into either of two recently described versions of optimal consensus for Ruk SH3 domain's interaction site, Px(P/A)xxR[25] or PxxxPR.[26] Conversely, the inability of ΔSH3-Ruk to interact with full-length p85α (Figure 2(e)) could be seen as an evidence that the interaction between Pro-rich region of Ruk and SH3 domain of p85α is not sufficient for formation of stable dimers. However, comparison of the interaction capabilities of ΔSH3-Ruk and Ruk_m indicates that the Pro-rich region of Ruk does play a role in heterodimerisation of at least certain Ruk isoforms with p85α. The only difference between these two Ruk isoforms is the presence of a SH3 domain, SH3C, which on its own does not interact with p85α *in vitro* (Figure 4) and is not required for interaction in HEK293 cells (Figure 2(h)). Nevertheless, in contrast to ΔSH3-Ruk, Ruk_m weakly interacts with full-length but not ΔSH3-p85α (Figures 2(c) and 3). Therefore, two domains of Ruk, SH3C and Pro-rich region, each of which is not capable of securing high affinity interaction of Ruk with full-length p85α, together are able to stabilise heterodimers of these proteins. Moreover, deletion of Pro-rich and BH domains in p85α makes possible interaction of such mutant protein not only with Ruk_l but also with ΔSH3-Ruk (Figure 8), clearly indicating that heteromerisation of these truncated proteins can be secured solely by interaction between the Pro-rich region of Ruk and SH3 domain of p85α.

How can these experimental data, schematically summarised in Figure 9(a), be used to explain the mechanism of interaction between Ruk and p85α? It has been demonstrated that p85α forms homodimers *via* SH3 domain/first Pro-rich region and BH/BH interactions.[27] This means that its SH3 domain is normally hindered by interaction with the Pro-rich block, which sequence perfectly fits the consensus of a binding site for SH3 domains of Ruk (see above). To make the SH3 domain of p85α able to interact with the Pro-rich domain of Ruk, its release from intrahomodimeric interaction is required. This could be achieved by either deletion of Pro-rich region, as in ΔBH/Pro-p85α, or ousting by other SH3 domains, for instance SH3 domains of Ruk. We propose that in a Ruk_l molecule SH3 domains could be similarly hindered by high affinity intrahomodimeric interactions with its own Pro-rich region (illustrated in Figure 9(b)). This explains why Ruk_l is not able to form heterodimers with ΔSH3-p85α, while Ruk proteins with the same set of SH3 domains but lacking a Pro-rich region, ΔPro-Ruk and ABC-Ruk, evidently dimerise with this protein. Therefore, the inability of a SH3 domain-bearing Ruk isoform to interact with ΔSH3-p85α could be seen as an indicator of strong intrahomodineric interactions between Pro-rich and SH3 domains of this isoform.

Using *in vitro* pull-down assay with GST-fusion SH3 domains of Ruk as baits we demonstrated that SH3A and, to lesser extent, SH3B but not SH3C of Ruk interact with Pro-rich region-containing Ruk proteins (Figure 6). This observation is consistent with results obtained in similar experiments with human orthologues of Ruk, CIN85[26] and CD2BP3,[19] and confirms that intramolecular interactions between SH3 domains and proline-rich blocks within a Pro-rich region of Ruk are possible. To assess which of four proline-rich blocks are critical for stabilisation of intramolecular interactions *in vivo* we generated mutants with several point mutations in each of the proline-rich blocks (Figure 5(a)) and studied their interaction with p85α and ΔSH3-p85α in HEK293 cells. A protein with mutations in the first block behaved as wild-type Ruk_l, whereas interaction patterns of P2 and P3 mutant proteins resembled interaction patterns of ΔPro-Ruk and ABC-Ruk (Figure 5(b)). We concluded that the first proline-rich block is dispensable but the others, especially P2 and P3, are important for stabilisation of intramolecular interactions between SH3 domains and Pro-rich region of Ruk. Interestingly, blocks P2, P3 and P4, share consensus sequence (I/L)PPx(R/K)P(E/R) absent in P1. Further experiments should elucidate whether this sequence is indeed responsible for intramolecular interaction with Ruk SH3 domains but it is already clear that such interaction does not require sequences described as optimal for interaction of Ruk SH3 domains with other proteins or synthetic peptides. Sequences that fit into a consensus Px(P/A)xxR, described by Kurakin *et al.*[25] are not present in the Pro-rich region of Ruk and the sequence PPKKPR that fits into a consensus PxxxPR suggested by Kowanetz *et al.*[26] is present only in the block P3. As a possible explanation for this discrepancy an allosteric effect of Ruk dimerisation *via* coiled-coil domains on conformation of SH3 and Pro-rich domains, resulting in their increased affinity to each other might be suggested. Consistent with this suggestion is our observation that deletion of C-terminal coiled-coil domain of Ruk_l allows the truncated protein to interact, although very weakly, with ΔSH3-p85α (Figure 2(i)), probably because the absence of coiled-coil domain weakens intramolecular interaction between Pro-rich region and SH3 domains, making the latter

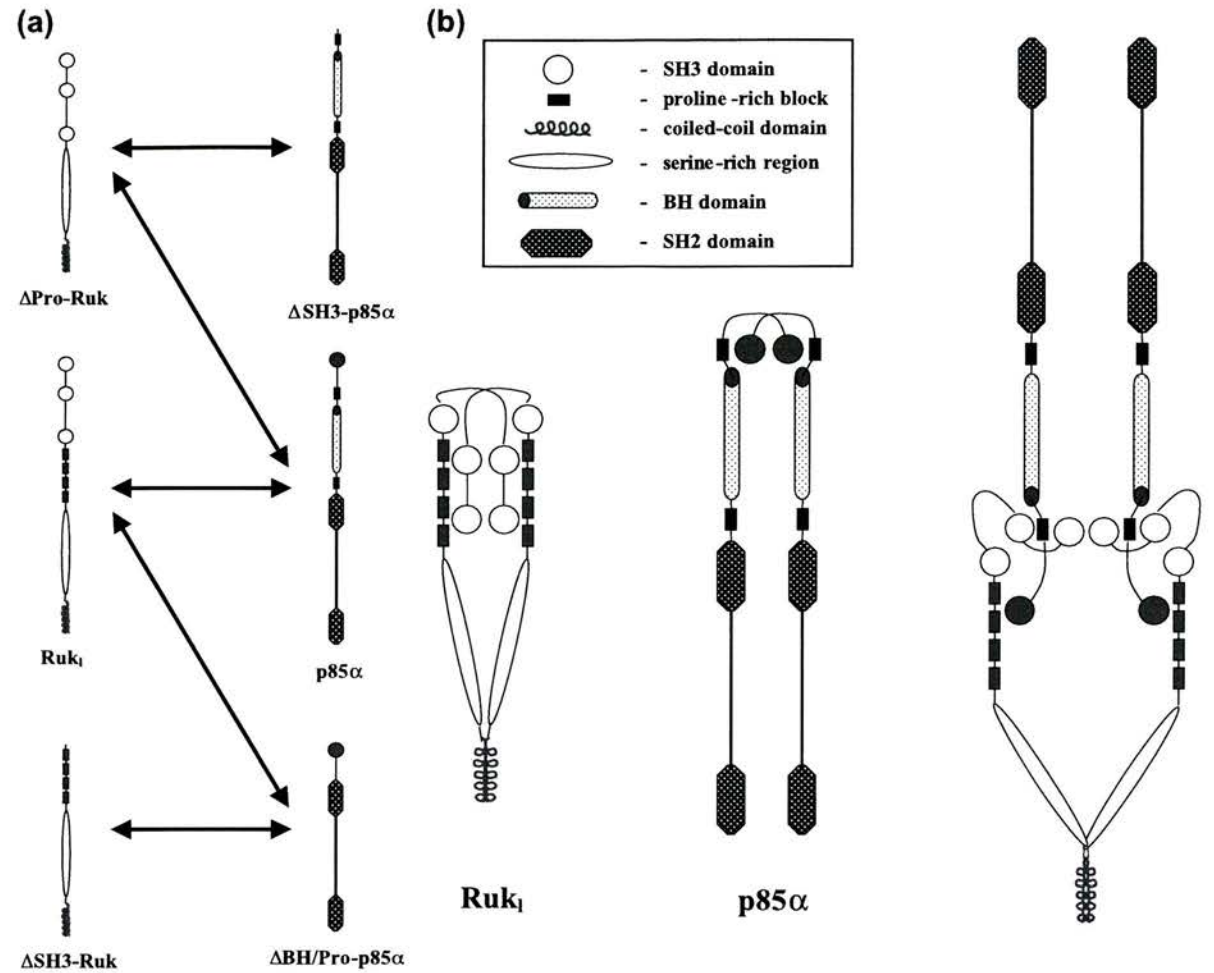

Figure 9. Hypothetical scheme of interaction between Ruk and p85α. Possible interactions between full-length and deletion mutants of Ruk and p85α are shown in a by arrows. Homodimers of full-length Ruk$_l$ and p85α and how they might form a heterodimer with each other are illustrated in (b).

more accessible for interaction with Pro-rich region of p85α. The role of the C-terminal coiled-coil domain of Ruk in homodimerisation and even formation of large protein complexes has been shown previously.[14,15,26] We also demonstrated the ability of coiled-coil-domain-only isoforms, Ruk$_h$ and Ruk$_s$, to interact with each other and longer Ruk isoforms *in vitro* (Figure 6) and in the yeast two-hybrid system (Figure 7 and data not shown). Moreover, in the yeast two-hybrid system Ruk$_h$ interacts weakly with Ruk$_l$ but strongly with ΔPro-Ruk (Figure 7). These results suggest that the affinity of coiled-coil domains in a Ruk$_l$ homodimer is higher than the affinity of coiled-coil domains of Ruk$_l$ and Ruk$_h$ in a heterodimer, but the absence of the Pro-rich region reduces the affinity in a ΔPro-Ruk homodimer and allows effective formation of heterodimers between Ruk$_h$ and ΔPro-Ruk. Taken together, our data demonstrate that interaction between coiled-coil domains and interaction between SH3 domains and Pro-rich regions reciprocally stabilise each other during dimerisation of two Ruk molecules. Internal deletions within the Ruk molecule, even if they did not directly affect interacting interfaces, as in the case of SH3C domain deletion in ΔC-Ruk (Figure 2(h)), could also destabilise intrahomodimeric interactions, probably because they change the distance between interacting domains. In the case of interaction between full-length p85α and Ruk$_l$ the major role in destabilisation of interactions between SH3 domains and Pro-rich region within Ruk$_l$ homodimer belongs to the SH3 domain of p85α because deletion of this domain completely abolished heterodimerisation with Ruk$_l$ (Figure 2(a)).

We believe that our experimental data strongly support the hypothesis that reciprocal ousting of SH3 domains of p85α and Ruk from their intrahomodimeric interactions with Pro-rich regions is crucial for interaction of full-length isoforms of these proteins. Further structural studies will be required to confirm this model of interaction illustrated in Figure 9(b). The intrahomodimeric Pro-rich to SH3 domain interactions might affect the ability of Ruk/CIN85/SETA/CD2BP3 isoforms to bind not only p85α but other proteins as well. Tibaldi and Reinherz suggested a similar effect of these intramolecular interactions on the efficiency of

Ruk/CIN85/SETA/CD2BP3 interaction with c-Cbl because in their experiments mutants lacking a Pro-rich region co-immunoprecipitated c-Cbl more efficiently than full-length protein.[19]

In conclusion, accumulating experimental evidence suggests that differences in domain organisation of various Ruk/CIN85/SETA/CD2BP3 isoforms affect their abilities to interact with each other and other signalling molecules, and, consequently, determines their different effect on intracellular processes.

Materials and Methods

Expression plasmids

For expression in HEK293 cells, cDNAs encoding various Ruk isoforms or mutants were subcloned under transcriptional control of a CMV promoter in pCMV5 vector. C-terminal FLAG-tag (DYDDDDK) was added to encoded proteins during subcloning by conventional PCR-based techniques. For construction of Ruk_l, Ruk_m, Ruk_h and Ruk_s expression plasmids, full coding regions of corresponding cDNA[21,22] were used. In the deletion mutant constructs fragments corresponding to the following amino acid residues of Ruk_l[21] protein were deleted: 2–99 (ΔA-Ruk), 274–327 (ΔC-Ruk), 2–327 (ΔSH3-Ruk), 2–432 (Ruk_e), 328–426 (ΔPro-Ruk), 354-stop codon (ABC-Ruk), 431-stop codon (ΔCterm-Ruk). For construction of plasmids expressing Ruk proteins with mutations in the Pro-rich region (shown in Figure 5), primers with relevant nucleotide substitutions, which resulted in substitutions of selected amino acids to alanine in the encoding protein, and a purposely introduced in-frame NotI site were designed. Combinations of these primers with N-terminal or C-terminal Ruk primers were used to amplify N-terminal or C-terminal fragments of Ruk_l coding regions, correspondingly. These fragments were digested with NotI and ligated together to obtain a fragment encoding a full-length protein with engineered mutations. All final plasmid constructs were verified by sequencing. Plasmids for expression of myc-tagged p85α and ΔSH3-p85α were described previously.[23] To generate a ΔBH/Pro-p85α plasmid an internal BglII-XhoI fragment of a plasmid encoded myc-tagged p85α protein was substituted with a synthetic double-stranded BglII-XhoI fragment. As the result, in the encoded protein amino acid residues 84–332 were substituted by three alanine residues.

Transient protein expression in HEK293 cells

HEK293 cells were cultured at 37 °C in an atmosphere of 5% CO_2 in Dulbecco's modified Eagle's medium (DMEM) containing 10% (v/v) foetal bovine serum (Invitrogen, Carlsbad, CA) and antibiotic/antimycotic solution (Sigma, St Louise, MO). Cells were plated into 10 cm diameter dishes and transfected with 10 μg of plasmid DNA by a modified calcium phosphate method.[28] At 24 hours after transfection, cells were washed twice with cold PBS and lysed in buffer A (50 mM Tris (pH 7.5), 1% Triton, 150 mM NaCl, 1 mM EDTA and Complete Protease Inhibitor Cocktail from Pierce, Rockford, IL), with ten passes through a 23 G syringe needle. After centrifugation at 14,000*g* for 20 minutes at 4 °C, proteins in the supernatant were analysed in SDS-PAGE, followed by Western blot analysis with rabbit polyclonal anti-Ruk,[21] anti-FLAG (Sigma, St Louise, MO) or anti-myc-tag (Santa Cruz Biotechnology Inc., Santa Cruz, CA) primary antibody. Secondary donkey anti-rabbit antibodies coupled to horseradish peroxidase (HRP) and ECL system from Amersham Pharmacia Biotech (St Albans, UK) were used for detection of the immunoreactive proteins. For co-expression experiments amounts of plasmids used for transfection were adjusted to obtain similar levels of expression of p85α and Ruk isoforms.

Immunoprecipitation

An aliquot of cleared supernatant (0.5 mg of total protein) from each transfection was mixed with 10 μl of anti-FLAG-tag antibody-immobilised beads (Anti-FLAG M2 affinity gel, Sigma, St Louise, MO). After a two hour incubation at 4 °C with constant mixing, beads were washed three times with TBS, twice with TBS plus 150 mM NaCl, resuspended in 40 μl of SDS-loading buffer without β-mercaptoethanol and bound proteins were eluted by boiling for two minutes. Immunoprecipitated proteins in eluates were analysed by SDS-PAGE and Western blotting as described above.

GST-fusion protein expression and pull-down experiments

The full-length coding regions of p85α and Ruk_s isoform or fragments corresponding to SH3 domains of Ruk were subcloned in pGEX vectors (Amersham Pharmacia Biotech, St Albans, UK) in-frame with glutathione *S*-transferase and used for transformation of *E. coli* B21 strain. Induction of fusion protein expression by IPTG and their purification on glutathione-Sepharose were performed as recommended by the manufacturer (Amersham Pharmacia Biotech, St Albans, UK). For pull-down experiments 5 μg of GST or GST-fusion protein bound to glutathione-Sepharose (approximately 20 μl of packed beads equilibrated in 50 mM Tris–HCl (pH 7.5), 150 mM NaCl, 1% Triton X-100) were incubated for four hours at room temperature with 300 μl (1.5 mg of total protein) of cleared lysate of HEK293 cells transiently transfected with Ruk or p85α expression plasmids. The cleared lysates were prepared as described above. The efficiencies of transfection were adjusted to obtain comparable levels of expression of Ruk isoforms in HEK293 cells and, consequently, equal amount of each isoform in pull-down reactions. The beads were washed three times with PBS/1% Triton X-100, three times with PBS and boiled in 50 μl of SDS-loading buffer. Eluted proteins were separated by SDS-PAGE and transferred onto PVDF membrane for Western blot analysis with anti-FLAG, anti-Ruk or anti-p85α antibodies.

Protein–protein interaction studies in yeast

For analysis of protein–protein interaction in the yeast two-hybrid system, coding regions of p85α, Ruk isoforms or Ruk mutants described above were cloned in pPC86 vector in-frame with GAL4 transcription activating domain (GAL4AD) or pPC97 vector in-frame with GAL4 DNA-binding domain (GAL4BD).[29] Protein–protein interaction assay was performed as described.[30] In brief, yeast strain Y153 was used to co-transform bait and prey plasmids, and transformants were selected by plating on synthetic dextrose leucine and tryptophan

dropout plate. To evaluate *LacZ* reporter gene *trans*-activation, filter β-galactosidase assay was used.

Acknowledgements

We are grateful to Peter Shepherd for p85α expression plasmids and Julia Wanless for excellent technical assistance. This work was supported by grants from the Association for International Cancer Research.

References

1. Dikic, I. (2002). CIN85/CMS family of adaptor molecules. *FEBS Letters*, **529**, 110–115.
2. Dustin, M. L., Olszowy, M. W., Holdorf, A. D., Li, J., Bromley, S., Desai, N. *et al.* (1998). A novel adaptor protein orchestrates receptor patterning and cytoskeletal polarity in T-cell contacts. *Cell*, **94**, 667–677.
3. Shih, N. Y., Li, J., Cotran, R., Mundel, P., Miner, J. H. & Shaw, A. S. (2001). CD2AP localizes to the slit diaphragm and binds to nephrin *via* a novel C-terminal domain. *Am. J. Pathol.* **159**, 2303–2308.
4. Shih, N. Y., Li, J., Karpitskii, V., Nguyen, A., Dustin, M. L., Kanagawa, O. *et al.* (1999). Congenital nephrotic syndrome in mice lacking CD2-associated protein. *Science*, **286**, 312–315.
5. Palmen, T., Lehtonen, S., Ora, A., Kerjaschki, D., Antignac, C., Lehtonen, E. & Holthofer, H. (2002). Interaction of endogenous nephrin and CD2-associated protein in mouse epithelial M-1 cell line. *J. Am. Soc. Nephrol.* **13**, 1766–1772.
6. Yuan, H., Takeuchi, E. & Salant, D. J. (2002). Podocyte slit-diaphragm protein nephrin is linked to the actin cytoskeleton. *Am. J. Physiol. Renal Physiol.* **282**, F585–F591.
7. Lehtonen, S., Zhao, F. & Lehtonen, E. (2002). CD2-associated protein directly interacts with the actin cytoskeleton. *Am. J. Physiol. Renal Physiol.* **283**, F734–F743.
8. Soubeyran, P., Kowanetz, K., Szymkiewicz, I., Langdon, W. Y. & Dikic, I. (2002). Cbl-CIN85-endophilin complex mediates ligand-induced downregulation of EGF receptors. *Nature*, **416**, 183–187.
9. Petrelli, A., Gilestro, G. F., Lanzardo, S., Comoglio, P. M., Migone, N. & Giordano, S. (2002). The endophilin-CIN85-Cbl complex mediates ligand-dependent downregulation of c-Met. *Nature*, **416**, 187–190.
10. Szymkiewicz, I., Kowanetz, K., Soubeyran, P., Dinarina, A., Lipkowitz, S. & Dikic, I. (2002). CIN85 participates in Cbl-b-mediated down-regulation of receptor tyrosine kinases. *J. Biol. Chem.* **277**, 39666–39672.
11. Dikic, I. & Giordano, S. (2003). Negative receptor signalling. *Curr. Opin. Cell. Biol.* **15**, 128–135.
12. Schmidt, M. H., Furnari, F. B., Cavenee, W. K. & Bogler, O. (2003). Epidermal growth factor receptor signaling intensity determines intracellular protein interactions, ubiquitination, and internalization. *Proc. Natl Acad. Sci. USA*, **100**, 6505–6510.
13. Haglund, K., Shimokawa, N., Szymkiewicz, I. & Dikic, I. (2002). Cbl-directed monoubiquitination of CIN85 is involved in regulation of ligand-induced degradation of EGF receptors. *Proc. Natl Acad. Sci. USA*, **99**, 12191–12196.
14. Verdier, F., Valovka, T., Zhyvoloup, A., Drobot, L. B., Buchman, V., Waterfield, M. & Gout, I. (2002). Ruk is ubiquitinated but not degraded by the proteasome. *Eur. J. Biochem.* **269**, 3402–3408.
15. Watanabe, S., Take, H., Takeda, K., Yu, Z. X., Iwata, N. & Kajigaya, S. (2000). Characterization of the CIN85 adaptor protein and identification of components involved in CIN85 complexes. *Biochem. Biophys. Res. Commun.* **278**, 167–174.
16. Borinstein, S. C., Hyatt, M. A., Sykes, V. W., Straub, R. E., Lipkowitz, S., Boulter, J. & Bogler, O. (2000). SETA is a multifunctional adapter protein with three SH3 domains that binds Grb2, Cbl, and the novel SB1 proteins. *Cell Signal.* **12**, 769–779.
17. Hutchings, N. J., Clarkson, N., Chalkley, R., Barclay, A. N. & Brown, M. H. (2003). Linking the T cell surface protein CD2 to the actin-capping protein CAPZ via CMS and CIN85. *J Biol Chem*, **278**, 22396–22403.
18. Schmidt, M. H., Chen, B., Randazzo, L. M. & Bogler, O. (2003). SETA/CIN85/Ruk and its binding partner AIP1 associate with diverse cytoskeletal elements, including FAKs, and modulate cell adhesion. *J. Cell. Sci.* **116**, 2845–2855.
19. Tibaldi, E. V. & Reinherz, E. L. (2003). CD2BP3, CIN85 and the structurally related adaptor protein CMS bind to the same CD2 cytoplasmic segment, but elicit divergent functional activities. *Int. Immunol.* **15**, 313–329.
20. Chen, B., Borinstein, S. C., Gillis, J., Sykes, V. W. & Bogler, O. (2000). The glioma-associated protein SETA interacts with AIP1/Alix and ALG-2 and modulates apoptosis in astrocytes. *J. Biol. Chem.* **275**, 19275–19281.
21. Gout, I., Middleton, G., Adu, J., Ninkina, N. N., Drobot, L. B., Filonenko, V. *et al.* (2000). Negative regulation of PI 3-kinase by Ruk, a novel adaptor protein. *EMBO J.* **19**, 4015–4025.
22. Buchman, V. L., Luke, C., Borthwick, E. B., Gout, I. & Ninkina, N. (2002). Organization of the mouse Ruk locus and expression of isoforms in mouse tissues. *Gene*, **295**, 13–17.
23. Beeton, C. A., Das, P., Waterfield, M. D. & Shepherd, P. R. (1999). The SH3 and BH domains of the p85alpha adapter subunit play a critical role in regulating class Ia phosphoinositide 3-kinase function. *Mol. Cell Biol. Res. Commun.* **1**, 153–157.
24. Bogler, O., Furnari, F. B., Kindler-Roehrborn, A., Sykes, V. W., Yung, R., Huang, H. J. & Cavenee, W. K. (2000). SETA: a novel SH3 domain-containing adapter molecule associated with malignancy in astrocytes. *Neuro-oncology*, **2**, 6–15.
25. Kurakin, A. V., Wu, S. & Bredesen, D. E. (2003). Atypical recognition consensus of CIN85/SETA/Ruk SH3 domains revealed by target-assisted iterative screening. *J. Biol. Chem.* **278**, 34102–34109.
26. Kowanetz, K., Szymkiewicz, I., Haglund, K., Kowanetz, M., Husnjak, K., Taylor, J. D. *et al.* (2003). Identification of a novel proline-arginine motif involved in CIN85-dependent clustering of Cbl and down-regulation of epidermal growth factor receptors. *J. Biol. Chem.* **278**, 39735–39746.
27. Harpur, A. G., Layton, M. J., Das, P., Bottomley, M. J., Panayotou, G., Driscoll, P. C. & Waterfield, M. D. (1999). Intermolecular interactions of the p85alpha regulatory subunit of phosphatidylinositol 3-kinase. *J. Biol. Chem.* **274**, 12323–12332.

28. Webster, G. A. & Perkins, N. D. (1999). Transcriptional cross talk between NF-kappaB and p53. *Mol. Cell Biol.* **19**, 3485–3495.
29. Chevray, P. M. & Nathans, D. (1992). Protein interaction cloning in yeast: identification of mammalian proteins that react with the leucine zipper of Jun. *Proc. Natl Acad. Sci. USA*, **89**, 5789–5793.
30. Durfee, T., Becherer, K., Chen, P. L., Yeh, S. H., Yang, Y., Kilburn, A. E. *et al.* (1993). The retinoblastoma protein associates with the protein phosphatase type 1 catalytic subunit. *Genes Dev.* **7**, 555–569.

Edited by M. Yaniv

(Received 13 April 2004; received in revised form 12 August 2004; accepted 20 August 2004)